Geochemical and petrographical investigation of the Waaikraal gold deposit, northwest of Brits, Transvaal.

by

Sabine Marie Charlotte Verryn

Submitted in partial fulfilment
of the requirements for the degree of
Magister Scientiae
in the Faculty of Science
of the
University of Pretoria
Pretoria

August 1989

ABSTRACT

The Waaikraal Gold Deposit is situated approximately 25 km northwest of Brits and 30 km northeast of Rustenburg.

The gold occurs in a sill-like body consisting of alternating layers and lenses of pyroxenite and a magnetite-rich rock, hosted in sediments belonging to the Rayton Formation of the Transvaal Sequence. The sediments are situated between the magnetite gabbros of the upper zone of the Bushveld Complex and the granites of the Lebowa Granite Suite.

The pyroxenite is composed of clinopyroxene (augite and hedenbergite), plagioclase (mainly andesine), orthoclase, quartz, amphibole (hastingsite and hastingsitic hornblende) and some magnetite and apatite. The magnetite-rich rock consists of magnetite, clinopyroxene (augite and hedenbergite) and plagioclase (mainly andesine). Olivine (fayalite), apatite and ilvaite are accessory constituents in the magnetite-rich rock.

The gold occurs in three different phases viz., very pure native gold, with Ag-content < 1.3 weight per cent, is the most prominent phase, in maldonite (Au_2Bi) and in a gold-copper compound ($CuAu_3$). It is associated with cobaltite (CoAsS), arsenopyrite (FeAsS), safflorite ($(Co,Fe)As_2$), native bismuth, bismuthinite (Bi_2S_3), joseite-B (Bi_4Te_2S) and chalcopyrite. Other ore minerals include pyrrhotite, pyrite and sphalerite.

The composition of silicates and the presence of high amounts of titanium in the magnetite grains suggest that the pyroxenite is related to the upper zone of the Bushveld Complex and that it crystallised from a highly differentiated upper zone type liquid, which was injected into the host rocks during the final stages of consolidation of the upper zone. The magnetite-rich rocks, on the other hand, are considered to be of sedimentary origin. Derivation of this rock from an iron-rich metamorphosed sediment is supported by its low titanium content, but comparison with iron-rich sediments shows that this possibility is unlikely. The presence of typical skarn minerals such as hedenbergite, magnetite and ilvaite, as well as the typical association of Cu, Co, As, Bi and Au with Fe, suggest that this rock could also be a calcic iron-skarn derived from sediments through metasoma-

tism by iron-rich fluids. The "original sediment" is most likely is a marl with a composition eqivalent to equal parts of shale and limestone.

The temperature range of formation of the ore minerals associated with the gold and the mode of occurrence of the gold suggests a possibly Bushveld related, hydrothermal origin for the gold, where the gold may have been transported as sulfide complexes.

SAMEVATTING

Die Waaikraal goudafsetting is ongeveer 25 km noordwes van Brits en 30 km noordoos van Rustenburg gelee.

Die goud kom voor in 'n plaatagtige liggam bestaande uit afwisselende lae en lense van pirokseniet en magnetietryk gesteentes, in sedimente van die Rayton Formasie van die Transvaal Opeenvolging. Die sedimente lê tussen magnetietgabbros van die bosone van die Bosveldkompleks en graniete van die Lebowa Graniet Suite.

Die pirokseniet bestaan uit klinopirokseen (ougiet en hedenbergiet), plagioklaas (hoofsaaklik andesien), ortoklaas, kwarts, amfibool (hastingsiet en hastingsitiese horingblende) met mindere magnetiet en apatiet. Die magnetietryk gesteente bestaan uit magnetiet, klinopirokseen (ougiet en hedenbergiet) en plagioklaas (hoofsaaklik andesien). Olivien (fayaliet), apatiet en ilvaiet is bykomstige bestanddele van die magnetietryk gesteente.

Die goud kom in drie verskillende fases voor, te wete as baie suiwer goud met 'n silwerinhoud < 1.3 gewigspersent, wat die volopste is, in maldoniet (Au_2Bi) en in 'n goud-koper verbinding ($CuAu_3$). Die goud is met kobaltiet (CoAsS), arseenpiriet (FeAsS), safflorit ($(Co,Fe)As_2$), bismut metaal, bismutiniet (Bi_2S_3), joseiet-B (Bi_4Te_2S) en chalkopiriet geassosieer. Ander ertsminerale sluit in pirrotiet, piriet en sinkblende.

Die samestelling van die silikate en die groot hoeveelhede titaan in die magnetietkorrels dui daarop dat die pirokseniet aan die bosone van die Bosveldkompleks verwant is. Hierdie gesteente het vermoedelik vanuit 'n hoogsgedifferensieerde bosone-tipe vloeistof gekristalliseer, wat gedurende die finale stadiums van konsolidasie van die bosone in die omgewingsgesteentes ingedring is. Die magnetietryk gesteentes aan die ander kant, mag van sedimentêre oorsprong wees, en wel van 'n ysterryk gemetamorfoseerde sediment, wat deur die lae titaaninhoud gesteun word. 'n Vergelyking met ysterryk sedimente toon egter dat hierdie moontlikheid onwaarskynlik is. Die teenwoordigheid van tipiese skarn minerale soos hedenbergiet, magnetiet en ilvaiet, sowel as die tipiese assosiasie van Cu, Co, As, Bi en Au met Fe dui daarop dat hierdie gesteente moontlik 'n kalsiese yster-skarn verteenwoordig wat deur metasomatose van oorspronklike sedimente deur ysterryk vloeistowwe sou kon ontstaan het. Die "oorspronklike sediment" was

hoogs waarskynlik ´n mergel met ´n samestelling gelyk aan gelyke dele skalie en kalksteen.

Die temperatuur van vorming van die ertsminerale geassosieer met die goud en die voorkomswyse van die goud dui op ´n waarskynlik Bosveld-verwante, hidrotermale oorsprong vir die goud, waar die goud waarskynlik as sulfiedkomplekse vervoer is.

TABLE OF CONTENTS

LIST OF TABLES

LIST OF FIGURES

1. INTRODUCTION

1.1 General

Waaikraal Gold Mine is situated on Portion 2 of the farm Waaikraal 396JQ in Bophuthatswana, approximately 25 km north-west of Brits and 30 km north-east of Rustenburg (see Fig. 2.1).

The mine itself is fairly small, with underground reef development only about 100 metres in extent.

The deposit is a sill-like body of magnetite-rich rock and pyroxenite in a large xenolith of Transvaal sediments wedged between the upper zone and the Lebowa Granite Suite of the Bushveld Complex.

A long standing problem has been the question of the relationship of the Waaikraal deposit to the Bushveld Complex. The aim of this investigation is therefore to ascertain whether the petrography, ore mineralogy and chemistry of the various minerals, as well as the geochemical signature of the rocks, could provide an answer to the above question, and information on the origin of the gold and its host rocks.

1.2 Historical Mining Background

According to Wagner (1926a), free gold in fairly coarse grains had long been known to occur in the surface soils on the farm Waaikraal. The gold was traced back to its source in 1925 by Mr. W.M. Edwards, who named his discovery the "Moorcroft Reef".

Open pit and underground mining activities started in 1926 and continued until about 1945, when mining ceased, possibly due to an intrusive dolerite dyke.

Bethanie Mining Corporation took over the mine in 1982 and their activities continued until the middle of 1986. This company mined underground and also reworked old slimes dumps.

1.3 Previous Investigations

Very few reports and publications are available on the gold deposit at Waaikraal.

The earliest study, and only official publication on this locality, was that by Wagner in 1926a, who described the major ore bearer as a pyroxenitic, quartz-bearing sill of soda gabbro, which he considered to belong to the Bushveld Complex. The gold was found to occur mainly with secondary limonite derived from oxidation of pyrrhotite and pyrite. The highest gold content was observed in the central part of the sill.

In a supplementary note, Wagner (1926b) described a greyish silvery-white mineral with a bright metallic lustre, which he considered to be krennerite, a telluride of gold.

Van Biljon (1974) briefly referred to the Waaikraal Gold Deposit and maintained that both the pyroxenitic quartz-bearing soda gabbro and the recrystallised ironstone (mainly magnetite) are products of replacement of banded cherty rocks over- and underlain by quartzite. The gold bearer is believed not to be injected into the ironstone as maintained by Wagner, but to be a replacement product.

The Waaikraal deposit was reinvestigated by the Bophuthatswana Geological Survey (Weston, 1980, 1981). Thin section study of samples collected in the quarry led Weston (1980) to the conclusions that the amount of magnetite decreases, while the amount of pyroxene increases from the top to the bottom of the sill and that there is a general increase in gold content towards the base of the sill.

Subsequent drilling down dip from the quarry indicated that the sequence of the rocks obtained from the cores is not identical to the sequence in the quarry (Weston, 1981). A magnetite-pyroxenite was believed to be the ore bearer although the gold values obtained were very low. Unfortunately, the drill cores were in a very bad condition and the exact drilling positions could not be obtained, which made a further study of those cores not feasable.

A mineralogical examination of the Moorcroft Reef was done by Swash in 1983. He states that the dominant ore mineral is joseite

$(Bi_4(TeS)_3)$ (a very soft silvery coloured mineral), with which the gold is nearly always associated.

2. GEOLOGY

The Waaikraal deposit occurs in sediments belonging to the Rayton Formation of the Transvaal Sequence (Geological Survey, 1981), wedged between the magnetite gabbros of the upper zone of the Bushveld Complex and granites of the Lebowa Granite Suite.

The area around Waaikraal Gold Mine was mapped in detail at a scale of 1:12 000 (Fig. 2.2). Because of the poor outcrops, the Bethanie Mining Corporation dug 1-3 metre deep survey pits in order to determine the extent of the ore body. Many of these pits did not penetrate the soil cover, others exposed some of the underlying rock, whereas few exposed a succession of rocks consisting of hornfels, magnetite-rich rock, pyroxenite and quartzite.

The detailed map (Fig. 2.2) includes many inferred contacts due to the poor exposure in the field. The positioning of the inferred faults is based on the outcrop pattern of the magnetite-rich rock and the pyroxenite in pits and trenches.

The oldest rocks in the area are the sediments belonging to the Transvaal Sequence. Quartzite is most abundant and consists of euhedral to subhedral interlocking quartz grains with 120° triple junctions. Small amounts of plagioclase, mica, chlorite and amphibole occupy the intergranular sites, whilst zircon is the only accessory mineral present.

Patchy outcrops of pyroxene-hornfels and calc-silicate hornfels probably represent remnants of originally interbedded shale and limestone. The sediments occupy the central part of the mapped area (Fig. 2.2) and host the ore body, which is an inclined, sill-like body of pyroxenite and magnetite-rich rock within the quartzite. Its lateral extension is uncertain because of the lack of outcrop. The distribution of the sill is largely inferred from the pits dug by Bethanie Mining Corporation. This investigation concentrates on exposures in the mine itself.

The ore body dips approximately 30° to the northeast and strikes in a northwest-southeast direction. The sill consists of an irregularly alternating succession of lenses and layers of pyroxenite and magnetite-rich rock with thin lenses and bands of magnetite-rich rock in the pyroxenite and the vice versa. Within the old workings the hanging wall consists of pyroxene-hornfels and the foot wall of quartzite.

The distribution of the two rock types throughout the mine was mapped and is presented, together with the distribution of the gold values in Figure 2.3. The profiles indicated in this figure do not represent the whole succession from the foot- to the hanging wall, because the entire sill was not always mined. It is evident from this diagram that the individual layers are discontinuous and could therefore be interpreted as large, lenticular bodies.

The southern area consists of magnetite gabbros of the upper zone of the Bushveld Complex, which contain a prominent northwest-southeast striking layer of magnetite. Some pegmatoid layers can be observed in the magnetite gabbros. Magnetite gabbro was also found in pits dug within the quartzite to the south of the mine.

The northern part of the mapped area is occupied by granite of the Lebowa Granite Suite (SACS, 1980). A small amount of granite has intruded along the contact between the magnetite gabbro and the quartzite to the south of the mine.

The area is intersected by three northwest-southeast striking dolerite dykes.

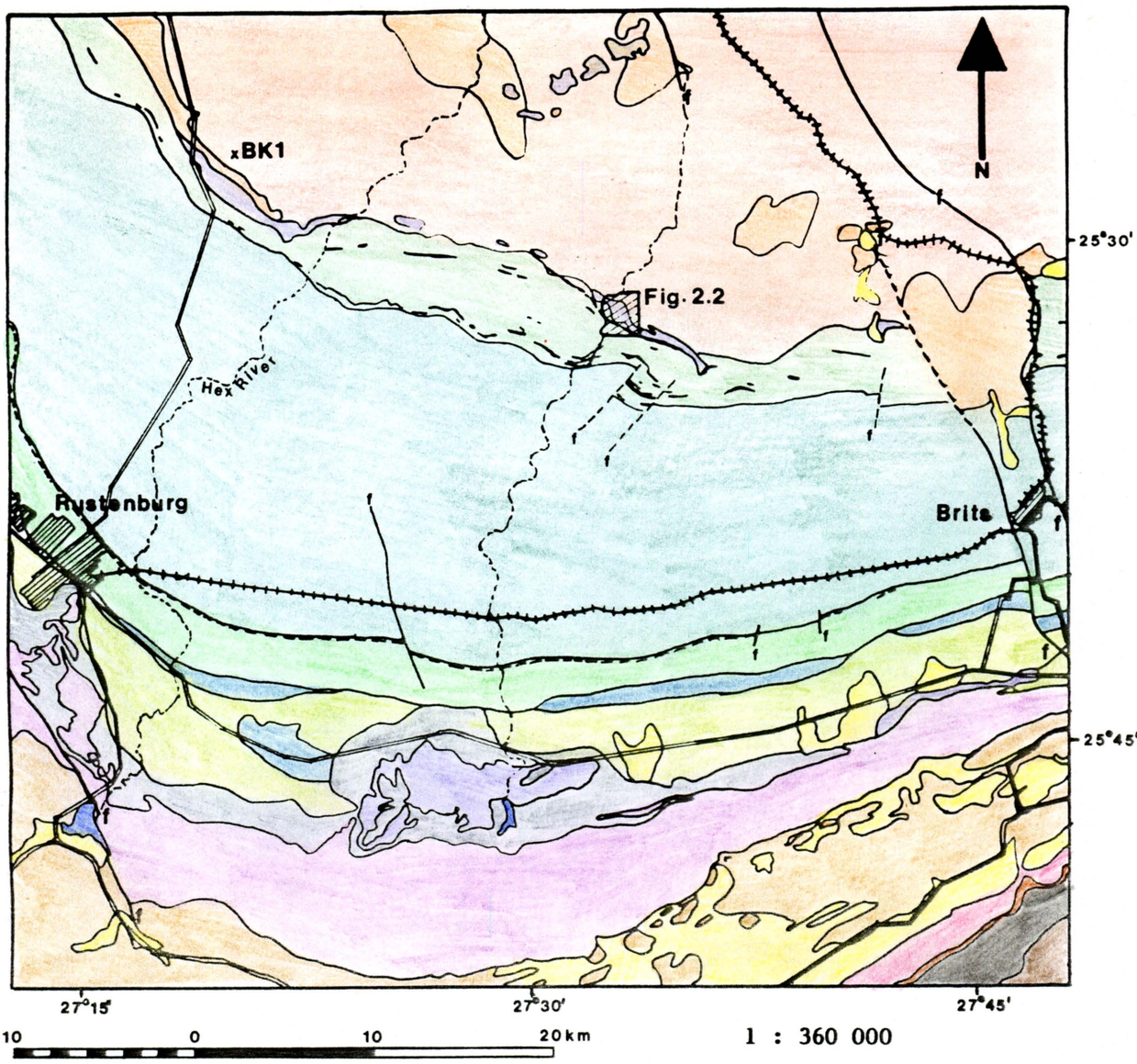

Figure 2.1 Simplified geological map of part of the western Bushveld Complex (modified after Geological Sheet 2526 (Rustenburg) 1 : 250 000, 1981)

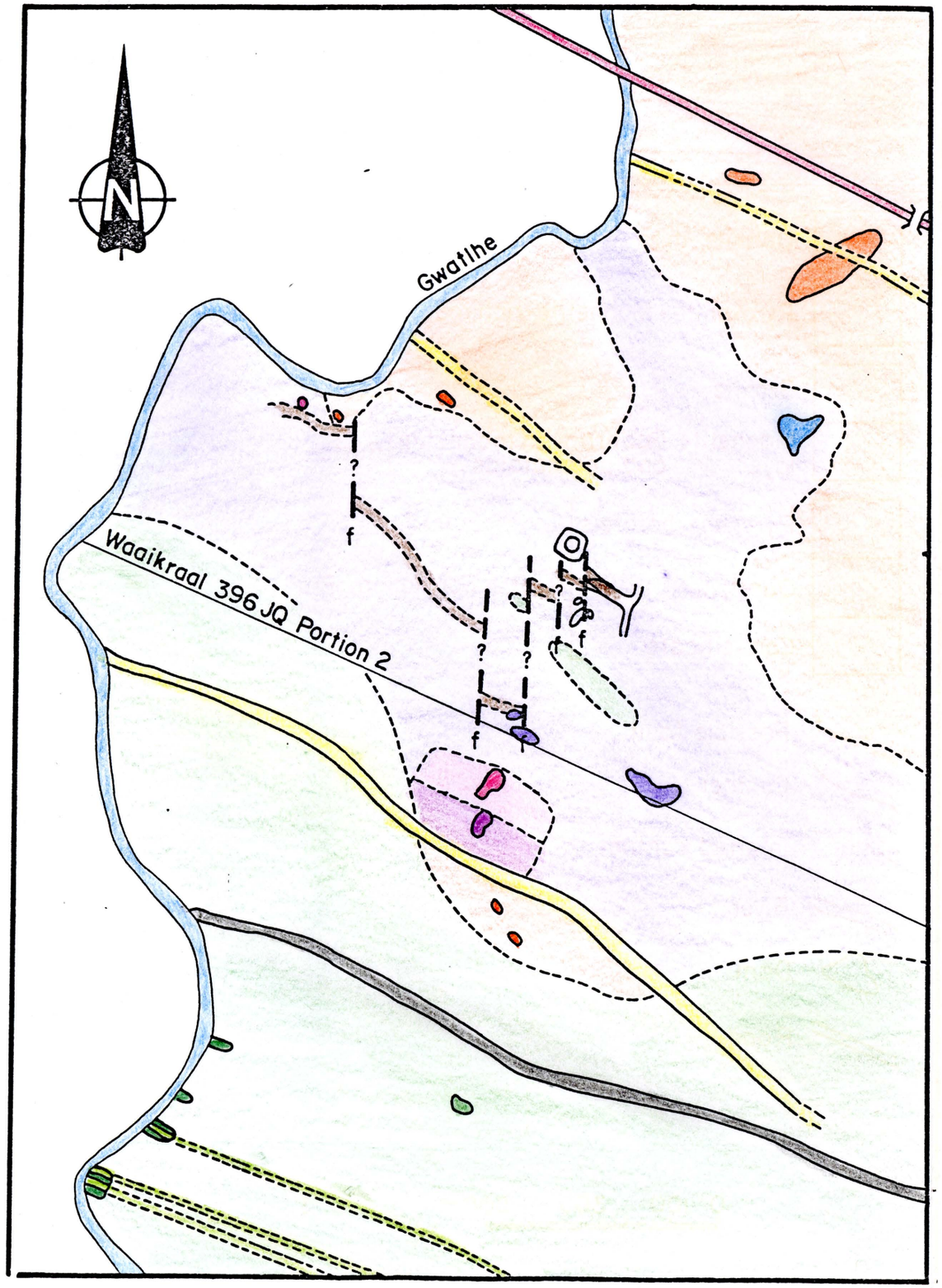

LEGEND

- Dolerite dyke
- Pyroxenite - Magnetite-rich rock 'sill'
- Granite — Lebowa Granite Suite
- Magnetite layer // — Gabbro with magnetite and pegmatoids -// — Rustenburg Layered Suite

(Lebowa Granite Suite + Rustenburg Layered Suite) → BUSHVELD COMPLEX

- Pyroxene hornfels
- Quartzite
- Calc-silicate

(Rayton Formation, Pretoria Group) → TRANSVAAL SEQUENCE

- ?f Possible fault
- Contact
- Inferred contact
- River
- Dam
- Road
- Gate
- Farm boundary
- Slimes dump
- Rock dump
- Quarry

0 100 300 500m

SCALE 1 : 12 000

Figure 2.2 Geological map of the area surrounding Waaikraal Gold Mine.

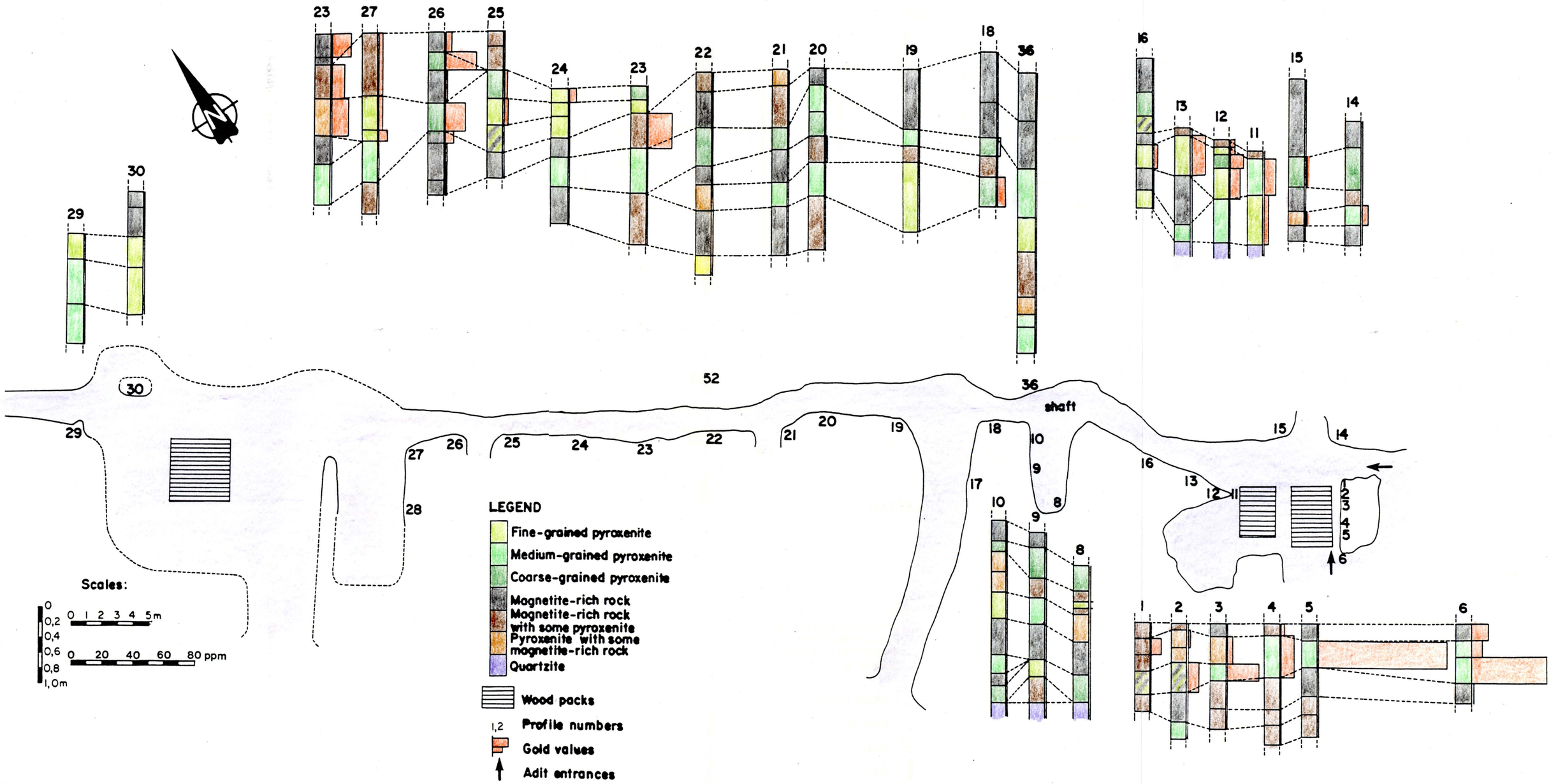

Figure 2.3 Mine plan indicating positions of sample profiles and gold distribution.

3. PETROGRAPHY

3.1 Petrography of the Ore Body

3.1.1 Modal Composition of the Pyroxenite and Magnetite-Rich Rock

The mineral content in the pyroxenite and magnetite-rich rock was established by pointcounting sixteen thin sections with a Swift Point Counter (Appendix 1). Between 790 and 1031 points were counted per section. Plagioclase is frequently altered and is indicated as such in the Appendix.

The two rock types, pyroxenite and magnetite-rich rock, were distinguished on the basis of their macroscopic appearance in the field and although their respective modal compositions can vary widely (Table 3.1), contacts between the two rock types are always sharp and readily discernable in the mine.

Table 3.1 Summary of the abundancy of minerals in pyroxenite and magnetite-rich rock.

Mineral	Volume %	
	Pyroxenite	Magnetite-rich rock
Clinopyroxene	50 - 90	10 - 60
Plagioclase	0 - 25	3 - 17
Orthoclase	1 - 7	-
Quartz	1 - 20	-
Hornblende	0 - 16	-
Olivine	-	0 - 28
Mica / Chlorite	0 - 2	0 - 5
Opaque	0 - 12	30 - 53
Accessory Minerals	0 - 2	0 - 1

3.1.2 Pyroxenite

Clinopyroxene is the major constituent of the pyroxenite at Waaikraal. It is anhedral and varies in grain size from less than one millimetre to more than a centimetre (Fig. 3.1) and is slightly pleochroic in shades of light green. Amphibole occurs as inclusions in the clinopyroxene and often surrounds ore minerals (Figures 3.1 and 3.2). The amphibole is strongly pleochroic in shades of green. No orthopyroxene was observed.

Plagioclase was only found interstitially. In many cases the plagioclase has undergone saussuritisation, possibly as a result of weathering and hydrothermal activities. Albite twinning is very common (Fig. 3.1).

The pyroxenite contains up to 18 volume per cent quartz (Table 3.1), which occurs mostly interstitially together with feldspar. Graphic intergrowth between quartz and feldspar is very common in this rock (Fig. 3.3). Individual quartz grains are often veined by fibrous biotite and chlorite (Fig. 3.4), which are restricted to the quartz grains and are probably caused by hydrothermal alteration (Moorhouse, 1959).

Magnetite in the pyroxenite occurs as discrete subhedral to anhedral grains of up to five millimetres in length. The grains contain abundant exsolution lamellae of ilmenite, but frequently also spinel exsolutions (Fig. 3.5). The magnetite is occasionally replaced by amphibole, sericite and other unidentified sheetsilicates with relic exsolution lamellae of ilmenite (Figures 3.6 and 3.7).

Accessory minerals are calcite (Fig.3.8) and apatite, which is usually present as large euhedral crystals imbedded in quartz and plagioclase (Fig. 3.9). The calcite usually occurs as vein fillings, in which case it is evidently of secondary origin. In sample WK 36.8, however, abundant calcite was found to occur as large grains intergrown with clinopyroxene and prehnite (Fig. 3.10). In this case, prehnite together with calcite probably is a hydrothermal alteration product of plagioclase.

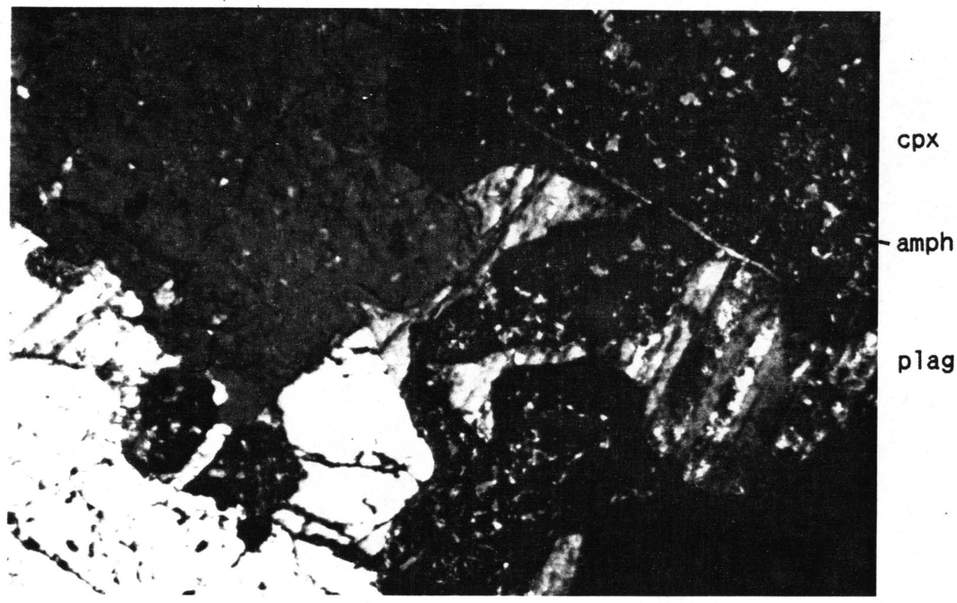

Figure 3.1 Clinopyroxene (cpx) with amphibole exsolutions (amph) and interstitial plagioclase (plag) in pyroxenite (WK 6.3).
Photomicrograph: transmitted light (TL), cross-polarized light (CPL). ⟷ 300 μm

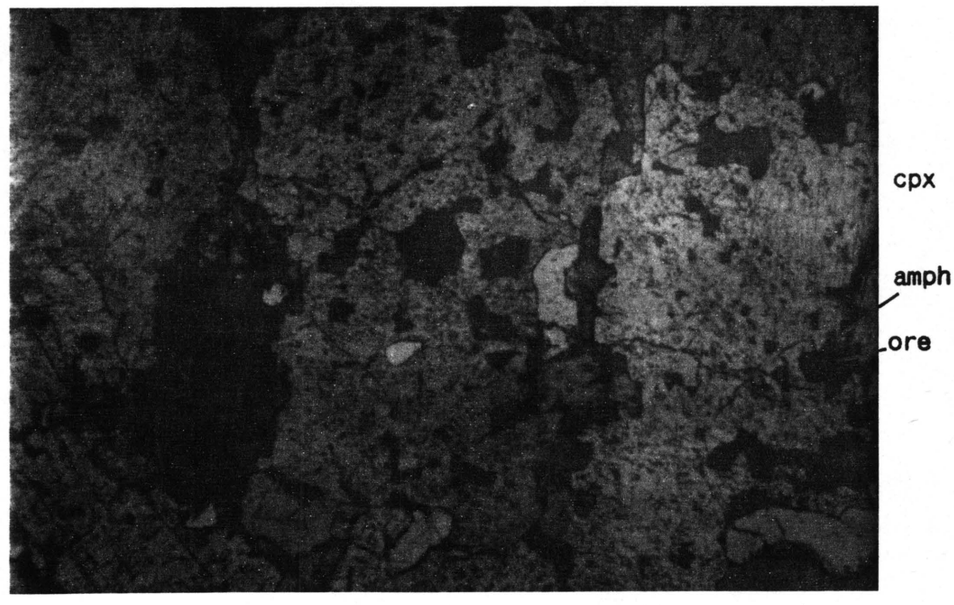

Figure 3.2 Amphibole exsolutions surrounding ore minerals in clinopyroxene. Pyroxenite WK 20.5.
Photomicrograph: TL, plane polarized light (PPL). ⟷ 300 μm

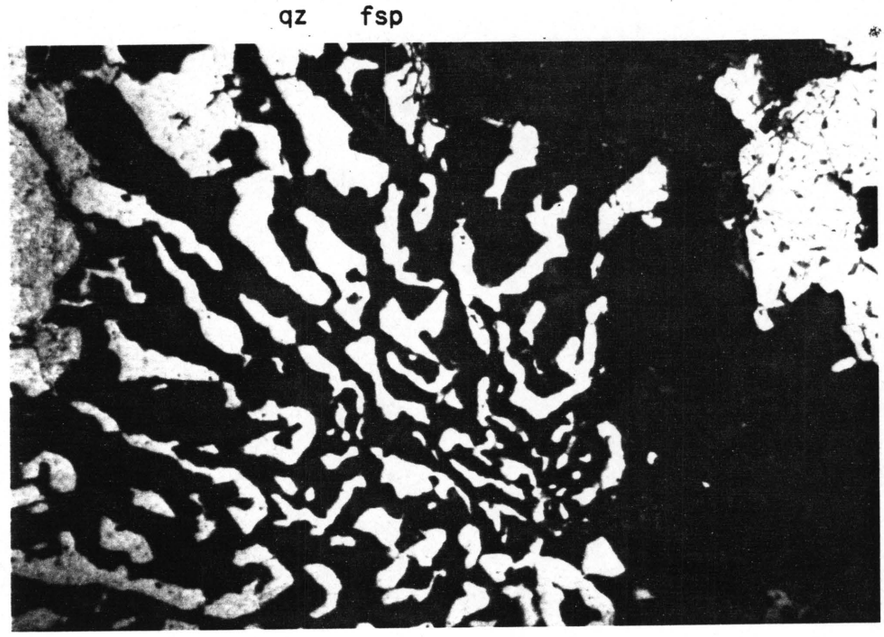

Figure 3.3 Graphic intergrowth between quartz (qz) and feldspar (fsp) in pyroxenite (WK 14.4). Photomicrograph: TL, CPL. ⟵⟶ 300 µm

Figure 3.4 Quartz grain veined by fibrous biotite (bte) and chlorite (chl) in pyroxenite (WK 14.4). Photomicrograph: TL, CPL. ⟵⟶ 300 µm

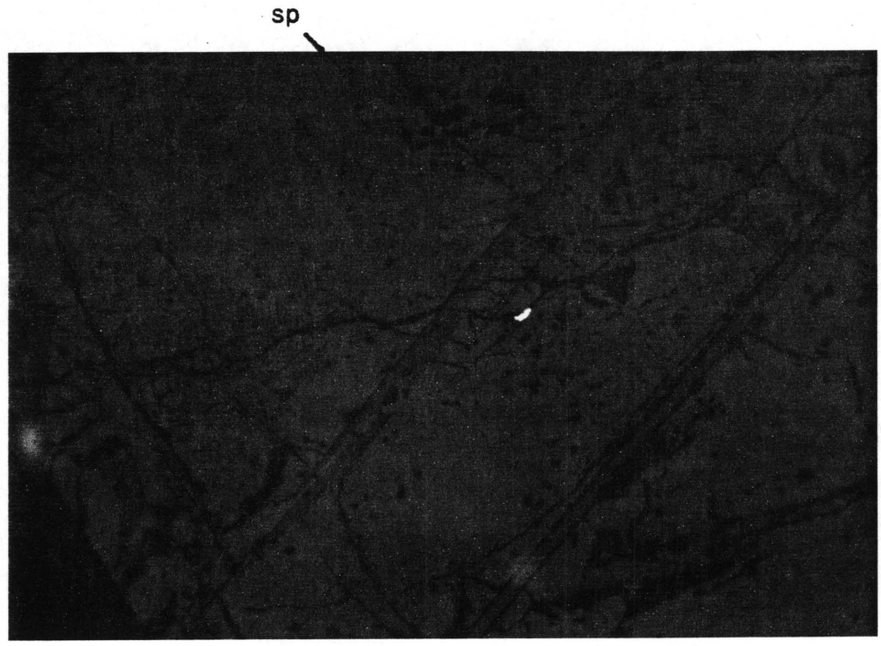

Figure 3.5 Magnetite (mt) with ilmenite (il) and spinel (sp) exsolutions in pyroxenite (WK 20.5). Photomicrograph: reflected light (RL), PPL.
100 µm

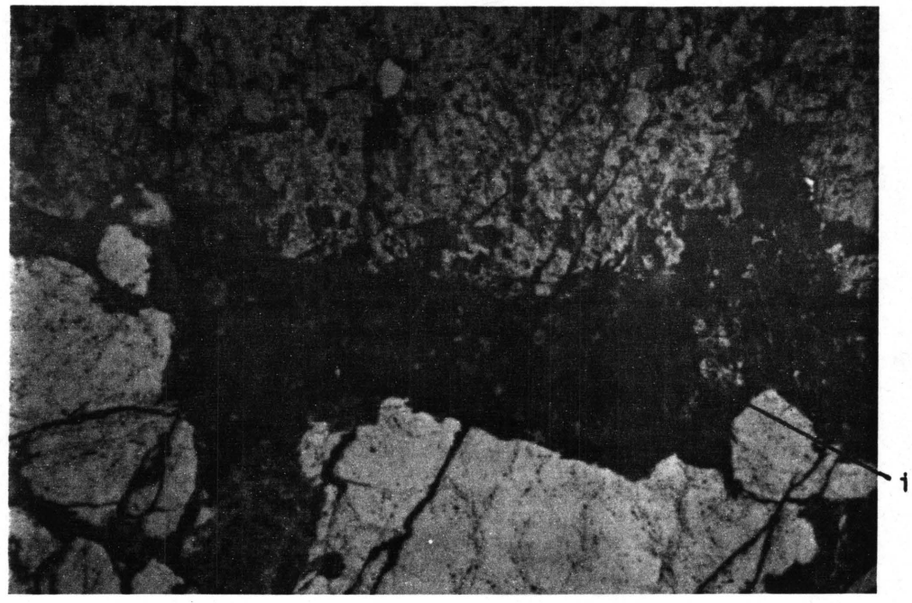

Figure 3.6 Magnetite grain replaced by amphibole, chlorite and other unidentified sheetsilicates with relic exsolution lamellae of ilmenite in pyroxenite (WK 12.3). Photomicrograph: TL, PPL.
300 µm

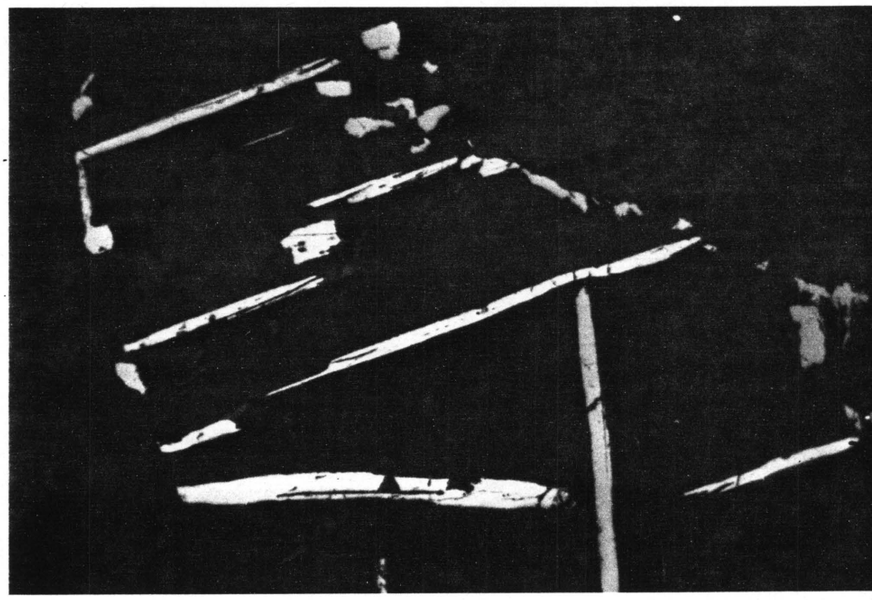

Figure 3.7 Magnetite grain replaced by amphibole, chlorite and other unidentified sheetsilicates with relic exsolution lamellae of ilmenite in pyroxenite (WK 12.3).
Photomicrograph: RL, PPL.

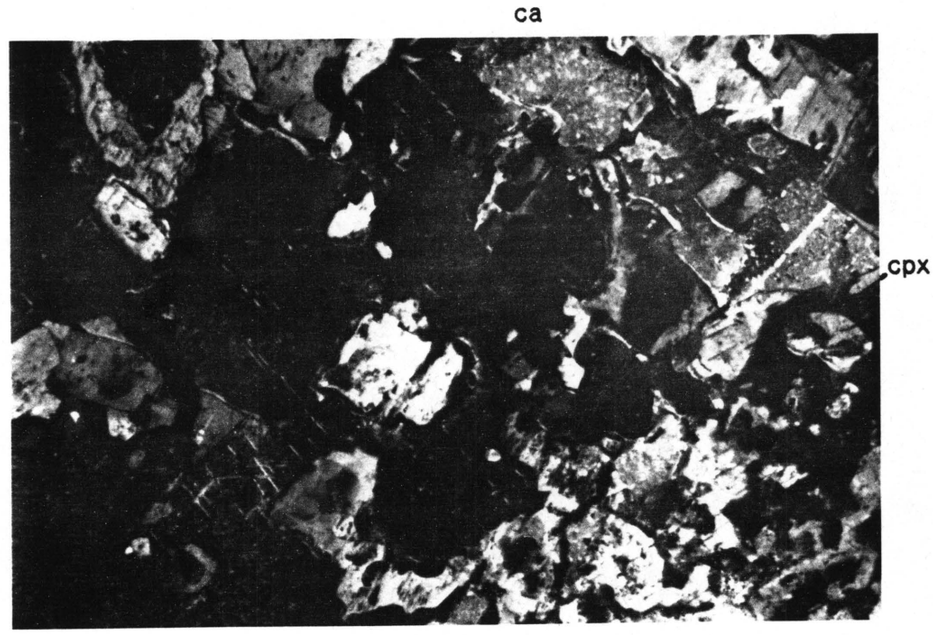

Figure 3.8 Calcite (ca) intergrown with clinopyroxene in pyroxenite (WK 36.8).
Photomicrograph: TL, CPL.

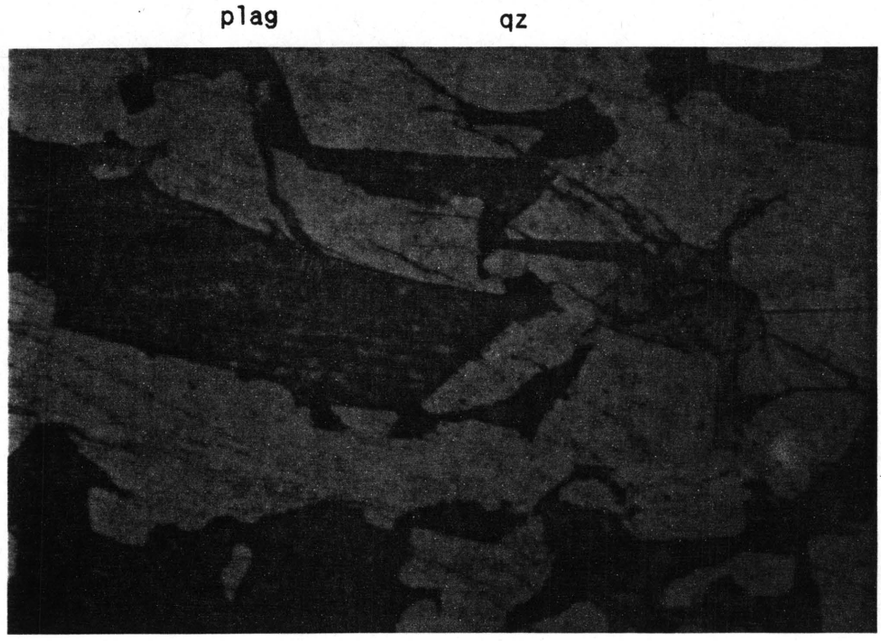

Figure 3.9 Apatite (ap) in graphic intergrowth between quartz and plagioclase in pyroxenite (WK 12.3).
Photomicrograph: TL, PPL. ⟵⟶ 300 µm

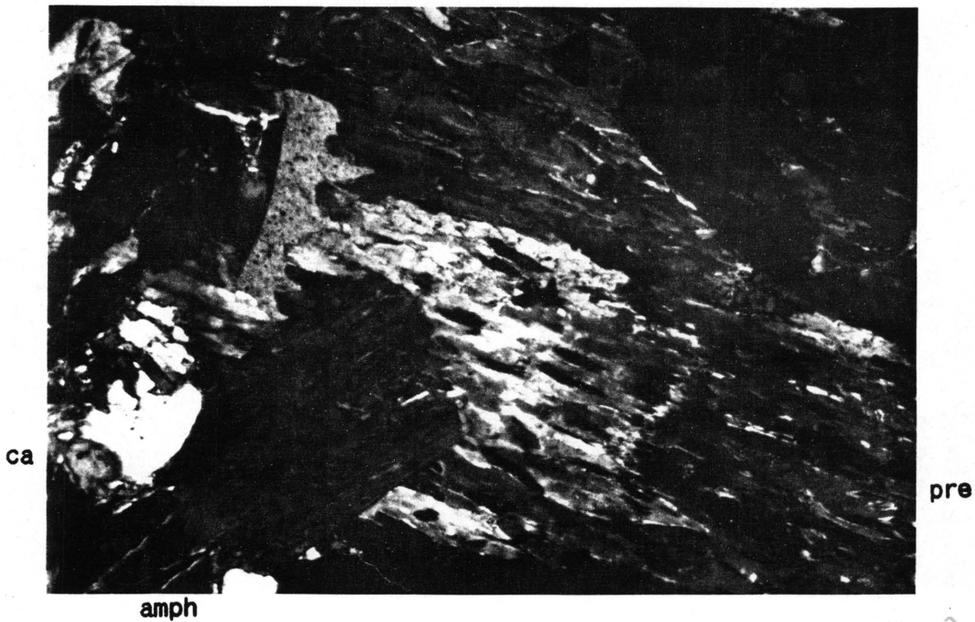

Figure 3.10 Prehnite (pre) and calcite as alteration product of plagioclase with some amphibole (amph) in pyroxenite (WK 36.6). ⟵⟶ 300 µm
Photomicrograph: TL, CPL.

3.1.3 Magnetite-Rich Rock

The clinopyroxene is more euhedral in the magnetite-rich rock than in the pyroxenite and does not contain any amphibole exsolutions. The grains are generally smaller than 2 millimetres in diameter, and frequently contain inclusions of small rounded to subhedral magnetite granules. Small clinopyroxene grains can also be found in magnetite were they are occasionally surrounded by plagioclase (Figures 3.11 and 3.12).

Larger (approximately 2 millimetres diameter) magnetite grains occur as anhedral to subhedral aggregates, which occasionally display 120° triple junctions. The magnetite of the magnetite-rich rock contains no ilmenite exsolutions, although spinel exsolutions occur throughout many of the grains (Fig. 3.13). Occasionally secondary magnetite occurs as rims surrounding several of the primary magnetite, or as veins together with chlorite and ilvaite. In polished section, the secondary magnetite is slightly darker than the primary magnetite (Fig.3.14).

Plagioclase occurs intersitially and is more altered than that in the pyroxenite, and apart from saussurite, clinozoisite was also identified as an alteration product (see Appendix 5.6 for composition) (Fig. 3.15).

Olivine was found to occur in one sample of magnetite-rich rock (WK 14.1). It occurs as anhedral grains together with clinopyroxene and magnetite (Fig. 3.16).

Ylvaite ($Ca(Fe^{2+},Mn,Mg)_2(Fe^{3+},Al)(SiO_4)_2OH$) was observed in several samples of magnetite-rich rock. This mineral is present together with primary and secondary magnetite, clinopyroxene and sometimes chlorite. It forms aggregates of subhedral prismatic crystals which are randomly orientated (Fig. 3.14). Ilvaite usually occurs as a late stage mineral in Ca-Fe-Si skarn deposits (Burt, 1971), but can also occur as a reaction product between plagioclase and fayalite-rich olivine (Tröger, 1969) and is described as the latter in the upper zone of the Bushveld Complex (Reynolds, 1985).

Thin veins often cut across grain boundaries of silicates and magnetite. They are generally filled with chlorite, but occasionally also contain some ilvaite and secondary magnetite (Fig. 3.17).

Apatite is found as an accessory mineral and occurs as small subhedral to euhedral inclusions in the clinopyroxene (Fig. 3.18).

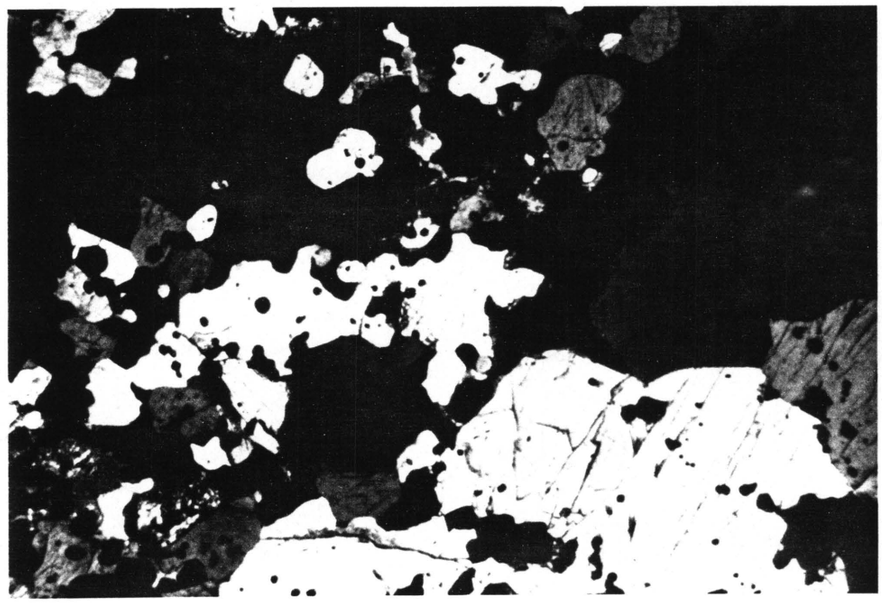

Figure 3.11 Typical texture of magnetite-rich rock (WK 12.2). Note the small rouded to subhedral inclusions of magnetite in the clinopyroxene (cpx).
Photomicrograph: TL, CPL.

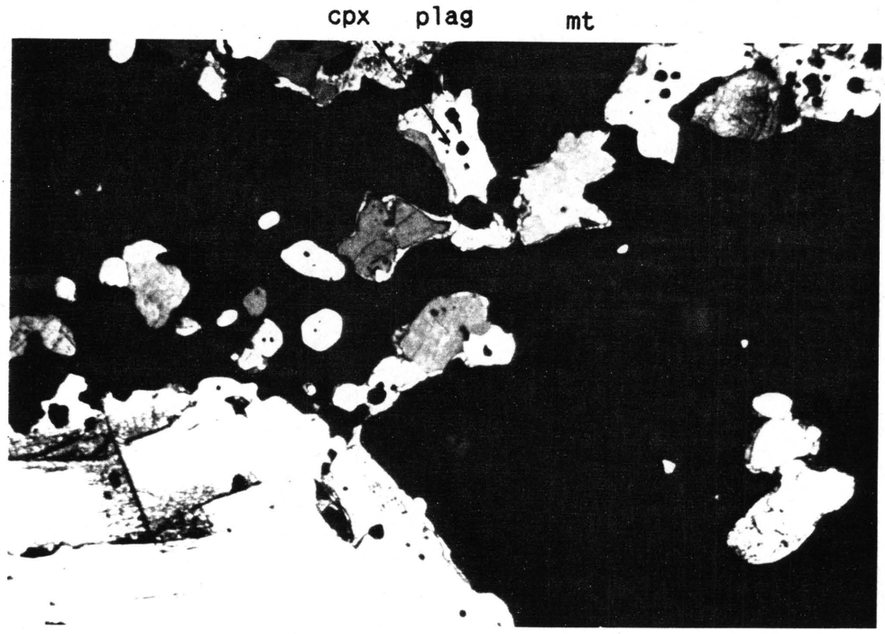

Figure 3.12 Clinopyroxene surrounded by plagioclase in magnetite grains. Magnetite-rich rock WK 28.3.
Photomicrograph: TL, CPL. ⟵⟶ 300 μm

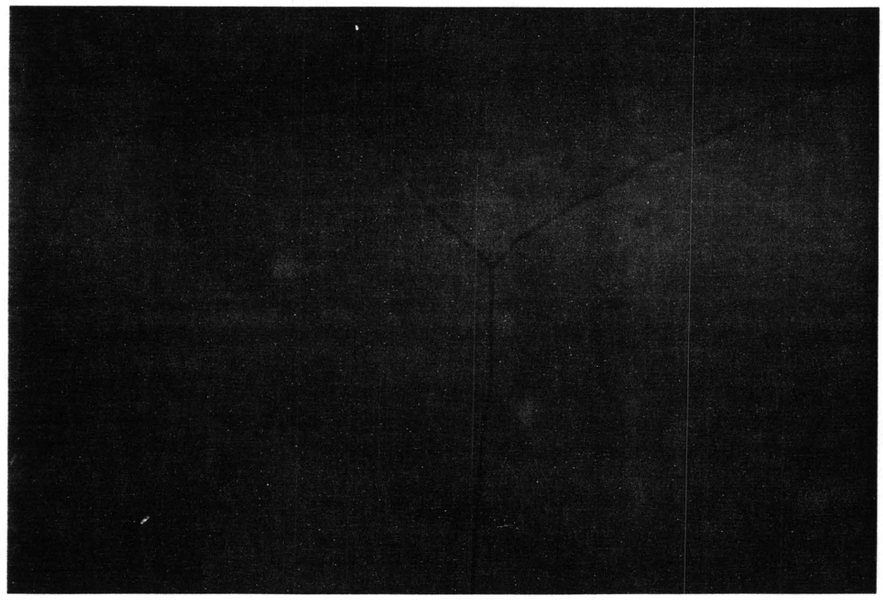

Figure 3.13 Magnetite with 120° interlocking angles and spinel exsolutions in magnetite-rich rock (WK 52.3).
Photomicrograph: RL, PPL. ⟵⟶ 100 μm

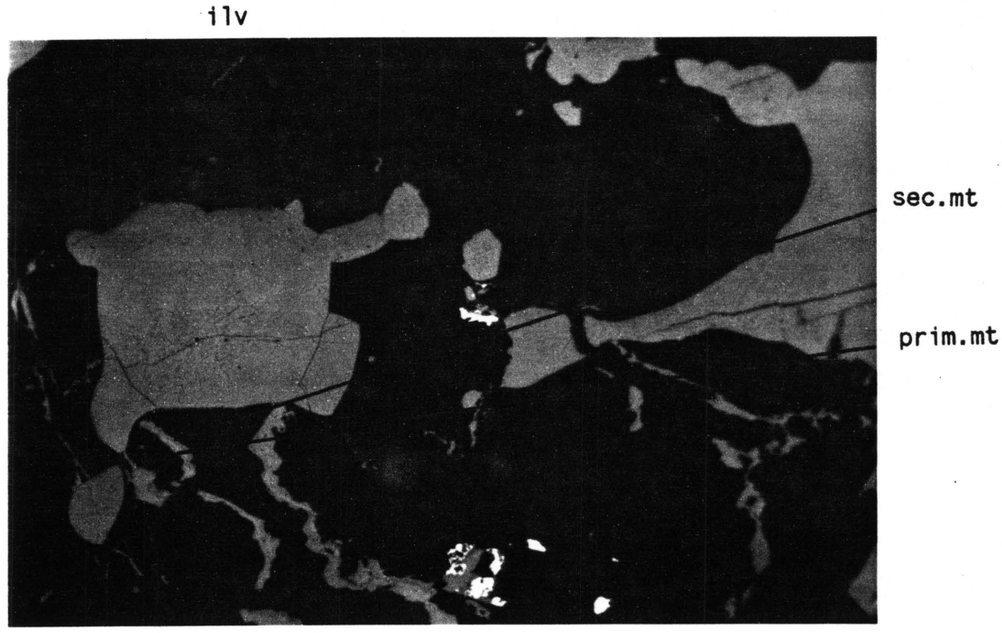

Figure 3.14 Primary and secondary magnetite with ilvaite (ilv) (dark grey to bluish grey) in magnetite-rich rock (WK 1).
Photomicrograph: RL, PPL. 100 µm

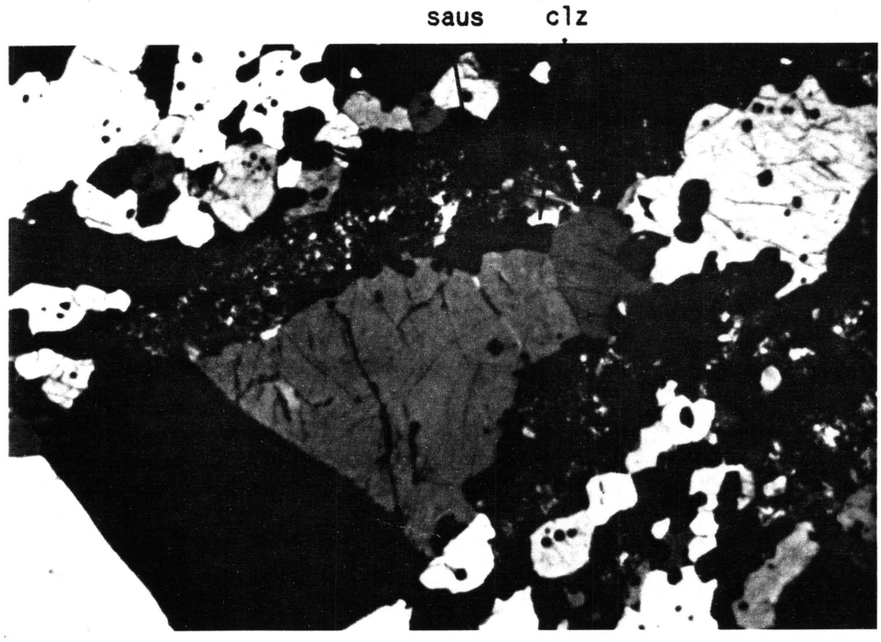

Figure 3.15 Plagioclase altered to saussurite (saus) and clinozoisite (clz) in magnetite-rich rock (WK 28.3).
Photomicrograph: TL, CPL. 300 µm

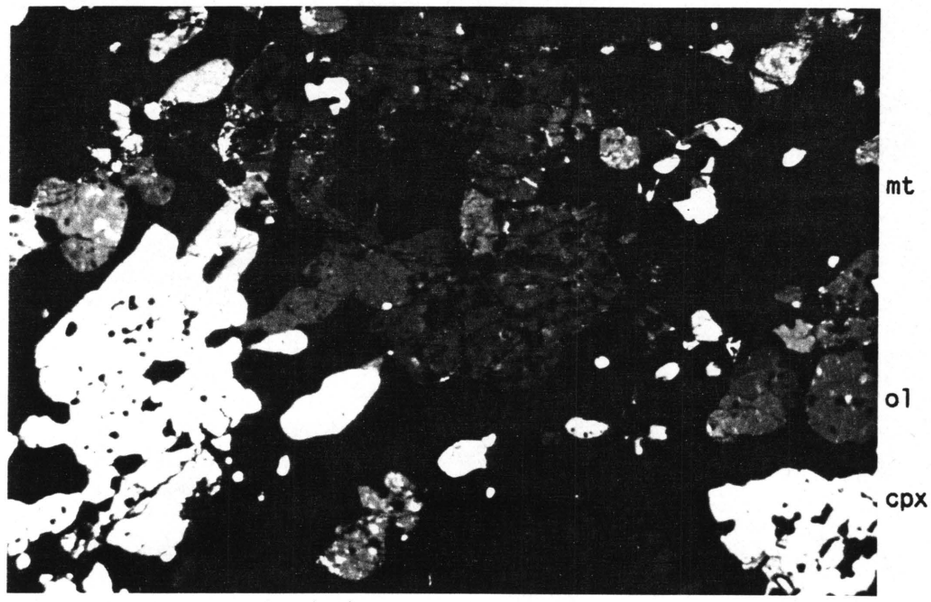

Figure 3.16 Olivine (ol) with clinopyroxene and magnetite in magnetite-rich rock (WK 14.1). Photomicrograph: TL, CPL. ⟵⟶ 300 μm

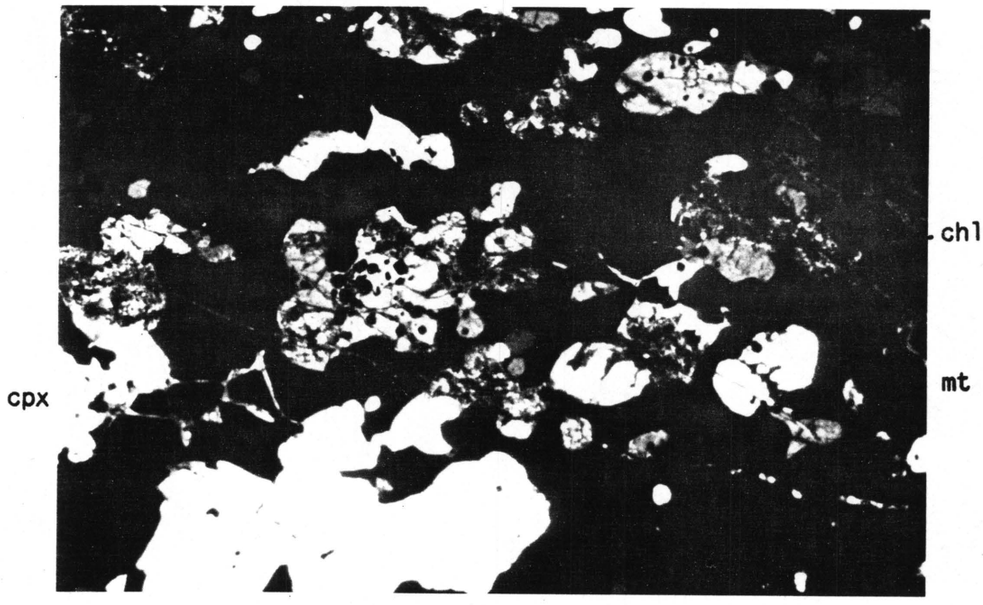

Figure 3.17 Chlorite veins in clinopyroxene and magnetite in magnetite-rich rock (WK 14.1). Photomicrograph: TL, CPL. ⟵⟶ 300 μm

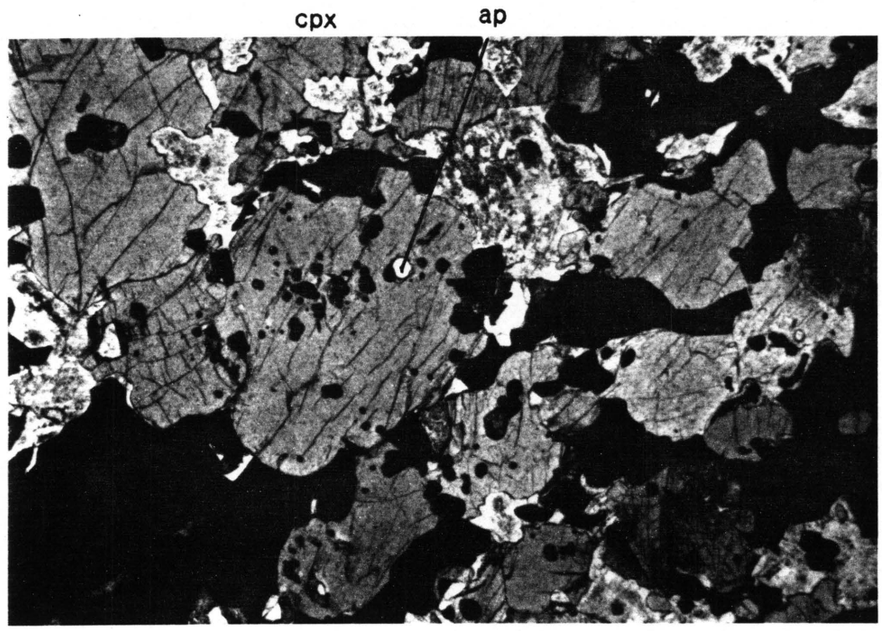

Figure 3.18 Apatite in clinopyroxene in magnetite-rich rock (WK 12.2).
Photomicrograph: TL, PPL.

3.2 Petrography of Pyroxene Hornfels, Calc-Silicate Hornfels, Magnetite Gabbro and Topmost Differentiates of the Bushveld Complex

The **pyroxene-hornfels** consists mainly of euhedral to subhedral grains of clinopyroxene, which often display 120° triple junctions and frequently contain inclusions of small plagioclase granules. The sites between the clinopyroxenes are filled with saussurite. The only accessory mineral is apatite.

Subhedral wollastonite is the major constituent of the **calc-silicate hornfels.** The interstitial sites are occupied by garnet (approximately $An_{60}Py_{40}$, determined by microprobe). Tremolite occurs in a few places.

The most abundant constituent of the nearby **magnetite gabbro** is euhedral to subhedral plagioclase. Clinopyroxene, orthopyroxene, plagioclase and magnetite occur interstitially, whereas biotite and chlorite often surround magnetite grains.

Due to the lack of exposure of the **topmost differentiates of the Bushveld Complex,** rocks from the top of the Bierkraal-1 borehole (location indicated in Figure 2.1) were used for comparison. Reynolds (1985) briefly described the mineralogy of the rocks from this borehole. The rocks under consideration here are generally medium grained (1-5 millimetres in diameter) ferrodiorites and ferrogabbros. They contain plagioclase and abundant Fe-rich olivine, which commonly alters to fine grained aggregates of chlorite and/or iddingsite. Ilvaite is present as a minor alteration product of the olivine. Very dark brownish-green amphibole, quartz and alkali feldspar are common. Apatite occurs as small, isolated subhedral crystals located interstitially between silicate minerals. Opaque oxide minerals (magnetite and ilmenite) are minor constituents.

4. ANALYTICAL PROCEDURES

4.1 Whole Rock Analyses

4.1.1 Sampling

172 Samples of between 4 and 8 kilograms, depending on coarseness of the rocks, were taken from 31 vertical sections at regularly spaced intervals in the accessible parts of the old mine workings. This yielded a good coverage of that part of the sill exposed in the mine. Footwall quartzite was sampled wherever it was accessible, but hanging wall pyroxene hornfels was not exposed in the mine. Sample localities are indicated in Figure 2.3.

Sampling was done by hammer and chisel and care was taken that samples did not extend over lithological contacts. Each sample was split; one half was used for gold fire assays and the other for thin sectioning and geochemical analysis.

Additional samples of the footwall quartzite were taken outside the mine along strike at intervals of about 15 metres (QZ 1-6). One sample of pyroxene hornfels (HF1) was taken at a face outside the mine above the easternmost entrance and four samples of calc-silicate hornfels were taken to the east of the mine.

Three samples of magnetite gabbro were collected south of the magnetite layer.

4.1.2 Sample Preparation

In order to eliminate samples with large amounts of weathered surfaces only 148 samples were crushed in two stages in a jaw crusher. The first stage reduced the samples to a grain size of 3-4 centimetres in diameter. Fragments with signs of weathering were removed, prior to further crushing to a grain size of approximately 5 millimeters diameter. Representative portions were then powdered to -200 mesh using a mill with a chrome steel container. Although the extent of chrome

contamination of the samples is not known, chrome values are indicated in the analytical tables and figures, but no conclusions are drawn from them. The presence of important cobalt-bearing mineral assemblages at Waaikraal prevented the use of tungsten carbide bowls, which are known to contain significant quantities of cobalt.

4.1.3 Analytical Procedures

Geochemical analyses were performed on an ARL 8420 XRF at the University of Pretoria. Operating conditions are presented in Appendix 2.1.

Major elements Si, Ti, Al, Fe, Mn, Mg, Ca, K, P, Cr and Ni were analysed on glass discs which were prepared according to the method of Norrish an Hutton (1969). 1.0000 g of Spectroflux, 0.1866 g of sample and 0.0134 g of $NaNO_3$ were used for the preparation of the discs.

The H_2O^- content was determined by weighing before and after heating to 110°C for a minimum of 4 hours. Loss (gain) on ignition was determined by weighing before and after heating the sample to 950°C for a minimum of 8 hours.

For Na and the trace elements Ba, Co, Cr, Cu, Ga, Mo, Nb, Ni, Pb, Rb, Sc, Sr, Th, U, V, Y, Zn and Zr approximately 15 grams of each sample powder was mixed with 12 drops of a binder (2% Moviol) and pelletized in aluminium cups.
Gold was analysed by fire assay at Rustenburg Platinum Mines.

Thin section investigation of the analysed rocks revealed the presence of bismuth bearing minerals. Seeing that the Bi_{L_β}-line interferes with the Th_{L_α}-line, Th values were discarded and are not shown in analytical tables (Appendix 3.2).

4.1.4 Reproducibility

Estimates for the reproducibility of analyses (Appendix 2.1.3) was obtained by calculating the standard deviation from duplicate analyses with the formula given by Kaiser and Specker (1956). Reproducibility was calculated for trace elements of whole rock analyses using two independantly prepared pellets for each of 10 samples.

4.1.5 Correction of Analyses

After matrix corrections (Norrish & Hutton, 1969) and after provision was made for loss (gain for most samples) of ignition and H_2O^-, all but 26 analyses yielded totals of more than 101.5 weight per cent.

In order to determine the reason for this deficiency in the analytical data, Pearson correlation coefficients were calculated between the total and the major elements analysed. The highest correlation was found to be between the total and Fe_2O_3 ($r = 0.64$) and also between the total and loss on ignition ($r = 0.53$). As these two parameters are closely linked it is presumed that the high totals of the analyses are connected to the high iron content of the samples. A plot of Fe_2O_3 against the total is presented in Fig. 4.1.

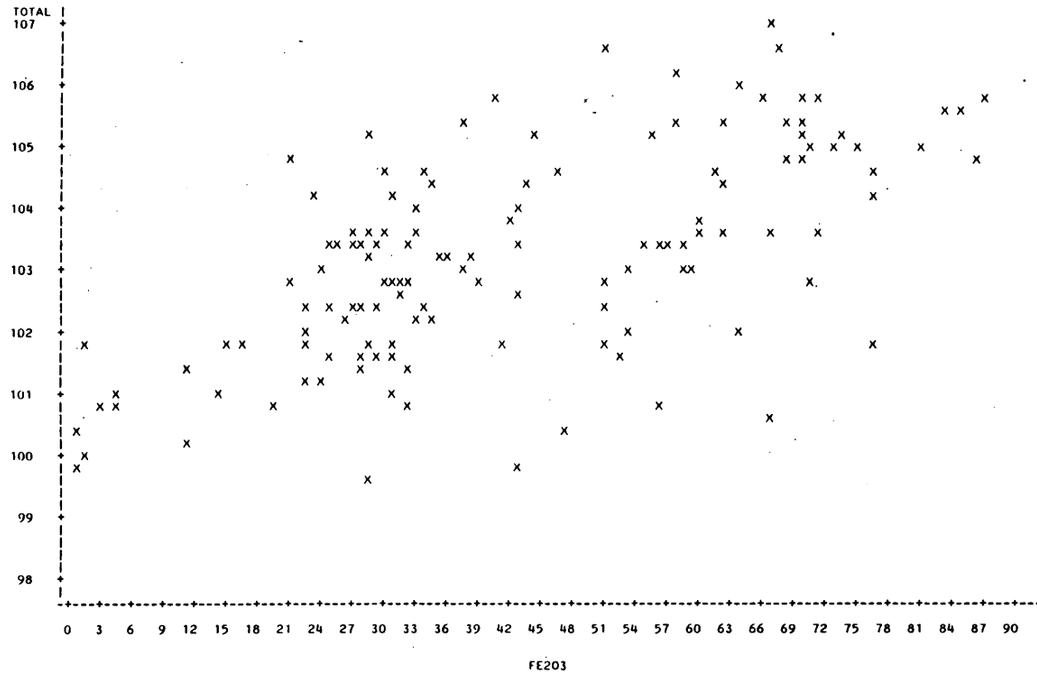

Figure 4.1 Plot of Fe_2O_3 content versus Total (in weight per cent).

The following factors could be the cause of these high totals:

1. The material was possibly not ashed long enough at 950°C.
2. The magnetite, which contains most of the Fe^{2+} to be oxidised at 950°C, was possibly not fully oxidised and could have oxidised further by the flux during melting. Consequently the mass of the sample analysed could have changed.
3. The calibration for Fe may not be correct.

The above three possibilities were evaluated in two different ways:

1. 5 grams of three samples with a high iron-content were ashed for 56 hours at 950°C and weighted at regular intervals, after heating at 110°C for 4 hours. The average gain in weight after heating to 950°C for 8 hours was 0.1179 grams. After a further 8 hours, the samples gained an average of another 0.0004 grams and after a further 16 hours there was another gain of 0.0055 grams. The amounts gained on further heating for 24 hours are negligable, and only amount to 0.12 per cent of the initial sample weight.

   Examination of polished sections of three ashed samples under reflected light showed that the core of the magnetite grains were often not fully oxidised (Fig. 4.2). Consequently, there is a distinct possibility that the magnetite only oxidised fully in the presence of the flux during preparation of the glass discs.

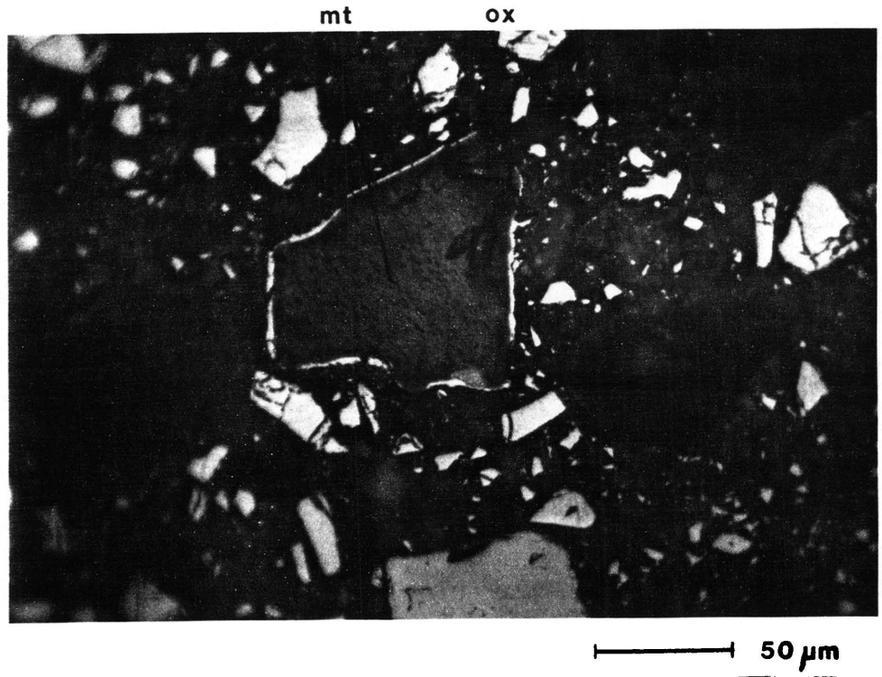

Figure 4.2 Polished section of ashed sample. Remnant of magnetite (mt) with oxidised rim (ox). Magnetite-rich rock WK 24.4.
Photomicrograph: reflected light, plane polarized light.

2. Four samples with varying iron contents were analysed wet chemically for Fe_2O_3 at ISCOR to determine possible inaccuracies of the calibration. Significant differences in the Fe_2O_3 content between analyses done at ISCOR and Pretoria University were detected (Table 4.1). The Fe_2O_3 contents of both analyses when plotted on a binary variation diagram (Fig. 4.3), yields a straight line relationship below the 1:1 line. The equation for the regression line is

$$ISCOR = 0.9347 * UP + 1.3375$$

and has a correlation coefficient of r = 0.9999.

Table 4.1 Fe_2O_3 contents of samples analysed at ISCOR and UP and ratios between them.

Sample	UP	ISCOR	Iscor/UP
WK 28.5	55.40	53.00	1.045
WK 3.1	68.34	65.40	1.045
WK 28.1	74.83	71.30	1.050
WK 14.1	87.25	82.80	1.054

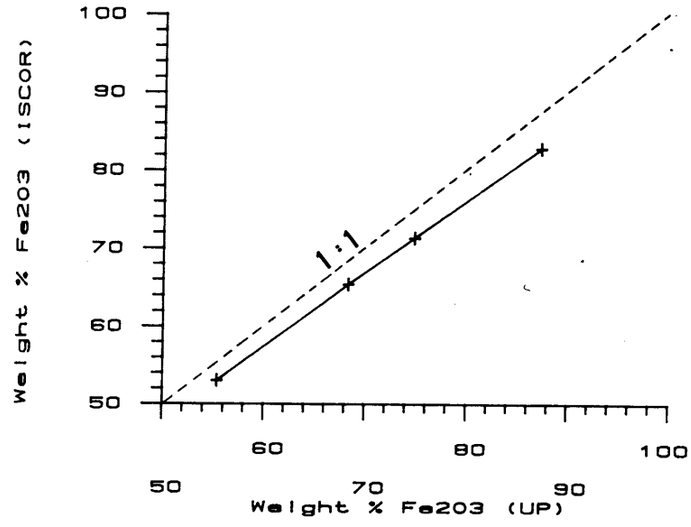

Figure 4.3 Plot of Fe_2O_3 content of samples analysed at the University of Pretoria versus ISCOR (in weight per cent).

Seeing that only 26 analyses have totals between 98.5 and 101.5 weight percent, it was decided to correct all the analyses for the Fe_2O_3 content as follows:

i) Analyses with an Fe_2O_3 content above 50 weight per cent were corrected using the formula of the regression line:

$$Fe_2O_3(corr) = 0.9347 * Fe_2O_3 + 1.3375$$

ii) Analyses with an Fe_2O_3 content below 50 weight per cent were corrected by dividing the Fe_2O_3 content obtained at UP by 1.045, which is the ratio between the two analyses for samples with the lowest iron content (Table 4.1).

These above corrections resulted in 82 samples with a total of between 98.5 and 101.5 weight per cent, which are presented in Appendix 3.1. 56 samples had a total above 101.5 and 6 samples below 98.5 weight per cent and are not represented in the appendix.

4.2 Analyses of Mineral Compositions

Mineral compositions of silicates, magnetite, ilmenite and other ore minerals were obtained by microprobe analyses on a JEOL 733 Superprobe with 4 spectrometers at the University of Pretoria. Operating conditions for the different minerals are summarised in Appendix 2.2.1, whilst analytical results are presented in Appendix 5.

Only analyses with totals ranging between 98.5 and 101.5 weight per cent were accepted for clinopyroxene, feldspars, magnetite and ore minerals. Due to the presence of water, OH^- and other light elements such as F and Cl which cannot be readily analysed with the electron microprobe, totals for the amphibole analyses usually do not add up to 100 per cent.

Total iron content is referred to as FeO, exept in the case of magnetite analyses, for which Fe_2O_3 was calculated, assuming stoichio-

metry.

Estimates for the reproducibility were calculated according to Kaiser and Specker (1956) (Appendix 2.2.3). Duplicate analyses of identical spots on minerals could only be obtained for clinopyroxene, magnetite, ilmenite and ore minerals. The sodium in albite-rich plagioclase evaporates when exposed to the electron-beam for too long. Limits of detection (Appendix 2.2.2) for microprobe analyses were determined at the 3 sigma level.

5. WHOLE ROCK GEOCHEMISTRY

5.1 Whole Rock Compositions of Pyroxenite and Magnetite-Rich Rock

Arithmetic means and standard deviations of each element analysed were calculated for the two different rock types. Although 70 samples of pyroxenite and 54 samples of magnetite-rich rock were analysed, the correction procedure for Fe_2O_3 outlined in chapter 4.1.5 resulted in 37 and 24 analyses with acceptable Fe_2O_3 values respectively. Nevertheless, all analyses were considered in the calculations for the remaining elements. Where concentrations of elements are below the lower limit of detection (l.l.d.) they were not included in the calculations. Consequently, the mean values and the standard deviations shown in Tables 5.1 and 5.2 are not always representative of the entire population, because they were calculated only from that part of the population with element values above the lower limit of detection (see N in Tables 5.1 and 5.2).

Table 5.1 Average whole rock compositions of pyroxenite (a) and magnetite-rich rock (b) (in weight per cent) (N = number of values > l.l.d., except for Fe_2O_3 which is explained in chapter 5.1).

a: Pyroxenite

Element	Mean	s	min	max	N
SiO_2	46.51	6.53	29.23	62.72	70
TiO_2	0.62	0.34	0.11	1.69	70
Al_2O_3	4.66	1.45	1.67	9.74	70
Fe_2O_3	31.81	9.21	21.38	54.32	37
MnO	0.58	0.11	0.31	1.01	70
MgO	1.57	0.85	0.22	4.07	70
CaO	15.28	2.11	7.89	21.20	70
Na_2O	0.90	0.35	< l.l.d.	2.14	69
K_2O	0.57	0.23	0.12	1.12	70
P_2O_5	0.08	0.06	< l.l.d.	0.37	57
Cr_2O_3	0.08	0.01	< l.l.d.	0.13	66
NiO	< l.l.d.	< l.l.d.	< l.l.d.	< l.l.d.	0

b: Magnetite-rich rock

Element	Mean	s	min	max	N
SiO_2	26.12	7.15	13.43	46.49	54
TiO_2	0.62	0.50	0.20	2.82	54
Al_2O_3	4.77	1.19	2.60	8.48	54
Fe_2O_3	60.87	14.21	31.38	82.89	24
MnO	0.56	0.19	0.38	1.24	54
MgO	0.49	0.33	0.10	1.67	54
CaO	10.07	3.67	1.91	21.29	54
Na_2O	0.33	0.27	< l.l.d.	1.21	30
K_2O	0.19	0.12	< l.l.d.	0.57	53
P_2O_5	0.04	0.02	< l.l.d.	0.09	24
Cr_2O_3	0.09	0.02	0.05	0.13	54
NiO	< l.l.d.	< l.l.d.	< l.l.d.	< l.l.d.	0

Table 5.2 Average trace element content of pyroxenite (a) and magnetite-rich rock (b) (in ppm). (N = number of values > l.l.d.).

a: Pyroxenite

Element	Mean	s	Min	Max	N
Zn	161	43	17	247	70
Cu*	22	14	< l.l.d.	109	67
Ni**	25	22	4	138	68
Co	234	151	4	667	70
Ga	11	4	< l.l.d.	24	62
Mo	5	2	< l.l.d.	11	18
Nb***	7	3	< l.l.d.	16	59
Zr	134	48	14	287	70
Y	28	17	11	112	70
Sr	60	28	9	158	70
Rb	24	13	< l.l.d.	103	66
U****	11	5	< l.l.d.	24	32
Pb	12	5	< l.l.d.	27	52
Cr	57	22	< l.l.d.	120	69
V	36	17	8	83	70
Ba	300	108	47	617	70
Sc	29	17	< l.l.d.	63	34
Au	4	12	0	83	70

* Extreme value of 1592 omitted in calculation of mean.
** Extreme values of 209 and 380 omitted in calculation of mean.
*** Extreme values of 90, 135, 152, 181 and 211 omitted in calculation of mean.
**** Extreme value of 103 omitted in calculation of mean.

b: Magnetite-rich rock

Element	Mean	s	min	max	N
Zn	32	25	16	205	54
Cu	21	20	6	152	54
Ni*	216	169	< l.l.d.	745	43
Co**	9	4	< l.l.d.	23	46
Ga	8	2	< l.l.d.	14	47
Mo	9	3	< l.l.d.	19	52
Nb	171	66	9	446	54
Zr	16	16	< l.l.d.	123	52
Y	56	36	3	173	54
Sr	13	8	< l.l.d.	44	48
Rb	6	5	< l.l.d.	18	16
U	22	17	< l.l.d.	58	21
Pb	-	-	< l.l.d.	16	1
Cr	91	32	21	209	54
V	57	27	< l.l.d.	120	49
Ba	161	108	41	627	54
Sc	< l.l.d.	< l.l.d.	<l.l.d.	< l.l.d.	0
Au	1	5	0	30	54

* Extreme value of 4853 omitted in calculation of mean.
** Extreme value of 259 omitted in calculation of mean.

5.2 Tukey-Test

The modified Tukey-test (Neave, 1979) was used to establish whether there is a significant geochemical difference between the pyroxenite and the magnetite-rich rock. The test compares the positions of the different populations (content of each element in pyroxenite and the magnetite-rich rock) and is based on the zero-hypothesis (H_o) that a difference exsists between the two rock types.

The critical values for the acceptance of H_o at a certain significance level (= error probability) for the evaluation of a difference in Fe_2O_3 had to be corrected because the ratio between the numbers of samples was too large.

The following are the critical values for the two-sided test and their corresponding error-probabilities (in parentheses).

for Fe_2O_3:	11	(5%)	14	(1%)	17	(0.1%)
all other elements:	10	(5%)	13	(1%)	16	(0.1%)

The results of the Tukey-test are indicated in Table 5.3 below:

Table 5.3 Results of Tukey-test performed to detect differences between pyroxenite and magnetite-rich rock

Element	Test Statistics	Error Probability*
SiO_2	85	<< 0.1 %
TiO_2	5	> 5 %
Fe_2O_3	47	<< 0.1 %
MnO	9	> 5 %
MgO	42	<< 0.1 %
CaO	23	< 0.1 %
Na_2O	44	<< 0.1 %
Zn	66	<< 0.1 %
Cu	3	> 5 %
Co	70	<< 0.1 %
Nb	74	<< 0.1 %
Zr	93	<< 0.1 %
Sr	83	<< 0.1 %
Cr	31	< 0.1 %
Ba	14	< 0.1 %
Au	4	> 5 %

* for H_o that there is a difference between the two rock types.

No evaluation of a difference can be made for P_2O_5, Sc, Pb, U, Rb, Mo and Ga because the lowest values for both populations lie below the limit of detection and it is therefore not possible to work out the test statistics. For Al_2O_3, V, Y and Ni the test can also not be applied, because here the highest and the lowest values observed come from the same rock type, even though one extreme value may be omitted in the modified Tukey-test.

The test does, however, indicate that significant differences exsist for most of the other elements. Only TiO_2, MnO, Cu and Au show error-probabilities higher than 5 per cent, which implies that the two rock types can not be distinguished on the basis of these elements.

The significant differences in the SiO_2, Fe_2O_3, MgO and CaO contents can readily be explained by the difference in the mineralogy of the two rock types. Si, Mg, Ca and some Fe are concentrated in clinopyroxene, quartz, plagioclase and amphibole, whereas the bulk of the Fe is concentrated in magnetite, which is much more abundant in the magnetite-rich rock.

5.3 Correlations between Different Elements analysed in Waaikraal Rocks

Element concentrations obtained for the pyroxenite and the magnetite-rich rock were used in Spearman correlation matrices for each rock type seperately (Appendix 4). Values below the lower limit of detection were omitted in the calculations.

In the magnetite-rich rock, very strong positive correlations ($r = 0.802$ to 0.866) between SiO_2, CaO and Al_2O_3 and very strong negative correlations ($r = -0.836$ to -0.976) between these elements and Fe_2O_3 result. MgO and K_2O show somewhat less pronounced positive correlations ($r = 0.441$ to 0.691) with SiO_2, CaO and Al_2O_3, and negative correlations ($r = -0.542$ to -0.715) with Fe_2O_3. SiO_2, CaO, Al_2O_3, MgO and K_2O are thought to reflect the silicate component (clinopyroxene, plagioclase, orthoclase and quartz) of the rock, whereas

Fe_2O_3 reflects the magnetite component.

A relatively strong negative correlation between TiO_2 and Fe_2O_3 (r = -0.668) indicates that TiO_2 is concentrated in silicates (r = 0.360 between TiO_2 and SiO_2) rather than in the magnetite, which is substantiated by the absence of ilmenite exsolutions in the magnetite.

The positive correlation between Al_2O_3 and Sr, Y, Ba, Zr and Nb (r = 0.370 to 0.883) indicates that these elements could have been adsorbed onto sheetsilicates or the feldspars, which is also supported by the positive correlation between Sr, Y, Zr, Ba and K_2O. A principal component analysis groups K_2O and Al_2O_3 together with Nb, Zr, Y, Ba and Sr in one factor and K_2O, Ba and Sr without Nb, Zr and Y in another factor. These inter-element relations indicate that Nb, Zr, Y, Ba and Sr were preferentially concentrated in sheetsilicates like clay minerals and mica, whereas Ba and Sr were also concentrated in orthoclase. Adsorbtion of Nb, Zr, Y, Ba and Sr onto clay minerals is mentioned for example by Tobschall (1975) to occur in the Steiger Slates (Vosges, France).

The positive correlation between Zn and Fe_2O_3 (r = 0.481) and negative correlations of Zn with CaO, Al_2O_3 and SiO_2 (r = -0.593 to -0.757) suggests that the Zn is contained in the magnetite.

Similar to the magnetite-rich rock, there is a very strong negative correlation (r = -0.894) between SiO_2 and Fe_2O_3 in the pyroxenite. SiO_2, MgO, Na_2O and K_2O are positively correlated with each other (r = 0.347 to 0.587) and negatively correlated with Fe_2O_3 (r = -0.499 to -0.894) reflecting the major mineralogical phases. Al_2O_3 shows positive correlations (r = 0.374 to 0.449) with Na_2O and K_2O and a negative one (r = -0.433) with CaO. Al_2O_3, Na_2O and K_2O are thought to represent the feldspar component of the pyroxenite, whereas the negative correlation between Al_2O_3 and CaO is reflected by the inverse proportion of modal clinopyroxene and plagioclase observed in these rocks. The CaO content of the feldspar is disguised by the CaO in the clinopyroxene, which results in a lack of correlation between CaO and the feldspar component (Al_2O_3, Na_2O and K_2O), whereas the Fe_2O_3 content of the clinopyroxene is disguised by the Fe_2O_3 in the magnetite, resulting in a negative correlation between Fe_2O_3 and SiO_2 or CaO.

The positive correlation between Fe_2O_3 and TiO_2 (r = 0.477), in contrast to the observed negative correlation in the magnetite-rich

rock, reflects the presence of ilmenite lamellae in the magnetite. Similar to the magnetite-rich rock there is a positive correlation between Zn and Fe_2O_3 (r = 0.342) and Zn and TiO_2 (r = 0.439), indicating the possible presence of Zn in the magnetite.

Nb shows a positive correlation with Fe_2O_3 (r = 0.475) and a negative correlation with SiO_2 (r = -0.509) and might therefore be concentrated together with the magnetite. Sr, Rb and Ba are positively correlated with each other (r = 0.479 to 0.602) as well as with Al_2O_3, Na_2O and K_2O (r = 0.348 to 0.631), suggesting their presence in feldspars.

5.4 Comparison of Waaikraal Rocks with Rocks of the Upper Zone of the Bushveld Complex

In an effort to determine any possible genetic link between the Waaikraal sill and the topmost differentiates of the Bushveld Complex, the major- and trace element contents of the pyroxenite and the magnetite-rich rocks from Waaikraal were compared with the compositions of the nearby exposed magnetite gabbro (Appendix 3 and Table 5.4), and also with samples from the top of the Bierkraal-1 borehole.

Six samples of the Bierkraal borehole (BK-1), between 428.5 and 563.5 metre deep (between 16.5 and 151.5 metre below the roof contact), were selected and the major- and trace element means were calculated from unpublished analytical data of R.K.W. Merkle (Table 5.4). In order to facilitate comparison of the analytical data, these means for the Bierkraal samples were used to normalise the means of the pyroxenite, magnetite-rich rock and magnetite gabbro (Fig. 5.1).

Table 5.4 Arithmetic means of major element (in weight per cent) and trace element (in ppm) content of magnetite gabbro (N = 3) and rocks from Bierkraal (N = 6).

Element	Magnetite Gabbro	Bierkraal
SiO_2	46.39	45.10
TiO_2	2.91	2.08
Al_2O_3	16.40	12.49
Fe_2O_3	18.75	24.49
MnO	0.20	0.41
MgO	3.97	2.31
CaO	9.05	8.67
Na_2O	3.55	5.05
K_2O	0.40	0.77
Zn	28	157
Cu	18	42
Ni	47	29
Co	25	63
Mo	3	7
Nb	30	13
Zr	6	127
Y	343	42
Sr	5	325
Rb	0	30
V	62	5

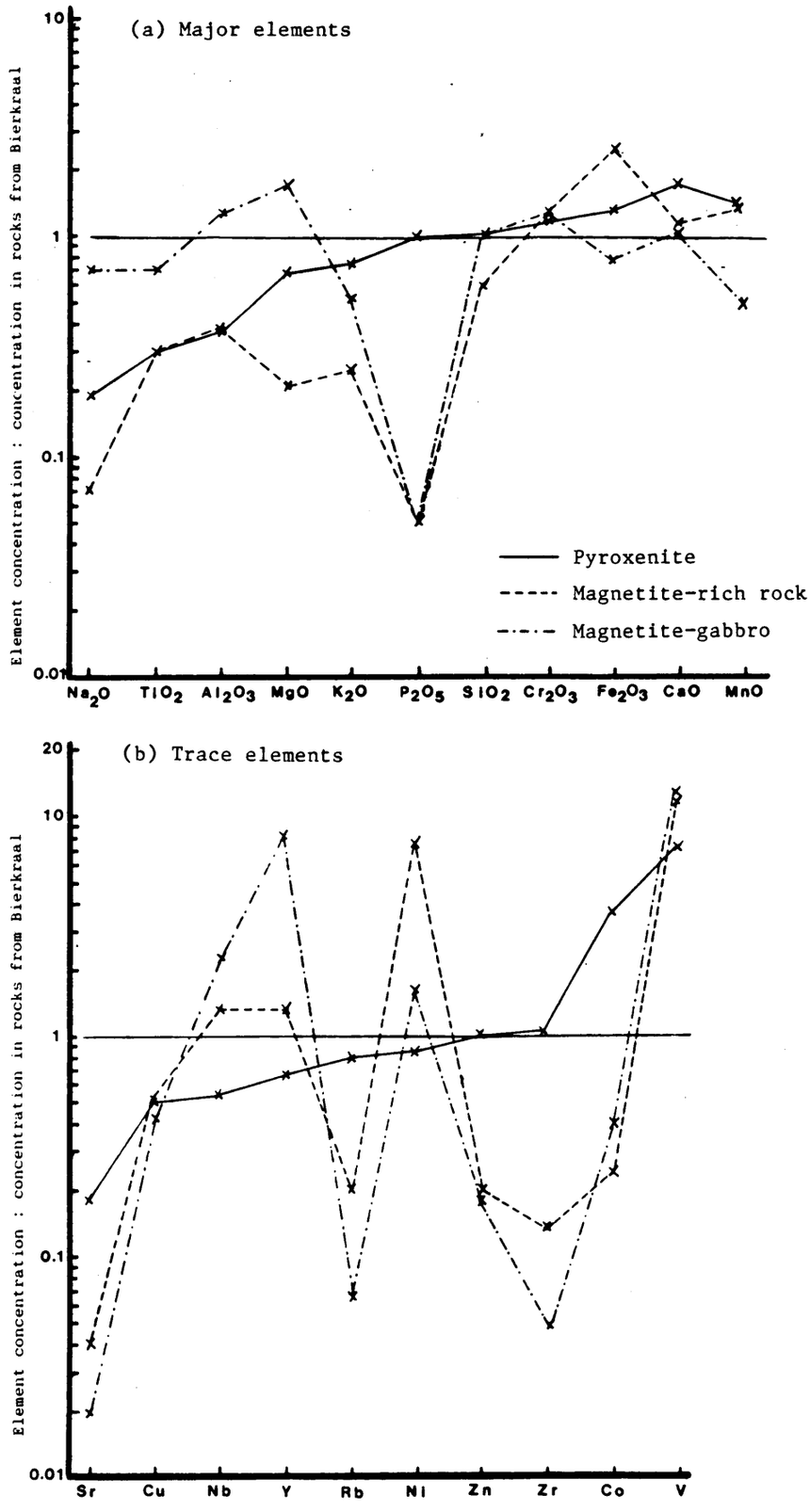

Figure 5.1 Arithmetic means of major- (a) and trace elements (b) of Waaikraal pyroxenite, Waaikraal magnetite-rich rock and magnetite gabbro normalised to topmost differentiates of the upper zone intersected by the Bierkraal borehole by division.

Significant differences can be detected between the different rock types. The higher MgO and V content and the lower Fe_2O_3 and TiO_2 content of the magnetite gabbro, in comparison with the samples from Bierkraal, indicate that the magnetite gabbros belong to a stratigraphically lower part of the upper zone than the samples from the Bierkraal borehole.

The magnetite-rich rocks are, compared to those from Bierkraal, depleted in most elements, except for Fe, V, Cr, Ni and to a lesser extent for Ca, Mn, Nb and Y, which reflect the much larger amounts of magnetite in the former. Interesting to note, however, is the low TiO_2 content, in spite of the large amount of magnetite and the similarity in trace element pattern between the magnetite-rich rock and the magnetite gabbro.

The resemblance between the rocks from Bierkraal and the pyroxenite is closer for the oxides Al_2O_3, MgO, P_2O_5, Fe_2O_3 and MnO and the elements Sr, Nb, Y, Rb, Ni, Zn, Zr and Co, than between the latter and the magnetite gabbros. The SiO_2 and CaO content in the pyroxenite is equally close to the Bierkraal samples and to the magnetite gabbro, whereas the Na_2O, TiO_2, K_2O, Cu and V content of the pyroxenite is closer to the magnetite gabbro. Na_2O, TiO_2 and K_2O occur in relatively low quantities, so that small differences in element content can result in large differences when normalised. Therefore it is assumed that the pyroxenite resembles the samples from Bierkraal closer than the magnetite gabbro, although the Al_2O_3, Na_2O, K_2O, Rb and Sr contents are lower and the CaO and Fe_2O_3 contents are higher in the pyroxenite than in the samples from Bierkraal. This is probably caused by the presence of less clinopyroxene and more feldspar than in the rocks from Bierkraal.

The plot MgO /(MgO + Fe_2O_3) versus Rb /(K_2O + Na_2O) (Fig. 5.2) indicates that the pyroxenites from Waaikraal are more differentiated rocks than the topmost differentiates of the upper zone intersected by the Bierkraal borehole. However, a comparison is difficult as the samples from Bierkraal represent a cumulate and the Waaikraal pyroxenite most likely represents a melt. In addition, the upper zone of the western Bushveld Complex does not necessarily represent products of uninterrupted differentiation of a homogeneous melt. Several cycles are reflected in the whole rock geochemistry and also in the concentration of normally incompatible elements like Nb, Y and Zr (Merkle

and Von Gruenewaldt, 1986). Therefore, the incompatible element content of the pyroxenite, when compared with upper zone rocks, are not necessary an unambiguous indication of the degree of differentiation.

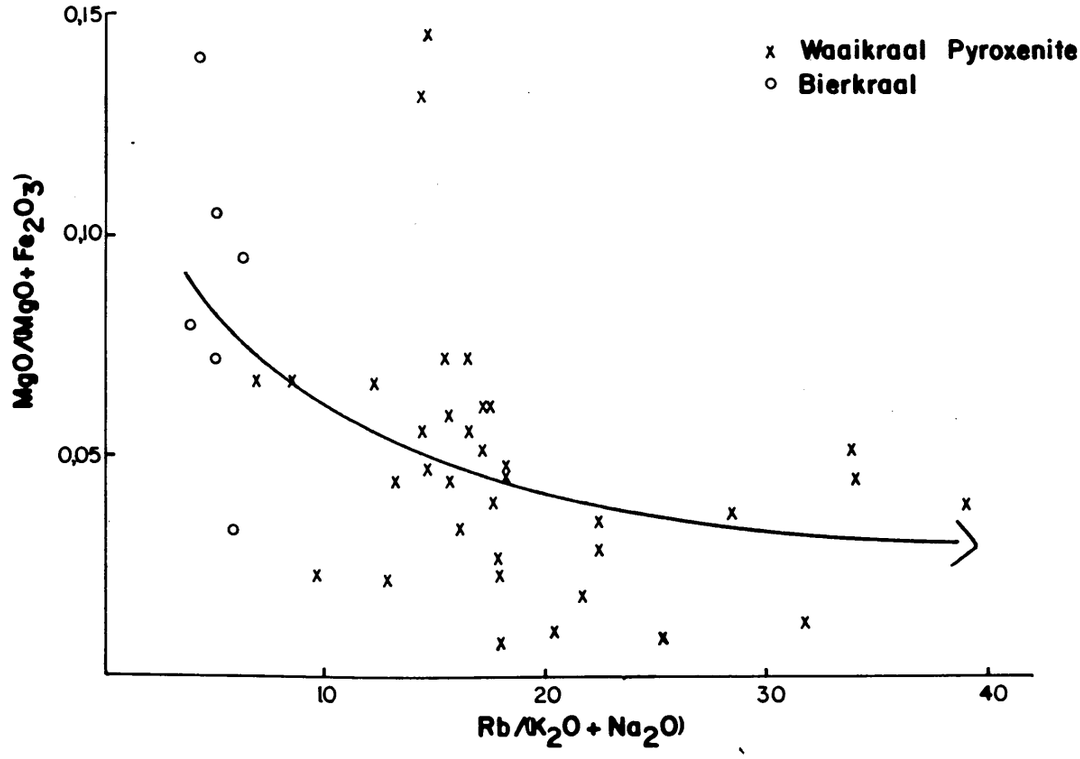

Figure 5.2 Plot of MgO /(MgO + Fe_2O_3) versus Rb /(K_2O + Na_2O) of Waaikraal pyroxenite and topmost differentiates of the upper zone intersected by the Bierkraal borehole, with an indication of the differentiation trend.

6. MINERAL CHEMISTRY

6.1 Pyroxene

The composition of the clinopyroxene in the ore body (20 thin sections), the magnetite gabbro (3 thin sections), the hornfels overlying the ore body and of ferrodiorite and ferrogabbro in the Bierkraal core was determined by electron microprobe. The analytical data is presented in Appendix 5.1. Each analysis represents the average of between 4 and 18 spot analyses with totals between 98.5 and 101.5 weight per cent.

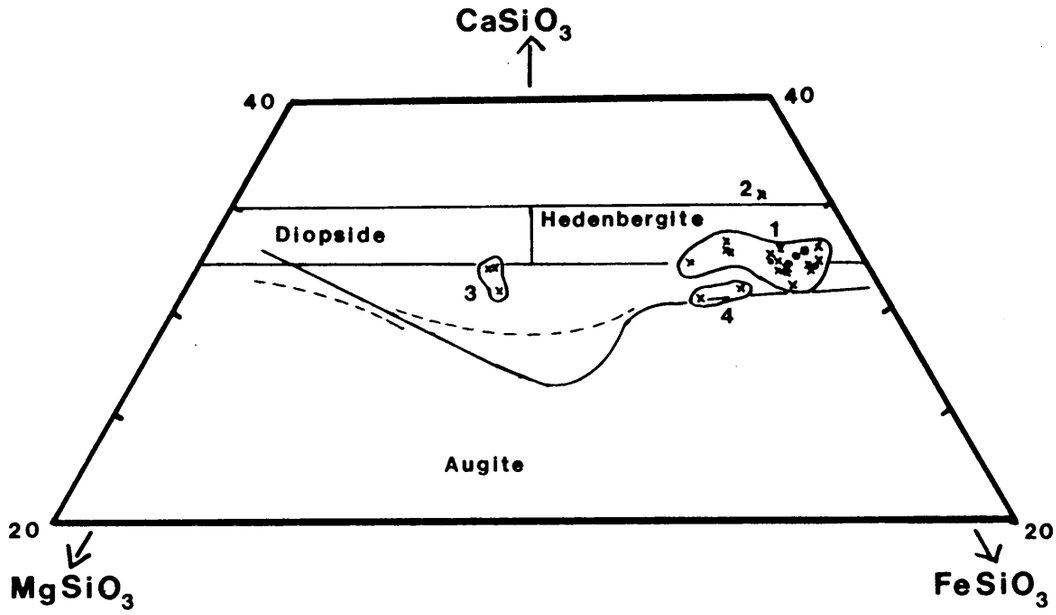

Figure 6.1 Composition of clinopyroxenes of Waaikraal pyroxenite (×) and magnetite-rich rock (•)(1), Waaikraal hornfels (2), magnetite gabbro (3) and topmost differentiates from the upper zone intersected by the Bierkraal borehole (4) plotted as molecular proportion $FeSiO_3$:$CaSiO_3$:$MgSiO_3$. Compositional trends of Ca-rich pyroxenes from the eastern Bushveld (solid line) and from the western Bushveld (dashed line) are after Atkins, 1969 and Markraaff, 1976 respectively. Clinopyroxene classification according to Morimoto (1988).

The compositions of the clinopyroxenes from the pyroxenite and from the magnetite-rich rock at Waaikraal overlap and plot on the boundary of the hedenbergite and the augite fields in the pyroxene quadrilateral (Field 1, Fig. 6.1).

Figure 6.1 illustrates that there is a considerable difference in Fe/Mg ratio between the clinopyroxene of the ore body (pyroxenite as well as magnetite-rich rock) and the magnetite gabbro. The clinopyroxene clearly suggests that the magnetite gabbro belong to a stratigraphically lower horizon of the Bushveld Complex than the rocks used from the Bierkraal borehole. It is interesting to note the similarity in composition of the clinopyroxenes of the latter locality and those from Waaikraal, although the Waaikraal pyroxenes are richer in Fe and Ca and plot above the crystallisation trend for clinopyroxenes from the eastern Bushveld Complex (Atkins, 1969).

6.2 Plagioclase

Plagioclase was analysed in 13 thin sections of the ore body (pyroxenite and magnetite-rich rock) and 3 thin sections of the nearby magnetite gabbro. Because no significant difference in composition within a grain was detected, only two points were analysed for most plagioclase grains, one at the edge and one in the middle of the grain, in order to account for compositional inhomogeneities.

The chemical composition of the plagioclase, together with the number of ions on the basis of 32 oxygen atoms and the molecular percentages of anorthite, albite and orthoclase are presented in Appendix 5.2.

The molecular percentages of anorthite, albite and orthoclase of plagioclases in the pyroxenite, the magnetite-rich rock, the magnetite gabbros and of plagioclase from the top of the upper zone in the Bierkraal borehole (Geraghty, unpublished results) are plotted in Fig. 6.2. Analyses were not averaged, as was done with the clinopyroxene data, due to the compositional variation within one thin section.

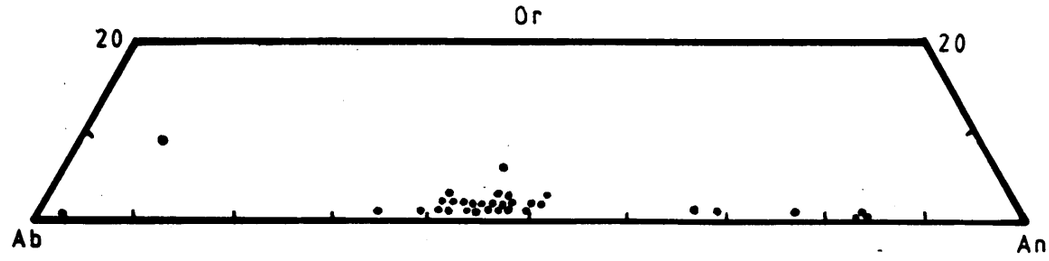

(a) Pyroxenite (17 obsevations hidden)

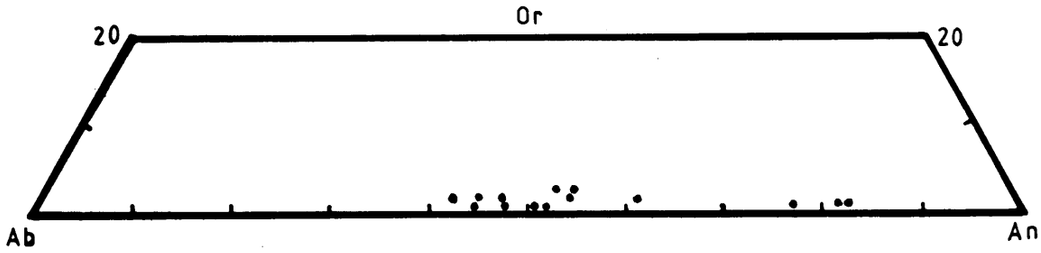

(b) Magnetite-rich rock (11 observations hidden)

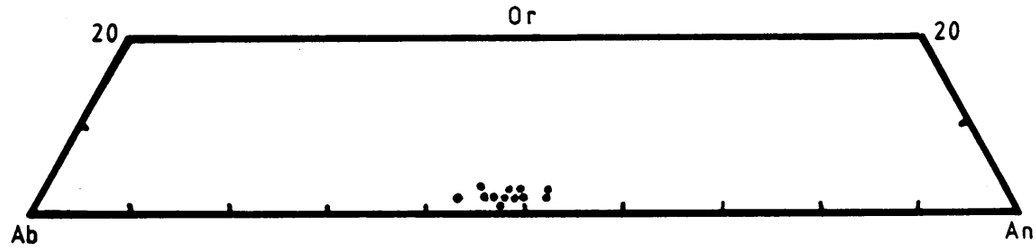

(c) Magnetite-gabbro (13 observations hidden)

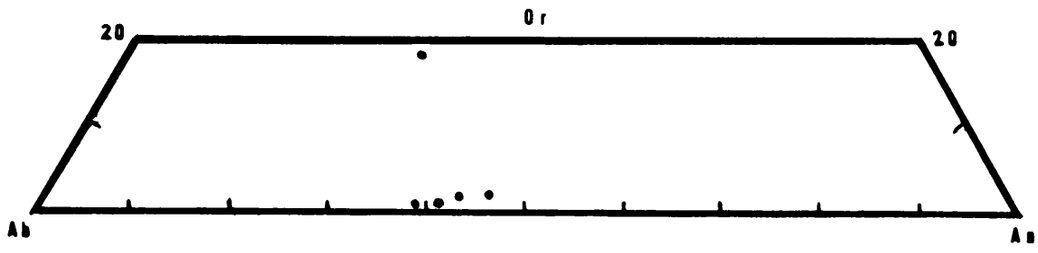

(d) Bierkraal borehole

Figure 6.2 Composition of plagioclase of pyroxenite (a), magnetite-rich rock (b), magnetite gabbro (c) and rocks from Bierkraal (d) plotted as molecular percentages anorthite, albite and orthoclase.

Table 6.1 Frequencies of different plagioclase compositions of pyroxenite, magnetite-rich rock and magnetite gabbro.

Sample	Rock-type	% Anorthite 0-10	10-30	30-50	50-70	70-90	90-100
WK 3.2	P	-	-	9	-	-	-
WK 5.2	P	1	-	6	-	-	-
WK 6.3	P	-	-	5	-	-	-
WK 12.2	P	1	-	-	3	4	-
WK 12.4	P	-	-	2	-	-	-
WK 13.2	P	-	-	1	-	-	-
WK 28.4	P	-	-	10	-	-	-
WK 14.4	P	-	-	2	2	-	-
WK 16.2	P	3	-	-	-	-	-
WK 4.1	M	-	-	1	5	1	-
WK 12.1	M	-	-	5	2	-	-
WK 28.3	M	-	-	-	-	1	-
WK 14.1	M	-	-	-	-	2	-
MG 1\2\3	MG	-	-	23	3	-	-

P = pyroxenite, M = magnetite-rich rock, MG = magnetite gabbro

The composition of plagioclase of the pyroxenite as well as the magnetite-rich rock varies considerably from grain to grain within one thin section with the majority of compositions around An_{30-50} (Table 6.1). In comparison, plagioclase of the magnetite gabbro was found to be very uniform in composition (An_{40-52}) and to be more anorthite-rich than the plagioclase at the top of the upper zone in the Bierkraal borehole. This again indicates that the magnetite gabbro belongs to a stratigraphically lower horizon of the Bushveld Complex than the rocks used from Bierkraal.

It is evident from Figure 6.2 and Table 6.1 that the different rock types can not be distinguished on the basis of the composition of the plagioclase. The composition of the plagioclase can, however, vary much more widely on thin section scale in the Waaikraal sill than in the other rock types, which could possibly the effect of hydrothermal activity, as will be discussed in more detail in a later section (chapter 9.1).

6.3 Amphibole

Amphibole analyses were obtained from 14 thin sections of pyroxenite. No amphiboles were detected in the magnetite-rich rock. The computer program by Spear and Kimball (1984) was used to calculate the number of ions on a basis of 24 oxygen atoms and to obtain four estimates for the Fe^{3+} content, viz., no Fe^{3+}, low Fe^{3+}, high Fe^{3+} and an average between the last two. In this study the average Fe^{3+} content was used.

The program calculates the numbers of ions in the amphibole formula on the basis of 24 (O,OH,F,Cl), and indicates the distribution of the elements between the different sites in the crystal structure.
The general form of the standard amphibole formula is:

$$A_{0-1}B_2C_5{}^{VI}T_8{}^{IV}O_{22}(OH,F,Cl)_2$$

T represents the tetrahedral sites, C represents the M1+M2+M3 sites, B the M4 sites and A the A sites (Deer et al., 1977).

The analyses, as well as the calculated numbers of ions in the amphibole formula, are presented in Appendix 5.3.

According to the classification of Leake (1978), all the amphiboles from the Waaikraal sill fall into the calcic amphibole group, with $(Ca + Na)_B > 1.34$ and $Na_B < 0.67$ (B: M_4 sites as shown above). Within the calcic amphibole group, most of the analyses can be classified as hastingsite and hastingsitic hornblende, although a few analyses fall into the compositional fields for ferro-edenite, ferro-edenitic hornblende, ferro-actinolite and ferro hornblende (Fig.6.3).

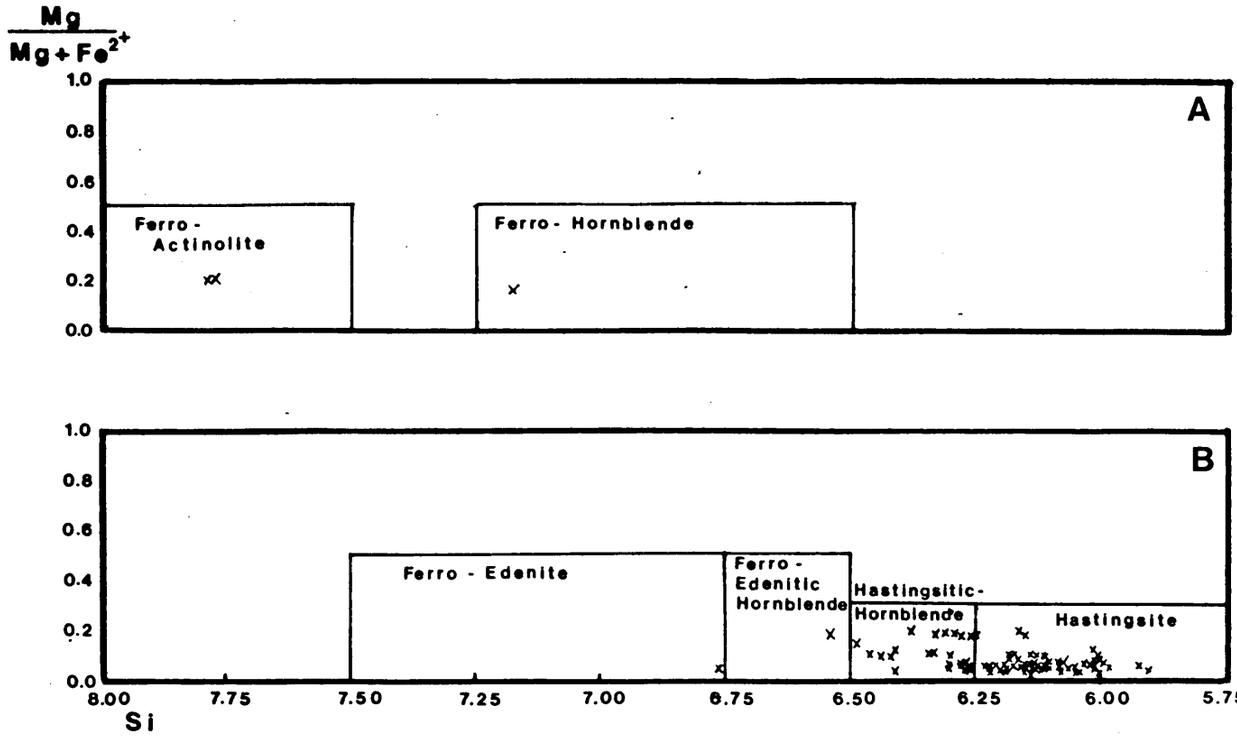

Figure 6.3 Plot of Mg /(Mg + Fe^{2+}) versus Si showing the compositional variation of amphiboles from the Waaikraal pyroxenite in terms of the nomenclature of Leake (1978). A for amphiboles with $(Na + K)_A < 0.50$ and Ti < 0.50 and B for amphiboles with $(Na + K)_A > 0.50$, Ti < 0.50 and $Fe^{3+} > Al^{VI}$.

Amphiboles of similar composition are described by Gulyaeva et al (1986) from Novogorbushinskoe in the far eastern USSR. Here amphiboles replace clinopyroxene in a hedenbergite-magnetite skarns with superimposed ore-mineralisation.

6.4 Olivine

Olivine was only encountered in one sample of magnetite-rich rock (WK 14.1) from which five grains were analysed by microprobe. The numbers of ions in the olivine formula on the basis of 4 oxygen atoms and the atomic ratios of Mg : Fe : Mn are presented in Appendix 5.4. The average of the five analyses is plotted in a compositional variation diagram together with compositions of olivines reported by Reynolds (1985) from the Bierkraal 1 borecore (Fig.6.4).

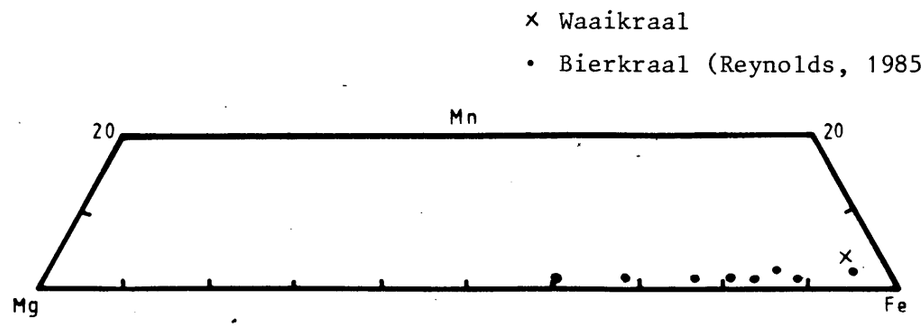

Figure 6.4 Composition of olivines from Waaikraal and Bierkraal plotted as ion proportion Fe:Mg:Mn (total Fe as Fe^{2+}).

From this plot, it can be seen that the olivine in the Waaikraal is chemically very similar to the olivines of the topmost differentiates of the upper zone intersected by the Bierkraal borehole.

6.5 Magnetite and Ilmenite

Analyses of magnetite grains and their ilmenite exsolution lamellae were obtained from three polished sections of pyroxenite and three polished sections of the magnetite gabbro. The magnetites from the magnetite-rich rock, which do not contain exsolution lamellae of ilmenite, were analysed in two polished sections. The microprobe analyses obtained were recalculated to determine the Fe^{3+} content assuming stoichiometry (Appendix 5.5).

The composition of the magnetite component of the ttanomagnetite grainsin the two rock types from the ore body is very similar and contain small ulvospinel exsolutions. The titanomagnetite of the pyroxenite, however, contains 10-30 volume per cent ilmenite exsolution lamellae, indicating an overall much higher Ti-content of the titanomagnetite grains as a whole. The TiO_2 content of the magnetite in the magnetite-rich rock ranges from only 0.2 to 2.8 weight per cent with a mean around 0.45 weight per cent (Fig. 6.5).

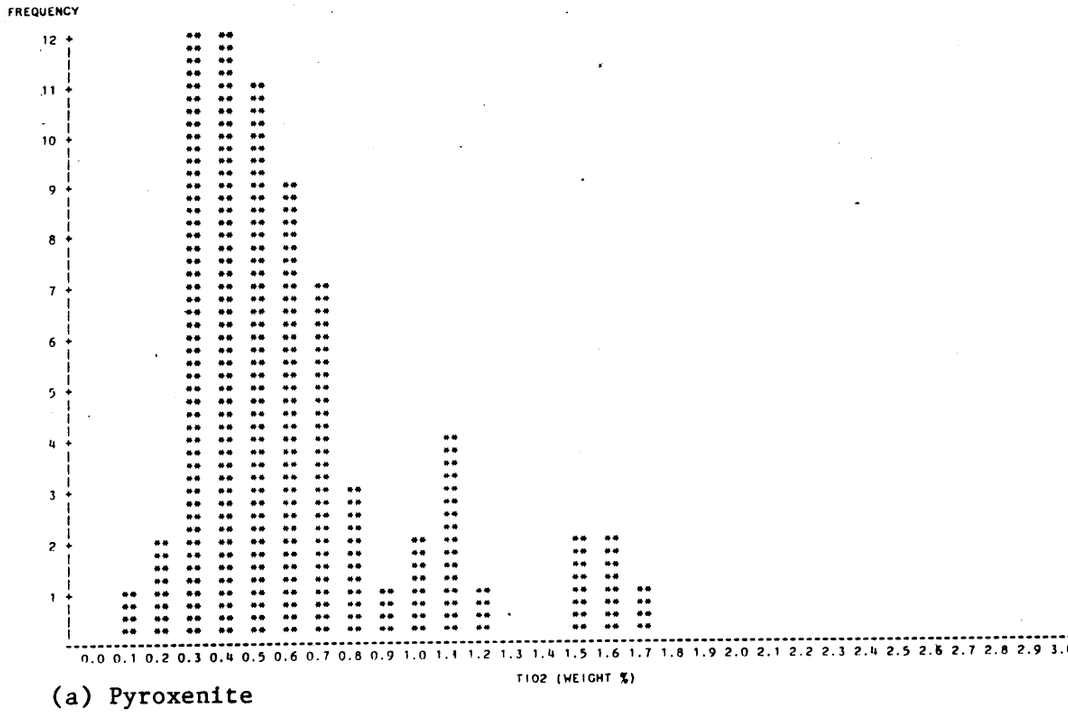

(a) Pyroxenite

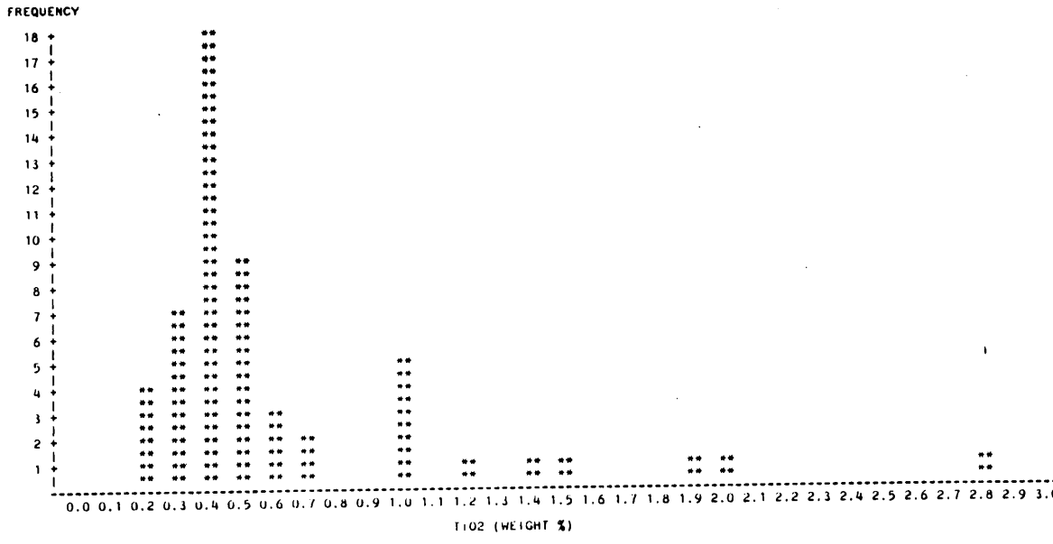

(b) Magnetite- rich rock

Figure 6.5 Distribution of TiO_2 in the magnetite of Waaikraal pyroxenite (a) and magnetite-rich rock (b) (in weight per cent).

The compositions of Waaikraal magnetites and ilmenites are compared with magnetites and ilmenites from the magnetite gabbros and from the Bierkraal borehole in Figure 6.6.

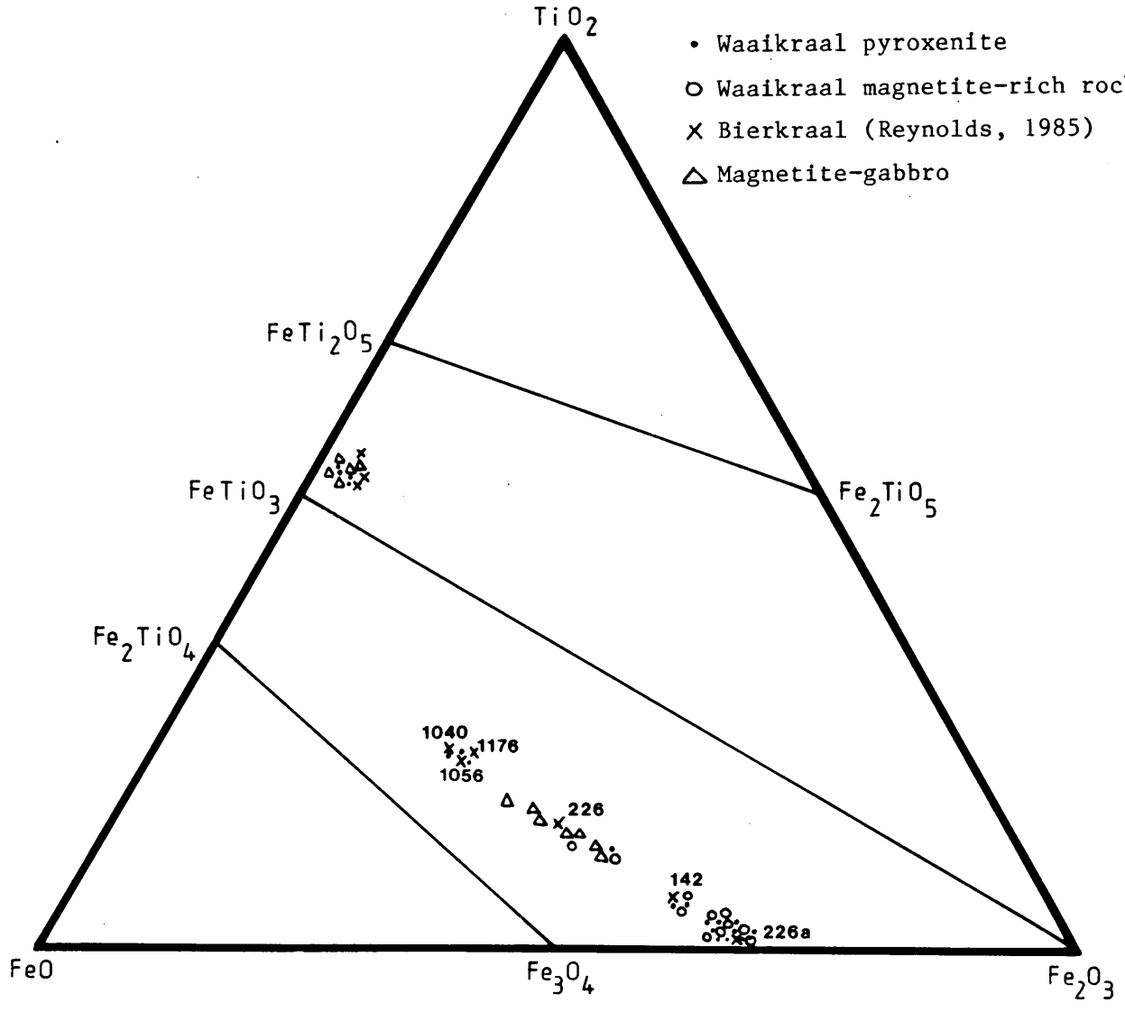

Figure 6.6 Composition of magnetite and ilmenite of the pyroxenite, magnetite-rich rock, magnetite gabbro and samples from Bierkraal (51 observations hidden). Numbers indicate drilling depth in metres below the roof contact in the Bierkraal borehole (226a = a late stage transgressive magnetite veinlet).

From Figure 6.6 it can be observed that the ilmenite analyses of the different rock types all plot in the same area, because of the very restricted solid solution field of ilmenite. The ilmenite of the Waaikraal pyroxenite, however, contains about 2 weight per cent MnO, whereas the ilmenite from the Bierkraal borehole contains only up to 0.67 weight per cent MnO. The MgO content of the ilmenite from Waaikraal pyroxenite is generally below the detection limit, whereas the ilmenite from Bierkraal contains up to 3 weight per cent MgO.

The composition of the magnetite on the other hand varies considerably, evidently in response to the amount of ulvospinel in either solid solution or as tiny exsolutions in the magnetite. Waaikraal magnetite of both the pyroxenite and the magnetite-rich rock corresponds best with the magnetites of the topmost rocks of the upper zone and with a late stage transgressive magnetite veinlet of the Bierkraal borehole (Reynolds, 1985).

7. GOLD AND ORE MINERALOGY OF THE ORE BODY

The variety of different ore minerals present can be devided into the following groups: Gold and gold compounds, bismuth minerals, diarsenides, sulfarsenides, iron sulfides, copper bearing sulfides and sphalerite. Each group will be delt with seperately with a description of the textural relations and of the associations at the end of this chapter.

7.1 Gold and Gold Compounds

Gold occurs in three different phases viz., as native gold, a gold-bismuth- and a gold-copper compound.

Compositions of the three phases were obtained by microprobe analyses. Although all minerals were analysed for Au, Ag, Hg, Pd, Fe, Cu, Rh and Bi; Pd, Rh and Hg were never found to be present in quantities above the detection limit (Appendix 6.1).

7.1.1 Gold

The native gold is very pure and contains only traces of Fe and Cu. The highest silver content found was 1.26 weight per cent which results in the grains being of a deep yellow colour under reflected light.

The highest concentrations of gold occur in the pyroxenite, but gold can occasionally also be present in high concentrations in the magnetite-rich rock. Figure 2.3 indicates the distribution of gold in the different rock types throughout the mine. The distribution is very irregular and follows no recognizable pattern.

In both rock types the gold occurs either as small individual anhedral grains in close proximity of other ore minerals such as bismuth bearing minerals, arsenides, diarsenides and chalcopyrite (see chapters 7.3 to 7.5 and 7.7)(Fig. 7.1), or in composite grains together with these ore minerals. In the latter case the gold occurs either as grains, up to 300 μm in diameter, or as veins within these minerals (Figures 7.2 and 7.3).

In the magnetite-rich rock the gold is often situated at 120° junctions between magnetite grains and also occurs together with other ore minerals in fractures of the magnetite, a feature also observed in the pyroxenite. This indicates that the gold was introduced after the formation of the host rocks.

In the pyroxenite, where the gold can also be present in clinopyroxene, it is often surrounded by amphibole and was probably introduced along cleavage planes of the pyroxene.

Generally, the grain size of the gold particles is smaller in the magnetite-rich rock than in the pyroxenite.

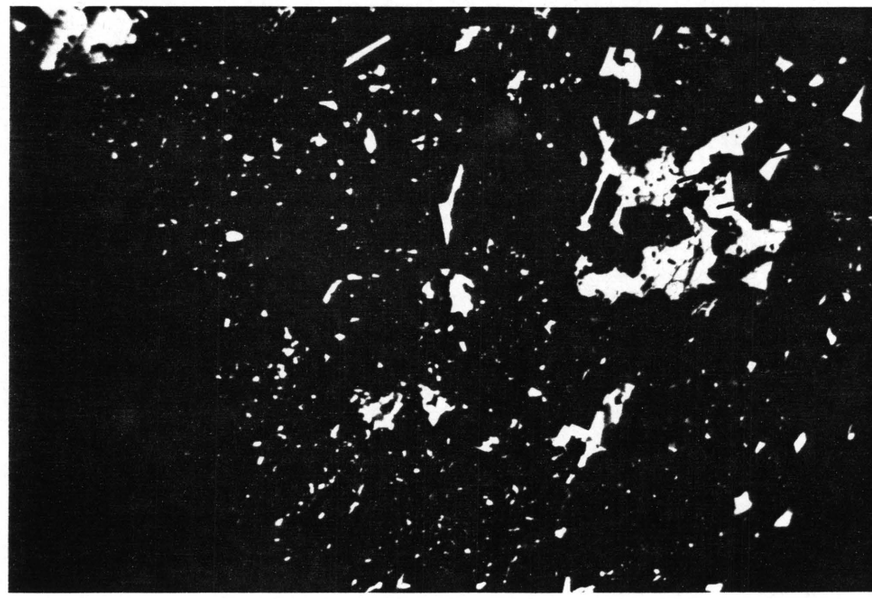

Figure 7.1 Individual gold grains (Au) together with joseite (jo) and safflorite (sa) in pyroxenite (WK 5.2).
Photomicrograph: Reflected light (RL), plane polarized light (PPL). 100 µm

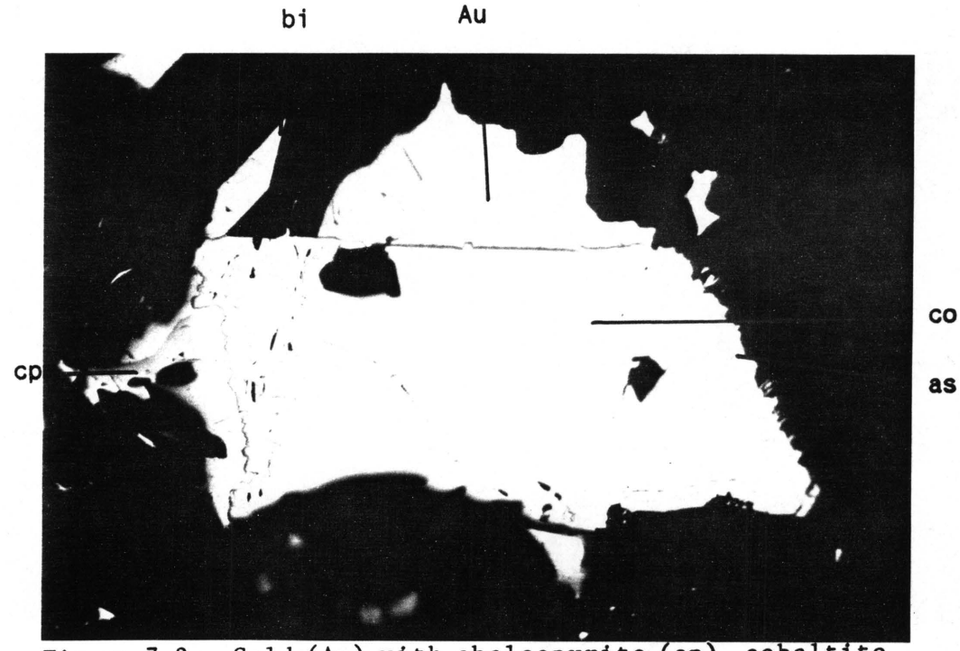

Figure 7.2 Gold (Au) with chalcopyrite (cp), cobaltite (co), arsenopyrite (as) and bismuthinite (bi) in pyroxenite (WK 5.2).
Photomicrograph: RL, PPL. 100 µm

a

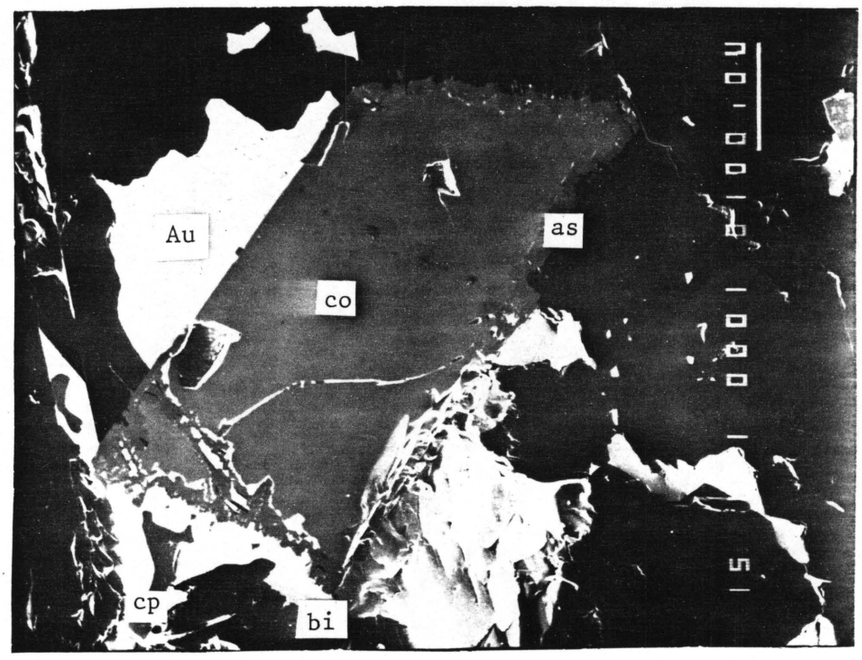

b

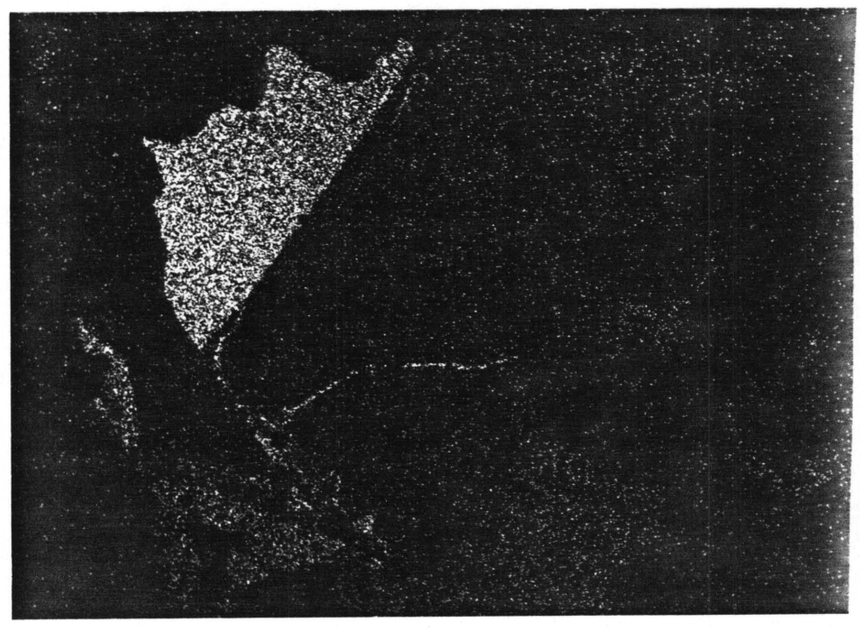

Figure 7.3 Gold (Au) with chalcopyrite (cp), cobaltite (co), arsenopyrite (as) and bismuthinite (bi) in pyroxenite (WK 5.2). 100 µm
a: Secondary electron image.
b: X-ray distribution pattern of Au.

7.1.2 Maldonite

Maldonite (Au_2Bi) is a very rare mineral, because its formation is limited to closely defined conditions at high temperatures (Ramdohr, 1980) and because it decomposes readily to Au and Bi. It was observed in only one sample (WK 52.3), but because it closely resembles joseite, its presence in other samples can not be excluded with certainty.

It was observed as droplets in massive safflorite (Fig. 7.4), and also together with joseite in safflorite, in silicates and interstitial to magnetite grains (Fig. 7.5). The droplets form chains and are considered to follow cracks which have subsequently healed, rather than original grain boundaries in the massive safflorite.

Microprobe analyses (see Appendix 6.1) established the presence of traces of silver and iron, apart from gold and bismuth.

Heating tests on mixtures of Au and Bi by Böhmke and Varndell (1986), revealed that a temperature of 500°C the two metals combined to form maldonite.

7.1.3 $CuAu_3$

Only one grain of a Au-Cu alloy, 60 µm in length and 20 µm in width, was encountered. It occurs attached to safflorite and has a golden colour with a slight greenish tint under reflected light (Fig. 7.6).

A microprobe analysis indicates a composition of 90.37 weight percent Au and 9.66 weight percent Cu, with traces of S and Ag (see Appendix 6.1). This corresponds to an Au-Cu alloy with the formula $CuAu_3$.

According to Hansen and Anderko (1958), there is a complete solid solution in the system Au-Cu below the solidification range of 1083° - 889°C. Below 410°C, solid state reactions occur and cause miscibility gaps between phases centered around the compositions Cu_3Au and CuAu (below 285°C) and CuAu and $CuAu_3$ (below 255°C). An ordered phase with

composition close to $CuAu_3$ is therefore stable below 255°C.

A natural compound with similar composition has been described by Oen and Kieft (1974) from Beni-Bousera, Morocco. Here the alloy contains 88.35 weight percent Au and 11.0 weight percent Cu, which corresponds to the formula $CuAu_{2.6}$.

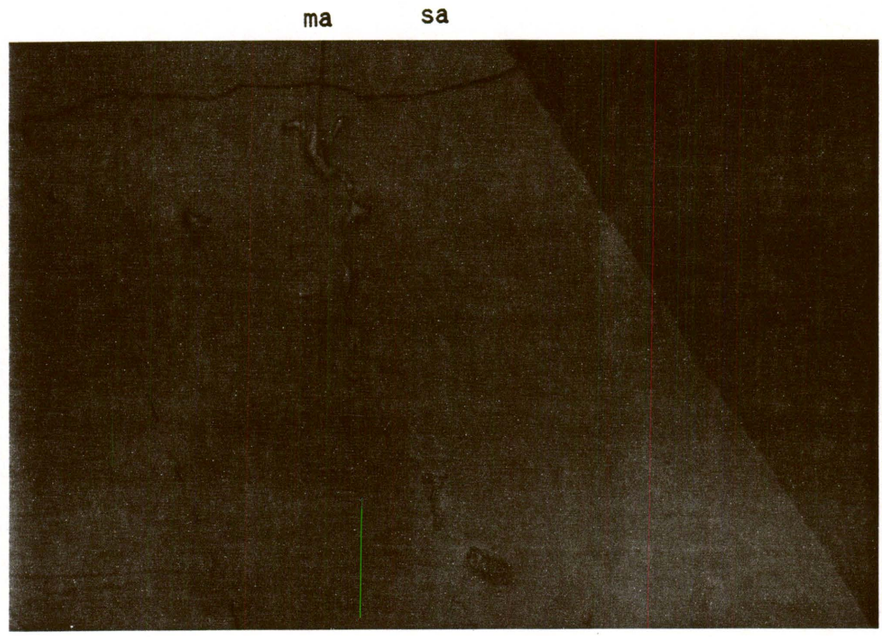

Figure 7.4 Droplets of maldonite (ma) in safflorite (sa) in magnetite-rich rock (WK 52.3). Photomicrograph: RL, PPL.

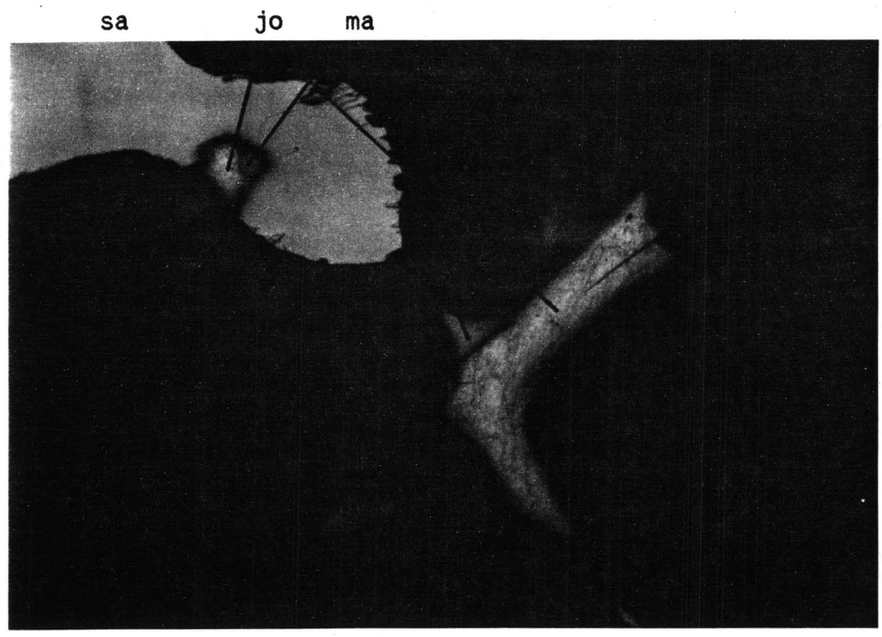

Figure 7.5 Maldonite (ma) together with safflorite (sa) and joseite (jo) between magnetite grains of the magnetite-rich rock (WK 52.3).
Photomicrograph: RL, PPL. ⟵⟶ 100 µm

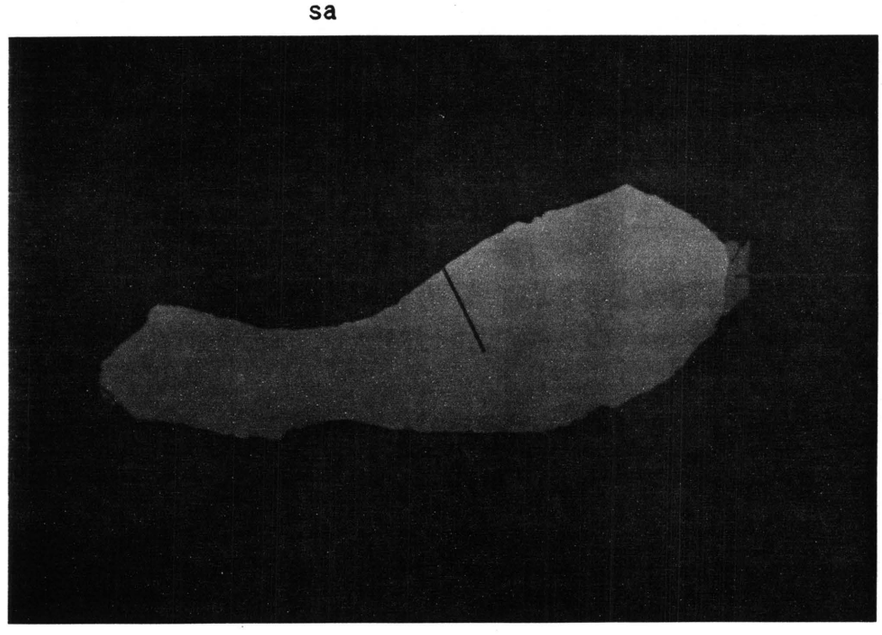

Figure 7.6 $CuAu_3$ attached to safflorite (sa) in magnetite-rich rock (WK 52.3).
Photomicrograph: RL, PPL. ⟵⟶ 100 µm

7.2 Bismuth Minerals

Three different bismuth-containing minerals (apart from maldonite) are present,viz. joseite, bismuthinite and native bismuth. All three minerals occur in both the pyroxenite and the magnetite-rich rock, but are more abundant in the pyroxenite.

The most frequent bismuth bearing mineral at Waaikraal is joseite. Of the two known modifications of joseite, only one out of 35 analysed grains turned out to be joseite-A (Bi_4TeS_2), the remaining grains being joseite-B (Bi_4Te_2S).

The analyses are presented in Appendix 6.2, from which it can be seen that joseite contains traces of Sb and As, apart from Bi, Te and S as major components.

Joseite occurs either interstitially between silicates or enclosed in them, and is generally surrounded by amphibole. It is mostly associated with bismuthinite, di- and sulfarsenides (see chapter 7.4 and 7.5) and gold (Fig. 7.7).

Yusa et al. (1979) described incongruent melting of joseite-B to joseite-A, tetradymite and liquid above 478°C.

Bismuthinite (Bi_2S_3) occurs as anhedral grains, often surrounding native bismuth (Fig. 7.8), but also together with joseite, gold and di- and sulfarsenides (see chapter 7.4 and 7.5). It contains, apart from Bi and S, also traces of Sb (Appendix 6.2).

The native bismuth contains up to 99.67 weight per cent bismuth and traces of Co, Ni and As (Appendix 6.2). It displays the very typical twinning (Ramdohr, 1980) which can be clearly observed under crossed nicols in reflected light (Fig. 7.9).

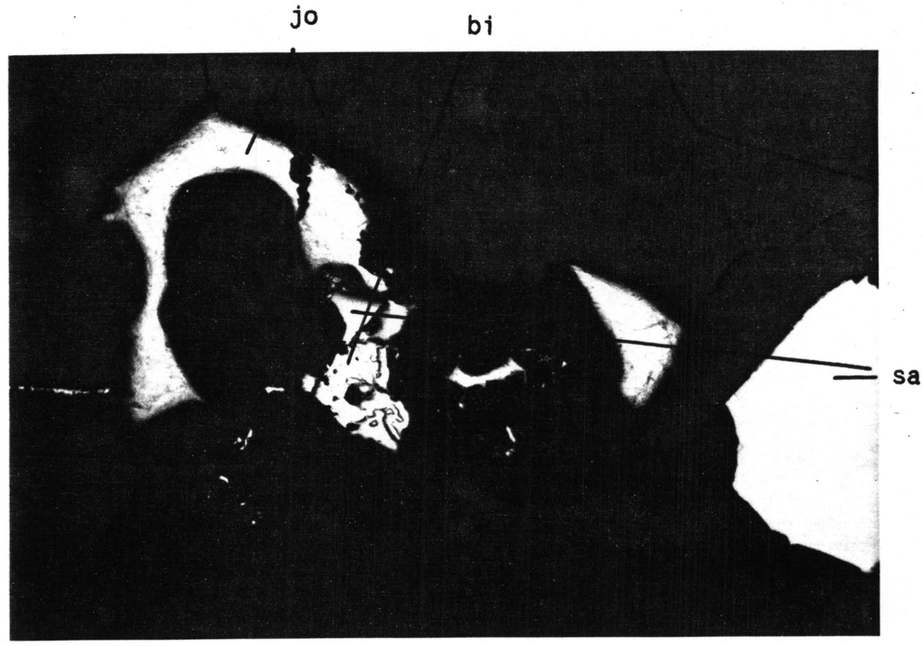

Figure 7.7 Joseite (jo), safflorite (sa) and bismuthinite (bi) in magnetite-rich rock (WK 52.3). Photomicrograph: RL, PPL. ⟵⟶ 100 µm

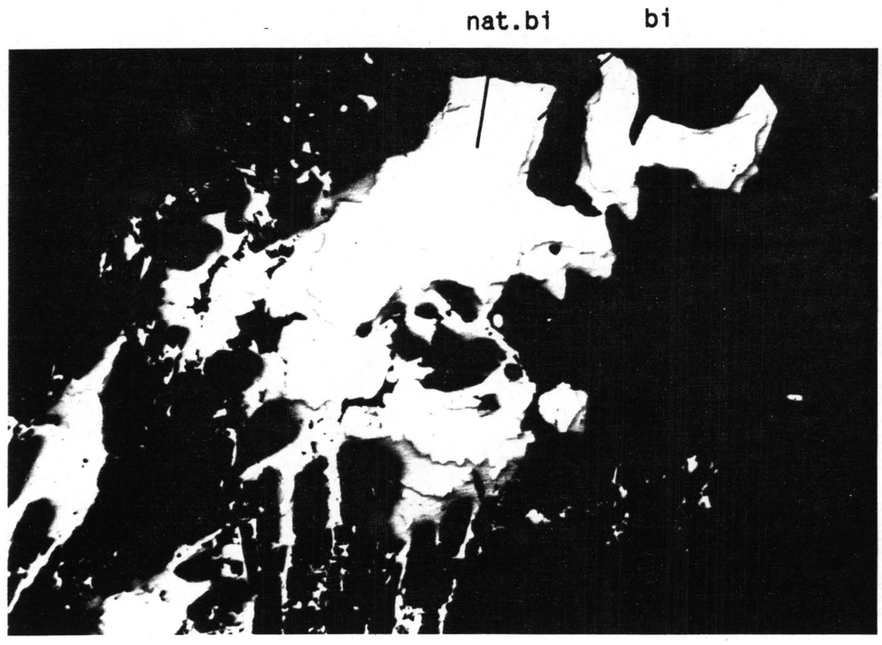

Figure 7.8 Native bismuth (nat bi) surrounded by bismuthinite (bi) in pyroxenite (WK 12.4).
Photomicrograph: RL, PPL. ⟵⟶ 100 µm

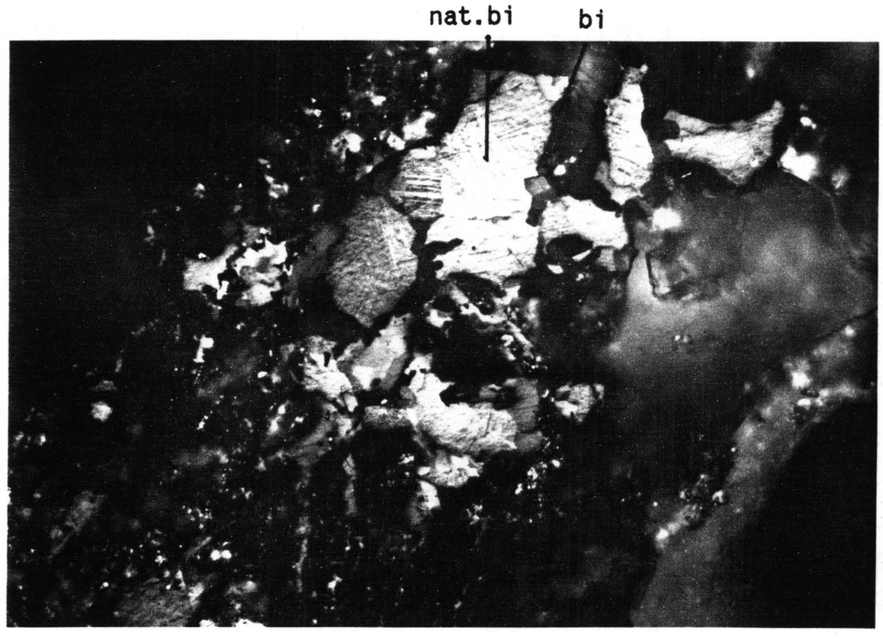

Figure 7.9 Native bismuth (nat bi) with typical twinning surrounding bismuthinite (bi) in pyroxenite (WK 12.4).
Photomicrograph: RL, cross polarized light (CPL).
⟵⟶ 100 µm

7.3 Diarsenides

Of the loellingite - safflorite - rammelsbergite ($FeAs_2$ - $CoAs_2$ - $NiAs_2$) group only members of the loellingite - safflorite solid solution series ($FeAs_2$ - $CoAs_2$) are encountered at Waaikraal.

The safflorite occurs as small individual idiomorphic grains interstitially to or within silicates (mainly clinopyroxene) of both rock types. Subhedral grains associated with, or even attached to, other ore minerals such as joseite, bismuthinite, minerals of the arsenopyrite group (see chapter 7.5) and gold are often observed.

In one sample (WK 52.3) safflorite occurs as large aggregates together with magnetite.

Different proposals for the terminology of the minerals in the loellingite - safflorite solid solution series exsist. Holmes (1947) has, for example, distinguished between safflorite and loellingite at 70 mole per cent $FeAs_2$, whereas Radcliffe and Berry (1968), who have worked on synthetic and natural specimens, recommend that loellingite be used only for material with less then 3 mole per cent $CoAs_2$.

Berry and Thompson (1962) classified safflorite into five types on the basis of different X-ray diffraction patterns, whilst Radcliffe and Berry (1968) gave compositional ranges for each type (Figure 7.10).

Results of microprobe analyses of minerals of the diarsenide group at Waaikraal (Appendix 6.3) were recalculated to mole per cent $FeAs_2$:$CoAs_2$:$NiAs_2$ and plotted on a ternary diagram (Figure 7.10). The solid solution series is clearly visible here and all the minerals are safflorite, according to the terminology of Radcliffe and Berry (1968). The most iron-rich mineral contains 4 mole per cent $CoAs_2$ and falls therefore just into the safflorite field. The highest $CoAs_2$ content encountered is 75 mole per cent.

Most analyses fall into fields I, III and IV of Berry and Thompson (1962). Two analyses fall outside any of the indicated fields and suggest that Fe-rich safflorite can contain higher Ni contents than originally suggested by Radcliffe and Berry (1968).

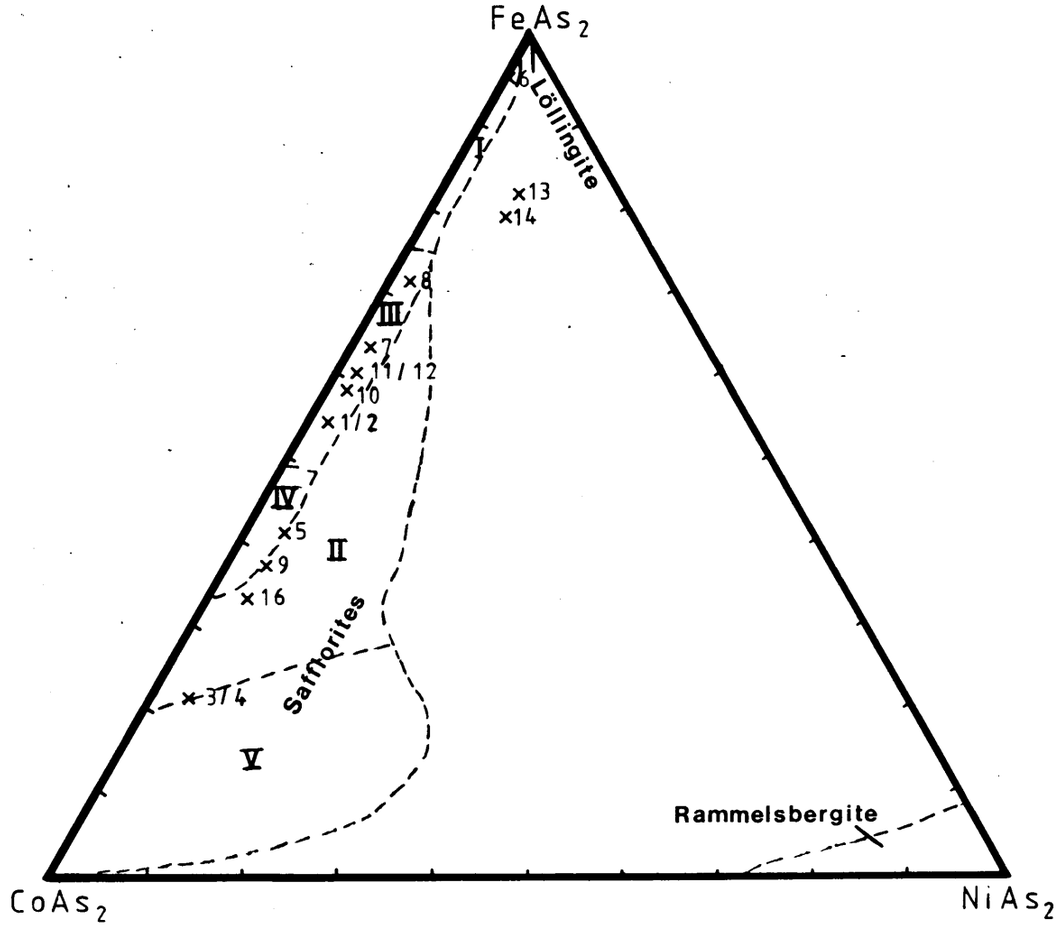

Figure 7.10 $FeAs_2$-$CoAs_2$-$NiAs_2$ ternary diagram indicating the compositional variation of safflorites from Waaikraal and the compositional fields of safflorite I-V and rammelsbergite (after Radcliffe and Berry, 1968) (in mol per cent)

The analytical data clearly suggests that the small idiomorphic grains (analyses 1 to 5, 7 and 9) display a considerable variation in composition, compared to the Fe-rich safflorites (analyses 6, 13 and 14), which are associated with gold and other ore minerals. Analyses 10 to 12 are of large aggregates of safflorite in sample WK 52.3, whereas analysis 16 is of a safflorite with a rim of cobaltite.

Safflorite usually belongs to the orthorhombic class (Roseboom, 1963; Radcliffe & Berry, 1968), but material with 80 - 100 mole per cent $CoAs_2$ is monoclinic (Radcliffe & Berry, 1971) and termed clinosafflorite. Radcliffe and Berry (1971), however, demonstrated that safflorite from the Cobalt area, Canada, with just below 75 mole per cent $CoAs_2$ can also be monoclinic. It is therefore possible that the rare mineral clinosafflorite also occurs at Waaikraal. Unfortunately only one safflorite grain analysed contains such a high cobalt content, and it was not possible to obtain X-ray data to support this

assumption.

The highest $NiAs_2$ content encountered in safflorite was 8 mole per cent (analysis 14) . The safflorites also contain traces of S and Bi.

7.4 Sulfarsenides

Sulfarsenides include those minerals which belong to the arsenopyrite - cobaltite - gersdorffite (FeAsS - CoAsS - NiAsS) group. The molar proportions of sulfaresenides at Waaikraal, determined by microprobe analyses (Appendix 6.4) are plotted in a ternary diagram (Fig. 7.11). Only cobaltite and arsenopyrite were found to occur in this deposit.

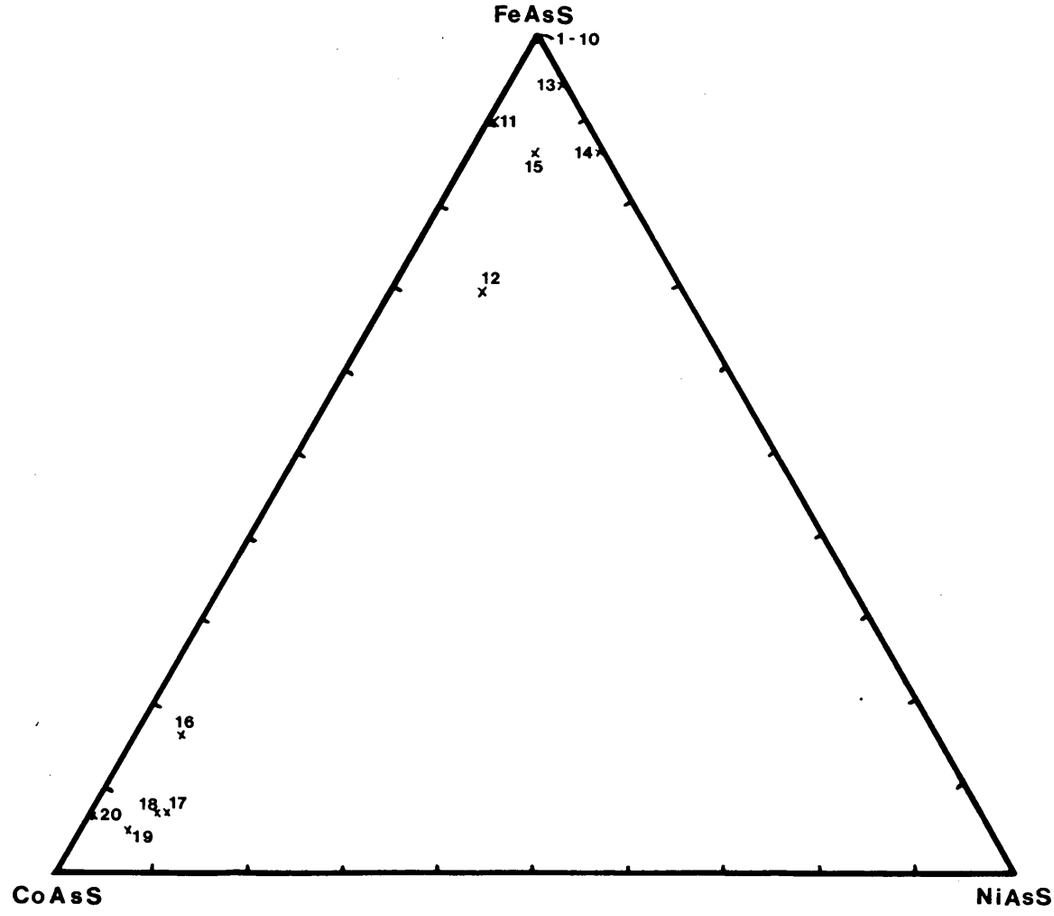

Figure 7.11 FeAsS-CoAsS-NiAsS ternary diagram indicating the compositional variation of cobaltites and arsenopyrites from Waaikraal (in mol per cent).

Cobaltite at Waaikraaal occurs as individual euhedral and as anhedral grains together with gold, joseite, bismuthinite, safflorite and arsenopyrite (Fig. 7.2). It can also completely enclose safflorite (Figures 7.12 and 7.13).

Cobaltites vary in composition from 79 - 94 mole per cent CoAsS, 5 - 16 mole per cent FeAsS and 0 - 8 mole per cent NiAsS. The ratio of (Co,Fe,Ni) : S : As is very close to 1 : 1 : 1.

Cobaltite occurs in two structural forms, isometric and orthorhombic (Giese & Kerr, 1965). At Waaikraal both structural types seem to be present as both isotropic and anisotropic grains were observed.

Arsenopyrites were found to occur either as euhedral or anhedral grains alone (Fig. 7.14) or occasionally together with gold, safflorite, bismuthinite, joseite, chalcopyrite and cobaltite (Fig. 7.2). Occasionally arsenopyrite surrounds cobaltite completely.

Arsenopyrites from Waaikraal vary in composition from pure FeAsS to (Fe,Co,Ni)AsS with up to 13 mole per cent NiAsS (4.73 weight per cent Ni) and up to 21 mole per cent CoAsS (7.09 weight per cent Co).

A plot of the arsenopyrites on a (Fe,Co,Ni) - As - S ternary diagram (Fig. 7.15) indicates that the pure arsenopyrites have a surplus of S and a deficiency of As, whereas the arsenopyrites containing Co and Ni have a deficiency of S and surplus of As.

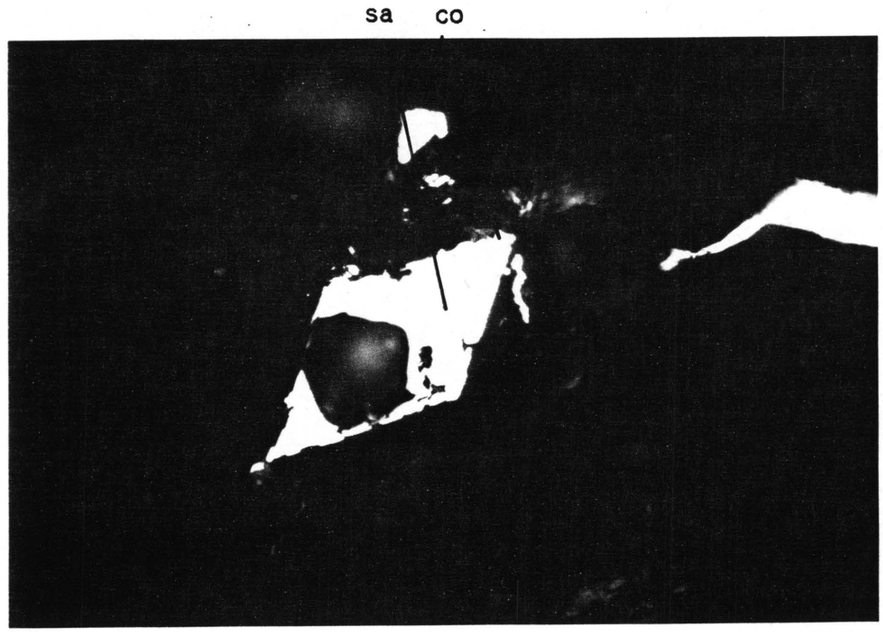

Figure 7.12 Cobaltite (co) enclosing safflorite (sa) in pyroxenite (WK 5.2).
Photomicrograph: RL, PPL. 50 µm

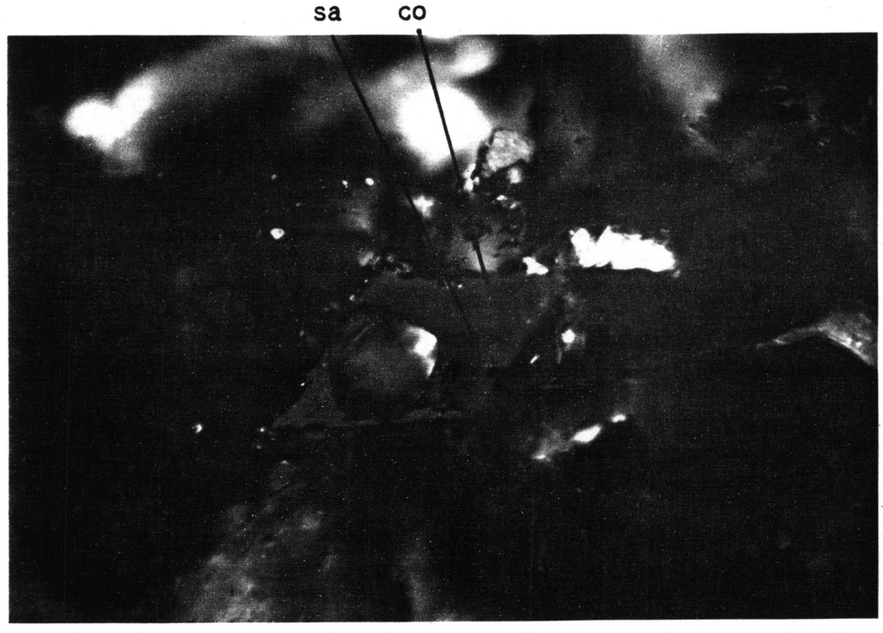

Figure 7.13 Cobaltite (co) enclosing safflorite (sa) in pyroxenite (WK 5.2).
Photomicrograph: RL, CPL. 50 µm

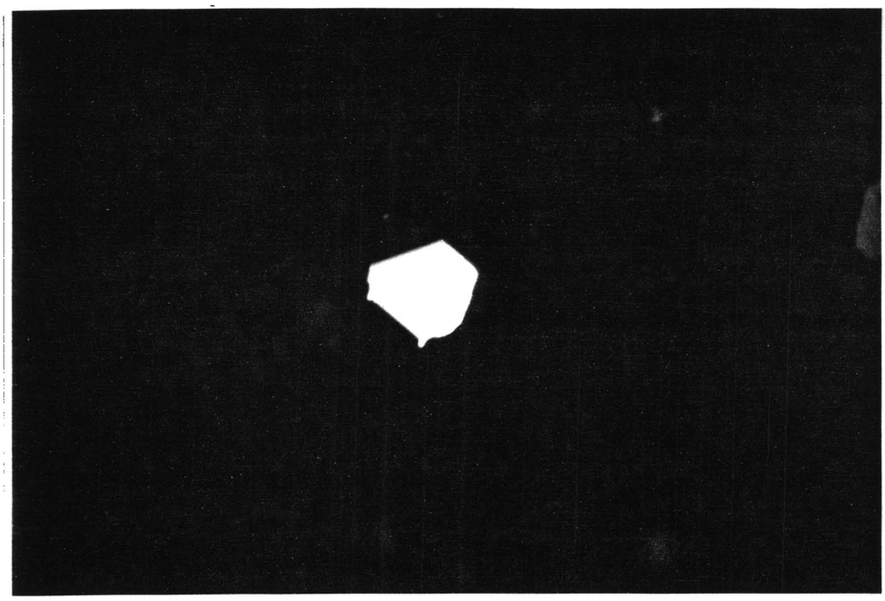

Figure 7.14 Euhedral grain of arsenopyrite in pyroxenite (WK 12.4).
Photomicrograph: RL, PPL. 50 µm

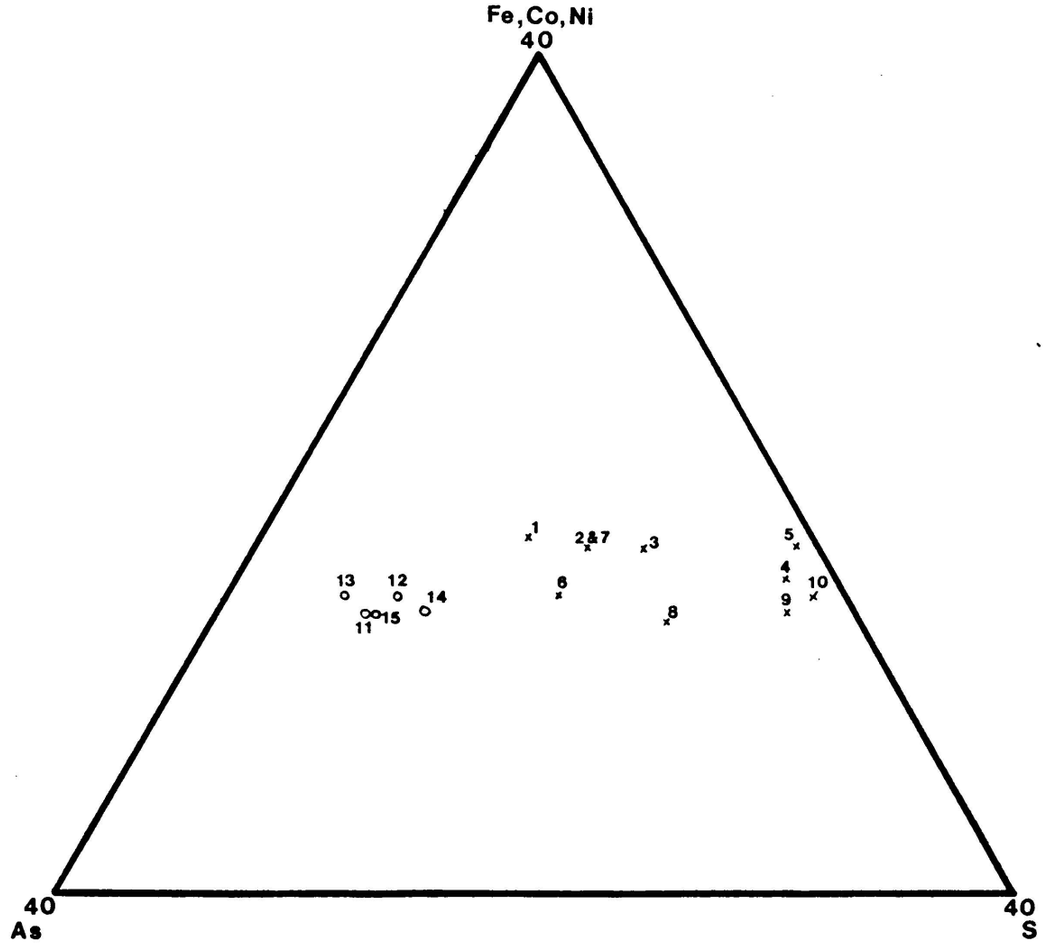

Figure 7.15 (Fe, Co, Ni)-As-S ternary diagram indicating the compositional variation of arsenopyrites from Waaikraal in mol per cent, (x) pure arsenopyrites, (o) arsenopyrites with up to 13 mol per cent Ni and up to 10 mol per cent Co.

7.5 Iron Sulfides

Both pyrrhotite and pyrite were only observed in large quantities in a few samples and tend to occur isolated from the other ore minerals such as the Bi-minerals, sulpharsenides, diarsenides and gold. They are often associated with chalcopyrite (Fig. 7.16) and occasionally with sphalerite (Fig. 7.17).

Members of the pyrrhotite group ($Fe_{1-x}S$) can be divided into two distinct compositional groups (Carpenter and Desborough, 1964). One group corresponds to stoichiometric FeS (troilite) and the other is an iron-deficient group with 47.8 - 46.5 atomic per cent iron (pyrrhotite). Only pyrrhotite, which contains a few exsolutions of pentlandite, was observed at Waaikraal.

At room temperature, the pyrrhotites can be divided into two groups, viz. monoclinic pyrrhotite (Fe_7S_8) with up to 46.67 atomic per cent Fe and hexagonal or intermediate pyrrhotite (Fe_9S_{10} - $Fe_{11}S_{12}$) with between 47.2 and 47.8 atomic per cent Fe (Morimoto et al, 1975). This variation of the pyrrhotites, together with the analytical uncertainty which is caused by the reproducibility of the analyses (see Appendix 2.2.3 and chapter 4.4), is illustrated in Figure 7.18.

The compositional variation of pyrrhotites at Waaikraal shown in Figures 7.18 and 7.19 indicates that the intermediate phase is dominant at Waaikraal.

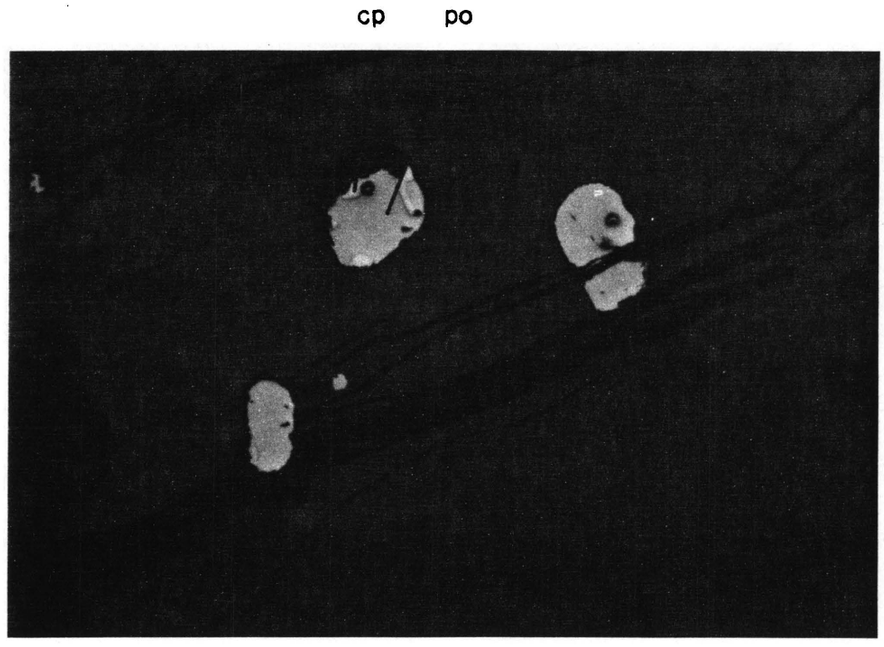

Figure 7.16 Pyrrhotite (po) and chalcopyrite (cp) in magnetite grains of magnetite-rich rock (WK 1).
Photomicrograph: RL, PPL.

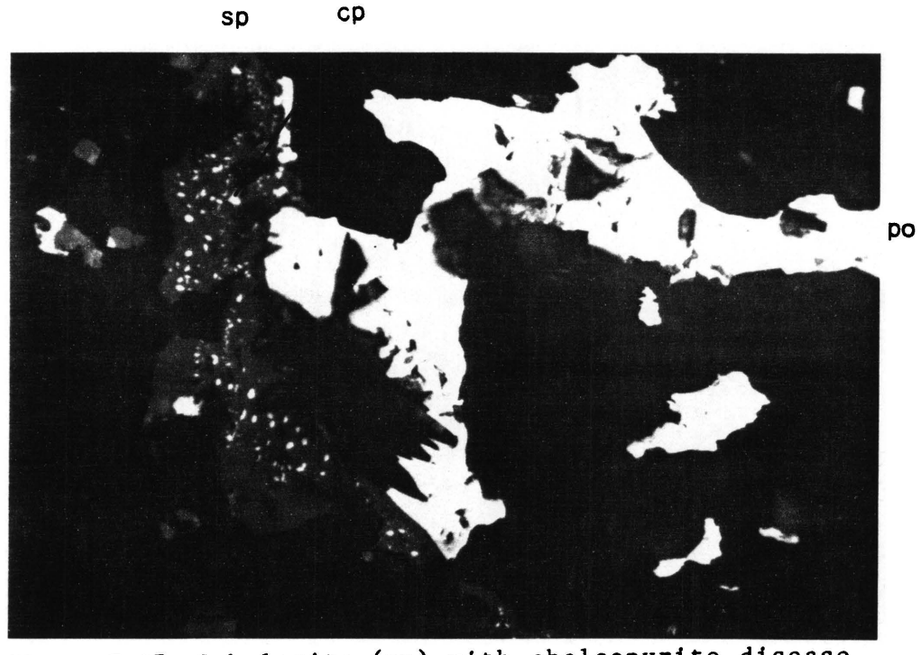

Figure 7.17 Sphalerite (sp) with chalcopyrite disease (cp) and pyrrhotite (po) in pyroxenite (WK 21.5).
Photomicrograph: RL, PPL.

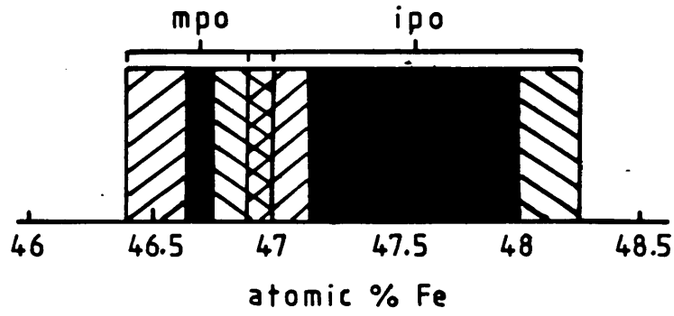

Figure 7.18 Compositional variation of pyrrhotite group minerals (black) and analytical uncertaity for 3 sigma (shaded) for this investigation (mpo = monoclinic pyrrhotite, ipo = intermediate pyrrhotite).

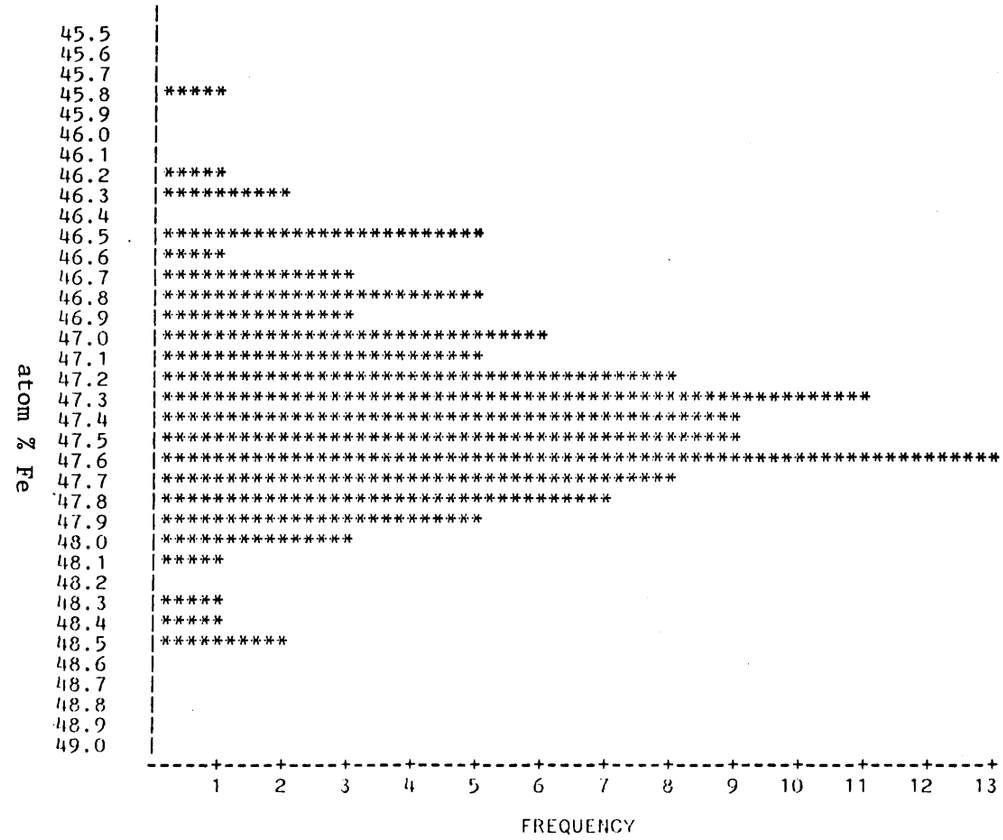

Figure 7.19 Compositional variation of pyrrhotites from Waaikraal (N = 110).

The presence of the two types of pyrrhotite is often clearly visible. Monoclinic pyrrhotite is concentrated as flamelike exsolution bodies in the intermediate pyrrhotite and has a higher reflectivity than the intermediate pyrrhotite. The exsolutions are concentrated at the edges and cracks of pyrrhotite grains.

Pyrite at Waaikraal can often be observed together with pyrrhotite or alone, is usually anhedral and occurs as large grains.

Together with the pyrite, an intermediate product ("Zwischenprodukt" (Ramdohr,1980)) can be observed (Fig. 7.20). This intermediate product consists of a very fine grained aggregate of, most probably, marcasite and pyrite and often forms concentric bodies. It shows distinct reflection pleochroism in white to light grey-green and weak anisotropy under crossed nicols of grey to green colours. According to Ramdohr (1980) the intensity of the anisotropy effects is dependant on the crystallographic orientation of the grain. The presence of the intermediate product suggests the beginning of supergene alteration (Ramdohr, 1980).

7.6 Copper - Bearing Sulfides

Chalcopyrite is the main copper sulfide at Waaikraal and occurs together with almost all the other ore minerals of the deposit, but is more abundant in the pyroxenite than in the magnetite-rich rock.

Chalcopyrite is present as anhedral grains within and between silicates and also as small droplets in sphalerite (Fig. 7.17). It is often associated with gold, which is either attached to or surrounded by it.

A few grains of chalcopyrite analysed by microprobe showed very little chemical variation. Traces of Ni are present. The analyses are presented in Appendix 6.6.

Covellite replaces chalcopyrite as a result of the beginning of supergene alteration and is therefore always associated with it.

7.7. Sphalerite

Sphalerite is present as anhedral grains. It is associated with pyrite and pyrrhotite. "Chalcopyrite disease" (Barton and Bethke, 1987), is common.

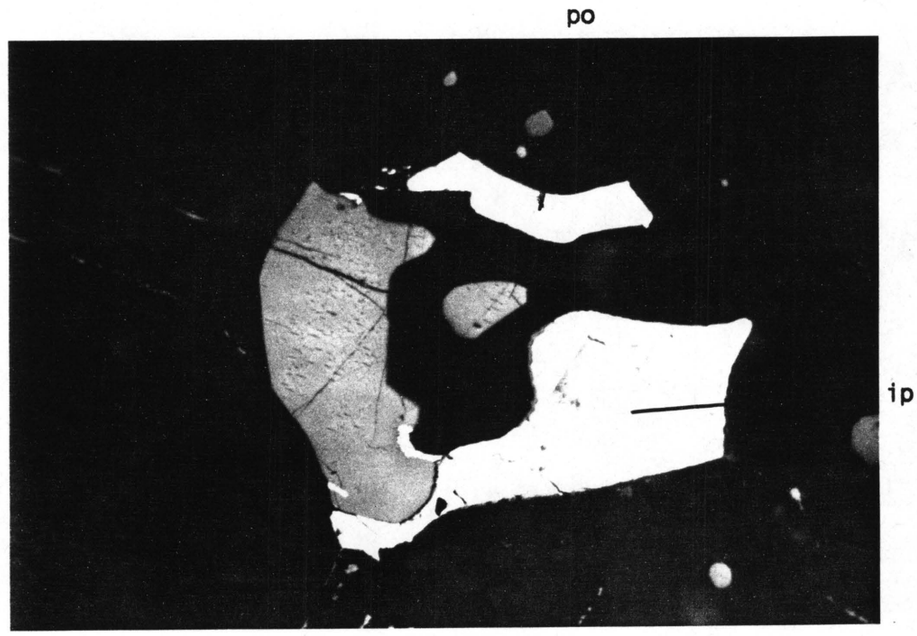

Figure 7.20 Intermediate product ("Zwischenprodukt") (ip) and pyrrhotite (po) in magnetite-rich rock (WK 1).
Photomicrograph: RL, PPL.

7.9 Summary of textural Relations of the Ore Minerals and Approximate Paragenetic Sequence

In the pyroxenite and the magnetite-rich rock from Waaikraal, two assemblages can be distinguished, viz. (i) safflorite, cobaltite, arsenopyrite, joseite, bismuthinite, native bismuth, chalcopyrite and gold and (ii) pyrrhotite, pyrite, chalcopyrite and sphalerite. Generally there is a greater abundancy of ore minerals in the pyroxenite than in the magnetite-rich rock.

In the pyroxenite joseite, together with bismuthinite and native bismuth frequently occurs as fillings of fractures in magnetite or silicate grains, interstitially between magnetite and silicates and also within clinopyroxene. When present within clinopyroxene they are often surrounded by amphibole and might have intruded along cleavage planes.

Safflorite, arsenopyrite and cobaltite are present as small grains interstitially to the silicates and oxides or occur in contact with the joseite, bismuthinite, native bismuth, chalcopyrite and gold.

Joseite was found surrounded by safflorite and vice versa. Native bismuth is frequently enclosed by bismuthinite (Figures 7.8 and 7.9) and cobaltite was found to enclose safflorite (Figures 7.12 and 7.13), both relations indicating a possible increase in sulfur activity during the ore forming processes. A rim of arsenopyrite around cobaltite (Fig.7.2) might be the result of an increase in iron. The large compositional variation of safflorites could indicate that safflorites have formed over a long period of time and/or from a wide variety of fluids during the evolution of the ore body.

Pyrrhotite, pentlandite, pyrite, chalcopyrite and sphalerite rarely occur in the pyroxenite and are generally not in contact with any of the other ore minerals mentioned above. This is probably a high temperature assemblage similar to that described by von Gruenewaldt (1976) and Merkle and von Gruenewaldt (1986) from the upper zone of the Bushveld Complex. Only in one instance was pyrite found to almost enclose an aggregate of arsenopyrite and safflorite, showing that this pyrite represents a later generation than the other ore mineral assemblages.

In the magnetite-rich rock safflorite, arsenopyrite and cobaltite grains are frequently encountered at contacts between magnetite and silicates, at triple junctions between magnetite grains, interstitially to silicates and in fractures of magnetite grains. Joseite, bismuthinite and gold occasionally occur in a similar way. Pyrite, pyrrhotite and chalcopyrite are found as large aggregates, often in contact with magnetite grains and as fillings of fractures. Occasionally chalcopyrite and pyrrhotite occurs as drop-like inclusions in magnetite (Fig. 7.16), which indicates that some of the magnetite must have crystallized after formation of the sulphide droplets.

Massive safflorite was observed in one sample of magnetite-rich rock (WK 52.3). Here maldonite forms droplets in safflorite and $CuAu_3$ is found in contact with the safflorite. Joseite, bismuthinite and gold are encountered within the safflorite, but safflorite also occurs surrounded by joseite and bismuthinite or intergrown with joseite.

From the above described textural relations the following approximate paragenetic sequence is suggested.

Table 7.1 Mineral assemblage and approximate paragenetic sequence at Waaikraal gold deposit.

	Mineralization I	Mineralization II	Supergene alteration
Gold		------	
Maldonite		--	
$CuAu_3$		--	
Safflorite		----------	
Joseite		----------	
Bismuthinite		--------	
native Bismuth		-------	
Cobaltite		----------	
Arsenopyrite		----------	
Chalcopyrite	----------	----------	
Pyrrhotite	----------		
Pentlandite	----------		
Pyrite	----------		----
Sphalerite	------		
Covellite			--
Zwischenprodukt			--

8. CONDITIONS OF ORE FORMATION

The close association of gold with a variety of different disulfides, sulfarsenides, alloys and sulfides allows an attempt to estimate the conditions of ore formation.

The **arsenopyrite** geothermometers and geobarometers described in the literature make use of assemblages containing arsenopyrite together with pyrite, pyrrhotite and loellingite (Clark, 1960, Barton, 1969, Kretschmar and Scott, 1976). At Waaikraal arsenopyrite was not encountered in association with any of these phases and therefore these arsenopyrite geothermometers could not be applied.

An indication of the temperature of formation of the arsenopyrite can, however, be obtained from the temperature stability of solid solutions in the FeAsS - CoAsS - NiAsS ternary diagram as determined at atmospheric pressures by Klemm (1965) (Fig. 8.1).

Analyses of arsenopyrites from Waaikraal plot in areas which indicate temperatures of $< 500^{o}C$. Cobaltites plot in the area of $< 400^{o}C$.

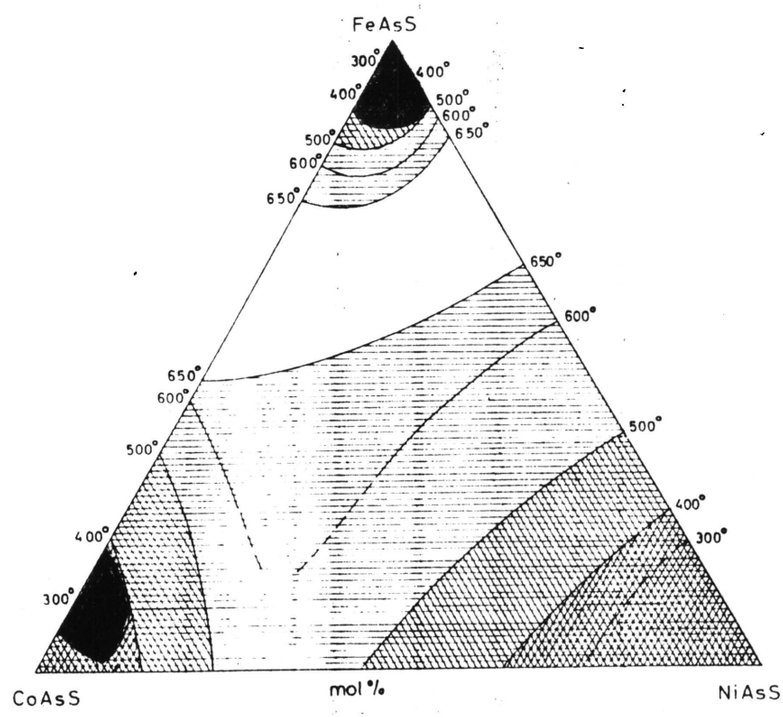

Figure 8.1 The solid solution fields in the ternary diagram FeAsS-CoAsS-NiAsS (after Klemm, 1965), black area : Waaikraal cobaltites and arsenopyrites.

Ripley (1972) could show that **safflorite** of composition $CoAs_2$ was stable from room temperature up to 900°C, $(Co_{0.5},Fe_{0.5})As_2$ was stable from room temperature to 800°C and $FeAs_2$ from room temperature to 700°C. This indicates that an increase in Fe-content results in a lower thermal stability. Waaikraal safflorites vary in composition from $(Co_{0.75}Fe_{0.25})As_2$ to $(Co_{0.04}Fe_{0.96})As_2$, indicating maximum temperature of formation for the Co-rich members of about 850°C and 700°C for the iron-rich members.

Bismuthinite and **native bismuth** often occur together with the gold. These two phases are stable together at a maximum temperature of approximately 880°C (Hansen and Anderko, 1958).

Differential thermal analysis of synthetic **joseite-B** by Yusa et al. (1979) showed an endothermic reaction at 478°C, at which joseite-B melts incongruently to joseite-A, tetradymite and liquid. Joseite-B alone is therefore only stable at temperatures below 478°C.

Maldonite forms at temperatures above 500°C (Böhmke and Varndell, 1986).

Thermal stabilities of **chalcopyrite** were extensively investigated (e.g. Yund and Kullerud, 1966, Barton, 1973 and Cabri, 1973).

The solid solution field of chalcopyrite decreases with decreasing temperature (Yund and Kullerud, 1966), but in the case of hydrothermal deposition of chalcopyrite, there could have been a rapid decrease in temperature as hot solutions entered cooler rocks and a high temperature composition of the chalcopyrite could have been frozen in. Where chalcopyrite occurs with the gold at Waaikraal no other sulfides of the system Cu-Fe-S are present. The composition of the chalcopyrite is very close to $CuFeS_2$. Therefore, the composition of the chalcopyrite from Waaikraal does not give an indication of formation temperature of the chalcopyrite.

Stabilities are summerised in Table 8.1 below.

Table 8.1 Thermal stabilities of ore minerals occuring with gold at Waaikraal

Ore Minerals	Stability Temperature	Source
Cobaltite	< 400°C	Klemm (1965)
Joseite-B	< 478°C	Yusa et al. (1979)
Arsenopyrite	< 500°C	Klemm (1965)
Safflorite (FeAsS)	< 700°C	Ripley (1972)
Safflorite ($(Co_{0.5},Fe_{0.5})As_2$)	< 800°C	Ripley (1972)
Bismuthinite & native Bismuth	< 880°C	Hansen & Anderko(1958)
Safflorite (CoAsS)	< 900°C	Ripley (1972)

The stability data of the ore minerals with which the gold at Waaikraal is associated indicates, that the gold mineralisation for cobaltite bearing assemblages took place at a maximum temperature (400°C).

From the observed mineral associations it is also possible to estimate temperature and sulfur activity conditions, which must have prevailed during deposition of these minerals, with the aid of a sulfur activity versus temperature diagram for joseite-B bearing (joseite-B is present in most gold bearing assemblages at Waaikraal) sulfidation reactions (Fig. 8.2).

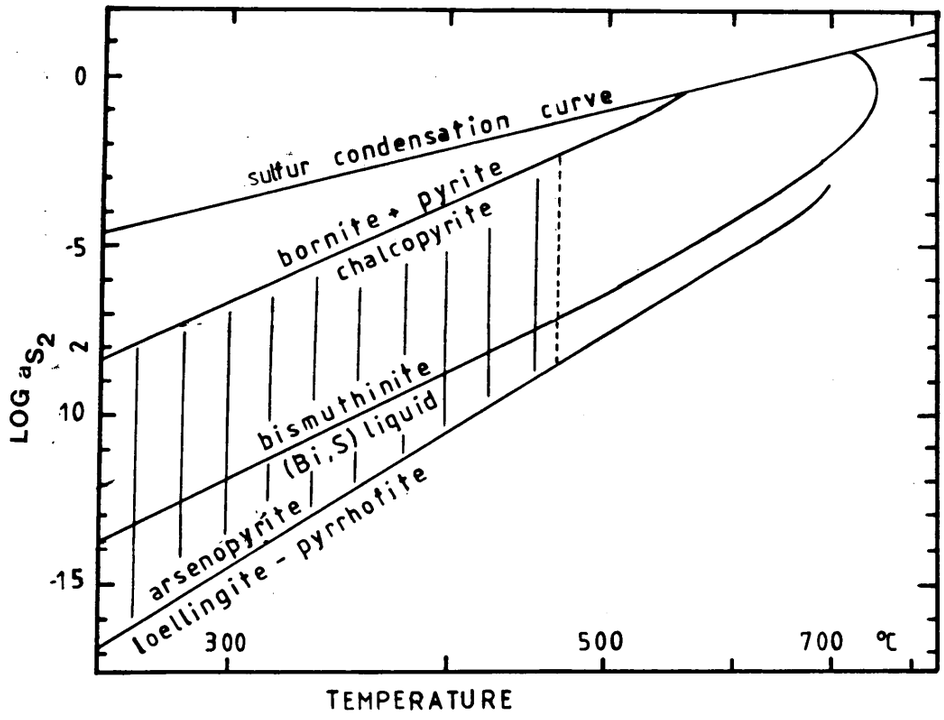

Figure 8.2 Activity of S_2 versus temperature diagram for selected sulfidation reactions (after Barton and Skinner, 1979). Shaded area: principal regime for joseite bearing assemblages from Waaikraal.

The absence of the assemblage loellingite + pyrrhotite and the presence of arsenopyrite in the ore mineral association places the general minimum sulfur activity at which the ore minerals crystallised above the buffer reaction loellingite + pyrrhotite = arsenopyrite in Figure 8.2. But, seeing that chalcopyrite is present without bornite + pyrite in this assemblage, sulfur activities must have been below that of the buffer reaction chalcopyrite = bornite + pyrite. The presence of joseite-B in the association places the maximum temperature of ore formation at 478°C. However, the coexistance of native bismuth and bismuthinite suggests the conditions of formation to have been close to or on the buffer reaction 2 Bi + 1.5 S_2 = Bi_2S_3.

9. POSSIBLE TRANSPORT AND ORIGIN OF THE GOLD

9.1 Hydrothermal Transport of the Gold

The temperature range of formation of the ore minerals associated with the gold (chapter 8) and the mode of occurrence of the gold as small grains and in veinlets suggest a hydrothermal origin of the gold.

Gold is transported by hydrothermal fluids over a wide temperature range, but the temperatures obtained for the mineralizing fluids of most gold deposits are in the range from 175°C to 450°C (Seward, 1984). This agrees well with the maximum temperature of deposition of gold associated with the joseite-B at Waaikraal of 478°C (chapter 8).

Generally, in aqueous systems gold occurs in two oxidation states, Au^{+} and Au^{3+}, but the activity of Au^{3+} is negligible in comparison to that of Au^{+} at 250°C to 400°C and a pH of four (Seward, 1984). It is therefore necessary to decide which of the Au^{+} complexes are of most importance in hydrothermal solutions.

Chloride- and sulfide complexes seem to dominate in hydrothermal solutions, although associated minerals indicate that other complexes are locally also important (Barnes, 1979). Tellurium, bismuth and/or arsenic complexes could indeed have been significant in the case of Waaikraal, if the minerals associated with the gold (e.g. bismuthinite, joseite, arsenopyrite etc.) are taken into consideration. Seward (1973) considers that complexes of the type $Au(Te)_3^{3-}$, $Au_2(Te)^{o}$ and $Au(Te_2)_2^{3-}$ are likely to occur in nature, but he also suggests that arsenothio complexes (e.g. $Au(AsS_2)^{o}$, $Au(AsS_3)^{2-}$) may be of importance, although no experimental data on their stability relations is available.

Chloride- and sulfide complexes of gold have been investigated by, among others, Helgeson and Garrels (1968), Henley (1973) and Seward (1973, 1984).

According to experiments at 25°C reported by Seward (1984) the most stable Au^{+} complexes are $Au(HS)_2^{-}$ and $Au(CN)_2^{-}$, whereas $AuCl_2^{-}$ is less

stable. $Au(HS)_2^-$ is considered by him to be responsible for gold transport in many hydrothermal ore-forming environments, whereas $AuCl_2^-$ will only be dominant in fluids containing high chloride and abnormally low reduced sulfur concentrations, or in fluids with elevated oxidation potential.

Seward (1973), conducted a study of solubility of gold at elevated temperatures and found that considerable quantities of gold may be transported in hydrothermal solutions as thio complexes, particularly in the near neutral pH region, where the $Au(HS)_2^-$ complex predominates at temperatures below 300°C. A decrease in temperature of an ascending ore solution and/or a change in pH would lead to deposition of gold and associated sulfides.

Henley (1973) has studied the solubility of gold in alkali chloride solutions at temperatures above 300°C. He noted that gold is readily soluble in these hydrothermal solutions although its solubility could decrease if other metals (which include most of the ore-metals) are present. Transport of these metals also involve solvation by chloride ligands.

Seeing that the gold at Waaikraal is associated with sulfides and sulfarsenides such as arsenopyrite, cobaltite and chalcopyrite, there is a strong possibility that the gold was transported as sulfide complexes. There are also indications that the fluid became progressively sulfidising during the evolution of the ore body, as is indicated by textural relations, e.g. native bismuth frequently surrounded by bismuthinite (Bi_2S_3) and safflorite ($CoAs_2$) enclosed by cobaltite (CoAsS). A study of the solubility of chalcopyrite in hydrothermal solutions at 200-350°C was conducted by Crerar and Barnes (1976) who concluded that CuCl predominates at 250-350°C, but that bisulfide complexing becomes more important below 250°C in weakly acidic solutions.

Transport of gold as complexes of tellurium, arsenic or bismuth is, because of the association of the gold with joseite, safflorite, cobaltite, arsenopyrite, bismuthinite and native bismuth, also likely, but the lack of experimental data on these complexes inhibits an evaluation of this possibility. There are hardly any hydrothermal solubility data available for arsenides and tellurides (Barnes, 1979). It is therefore not possible to draw any conclusions on the composi-

tion of fluids in which these elements were transported and from which the ore minerals were deposited.

Cole and Drummond (1986) studied the effect of hydrothermal transport and boiling on Ag/Au ratios in solutions. Their transport calculations indicate that low Ag/Au ratios (< 1 as in the case of Waaikraal) result from conditions dominated by low temperature (< 250°C), low Cl^- and moderate to high pH (> 5). Such solutions are dominated by $Au(HS)_2^-$ rather than $AuCl_2^-$. In approximately 90 per cent of cases where Ag/Au < 1, temperatures of 150 - 200°C prevail. Ag/Au ratios > 1 indicate dominance of $AuCl_2^-$ complexes. Shikazono and Shimizu (1987), on the other hand found the opposite relationship between Ag/Au ratios and sulfide- and chloride complexing.

In order to apply the findings of Cole and Drummond and to ascertain whether the Waaikraal ores were deposited under boiling hydrothermal conditions, fluid inclusion studies are required but were unfortunately not possible in the framework of this investigation.

From the available data and the literature it can be concluded that the most likely form of gold transport at Waaikraal was as sulfide complexes in hydrothermal solutions and that the gold, where associated with joseite, was deposited at temperatures below 478°C.

9.2 Platinum-Group Element Content of Selected Waaikraal Rocks and Possible Origin of the Gold

If the gold at Waaikraal is related to the Bushveld Complex, platinum-group elements may have been transported and concentrated together with the gold. Two samples of Waaikraal pyroxenite were therefore submitted for analyses of the platinum-group elements and gold to Sheen Analytical Services Ltd., Perth, Western Australia (Table 9.1).

Table 9.1 Platinum group lement concentrations (in ppb) in Waaikraal pyroxenite (WK 5.2 and WK 6.3, average of two determinations), UG-2 (averages after von Gruenewaldt et al., 1986) and Merensky Reef (MR) (after Barnes et al., 1985), marginal rocks (basaltic and tholeitic suites) (after Davies and Tredoux, 1985) and C-1 chondrites (after Naldrett and Duke, 1980).

	Os	Ir	Ru	Rh	Pt	Pd	Au	PGE/Au
WK 5.2	2	4.75	5.5	1.0	24	3.5	17050	0.002
WK 6.3	5	7.5	8.75	2.0	57.5	6.25	32000	0.003
UG-2	111	157	946	507	2950	1920	56	117.70
MR	63	74	430	240	3740	1530	310	19.60
basaltic	-	0.35	3.0	1.4	17.0	12.0	3.05	11.07
tholeitic	-	0.09	1.5	0.4	11.0	6.0	2.44	7.78
C-1	514	540	690	200	1020	545	152	23.09

The PGE concentrations of the Waaikraal pyroxenite normalised to C-1 chondrite values (Naldrett and Duke, 1980) display a very flat pattern, except for a positive anomaly for Pt (Fig. 9.1). Upper zone rocks from the eastern Bushveld (Harney et al., manuscript in preparation) show a very similar pattern with the exception of Pt, which shows a negative anomaly.

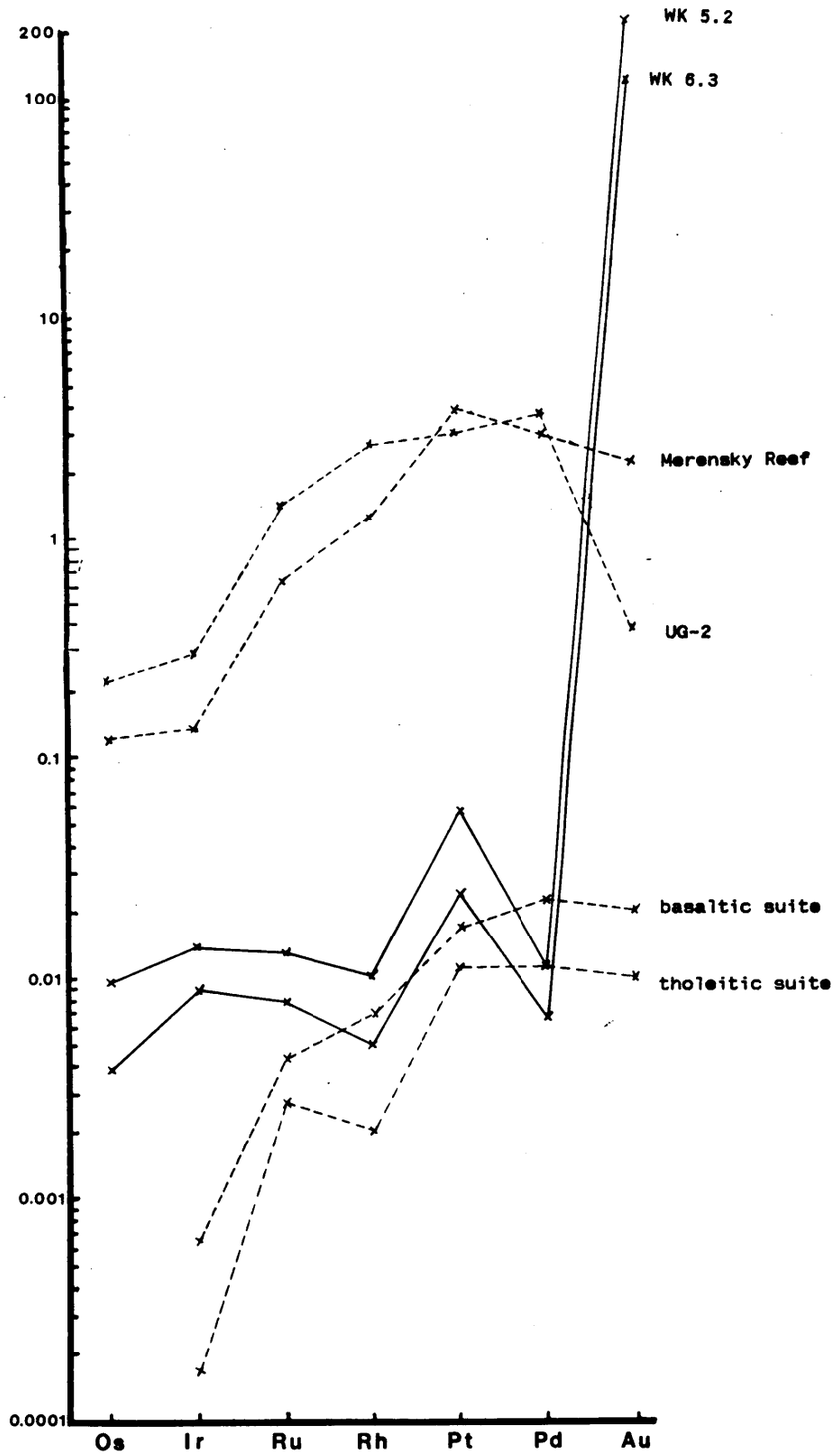

Figure 9.1 Chondrite - normalised PGE and Au concentrations of Waaikraal pyroxenite (WK 5.2 and WK 6.3), UG-2, Merensky Reef and marginal rocks of the Bushveld Complex (basaltic and tholeitic suites) (for sources see Table 9.1).

The gold contents of the UG-2 and, to a lesser degree, the Merensky Reef are depleted relative to the PGE if compared with marginal rocks of the Bushveld Complex (Davies and Tredoux, 1985), which are believed to represent parental magmas of the Complex. It is unlikely that this "depletion" is a function of differences in the respective distribution coefficients.

Naldrett and Duke (1980) give distribution coefficients (D) between coexisting sulfide and silicate liquids of 1000 for Pt and 1500 for Pd. Campbell and Barnes (1984), however, suggest that the distribution coefficients are as high as 10^5. Finstadt and Heier (1972) estimate D for Ir to be >1000 and for Au to be >500, whereas Brett (1971) estimates D_{Au} to be 130. Distribution coefficients of this magnitude (500) are unlikely to cause noticable fractionation of PGE and gold in a magma chamber, because most of the gold, as well as the PGE will be concentrated in the sulfide liquid. Therefore, the depletion of Au relative to the PGE in the UG-2 and the Merensky Reef compared with their suggested parental magma can not be attributed to differences in the distribution coefficient.

Von Gruenewaldt (1976) could demonstrate on the basis of a detailed mineralogical investigation of the upper zone in the eastern Bushveld that the upper 1000 metres of olivine gabbro crystallised from a sulfur oversaturated magma. The numerous immiscible sulfide droplets in these rocks evidently extracted any PGE and Au in the magma, so that it can be assumed that there was no progressive enrichment of gold towards the top of the upper zone. This is also substantiated by the absence of any significant known gold deposits in the roof of the Bushveld Complex. It is therefore assumed that the gold, together with some PGE, rather occurs disseminated throughout the upper zone and was mobilised at the postmagmatic stage by hydrothermal fluids to cause localised enrichments in the roof of the Complex.

Not much data is available on the mobility of the PGE in hydrothermal fluids. Barnes et al. (1985) interpret positive correlations between Au and Pt anomalies in rocks which were subjected to mild talc-carbonate alteration by concomitant mobility of Au and Pt. Schiffries (1982) assumes that a chloride complex can, at least at low temperatures, discriminate between the PGE, leading to a PGE distribution pattern which is highly skewed towards Pt.

As discussed in Chapter 9.1, the gold at Waaikraal was most likely

transported as sulfur complexes. According to Mountain and Wood (1988), Pt and Pd are more likely to be transported as sulfur complexes than as chloride complexes and, if conditions are favourable, Au and Pt could possibly be deposited together from bisulfide solutions. The solubility of Au as a bisulfide complex appears to be many orders of magnitude higher than that of Pt (Mountain and Wood,1988), which is also shown by the small Pt/Au ratio at Waaikraal. No thermodynamic data on bisulfide complexing of the other PGE is available, but, if transport through bisulfide complexing is assumed, their solubilities seem fairly uniform and lower than that for Pt. The positive Pt anomaly of the Waaikraal pyroxenite compared with the negative anomaly of the upper zone rocks from the eastern Bushveld could possibly be explained by the selective transport of some PGE together with the gold in the hydrothermal fluids.

10. THE ORIGIN OF THE GOLD-BEARING PYROXENITE AND MAGNETITE-RICH ROCKS FROM WAAIKRAAL

10.1 Introduction

Comparison of the whole rock composition and trace element content of the pyroxenite and the magnetite-rich rock from Waaikraal with rocks from the upper zone of the Bushveld Complex show that the pyroxenite might have crystallised from a highly differentiated upper zone type liquid (chapter 5.4). This assumption is supported by the compositional similarities of clinopyroxenes, plagioclase and magnetite of Waaikraal pyroxenite and rocks from the topmost part of the upper zone intersected by the Bierkraal borehole (see chapters 6.1, 6.2 and 6.5 respectively).

Seeing that the magnetite grains in the pyroxenite contain exsolution lamellae of ilmenite, whereas the magnetite grains of the magnetite-rich rock do neither contain ilmenite lamellae nor high concentrations of titanium (chapters 3.1.3 and 6.5) different origins for the two rock types at Waaikraal are proposed, although the compositions of the silicates are very similar (chapters 6.1, 6.2 and 6.4).

10.2 Other Ti-Poor Magnetite-Rich Rocks in the Bushveld

Van Biljon (1949) considers certain garnet-magnetite rocks from Zeekoegat, to be the products of hydrothermal solutions which followed and replaced calcareous parts of sediments. The sediments, mainly quartzite and limestone, belong to the same stratigraphic unit as the sediments at Waaikraal (Geological Survey, 1981). The garnet-magnetite is also marked by a very low titanium content (0.40 weight per cent) and except for the Fe-content (which is higher in the magnetite-rich rocks from Waaikraal) and the Ca-content (which is lower than in the garnet-magnetite rock), the whole rock compositions of both rock types are very similar (Table 10.1). The differences can be ascribed to different modal proportions, where the magnetite-rich rock from Waaikraal contains less silicates (clinopyroxene) compared to the garnet-

magnetite rock from Zeekoegat.

Magnetite-rich rock with a low titanium content also occurs in the Dwars River Fragment, a sequence of quartzite, hornfels and metamorphosed dolomitic limestone of the Pretoria Group in the vicinity of Kennedy's Vale, District Lydenburg. The origin of the magnetite-rich rock is not quite clear, but the low titanium content (Table 10.1) points to a sedimentary origin, whereas the presence of garnet suggests a skarn (Van Rensburg, 1962).

Table 10.1 Whole rock composition of a garnet-magnetite rock from Zeekoegat (van Biljon, 1949), magnetite rock from the Dwars River Fragment (van Rensburg, 1962), and the means of Waaikraal magnetite-rich rock for comparison (all iron as Fe_2O_3).

	garnet-magnetite rock	magnetite rock	Waaikraal magnetite-rich rock
SiO_2	29.18	4.82	26.12
TiO_2	0.40	0.20	0.62
Al_2O_3	4.48	4.89	4.77
Fe_2O_3	32.74	54.52	60.87
FeO	5.75	21.34	-
MnO	0.33	1.02	0.56
MgO	0.89	9.09	0.49
CaO	25.51	0.27	10.07
Na_2O	-	-	0.33
K_2O	-	-	0.19
P_2O_5	0.09	0.09	0.04
Cr_2O_3	trace	-	0.09
V_2O_5	-	0.74	-
H_2O^+	0.28	3.00	
H_2O^-	0.10	0.15	
	99.75	100.13	104.15

10.3 Sedimentary Origin of the Magnetite-Rich Rocks

The two most important varieties of iron-rich sediments are banded iron formations and oolitic ironstones (Maynard, 1983). Amongst the banded iron formations, two types are dominant: Algoma- and Lake Superior type deposits (Gross, 1980). The presence of clinopyroxenes in metamorphic iron formations has been described by Kranck (1961) and Immega and Klein (1976), but clinopyroxene generally occurs together with Fe-rich orthopyroxene in these rocks.

The means of major- and trace elements of the magnetite-rich rocks from Waaikraal (Tables 5.1 and 5.2) are compared with these two types of iron formations Figure 10.1.

Typical goethitic, hematitic, chamositic and sideritic ironstones were normalised to Waaikraal magnetite-rich rock and plotted in Figure 10.2. Unfortunately, only major element data could be obtained for the different oolitic ironstones.

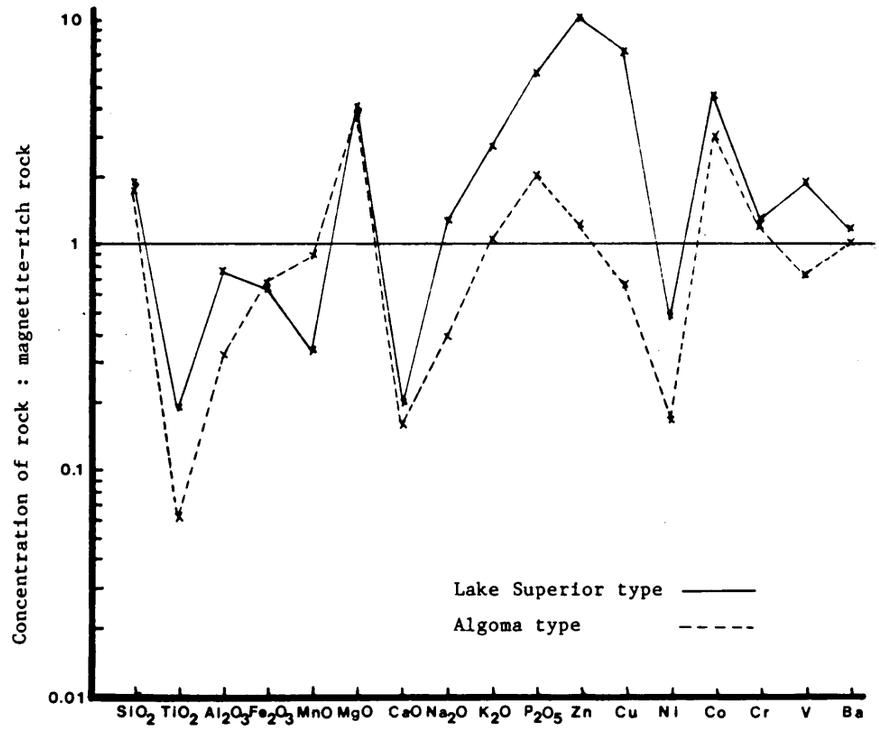

Figure 10.1 Average major- and trace element concentration of Algoma- and Lake Superior type iron formation (after Gross, 1980) normalised to Waaikraal magnetite-rich rock.

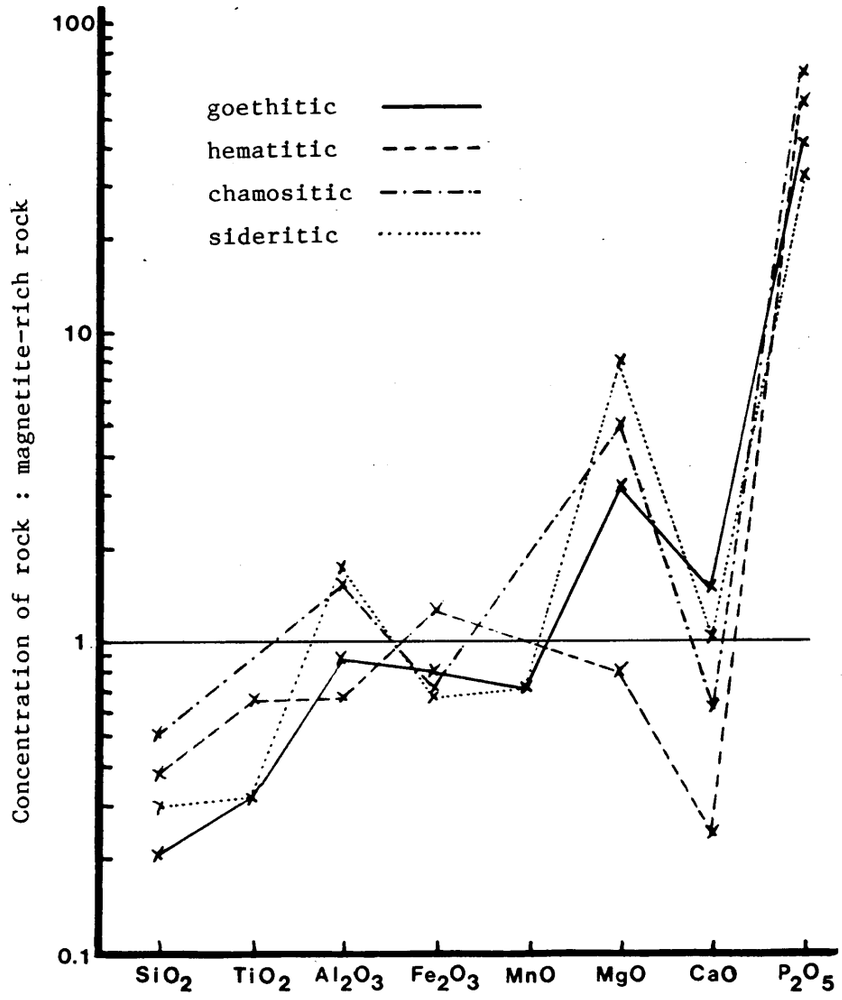

Figure 10.2 Average major element concentration of typical goethitic, hematitic, chamositic and sideritic ironstones (after Maynard, 1983) normalised to Waaikraal magnetite-rich rock.

Figures 10.1 and 10.2 show that there are significant compositional differences between the magnetite-rich rock from Waaikraal and typical ironstones as well as between Waaikraal magnetite-rich rock and iron formations. It is therefore unlikely that the magnetite-rich rock at Waaikraal can be considered as an original iron-rich sediment.

10.4 Skarn Origin of the Magnetite-Rich Rock

According to Verkaeren and Bartholomé (1979) it is well known that iron oxide deposits may form in the vicinity of an intrusive as a result of iron being introduced into a limestone by metasomatic fluids. The magnetite-rich rock from Waaikraal might therefore represent a skarn, which could have evolved along the common pattern of a skarn (Einaudi et al., 1981); viz:

(1) isochemical contact metamorphism accompanying emplacement of the magma;
(2) metasomatism (skarn formation) accompanying crystallisation of the magma and evolution of the ore fluid;
(3) retrograde alteration and ore deposition accompanying final cooling of the system;

A skarn origin of the magnetite-rich rock from Waaikraal is supported by the presence of typical skarn minerals such as hedenbergite (see capter 6.1), magnetite and ilvaite (see chapter 3.1.3) and the metal association of Co, Cu, As and Au with Fe. The magnetite-rich rock could be classified as a calcic iron-skarn as described by Zharikov (1970) and Einaudi and Burt (1982), derived from sediments through metasomatism by iron-rich fluids.

In order to determine whether the magnetite-rich rock does indeed represent metasomatised sediments, it has to be established whether any evidence for the "original sediment", that is the sediment before introduction of iron-rich fluids, can be found.

Calc-silicates and quartzite occur in the vicinity of Waaikraal gold mine and shale has been described by van Biljon (1949) and Visser (1969) to be present in the Rayton Formation. These three sediment types and a combination of shale with calc-silicate were selected as potential "original sediments". Average whole rock compositions of the calc-silicates and quartzites from Waaikraal as well as the composition of a shale from Zeekoegat (van Biljon, 1949) are presented in Table 10.2.

In order to deduce an "original sediment" composition from the magnetite-rich rocks, the iron content of the average whole rock composition of the Waaikraal magnetite-rich rock is made equal to the respective iron content of the sediments. The concentration of the remaining elements in the magnetite-rich rocks were than increased proportionally to yield the recalculated analyses of the Waaikraal magnetite-rich rock in Table 10.2. The compositions of the calc-silicate, quartzite, shale and mixture of shale and calc-silicate are then normalised to the respective adjusted compositions of the magnetite-rich rock and plotted in Figure 10.3.

Table 10.2 Average whole rock composition of Waaikraal calc-silicate (N = 4) (WK-CS), Waaikraal quartzite (N = 9) (WK-QZ), shale from Zeekoegat (van Biljon ,1949) and a combination (1 : 1) of calc-silicate and shale; together with their respective recalculated (as described in chapter 10.4) magnetite-rich rock from Waaikraal.

	WK-CS	WK-QZ	Shale	WK-CS + Shale
SiO_2	51.10	84.41	57.8	54.45
TiO_2	0.10	0.13	0.8	0.45
Al_2O_3	1.33	4.06	19.3	10.32
Fe_2O_3	2.16	4.41	8.5	5.33
MnO	0.28	0.10	0.07	0.18
MgO	0.51	0.88	1.2	0.86
CaO	43.89	3.57	0.3	22.10
Na_2O	<1.l.d.	1.01	1.0	0.50
K_2O	0.06	1.50	5.1	2.58
P_2O_5	0.15	0.14	0.02	0.09
Cr_2O_3	0.08	0.10	-	0.04
recalculated Waaikraal magnetite-rich rock				
SiO_2	59.05	57.69	55.22	57.13
TiO_2	1.40	1.37	1.31	1.36
Al_2O_3	10.78	10.54	10.08	10.43
Fe_2O_3	2.16	4.41	8.5	5.33
MnO	1.26	1.24	1.18	1.22
MgO	1.11	1.08	1.04	1.07
CaO	22.76	22.24	21.29	22.03
Na_2O	0.75	0.73	0.70	0.72
K_2O	0.43	0.42	0.40	0.42
P_2O_5	0.09	0.09	0.08	0.09
Cr_2O_3	0.20	0.20	0.19	0.20

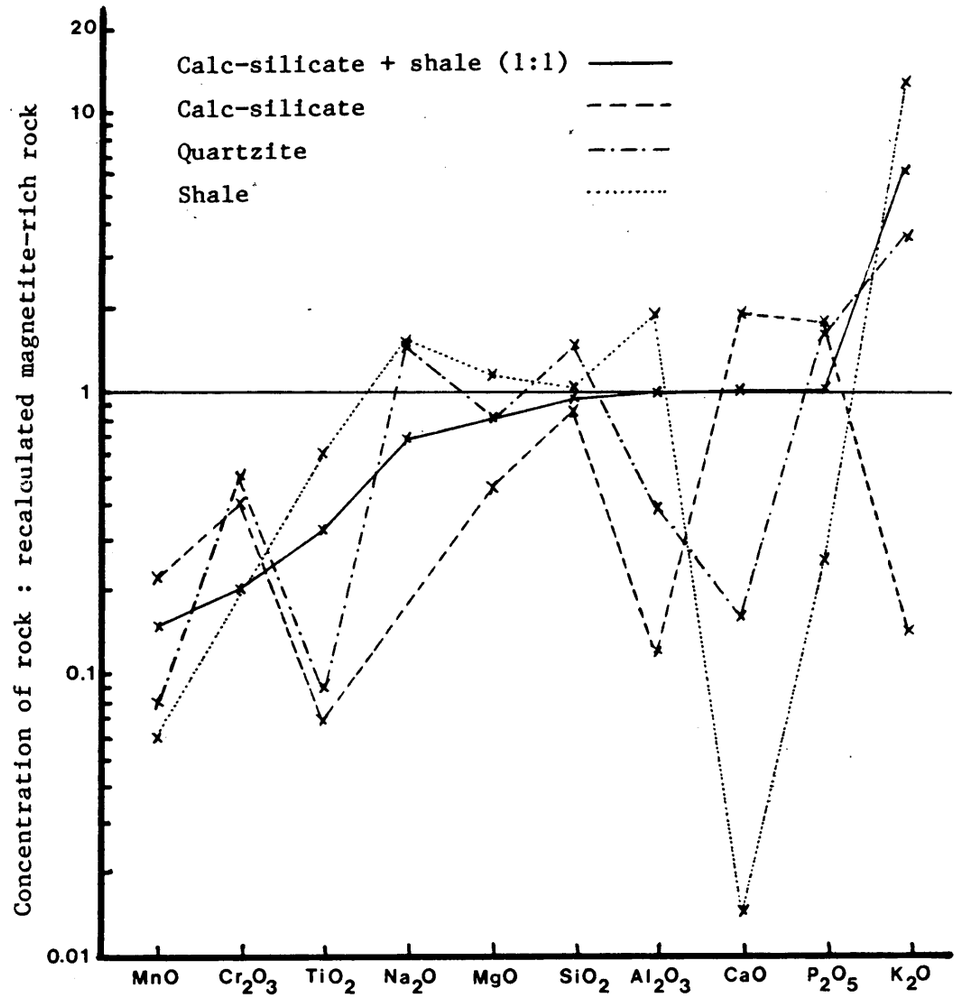

Figure 10.3 Average major element concentration of Waaikraal calc-silicate, Waaikraal quartzite, shale from Zeekoegat (van Biljon, 1949) and a combination of shale and calc-silicate (1 : 1) normalised to their respective recalculated (as described in chapter 10.3) Waaikraal magnetite-rich rock.

Figure 10.3 shows that the "original sediment", from which the magnetite-rich rock might have formed is most likely a combination of equal parts of shale and calc-silicate. CaO, P_2O_5, SiO_2, MgO, Al_2O_3 and Na_2O contents compare very well. K_2O is enriched in the sediment compared with the recalculated magnetite-rich rocks, possibly reflecting a smaller than average proportion of clay minerals in the unmetasomatised sediment or a potassium loss during metamorphism and hydrothermal activity. MnO was most likely transported together with the iron, but was not recalculated in the same way, causing the larger amount of MnO present in the recalculated magnetite-rich rocks. Cr_2O_3 is present in concentrations close to the detection limit, where small errors can cause large differences in comparative studies of this nature. TiO_2 is twice as high in the recalculated magnetite-rich rocks compared with the sediment, but the actual difference is only 0.91 weight per cent.

10.5 Conclusion

In conclusion it is favoured that the pyroxenite is related to the upper zone of the Bushveld Complex and that it crystallised from a highly differentiated upper zone type liquid, which was injected into the host rocks during the final stages of consolidation of the upper zone. The host rock probably consisted of a marl, with a composition equivalent to equal parts of shale and limestone. The latter recrystallised to calc-silicate rock during the emplacement of the Bushveld Complex. Introduction of the highly fractionated iron-rich liquids into the host rock gave rise to the pyroxenite and to conditions favourable for reconstructing the marl into the magnetite-rich rock.

11. SUMMARY AND CONCLUSION

The gold at Waaikraal occurs in a sill-like body of alternating layers and lenses of pyroxenite and magnetite-rich rock, hosted in sediments belonging to the Rayton Formation of the Transvaal Sequence. The sediments are situated between the magnetite gabbros of the upper zone of the Bushveld Complex and the granites of the Lebowa Granite Suite.

Clinopyroxene (hedenbergite and augite) with inclusions of amphibole (mainly hastingsite and hastingsitic hornblende) is the major constituent of the pyroxenite. Plagioclase (mainly andesine) and quartz occur interstitially. Magnetite with abundant exsolution lamellae of ilmenite, but frequently also spinel occurs as discrete grains. Accessory minerals are calcite, apatite and occasionally prehnite. The magnetite-rich rock consists mainly of magnetite and clinopyroxene (hedenbergite and augite). The magnetite does not contain any ilmenite exsolution lamellae, although spinel exsolutions occur throughout many of the grains. The clinopyroxene does not contain any inclusions of amphibole. Small clinopyroxene grains can be found within magnetite grains and vice versa. Plagioclase (mainly andesine) occurs interstitially. Abundant olivine (fayalite) was found in one sample and ilvaite was encountered in several samples of magnetite-rich rock. It is present together with primary and secondary magnetite and sometimes chlorite. An accessory mineral is apatite.

The sediments, which host the ore body are mainly quartzite and pyroxene hornfels. Calc-silicate hornfels (mainly wollastonite and garnet) occurs in places. The most abundant constituent of the magnetite gabbro exposed close to the deposit is plagioclase. Clinopyroxene, orthopyroxene, orthoclase and magnetite occur interstitially. Due to the lack of exposure of the topmost differentiates of the Bushveld Complex, rocks (ferrodiorite and ferrogabbro) from the top of the Bierkraal 1 borehole were used for comparison.

The mineralogical differences of the pyroxenite and the magnetite-rich rock are reflected in Spearman correlation matrices, which were obtained of whole rock- and trace element composition for each rock type separately. The modified Tukey test (Neave, 1979) also established, that there are significant differences between the two rock

types, which can readily be explained by the different mineralogy.

Comparison of the compositions of Waaikraal pyroxenite, magnetite-rich rock, magnetite gabbro and the topmost differentiates from the Bushveld Complex, revealed that the magnetite gabbro, exposed close to the deposit, belongs to stratigraphically lower part of the upper zone than the samples taken from the Bierkraal borehole. This is supported by the compositions of the clinopyroxene and the plagioclase. The magnetite-rich rocks are, compared to those from Bierkraal, depleted in most elements except for Fe, V, Cr, Ni, and to a lesser extend Ca, Mn, Nb and Y, which reflect the much larger amount of magnetite in the former. Interesting to note, however, is the low TiO_2 content, in spite of the large amounts of magnetite in the magnetite-rich rock. The resemblance between the rocks from Bierkraal and the pyroxenite is generally closer than between the latter and the magnetite gabbro. The plot $MgO/(MgO+Fe_2O_3)$ versus $Rb/(K_2O+Na_2O)$ (Fig.5.2) indicates that the pyroxenites from Waaikraal are more differentiated rocks than the topmost differentiates of the upper zone intersected by the Bierkraal borehole.

Analyses of mineral compositions showed that the composition of the clinopyroxene of the pyroxenite and the magnetite-rich rock overlap and plot on the boundary of the hedenbergite and augite fields of the pyroxene quadrilateral. The composition of the plagioclase of the pyroxenite as well as the magnetite-rich rock varies considerably from grain to grain within one thin section, with the majority of compositions around An_{30-50}. All amphibole in the pyroxenite fall into the calcic amphibole group according to the classification of Leake (1978). Most of the analyses can be termed hastingsite and hastingsitic hornblende, although a few analyses fall into the compositional fields for ferro-edenite, ferro-edenitic hornblende, ferro-actinolite and ferro-hornblende (Fig. 6.3). The ranges of composition of the magnetite itself in the two rock types of the ore body overlap. The magnetite in the pyroxenite, however contains 10-30 volume per cent ilmenite exsolution, indicating an overall much higher Ti-content of the magnetite/ilmenite grains as a whole. The composition of the magnetite varies considerably, evidently in response to the amount of ulvospinel in either solid solution or as tiny exsolutions in the magnetite. The composition of the Waaikraal magnetite of both rock types corresponds best with the magnetites from the topmost rocks of

the upper zone (Fig. 6.6).

In the pyroxenite and magnetite-rich rock from Waaikraal, two assemblages of ore minerals can be distinguished, viz. (i) safflorite, arsenopyrite, cobaltite, joseite, bismuthinite, native bismuth calcopyrite and gold and (ii) pyrrhotite, pyrite, chalcopyrite and sphalerite. The first group represents the later generation. Generally there is a greater abundance of ore minerals in the pyroxenite than in the magnetite-rich rock. Apart from very pure native gold, two gold bearing compounds occur. These are maldonite (Au_2Bi) and $CuAu_3$. The most frequent encounterd bismuth-bearing mineral is joseite-B (Bi_4Te_2S), but bismuthinite (Bi_2S_3) also occurs, often surrounding native bismuth. The composition of the safflorite varies from loellingite- ($FeAs_2$) to safflorite ($CoAs_2$) -rich members with up to 8 mole per cent $NiAs_2$. Cobaltite (CoAsS) and arsenopyrite (FeAsS) were the only sulfarsenides found to occur in the Waaikraal deposit. Chalcopyrite is the main copper-bearing sulfide and occurs together with almost all of the other ore minerals of the deposit. It is also present as small droplets in sphalerite. Intermediate and monoclinic pyrrhotite (the intermediate phase is dominant) is often found together with pyrite and chalcopyrite.

The close association of gold with a variety of different ore minerals allows to estimate the temperature conditions of ore formation. The available literature indicates the following maximum temperatures of formation: arsenopyrite 500°C, cobaltite 400°C, safflorite 850°C, bismuthinite + native bismuth 880°C and joseite-B 478°C.

The temperature range of formation of the ore minerals associated with the gold and the mode of occurrence of the gold as small grains and in veinlets suggests a hydrothermal origin of the gold. Seeing that the gold at Waaikraal is associated with sulfides and sulfarsenides such as arsenopyrite, cobaltite and chalcopyrite, there is a strong possibility that the gold was transported as sulfide complexes. There are also indications that the fluid became progessively sulfidizing during the evolution of the ore body, as is indicated by textural relations, e.g. native bismuth frequently surrounded by bismuthinite and safflorite enclosed by cobaltite.

Platinum-group element analyses of two samples of pyroxenite from Waaikraal revealed that the C-1 chondrite normalized pattern is very flat, except for a positive anomaly for Pt. The concentration of PGE

is very low. It is assumed that the gold, together with some PGE occurs dissiminated throughout the upper zone of the Bushveld Complex and was mobilized at the postmagmatic stage by hydrothermal fluids to cause localized enrichments in the roof of the complex.

Comparison of the whole rock composition and trace element content of the pyroxenite and the magnetite-rich rock with rocks from the upper zone of the Bushveld Complex shows that the pyroxenite might have crystallized from a highly differentiated upper zone type liquid. This assumption is supported by the compositional similarities of clinopyroxene, plagioclase and magnetite of Waaikraal pyroxenite and rocks from the topmost part of the upper zone intersected by the Bierkraal borehole. Seeing that the magnetite grains of the magnetite-rich rock do neither contain ilmenite exsolution lamellae, nor high concentrations of titanium, in contrast to the magnetite grains of the pyroxenite, a different, possibly sedimentary origin of the magnetite-rich rock is proposed. Comparison of the magnetite-rich rock with the two most important varieties of iron-rich sediments (banded iron formation and oolitic iron stones) revealed that there are significant differences between the composition of the magnetite-rich rock from Waaikraal and those sediments. It is therefore unlikely that the magnetite-rich rock can be considered as an original iron-rich sediment. A skarn origin of the magnetite-rich rock is supported by the presence of typical skarn minerals such as hedenbergite, ilvaite and magnetite and the metal association of Co, Cu, As and Au with Fe. Comparison of the magnetite-rich rock with quartzite, shale, calc-silicate and a combination of shale and calc-silicate, after equating the iron content of the average whole rock composition of the magnetite-rich rock with the iron content of the sediments, showed that the "original sediment" most likely was a marl with a composition equivalent to equal parts of shale and limestone.

REFERENCES

ATKINS, F.B. (1969) Pyroxenes of the Bushveld Intrusion, South Africa. **Journal of Petrology 10,** 222-249.

BARNES, S.-J., NALDRETT, A.J. and M.P. GORTON (1985) The origin of the fractionation of platinum-group elements in terrestrial magmas. **Chemical Geology 53,** 303-323.

BARNES, H.L. (1979) Solubility of ore minerals. **In: Barnes, H.L., (Ed.) Geochemistry of Hydrothermal Ore Deposits.** John Wiley & Sons, 404-460.

BARTON, P.B., Jr. (1969) Thermochemical study of the system Fe-As-S **Geochimica et Cosmochimica Acta 33,** 841-857.

BARTON, P.B., Jr. (1973) Solid solutions in the system Cu-Fe-S. Part I The Cu-S and CuFe-S joins. **Economic Geology 68,** 455-465.

BARTON, P.B., Jr. and P.M. BETHKE (1987) Chalcopyrite disease in sphalerite: Pathology and epidemiology. **American Mineralogist 72,** 451-467.

BARTON, P.B. Jr. and B.J. SKINNER (1979) Sulfide mineral stabilities. **In: Barnes, H.L., (Ed.) Geochemistry of Hydrothermal Ore Deposits.** John Wiley & Sons, 278-403.

BERRY, L.G. and R.M. THOMPSON (1962) X-ray powder data for ore minerals. **Geological Society of America, Memoir 85.**

BÖHMKE, F.C. and B.J. VARNDELL (1986) Gold in granulites at Renco Mine, Zimbabwe. **In: Anhaeuser, C.R. and S. Maske (Eds.), Mineral Deposits of South Africa, Volumes I and II, Geological Survey of South Africa, Johannesburg,** 221-230.

BRETT, R. (1971) The earth's core: speculations on its chemical equilibrium with the mantle. **Geochimica et Cosmochimica Acta 35,** 203-221.

BURT, D.M. (1971) Multisystems analyses of the relative stabilities of babingtonite and ilvaite. **Carnegie Institution Washington, Yearbook 70,** 189-195.

CABRI, L.J. (1973) New data on phase relations in the Cu-Fe-S system. **Economic Geololgy 68,** 443-454.

CAMPBELL, I.H. and S.J. BARNES (1984) A model for the geochemistry of the platinum-group elements in magmatic sulfide deposits. **Canadian Mineralogist 22,** 151-160.

CARPENTER, R.H. and G.A. DESBOROUGH (1964) Range in solid solution and structure of naturally occuring troilite and pyrrhotite. **American Mineralogist 49,** 1350-1365.

CLARK, L.A. (1960) The Fe-As-S system: Phase relations and applications. **Economic Geology 55,** 3345- 3381 and 1631- 1652.

COLE, D.R. and S.E. DRUMMOND (1986) The effect of transport and boiling on Ag/Au ratios in hydrothermal solutions: a preliminary assessment and possible implications for the formation of epithermal precious-metal ore deposits. **Journal of Geochemical Exploration 25,** 45-79.

CRERAR, D.A. and H.L. BARNES (1976) Ore solution chemistry V. Solubilities of chalcopyrite and chalcosite assemblages in hydrothermal solution at 200° and 350°C. **Economic Geology 71,** 772-794.

DAVIES, G. and M. TREDOUX (1985) The platinum-group elements and gold contents of the marginal rocks of the Bushveld Complex. **Economic Geology 80,** 838-848.

DEER, W.A., HOWIE, R.A. and J. ZUSSMAN (1977) **An Intoduction to Rock Forming Minerals.** Longman Group Limited, London, 528 pages.

EINAUDI, M.T., MEINERT, L.D. and R.J. NEWBERRY (1981) Skarn deposits. **Economic Geology 75th Anniversary Volume,** 317-391.

EINAUDI, M.T. and D.M. BURT (1982) Introduction - terminology, classification and composition of skarn deposits. **Economic Geology 77,** 745-754.

FINSTADT, K.G. and K.S. HEIER (1972) The distribution of some elements between the metal and silicate phases obtaines in a smelting reduction process of dunite from Almklovdalen, West Norway, **Earth and Planetary Science Letters 16,** 209-212.

GEOLOGICAL SURVEY (1981) Geological Sheet 2526 (Rustenburg) 1:250 000, **Geological Survey of South Africa.**

GIESE, R.F. and P.F. KERR (1965) The crystal structures of ordered and disordered cobaltite. **American Mineralogist 50,** 1002-1014.

GROSS, G.A. (1980) A classification of iron formation based on depositional environments. **Contributions to Mineralogy and Petrology 18,** 215-222.

GULYAEVA, T.YA., GORELIKOVA, N.V. and A. KARABTSOV (1986) High potassium-chlorine bearing hastingsites in skarn from Primorge, Far East USSR. **Mineralogical Magazine 50,** 724-728.

HANSEN, M. and K. ANDERKO (Eds.) (1958) **Constitution of Binary Alloys.** McGraw-Hill Book Company, Inc., 1305 pages.

HELGESON, H.C. and R.M. GARRELS (1968) Hydrothermal transport and deposition of gold. **Economic Geology 63,** 622-635.

HENLEY, R.W. (1973) Solubility of gold in hydrothermal chloride solutions. **Chemical Geology 11,** 73-87.

HOLMES, R.J. (1947) Higher mineral arsenides of cobalt, nickel and iron. **Geological Society of America, Bulletin 58,** 299-392.

IMMEGA, I.P. and C. KLEIN (1976) Mineralogy and petrology of some metamorphic precambrian iron-formations in Southwestern Montana. **American Mineralogist 61,** 1117-1144.

KAISER, H. and H. SPECKER (1956) Bewertung und Vergleich von Analysenverfahren. **Zeitschrift für Analytische Chemie 149,** 46-66.

KLEMM, D.D. (1965) Synthesen und Analysen in den Dreiecksdiagrammen FeAsS-CoAsS-NiAsS und FeS_2-CoS_2-NiS_2. **Neues Jahrbuch für Mineralogie, Abhandlungen 103,** 205-255.

KRANCK, S.H. (1961) A study of phase equilibria in a metamorphic iron formation. **Journal of Petrology 2,** 137-184.

KRETSCHMAR, U. and S.D. SCOTT (1976) Phase relations involving arsenopyrite in the system Fe-As-S and their application. **Canadian Mineralogist 14,** 364-386.

LEAKE, B.E. (1978) Nomenclature of amphiboles. **American Mineralogist 63,** 1023-1052.

MARKGRAAF, J. (1976) Pyroxenes of the Western Bushveld Complex, South Africa, **Transactions of the Geological Society of South Africa 79,** 217-224.

MAYNARD, J.B. (1983) **Geochemistry of Sedimentary Ore Deposits.** Springer Verlag, New York Inc., 305 pages.

MERKLE, R.K.W. and G. VON GRUENEWALDT (1986) Compositional variation of Co-rich pentlandite: Relation to the evolution of the upper zone of the eastern Bushveld Complex, South Africa. **Canadian Mineralogist 24,** 529- 546.

MOORHOUSE, W.W. (1959) **The Study of Rocks in Thin Section.** Harper & Row, Publishers, New York and Evanston, 514 pages.

MORIMOTO, N., GYOBU, A. MUKAIYAMA, H. and E. ZZAWA (1975) Crystallography and stability of pyrrhotites. **Economic Geology 70,** 824-833.

MORIMOTO, N. Chairman Subcomittee on Pyroxenes I.M.A. (1988) Nomenclature of pyroxenes. **Mineralogical Magazine 52,** 535-550.

MOUNTAIN, B.W. and S.A. WOOD (1988) Solubility of platinum-group elements in hydrothermal solutions: Thermodynamic and physical chemical constraints. **In: H.M. Prichard et al. (Eds.) Geo-Platinum 87,** Elsevier Applied Science, London and New York, 57-82.

NALDRETT, A.J. and J.M. DUKE (1980) Platinum metals in magmatic sulfide ores. **Science 208, Number 4451,** 1417-1424.

NEAVE, H.R. (1979) Quick and simple tests based on extreme observations. **Journal of Quality Technology 11,** 66-79.

NORRISH, K. and J.T. HUTTON (1969) An accurate X-ray spectrographic method for the analysis of a wide range of geological samples. **Geochimica et Cosmochimica Acta 33,** 431-453.

OEN, I.S. and C. KIEFT (1974) Nickeline with pyrrhotite and cubanite exsolutions, Ni-Co-rich loellingite and an Au-Cu-alloy in Cr-Ni-ores from Beni-Bousera, Morocco. **Neues Jahrbuch für Mineralogie, Monatshefte 1,** 1-8.

RADCLIFFE, D. and L.G. BERRY (1968) The safflorite-loellingite solid solution series. **American Mineralogist 53,** 1856-1881.

RADCLIFFE, D. and L.G. BERRY (1971) Clinosafflorite: a monoclinic polymorph of safflorite. **Canadian Mineralogist 10,** 877-881.

RAMDOHR, P. (1980) **The Ore Minerals and their Intergrowths. 2nd ed., Volume 1 and 2.** Pergamon Press, 1207 pages.

REYNOLDS, I.M. (1985) Contrasted mineralogy and textural relationships in the uppermost titaniferrous magnetite layers of the Bushveld Complex in the Bierkraal area north of Rustenburg. **Economic Geology 80,** 1027-1048.

RIPLEY, L.G. (1980) Crystal growth part IV: The arsenides and sulpharsenides of cobalt, iron and nickel. **Departement of Energy, Mines and Resouces, Mines Branch., Ottawa-Mineral Science Division, Sulphide Research Contribution No.56, Research Report R238.** 112 pages.

ROSEBOOM, E.H. (1963) Co-Ni-Fe diarsenides: compositions and cell dimensions. **American Mineralogist 48,** 271-299.

SOUTH AFRICAN COMMITTEE FOR STRATIGRAPHY (SACS) (1980) **Stratigraphy of South Africa, Part I (Comp. L.E. Kent) Lithostratigraphy of the Republic of South Africa, South West Africa/Namibia, and the Republics of Bophutatswana, Transkei and Venda.** South Africa, Geological Survey, Handbook 8, 690 pages.

SCHIFFRIES, C.M. (1982) The petrogenesis of a platiniferous dunite pipe in the Bushveld Complex: Infiltration metasomatism by a chloride solution. **Economic Geology 77,** 1439-1453.

SEWARD, T.M. (1973) Thio complexes of gold in the transport of gold in hydrothermal ore solutions. **Geochimica et Cosmochimica Acta 37,** 379-399.

SEWARD, T.M. (1984) The transport and deposition of gold in hydrothermal systems. **In: Forster, R.P. (Ed) Gold '82: The Geology, Geochemistry and Genesis of Gold Deposits. Geological Society of Zimbabwe, special Publication No.1,** A.A. Balkema, Rotterdam, 165-181.

SHIKAZONO, N. and M. SHIMIZU (1987) The Ag/Au ratio of native gold and electrum and the geochemical environment of gold vein deposits in Japan. **Mineralium Deposita 22,** 309-314.

SPEAR, F.S. and K.L. KIMBALL (1984) RECAMP - a Fortran IV program for estimating Fe^{3+} contents in amphiboles. **Computer and Geosciences 10,** 317-325.

SWASH, P.M. (1983) Mineralogical examination of the Moorcroft Reef Waaikraal No. 396JQ. **Confidential Communication No. C244M, Council for Mineral Technology, Randburg.**

TOBSCHALL, H.J. (1975) Geochemische Untersuchungen zum stofflichen Bestand und Sedimentationsmilieu paläozoischer mariner Tone: Die Gehalte der Hauptelemente und Spurenelemente Ni, Cu, Zn, Rb, Sr, Y, Zr, Nb und Ba in den Steiger Schiefern (Vogesen). **Chemie der Erde 34,** 105-167.

TRÖGER, W.E. (1969) **Optische Bestimmung der gesteinsbildenden Minerale, Teil 2.** E. Schweizerbart´sche Verlagsbuchhandlung. Nägele und Obermiller, Stuttgart, 822 pages.

VAN BILJON, S. (1949) The transformation of the upper part of the Pretoria Series in the Bushveld Igneous Complex. **Transactions and Proceedings of the Geological Society of South Africa 52,** 1-197.

VAN BILJON, S. (1974) Transformation and deformation of the Pretoria Series in the south-western part of the Bushveld Complex. **Transactions of the Geological Society of South Africa,** 17-29.

VAN RENSBURG, W.C.J. (1962) **The Geology of the Dwars River Fragment and the Ore - Minerals of the Magnetite Deposit on Kennedy´s Vale 361KT, Eastern Transvaal.** unpublished MSc Thesis, University of Pretoria, South Africa, 94 pages.

VERKAEREN, J. and P. BARTHOLOME´ (1979) Geology of the San Leone magnetite skarn deposit (S.W. Sardinia). **Economic Geology 74,** 53-66.

VISSER, J.N.J. (1969) **´n Sedimentologiese Studie van die Serie Pretoria in Transvaal.** Unpublished DSc Thesis, University of the Orange Free State, South Africa, 263 pages.

VON GRUENEWALDT, G. (1976) sulfides in the upper zone of the Bushveld Complex. **Economic Geology 71,** 1324-1336.

VON GRUENEWALDT, G., HATTON, C.J., MERKLE, R.K.W. and S.B. GAIN (1986) Platinum-group element - chromitite associations in the Bushveld Complex. **Economic Geology 81,** 1067-1079.

WAGNER, P.A. (1926a) A new gold discovery in the Rustenburg district, Transvaal. **Transactions of the Geological Society of South Africa 29,** 95-108.

WAGNER, P.A. (1926b) Supplementary note on a new gold discovery in the Rustenburg district, Transvaal. **Transactions of the Geological Survey of South Africa 29,** 141-143.

WESTON, S. (1980) Report on gold deposit Waaikraal 396JQ. **Bophutatswana Geological Survey Report.**

WESTON, S. (1981) Report on drilling operations at gold deposit Waaikraal 396JQ. **Bophutatswana Geological Survey Report.**

YUND, R.A. and G. KULLERUD (1966) Thermal stability of assemblages in the Cu-Fe-S system. **Journal of Petrology 2,** 381- 404.

YUSA, K., KITAKAZE, A. and A. SUGAKI (1979) Synthesized bismuth-tellurium-sulphur system minerals (IX). **Science Reports of the Tohoku University, 3rd Series 14(2),** 121-133.

ZHARIKOV, V.A. (1970) Skarns. **International Geology Reviews 12,** 541-559, 619-647 and 760-775.

ACKNOWLEDGEMENTS

I would like to express my deepest gratitude to Prof. G. von Gruenewaldt and Dr. R.K.W. Merkle who both rendered invaluable assistance in the form of guidance, discussions and criticism.

Mr. P. Nel, I owe a special thank you for initiating the project and providing assistance during my field work.

Furthermore I would like to thank Hannele Horsch for assistance with the microprobe analyses and Dr. M.R. Sharpe for the XRF-analyses.

I am also very grateful to Prof. E.B. Fürtsch, who gave me the work environment, which made it possible for me to complete this study.

To the staff of the Bushveld Research Institute and the Departement of Geology of the University of Pretoria goes a special thank you for numerous fruitful discussions.

Last, but not least, I would like to thank my husband Steve for his thoughtful assistance and support.

APPENDIX 1

Modal Analyses of Selected Waaikraal Pyroxenite and Magnetite-Rich Rocks

a: Pyroxenite

Sample No.	WK 3.2	WK 6.3	WK 12.4	WK 12.3	WK 28.4	WK 21.5	WK 20.5	WK 16.2	WK 14.4
Clinopyroxene	67.57	64.89	74.30	51.39	63.92	52.73	47.09	91.71	64.64
Plagioclase	8.25	20.08	12.79*	25.58	5.52	19.40*	20.04*	0.34	9.31*
Orthoclase	6.49	3.39	1.46	1.52	-	6.91*	2.80	1.34	6.82
Quartz	8.02	2.91	5.85	18.35	1.18	1.90	8.19	0.45	6.20
Hornblende	5.78	6.11	2.92	0.76	15.18	14.49	10.67	4.26	9.55
Mica/Chlorite	-	-	0.12	0.63	0.94	1.68	0.32	0.22	-
Opaque	3.42	2.23	1.95	1.52	11.75	0.56	9.16	0.34	2.85
Accessory	0.47	0.39	0.61	0.25	0.71	2.33	1.73	1.34	0.51
Sum	100.00	100.00	100.00	100.00	100.00	100.00	100.00	100.00	100.00
Points counted	840	1031	821	790	851	897	928	893	806

b: Magnetite-rich rock

Sample No.	WK 28.3	WK 4.1	WK 6.1	WK 14.1	WK 15.3	WK 12.1	WK 17.3
Clinopyroxene	43.64	57.54	50.18	10.53	51.38	44.59	47.16
Plagioclase	11.73+	10.41+	3.15*	3.27	10.88*	5.91*	16.59
Orthoclase	-	0.40	-	-	-	-	-
Quartz	-	0.13	-	-	-	-	-
Hornblende	-	-	-	0.12	-	-	-
Mica/Chlorite	-	-	-	5.08	0.13	-	-
Opaque	44.30	30.98	46.30	52.42	37.13	49.39	36.14
Accessory	0.11	0.54	0.37	0.25	0.48	0.11	0.11
Olivine	-	-	-	28.33	-	-	-
Sum	100.00	100.00	100.00	100.00	100.00	100.00	100.00
Points counted	912	790	825	826	800	897	844

\+ partly altered

* altered

APPENDIX 2

2.1 XRF Analyses

2.1.1 Instrumentation and Operating Conditions for XRF Analyses

Instrumentation: All XRF analyses were done on an ARL 8420 XRF. A Rh end window tube was used at 50 mA and 50 kV.

List of analysed elements with the corresponding instrumental setup.

Element K -line	Peak Position 2theta	Analysing Crystal	Detector
Si	109.21	PET	FPC-6
Ti	86.14	LIF200	FPC-6
Al	145.12	PET	FPC-6
Fe	57.52	LIF200	FPC-6
Mn	62.97	LIF200	FPC-6
Mg	20.13	AX06	FPC-1
Ca	100.22	LIF200	FPC-6
Na	24.29	AX06	FPC-1
K	136.69	LIF200	FPC-6
P	141.03	GE	FPC-6
Cr	69.36	LIF200	FPC-6
Ni	48.67	LIF200	FPC-6
Zn	41.83	LIF200	FPC-6
Cu	45.03	LIF200	FPC-6
Ni	48.67	LIF200	FPC-6
Co	52.84	LIF200	FPC-6
Ga	38.95	LIF200	SC
Mo	28.90	LIF220	SC
Nb	30.44	LIF220	SC
Zr	32.10	LIF220	SC
Y	33.87	LIF220	SC
Sr	35.85	LIF220	SC
Rb	37.99	LIF220	SC
U*	37.30	LIF220	SC
Th*	39.23	LIF220	SC
Pb**	28.26	LIF200	SC
Cr	107.06	LIF220	FPC-6
V	123.26	LIF220	FPC-6
Ba*	87.14	LIF200	FPC-6
Sc	97.68	LIF200	FPC-6

AX06 = 56A synthetic multilayer crystal
FPC-6 = 4µm polypropylene window
FPC-1 = 1µm polypropylene window
* = L_α -line
** = L_β -line

2.1.2 Lower Limits of Detection

Element	l.l.d. (weight %)
TiO_2	0.01
MnO	0.01
Na_2O	0.01
K_2O	0.01
P_2O_5	0.02
Cr_2O_3	0.05
NiO	0.04
	l.l.d. (ppm)
Zn	4
Cu	4
Ni	4
Co	4
Ga	4
Mo	2
Nb	3
Zr	3
Y	3
Sr	3
Rb	2
U	5
Th	5
Pb	5
Cr	10
V	8
Ba	15
Sc	8

2.1.3 Reproducibility

Reproducibility (in ppm) was calculated for trace elements according to chapter 4.1.4 (N = 20).

Element	ppm
Zn	3.20
Cu	7.08
Ni	5.01
Co	2.90
Ga	2.95
Mo	3.23
Nb	3.96
Zr	3.41
Y	4.27
Sr	2.12
Rb	1.67
U	7.28
Th	6.89
Pb	3.11
Cr	421.87
V	115.48
Ba	11.15
Sc	3.18

2.2 Microprobe Analyses

2.2.1 Instrumentation and Operating Conditions

All microprobe analyses were done as spot measures on a JEOL Superprobe 733 with a wave dispersive system. For full ZAF corrections the program FZAFM was used.

a.: Silicates

Element	Standard	Counting Time in seconds Peak	Background
Al	Al_2O_3 (100%)	20	10
Mg	MgO (100%)	20	10
Ti	TiO_2 (100%)	20	10
Cr	Cr_2O_3 (100%)	20	10
Mn	MnO (100%)	20	10
Fe	Hematite	20	10
Na	Albite	20	10
Si	Quartz	20	10
K	Sanidine	20	10
Ca	Wollastonite	20	10

Accelerating voltage : 15 kV
Probe current measured on Faraday cage : $0.2 * 10^{-7}$ A

b.: Magnetite

Element	Standard	Counting Time in seconds Peak	Background
Mg	MgO (100%)	50	10
Cr	Cr_2O_3 (100%)	50	10
V	VO_2 (100%)	50	10
Al	Al_2O_3 (100%)	20	10
Ti	TiO_2 (100%)	20	10
Mn	MnO (100%)	20	10
Fe	Hematite	20	10
Si	Quartz	20	10
Ca	Wollastonite	20	10

Accelerating voltage : 20 kV
Probe current measured on Faraday cage : $0.2 * 10^{-7}$ A

c: Cobalt-Sulphides

Element	Standard	Counting Time in seconds Peak	Background
S	Arsenopyrite	50	20
Fe	Arsenopyrite	50	20
As	Arsenopyrite	50	20
Sb	Sb_2S_3	50	20
Co	CoS_2	50	20
Ni	Millerite	50	20
Bi	Bismuthinite	50	20

Accelerating voltage : 15 kV
Probe current measured on Faraday cage : $0.5 * 10^{-7}$ A

d: Bismuth-Sulphides

Element	Standard	Counting Time in seconds Peak	Background
Bi	Bismuthinite	50	20
S	Bismuthinite	50	20
Co	CoS_2	50	20
Ni	Millerite	50	20
As	Arsenopyrite	50	20
Te	Altaite	50	20
Sb	Sb_2S_3	50	20

Accelerating voltage : 15 kV
Probe current measured on Faraday cage : $0.5 * 10^{-7}$ A

e: Pyrrhotite and Chalcopyrite

Element	Standard	Counting Time in seconds Peak	Background
Fe	Troilite	50	20
S	Troilite	50	20
As	Arsenopyrite	50	20
Ni	Millerite	50	20
Co	CoS_2	50	20
Cu	Chalcopyrite	50	20

Accelerating voltage : 15 kV
Probe current measured on Faraday cage : $0.5 * 10^{-7}$ A

f: Gold and Gold Compounds

Element	Standard	Counting Time in seconds Peak	Background
Au	100% Au	50	20
Ag	100% Ag	50	20
Cu	100% Cu	50	20
Fe	100% Fe	50	20
Bi	Bismuthinite	50	20
Pd	Pd_8Sb_3	50	20
Hg	Pd_3HgTe_3	50	20
Rh	100% Rh	50	20

Accelerating voltage : 20 kV
Probe current measured on Faraday cage : $0.2 * 10^{-7}$ A

2.2.2 Limits of Detection (in weight per cent)

Limits of detection were determined at the 3 sigma level on the background at the peak position.

a: Silicates

- determined on clinopyroxene

SiO_2	0.03
CaO	0.03
Na_2O	0.02
K_2O	0.03
Cr_2O_3	0.06
MgO	0.05
Al_2O_3	0.05
FeO	0.04
MnO	0.05
TiO_2	0.04

b: Magnetite

- determined on magnetite

SiO_2	0.05
CaO	0.03
TiO_2	0.02
V_2O_3	0.03
Cr_2O_3	0.02
MgO	0.02
Al_2O_3	0.03
MnO	0.03

c: Bismuth-Sulphides

- determined on bismuthinite

S	0.02
Ni	0.03
Co	0.03
Te	0.04
As	0.21
Sb	0.01

d: Arsenopyrite /Co-Sulphides

- determined on cobaltite

S	0.02
Sb	0.03
As	0.13
Co	0.02
Fe	0.02
Ni	0.02
Bi	0.81

e: Chalcopyrite / Pyrrhotite

- determined on pyrrhotite

Co	0.02
Cu	0.03
Ni	0.02

f: Gold / Gold Compounds

- determined on native gold

Ag	0.09
Cu	0.02
Fe	0.02
Bi	0.02

2.2.3 Reproducibility (in weight per cent; < l.l.d. = less than lower limit of detection)

a: Clinopyroxene (N=60)

Na_2O	0.03
SiO_2	0.23
FeO	0.25
K_2O	0.01
Al_2O_3	0.04
MgO	0.04
MnO	0.04
CaO	0.41
Cr_2O_3	0.01

b: Magnetite (N=60)

SiO_2	< l.l.d.
TiO_2	0.18
FeO	0.47
MgO	0.01
CaO	< l.l.d.
MnO	0.02
Al_2O_3	0.09
Cr_2O_3	0.01
V_2O_3	0.01

c: Pyrrhotite (N=60)

As	< l.l.d.
S	0.18
Fe	0.26
Ni	0.01
Cu	< l.l.d.
Co	0.01

d: Chalcopyrite (N=24)

As	< l.l.d.
S	0.19
Fe	0.22
Ni	< l.l.d.
Cu	0.08
Co	0.01

e: Joseite-B (N=32)

S	0.02
Bi	0.31
Te	0.08
As	< l.l.d.
Ni	< l.l.d.
Sb	< l.l.d.
Co	< l.l.d.

f: Bismuthinite (N=12)

S	0.12
Bi	0.70
Te	< l.l.d.
As	< l.l.d.
Ni	< l.l.d.
Sb	< l.l.d.
Co	< l.l.d.

f: Arsenopyrite (N=12)

Co	0.02
Ni	< l.l.d.
Fe	0.08
S	0.11
As	0.47
Sb	< l.l.d.
Bi	0.32

APPENDIX 3

3.1 Whole rock composition in weight per cent of Waaikraal pyroxenite, magnetite-rich rock, quartzite, pyroxene hornfels, calc-silicate and magnetite gabbro (all iron as Fe_2O_3, <11d = less than lower limit of detection; NiO < 11d)

a: Pyroxenite

Sample	SiO_2	TiO_2	Al_2O_3	Fe_2O_3	MnO	MgO	CaO	Na_2O	K_2O	P_2O_5	Cr_2O_3	LOI	H_2O^-	TOTAL
WK2.2	40.51	1.69	2.94	39.14	0.62	0.93	14.92	0.48	0.24	<11d	0.09	-1.69	0.20	100.08
WK2.3	29.80	0.79	5.40	53.97	0.44	0.48	10.32	0.58	0.41	0.06	0.08	-1.37	0.18	101.15
WK2.4	41.60	1.46	4.72	36.77	0.61	1.07	14.68	0.67	0.54	<11d	0.09	-0.97	0.24	101.49
WK5.2	50.32	0.42	4.59	26.43	0.57	1.24	16.22	1.21	0.78	0.07	<11d	-0.99	0.22	101.12
WK6.2	30.64	1.14	4.53	54.32	0.44	0.43	9.41	0.70	0.35	0.05	0.10	-1.30	0.20	101.01
WK6.3	50.88	0.36	3.93	27.13	0.60	1.29	14.93	0.91	0.79	0.07	0.08	-0.79	0.29	100.48
WK7.1	48.87	0.29	2.92	28.93	0.66	1.35	18.20	0.67	0.30	0.04	0.09	-1.04	0.21	101.49
WK9.3	30.52	0.49	6.86	48.93	0.46	0.59	12.54	0.17	0.35	0.02	0.06	-1.23	0.13	99.89
WK10.3	29.32	0.51	5.69	52.77	0.44	0.63	12.16	0.35	0.28	0.03	0.09	-1.23	0.17	101.21
WK10.7	48.14	0.51	4.56	30.78	0.54	0.87	14.66	0.95	0.94	0.05	0.09	-0.89	0.18	101.38
WK10.9	50.66	0.31	3.80	26.83	0.63	0.93	17.33	0.69	0.48	0.05	0.09	-0.83	0.25	101.23
WK11.2	46.56	0.21	2.01	30.11	0.77	1.16	21.20	0.41	0.12	<11d	0.08	-1.50	0.24	101.37
WK11.3	49.95	0.43	3.37	27.81	0.66	1.51	16.69	0.85	0.45	0.05	0.09	-0.89	0.16	101.13
WK12.2	48.54	0.73	4.01	30.14	0.59	1.50	15.30	0.86	0.56	<11d	0.09	-1.24	0.23	101.32
WK12.3	53.50	0.46	6.16	23.22	0.50	0.95	12.42	1.50	1.12	0.02	0.08	0.00	0.23	100.16
WK12.5	49.32	0.70	3.79	29.68	0.54	1.22	14.86	0.75	0.50	0.07	0.09	-1.19	0.18	100.52
WK13.2	48.47	0.42	3.73	27.42	0.65	1.59	17.89	0.88	0.57	<11d	0.06	-1.23	0.11	100.57
WK13.4	62.72	0.16	1.67	21.38	0.73	0.22	14.11	0.26	0.13	0.02	0.09	-0.77	0.14	100.87
WK14.4	40.44	0.71	4.62	41.14	0.54	0.98	12.84	0.75	0.42	<11d	0.07	-1.16	0.15	101.50
WK15.4	44.63	0.59	4.76	33.22	0.60	1.19	15.00	0.86	0.48	0.02	0.06	-0.88	0.22	100.76
WK16.2	48.01	0.11	1.89	30.77	0.78	0.69	18.44	0.27	0.12	<11d	0.07	-1.92	0.12	99.35
WK17.6	48.87	0.46	6.16	26.41	0.45	1.43	14.62	0.70	0.70	0.09	0.08	0.22	0.18	100.39
WK18.3	53.04	0.30	5.55	26.37	0.57	1.55	15.01	1.18	0.98	0.06	0.06	-0.77	0.18	104.08
WK19.4	48.82	0.28	3.67	26.70	0.63	1.67	17.13	0.68	0.53	0.07	0.06	0.73	0.23	101.20
WK20.3	50.20	0.37	3.91	25.75	0.71	1.83	16.76	1.11	0.67	0.06	0.07	-0.31	0.15	101.28
WK20.5	55.17	0.33	5.97	21.85	0.46	1.43	13.47	1.44	1.11	0.08	0.07	-0.43	0.15	101.10
WK21.3	50.88	0.44	4.45	25.76	0.61	2.01	15.73	1.11	0.63	0.04	0.08	-0.74	0.14	101.14
WK21.5	46.92	0.95	3.69	29.18	0.57	1.90	16.58	0.95	0.49	0.04	0.06	-1.26	0.20	100.27
WK22.3	51.01	0.44	4.15	24.97	0.62	2.24	16.60	0.97	0.68	0.13	0.09	-1.12	0.31	101.10
WK24.1	44.91	0.76	4.57	31.05	0.63	1.43	15.70	1.11	0.41	<11d	0.07	-0.77	0.16	100.04
WK26.2	46.69	0.73	3.51	29.87	0.59	2.15	16.87	0.86	0.43	0.05	0.07	-0.67	0.19	101.35
WK26.4	42.06	1.49	4.28	36.12	0.48	2.78	13.24	0.80	0.54	0.18	0.10	-0.79	0.13	101.42
WK27.2	51.40	0.98	4.00	24.03	0.49	4.07	14.18	0.92	0.52	0.22	<11d	0.23	0.29	101.36
WK28.4	52.27	0.52	4.24	23.47	0.51	3.55	14.01	1.10	0.62	0.08	0.09	-0.14	0.17	100.50
WK36.6	32.37	0.47	5.37	49.12	0.68	0.92	11.26	0.32	0.56	0.02	0.08	-0.87	0.10	100.40
WK36.7	41.67	0.59	5.99	32.47	0.51	1.59	15.22	0.49	0.87	0.03	0.06	1.25	0.17	100.91
WK36.8	44.48	0.73	8.34	23.10	0.31	1.69	15.07	0.94	0.80	0.13	0.06	4.19	0.23	100.08

b: Magnetite-Rich Rock

Sample	SiO_2	TiO_2	Al_2O_3	Fe_2O_3	MnO	MgO	CaO	Na_2O	K_2O	P_2O_5	Cr_2O_3	LOI	H_2O^-	TOTAL
WK3.5	32.27	0.39	5.71	55.67	1.00	0.37	7.84	0.17	0.38	<11d	0.08	-3.01	0.06	100.94
WK4.5	27.93	0.38	5.38	56.92	0.83	0.25	10.48	<11d	0.24	<11d	0.07	-2.22	0.17	100.44
WK5.4	22.78	0.20	3.04	72.59	1.24	0.22	3.16	<11d	0.16	<11d	0.07	-3.04	0.17	100.61
WK9.5	20.50	0.28	4.23	67.68	0.40	0.14	8.76	0.04	0.10	<11d	0.10	-2.35	0.34	100.23
WK9.7	27.73	0.41	5.37	57.15	0.47	0.34	10.68	0.12	0.18	<11d	0.07	-1.98	0.44	100.99
WK10.1	22.21	0.47	4.58	63.76	0.48	0.52	9.98	0.06	0.24	<11d	0.10	-2.10	0.27	100.59
WK10.8	27.07	0.49	5.46	57.46	0.45	0.38	10.64	0.18	0.35	<11d	0.07	-1.51	0.11	101.17
WK13.3	30.84	0.57	5.64	50.31	0.55	0.49	11.32	0.39	0.44	<11d	0.09	-1.39	0.20	99.46
WK14.1	13.43	0.23	2.81	82.89	0.61	0.15	3.95	0.06	0.04	0.02	0.10	-2.97	0.09	101.42
WK14.5	15.90	0.25	3.55	77.29	0.57	0.27	5.57	0.03	0.01	<11d	0.08	-2.59	0.18	101.12
WK15.5	30.08	0.42	5.84	50.81	0.47	0.39	13.82	0.09	0.19	0.02	0.08	-1.66	0.25	100.81
WK17.5	25.97	0.39	5.19	59.23	0.47	0.26	10.63	0.07	0.17	<11d	0.07	-1.70	0.06	100.82
WK18.1	20.88	0.62	3.37	67.43	0.45	0.36	8.20	0.18	0.07	0.02	0.09	-2.33	0.26	99.61
WK19.3	36.49	1.16	5.91	40.99	0.60	0.97	14.48	0.63	0.37	0.05	0.10	-1.26	0.32	100.81
WK20.4	23.63	0.62	4.67	61.10	0.42	0.38	9.55	0.16	0.31	0.05	0.08	-2.02	0.30	99.25
WK20.6	31.22	0.47	5.72	49.00	0.57	0.37	14.43	0.18	0.13	<11d	0.10	-1.68	0.28	100.79
WK21.6	38.61	0.43	7.26	37.38	0.56	0.65	16.95	0.13	0.05	0.02	0.10	-1.41	0.37	101.10
WK22.4	21.09	0.33	3.66	72.89	0.94	0.10	4.87	<11d	0.20	0.04	0.08	-3.56	0.22	100.87
WK25.1	46.49	0.42	3.71	31.38	0.58	1.21	16.33	0.90	0.28	<11d	0.07	-0.89	0.21	100.69
WK26.5	27.91	0.95	5.09	56.23	0.56	0.88	9.79	0.67	0.16	<11d	0.08	-2.13	0.21	100.40
WK27.5	30.54	2.01	4.59	51.29	0.48	1.20	10.29	0.60	0.23	0.02	0.09	-1.57	0.06	99.84
WK30.2	14.78	0.21	2.60	78.82	0.44	0.13	6.85	<11d	<11d	0.02	0.10	-2.65	0.15	101.47
WK36.1	16.55	0.26	3.32	80.39	1.14	0.38	2.54	<11d	0.06	<11d	0.12	-3.53	0.25	101.49
WK36.2	15.30	0.37	2.88	82.10	1.03	0.28	1.91	<11d	0.02	<11d	0.09	-3.57	0.11	100.53

c: Pyroxene Hornfels

Sample	SiO_2	TiO_2	Al_2O_3	Fe_2O_3	MnO	MgO	CaO	Na_2O	K_2O	P_2O_5	Cr_2O_3	LOI	H_2O^-	TOTAL
HF1	45.16	0.32	7.99	21.43	0.70	1.10	22.43	0.71	0.20	0.08	<lld	-0.08	0.15	100.22

d: Quartzite

Sample	SiO_2	TiO_2	Al_2O_3	Fe_2O_3	MnO	MgO	CaO	Na_2O	K_2O	P_2O_5	Cr_2O_3	LOI	H_2O^-	TOTAL
WK9.8	86.46	0.10	3.46	3.95	0.09	0.47	3.02	1.16	1.12	0.42	0.09	0.35	0.17	100.86
WK11.4	74.29	0.12	2.47	11.07	0.28	1.15	8.81	0.74	0.45	0.16	0.09	-0.05	0.14	99.73
WK13.5	90.65	0.08	3.81	0.82	0.01	<lld	0.20	2.07	1.86	<lld	0.12	0.67	0.12	100.42
QZ1	57.86	0.42	8.68	11.07	0.34	4.57	14.61	1.14	1.52	0.34	0.07	0.21	0.09	100.93
QZ2	93.36	0.06	2.39	2.54	0.06	<lld	0.55	0.45	0.88	0.03	0.11	0.27	0.08	100.78
QZ3	86.01	0.11	4.17	4.62	0.07	0.64	1.96	0.58	1.98	0.06	0.11	0.18	0.14	100.66
QZ4	88.94	0.07	3.47	1.78	0.03	0.83	1.50	0.69	1.91	0.11	0.09	0.35	0.08	99.85
QZ5	89.94	0.09	4.32	0.94	0.02	<lld	0.83	1.14	2.06	0.07	0.10	0.17	0.14	99.82
QZ6	91.93	0.11	3.81	1.27	0.02	0.27	0.67	1.13	1.71	0.02	0.10	0.33	0.13	101.50

e: Calc-Silicate

Sample	SiO_2	TiO_2	Al_2O_3	Fe_2O_3	MnO	MgO	CaO	Na_2O	K_2O	P_2O_5	Cr_2O_3	LOI	H_2O^-	TOTAL
CS1	50.92	0.07	1.26	1.99	0.28	0.51	43.36	<lld	0.01	0.23	0.07	0.62	0.05	99.37
CS2	51.27	0.13	1.31	1.97	0.25	0.45	43.70	<lld	0.19	0.02	0.06	1.47	0.09	100.91
CS3	51.55	0.12	1.50	2.45	0.30	0.54	44.49	<lld	0.02	0.20	0.09	1.03	0.06	102.62
CS4	50.67	0.07	1.25	2.22	0.29	0.52	43.99	<lld	0.02	0.15	0.09	0.95	0.04	100.26

f: Magnetite-Gabbro

Sample	SiO_2	TiO_2	Al_2O_3	Fe_2O_3	MnO	MgO	CaO	Na_2O	K_2O	P_2O_5	Cr_2O_3	LOI	H_2O^-	TOTAL
MG1	47.51	3.39	18.42	15.53	0.14	2.58	9.48	3.93	0.54	0.04	0.09	-0.53	0.04	101.16
MG2	45.31	2.78	14.65	21.88	0.24	5.06	8.88	3.42	0.29	0.02	0.09	-1.14	0.00	101.48
MG3	46.35	2.55	16.13	18.84	0.21	4.26	8.78	3.29	0.38	0.06	0.10	-1.03	0.10	100.02

3.2 Trace element content in ppm of pyroxenite, magnetite-rich rock, pyroxene hornfels, quartzite and magnetite-gabbro (<11d = below the lower limit of detection, na = not analysed, for Au 0 indicates quantities of less than 0.5 ppm)

a: Pyroxenite

Sample	Zn	Cu	Ni	Co	Ga	Mo	Nb	Zr	Y	Sr	Rb	U	Pb	Cr	V	Ba	Sc	Au
WK2.2	27	26	380	14	<11d	4	90	15	48	9	7	<11d	<11d	112	54	150	<11d	2
WK2.3	187	17	8	399	7	6	9	155	17	66	25	12	8	52	20	254	<11d	0
WK2.4	183	17	16	406	17	<11d	8	127	17	65	27	<11d	6	74	46	351	24	7
WK3.2	159	19	13	305	9	<11d	8	106	21	54	20	<11d	8	28	11	238	<11d	4
WK3.3	159	22	23	407	15	<11d	6	107	18	83	23	<11d	14	66	32	384	<11d	21
WK5.2	144	29	13	407	9	<11d	11	138	24	74	31	5	12	53	37	382	22	83
WK6.2	181	30	23	409	11	<11d	13	141	12	58	19	24	5	41	32	275	<11d	6
WK6.3	154	41	16	478	4	<11d	<11d	120	23	50	31	23	<11d	51	17	346	8	48
WK7.1	155	26	21	300	<11d	<11d	5	123	26	33	33	<11d	<11d	48	27	206	<11d	3
WK8.5	165	15	15	358	12	<11d	9	134	18	63	16	10	14	43	8	231	10	0
WK9.2	164	24	16	327	5	3	7	135	27	85	27	5	11	40	46	467	12	0
WK9.3	17	24	29	4	5	11	211	21	112	24	<11d	<11d	<11d	92	53	225	<11d	0
WK9.4	175	14	14	376	9	3	7	138	19	66	23	<11d	<11d	53	27	336	<11d	0
WK9.6	157	21	18	584	19	<11d	7	145	17	77	26	14	11	53	24	430	11	0
WK10.2	184	26	19	270	5	<11d	9	119	19	84	21	<11d	6	53	41	424	<11d	0
WK10.3	196	17	8	45	<11d	6	16	219	31	106	20	14	9	50	35	215	<11d	0
WK10.4	169	21	15	187	5	<11d	5	207	24	108	21	<11d	<11d	45	19	312	<11d	0
WK10.5	155	25	9	296	5	<11d	5	169	24	83	30	<11d	14	44	28	617	9	0
WK10.7	162	16	6	438	7	<11d	9	158	20	39	34	16	19	70	25	420	<11d	0
WK10.9	147	59	35	218	6	<11d	<11d	137	28	38	19	7	<11d	56	61	218	<11d	0
WK11.2	160	14	13	248	<11d	<11d	8	84	16	19	15	<11d	12	25	19	96	<11d	8
WK11.3	163	42	26	418	8	<11d	<11d	152	16	50	44	<11d	<11d	104	31	263	18	3
WK12.2	167	23	21	375	12	<11d	10	135	19	58	26	<11d	12	57	12	273	13	3
WK12.3	163	109	22	296	11	<11d	5	182	13	85	103	103	<11d	69	46	410	<11d	10
WK12.4	157	45	32	426	12	<11d	3	148	20	71	49	<11d	<11d	73	59	323	20	8
WK12.5	138	18	49	390	15	<11d	4	153	21	40	22	<11d	<11d	120	51	261	<11d	0
WK13.2	162	20	23	329	5	<11d	3	142	33	49	24	6	10	54	49	342	25	10
WK13.4	137	<11d	21	28	<11d	<11d	5	80	11	22	8	<11d	6	81	9	47	<11d	0
WK14.4	215	22	12	328	13	4	11	149	18	59	21	<11d	11	79	31	370	<11d	3
WK15.2	193	27	28	319	16	3	13	149	18	63	20	12	14	83	57	413	<11d	1
WK15.4	182	17	15	349	11	<11d	4	173	21	58	30	7	12	43	20	410	<11d	1
WK16.2	166	14	4	147	6	<11d	<11d	68	18	24	5	19	<11d	<11d	26	100	<11d	0
WK16.5	164	13	8	332	5	6	8	206	27	69	21	<11d	<11d	64	35	194	<11d	3
WK16.7	177	18	20	394	20	<11d	6	132	22	43	20	<11d	9	59	27	288	<11d	1
WK17.2	165	21	10	342	10	<11d	4	126	29	50	22	<11d	14	56	29	344	31	
WK17.4	149	11	23	667	11	<11d	6	126	12	31	10	<11d	17	41	47	197	<11d	0
WK17.6	129	1592	67	169	13	3	6	185	25	64	24	<11d	14	103	27	181	<11d	0
WK18.3	160	13	10	184	10	3	6	138	23	93	31	<11d	18	49	30	419	<11d	2
WK18.5	161	20	19	292	12	<11d	6	157	21	61	31	19	12	72	17	442	14	5
WK19.2	172	20	14	199	6	<11d	7	140	26	70	24	7	8	20	24	423	9	0
WK19.4	174	17	26	120	10	<11d	4	114	19	43	19	<11d	18	41	11	186	<11d	0
WK20.2	159	21	8	209	7	<11d	<11d	123	30	29	15	<11d	12	17	17	414	<11d	1
WK20.3	177	20	19	181	6	<11d	<11d	145	25	36	22	<11d	<11d	27	19	273	<11d	1
WK20.5	141	24	16	131	7	3	4	189	16	101	45	7	17	51	32	581	<11d	0
WK21.3	178	23	21	226	15	<11d	4	138	24	72	27	10	7	38	10	310	30	0
WK21.5	181	19	20	232	11	<11d	9	126	17	61	25	8	10	50	42	317	36	0
WK22.3	24	27	209	12	<11d	7	152	25	70	26	<11d	20	<11d	106	61	316	24	0
WK22.7	168	13	119	76	8	<11d	6	175	28	52	32	<11d	13	84	62	290	<11d	0
WK23.1	171	21	18	192	11	<11d	6	126	28	64	19	9	12	52	17	271	48	0
WK23.4	175	9	11	64	11	5	5	256	29	78	29	<11d	10	67	39	316	<11d	0
WK23.5	27	17	56	12	<11d	6	181	14	49	14	<11d	12	<11d	74	83	163	<11d	0
WK24.1	190	16	16	203	8	<11d	5	142	26	65	20	5	23	44	25	267	<11d	4
WK24.2	147	13	31	149	9	<11d	6	154	16	144	39	5	16	61	41	392	9	1
WK24.3	180	11	21	164	9	<11d	6	132	29	56	26	<11d	8	45	35	265	44	1
WK24.5	194	13	11	181	8	<11d	8	104	23	50	16	12	7	33	49	207	36	1
WK25.3	24	35	138	9	<11d	6	135	31	64	28	<11d	<11d	<11d	97	12	311	38	0
WK26.2	176	18	18	364	7	<11d	8	127	27	35	11	<11d	6	40	38	140	21	20
WK26.4	214	19	13	162	13	3	6	118	34	55	22	<11d	9	34	25	253	53	12
WK27.2	203	21	16	86	11	<11d	5	143	32	49	21	15	13	39	50	326	63	3
WK27.3	177	12	7	157	13	<11d	6	194	29	54	19	6	20	40	34	293	60	7
WK28.4	162	15	29	195	14	<11d	4	119	31	49	25	12	9	72	51	311	58	10
WK29.2	142	11	20	34	18	<11d	4	84	22	158	30	10	5	48	33	420	15	0
WK29.3	146	16	27	38	11	<11d	3	86	27	135	23	8	6	47	46	280	56	1
WK30.3	199	24	30	50	15	<11d	5	106	31	58	16	9	20	49	34	284	54	0
WK30.4	186	21	18	58	14	<11d	9	128	26	95	20	<11d	<11d	59	43	403	32	0
WK36.3	186	27	27	244	8	<11d	5	123	29	59	30	<11d	25	46	35	312	30	0
WK36.4	193	26	22	239	9	<11d	4	136	23	50	28	<11d	27	71	41	321	27	1
WK36.6	219	13	48	46	14	4	9	166	27	43	19	<11d	11	51	59	207	<11d	1
WK36.7	166	27	70	50	21	<11d	10	163	49	32	20	<11d	11	48	82	184	<11d	1
WK36.8	247	<11d	39	18	24	<11d	13	287	97	44	12	7	9	55	79	91	13	0

b: Magnetite-Rich Rock

Sample	Zn	Cu	Ni	Co	Ga	Mo	Nb	Zr	Y	Sr	Rb	U	Pb	Cr	V	Ba	Sc	Au
WK3.1	25	20	110	8	8	6	118	12	42	5	<11d	<11d	<11d	60	57	121	<11d	0
WK3.5	22	18	272	4	<11d	9	102	9	50	20	<11d	<11d	<11d	57	42	95	<11d	0
WK4.5	26	19	<11d	<11d	<11d	6	240	12	63	20	<11d	<11d	<11d	82	34	181	<11d	0
WK5.4	36	15	78	7	7	7	84	<11d	11	5	3	5	<11d	96	63	79	<11d	1
WK6.1	34	33	273	4	10	5	159	13	29	6	<11d	<11d	<11d	68	51	65	<11d	10
WK8.6	28	13	<11d	4	6	9	180	9	35	6	<11d	<11d	<11d	103	66	234	<11d	0
WK9.1	28	15	53	12	7	11	140	4	19	8	<11d	<11d	<11d	84	<11d	202	<11d	0
WK9.5	34	13	<11d	<11d	4	9	184	14	46	7	<11d	<11d	<11d	56	46	205	<11d	0
WK9.7	25	11	124	8	7	7	182	15	72	11	<11d	<11d	<11d	69	19	235	<11d	0
WK10.1	26	18	67	7	8	10	221	19	56	12	<11d	5	<11d	63	45	123	<11d	0
WK10.6	26	15	108	8	5	6	191	14	41	16	3	<11d	<11d	107	79	315	<11d	0
WK10.8	26	19	277	4	6	6	184	17	108	24	<11d	<11d	<11d	82	42	409	<11d	0
WK13.3	40	26	144	8	<11d	5	175	21	58	29	5	<11d	<11d	83	69	627	<11d	0
WK14.1	36	13	78	7	8	11	124	4	3	6	6	<11d	<11d	58	43	97	<11d	0
WK14.3	26	13	184	<11d	12	12	214	17	72	13	4	24	<11d	105	45	85	<11d	0
WK14.5	31	24	107	6	6	10	166	10	50	10	<11d	<11d	<11d	60	12	68	<11d	0
WK15.1	32	7	<11d	<11d	12	9	139	18	18	<11d	<11d	<11d	<11d	64	68	56	<11d	0
WK15.3	26	16	161	13	10	15	175	17	38	10	4	11	<11d	55	68	200	<11d	0
WK15.5	23	9	<11d	4	10	14	301	15	89	15	<11d	<11d	<11d	209	45	202	<11d	0
WK16.3	22	20	134	10	4	7	175	24	86	24	<11d	11	<11d	133	71	231	<11d	0
WK16.6	20	14	30	6	<11d	11	196	19	106	16	<11d	6	<11d	60	120	91	<11d	1
WK17.1	30	14	63	8	8	9	201	24	67	20	<11d	13	<11d	74	78	288	<11d	1
WK17.3	26	9	121	<11d	8	11	220	17	63	8	17	<11d	<11d	125	69	256	<11d	0
WK17.5	25	11	<11d	5	7	3	211	13	105	13	3	<11d	<11d	77	34	161	<11d	1
WK18.1	32	48	339	12	7	9	118	15	21	7	<11d	16	<11d	99	102	75	<11d	1
WK19.3	21	19	112	9	4	7	141	23	87	21	<11d	<11d	<11d	122	100	373	<11d	0
WK20.4	46	13	142	10	8	11	185	14	96	19	<11d	<11d	<11d	73	79	290	<11d	1
WK20.6	21	26	146	8	7	14	232	15	90	12	<11d	44	<11d	48	49	111	<11d	0
WK21.4	28	30	262	12	12	11	151	8	74	13	<11d	39	<11d	69	<11d	186	<11d	0
WK21.2	31	18	335	11	4	12	107	9	39	12	<11d	58	<11d	76	102	242	<11d	0
WK21.6	17	42	118	8	8	7	446	25	151	6	7	48	<11d	111	37	76	<11d	0
WK22.1	17	26	210	7	<11d	6	117	21	76	26	4	<11d	<11d	102	70	305	<11d	0
WK22.2	23	8	<11d	7	9	8	259	21	89	13	<11d	16	<11d	109	113	178	<11d	0
WK22.4	26	23	40	<11d	9	13	206	5	42	13	<11d	20	<11d	90	29	118	<11d	0
WK22.6	19	14	<11d	12	5	8	307	20	173	8	<11d	<11d	<11d	102	<11d	115	<11d	0
WK23.3	23	22	339	8	9	7	178	13	62	11	<11d	<11d	<11d	100	20	167	<11d	0
WK24.4	31	6	152	14	9	8	151	14	29	10	<11d	<11d	<11d	128	29	142	<11d	0
WK24.6	29	25	476	14	6	6	162	9	40	5	<11d	8	<11d	100	69	96	<11d	0
WK25.1	205	26	7	259	12	<11d	9	123	26	44	10	<11d	16	21	34	130	<11d	0
WK25.6	16	15	12	12	<11d	11	269	12	90	19	<11d	<11d	<11d	78	<11d	158	<11d	0
WK26.1	29	17	279	9	11	7	178	9	29	11	<11d	<11d	<11d	66	15	54	<11d	4
WK26.3	33	6	436	15	10	12	162	9	32	13	18	<11d	<11d	107	67	83	<11d	2
WK26.5	30	19	745	16	7	6	123	7	50	7	<11d	57	<11d	99	63	132	<11d	6
WK26.7	32	14	211	15	7	7	176	7	32	<11d	<11d	<11d	<11d	84	80	60	<11d	0
WK27.5	22	37	481	17	5	7	155	14	49	3	4	6	<11d	142	120	162	<11d	0
WK28.1	33	10	717	6	11	<11d	151	10	19	<11d	<11d	<11d	<11d	107	40	41	<11d	12
WK28.3	27	6	258	8	14	3	142	5	42	8	<11d	<11d	<11d	113	23	85	<11d	7
WK28.5	28	41	365	15	5	7	141	10	54	20	<11d	<11d	<11d	157	24	166	<11d	1
WK30.2	48	13	211	7	8	19	92	<11d	10	9	<11d	21	<11d	89	30	53	<11d	0
WK30.1	16	12	142	7	<11d	5	158	19	116	8	7	10	<11d	115	<11d	126	<11d	0
WK36.1	30	11	<11d	7	6	4	119	9	12	<11d	4	<11d	<11d	72	67	57	<11d	1
WK36.2	33	29	<11d	8	7	13	86	8	5	<11d	7	<11d	<11d	67	40	48	<11d	0
WK36.5	31	25	386	23	6	10	110	10	36	13	<11d	9	<11d	160	60	173	<11d	0
WK52.3	51	152	4853	<11d	7	10	133	12	15	<11d	<11d	30	<11d	86	65	64	<11d	30

c: Pyroxene Hornfels

Sample	Zn	Cu	Ni	Co	Ga	Mo	Nb	Zr	Y	Sr	Rb	U	Pb	Cr	V	Ba	Sc	Au
HF1	171	7	6	22	14	<11d	5	192	21	65	9	16	9	55	18	88	<11d	na

d: Quartzite

Sample	Zn	Cu	Ni	Co	Ga	Mo	Nb	Zr	Y	Sr	Rb	U	Pb	Cr	V	Ba	Sc	Au
WK9.8	31	<11d	13	18	5	3	4	111	19	22	37	5	<11d	244	46	391	<11d	0
WK11.4	53	4	33	37	4	<11d	<11d	98	17	23	17	<11d	9	136	43	98	<11d	1
WK13.5	157	20	98	13	16	<11d	8	84	32	107	91	13	10	127	79	756	<11d	0
QZ1	11	<11d	<11d	<11d	5	3	4	141	11	18	56	<11d	6	324	33	618	<11d	na
QZ2	13	10	<11d	7	6	4	3	89	6	13	25	<11d	5	211	24	230	<11d	na
QZ3	27	6	318	6	6	<11d	4	122	11	19	56	<11d	<11d	199	56	505	<11d	na
QZ4	24	6	15	5	5	<11d	3	102	16	31	56	5	<11d	222	96	968	<11d	na
QZ5	15	4	4	<11d	5	4	5	150	11	36	63	6	7	242	34	796	<11d	na
QZ6	8	<11d	7	7	<11d	4	3	191	10	7	44	<11d	<11d	173	54	348	<11d	na

e: Magnetite-Gabbro

Sample	Zn	Cu	Ni	Co	Ga	Mo	Nb	Zr	Y	Sr	Rb	U	Pb	Cr	V	Ba	Sc	Au
MG1	25	15	27	28	<11d	8	37	4	377	10	<11d	<11d	<11d	122	80	180	18	na
MG2	40	20	61	23	<11d	<11d	24	7	315	<11d	<11d	<11d	<11d	143	76	90	18	na
MG3	18	19	54	24	<11d	<11d	28	7	337	4	<11d	<11d	<11d	96	31	156	10	na

a: Pyroxenite

	TI02	AL203	FE203	MNO	MGO	CAO	NA20	K20	P205	AU	BA	CO	CR	CU	GA	MO	NB	NI	PB	RB	SC	SR	U	V	Y	ZN	ZR	
SI02	-0.56523 0.0001 70	-0.19269 0.1100 70	-0.89378 0.0001 37	0.03166 0.7948 70	0.46148 0.0001 70	0.33611 0.0044 70	0.52231 0.0001 69	0.50508 0.0001 70	0.24027 0.0718 57	0.05255 0.6657 70	0.26815 0.0248 70	-0.08208 0.4994 70	-0.03765 0.7588 69	0.16794 0.1710 68	-0.18441 0.1513 62	-0.41481 0.0870 18	-0.50850 0.0001 64	0.02756 0.8208 70	0.10788 0.4465 52	0.41485 0.0005 66	0.11949 0.5009 34	0.05474 0.6526 70	0.07592 0.6746 33	-0.16324 0.1769 70	-0.00417 0.9727 70	-0.35212 0.0028 70	-0.11790 0.3310 70	SI02
TI02	1.00000 0.0000 70	0.18773 0.1196 70	0.47655 0.0029 37	-0.39008 0.0008 70	0.07018 0.5637 70	-0.48955 0.0001 70	-0.02194 0.8580 69	-0.16807 0.1643 70	0.19010 0.1567 57	0.07392 0.5431 70	0.03585 0.7683 70	0.13980 0.2484 70	0.07324 0.5498 69	-0.02315 0.8513 68	0.43152 0.0005 62	-0.15954 0.5212 18	0.27460 0.0281 64	0.04418 0.7165 70	-0.13045 0.3566 52	-0.26192 0.0336 66	0.49476 0.0029 34	0.12333 0.3091 70	0.00261 0.9885 33	0.23025 0.0552 70	0.05683 0.6403 70	0.41852 0.0001 70	0.06173 0.6117 70	TI02
AL203		1.00000 0.0000 70	0.11155 0.5110 37	-0.57222 0.0001 70	-0.05067 0.6770 70	-0.43339 0.0002 70	0.37411 0.0015 69	0.44920 0.0001 70	0.06643 0.6234 57	-0.19995 0.0970 70	0.29779 0.0123 70	-0.29037 0.0148 70	0.20138 0.0971 69	0.02229 0.8568 68	0.18900 0.1412 62	0.22518 0.3690 18	0.11213 0.3777 64	0.08934 0.4620 70	-0.03528 0.8039 52	0.34785 0.0042 66	-0.05007 0.7785 34	0.59005 0.0001 70	-0.20029 0.2637 33	0.24855 0.0380 70	0.16189 0.1806 70	0.01516 0.9008 70	0.38754 0.0009 70	AL203
FE203			1.00000 0.0000 37	-0.10327 0.5830 37	-0.49923 0.0017 37	-0.28900 0.0828 37	-0.57461 0.0002 37	-0.50587 0.0014 37	-0.36308 0.0529 29	0.06738 0.6919 37	-0.13171 0.4371 37	0.18540 0.2720 37	-0.05099 0.7677 36	-0.26849 0.1189 35	0.01195 0.9491 31	0.51797 0.1027 11	0.47454 0.0061 32	-0.20779 0.2172 37	-0.20378 0.3180 26	-0.23253 0. . .3 35	-0.13216 0.6524 14	-0.02017 0.9057 37	0.06437 0.7935 19	0.02574 0.8798 37	0.01804 0.9156 37	0.14156 0.4385 17	-0.01221 0.9428 37	FE203
MNO				1.00000 0.0000 70	-0.24902 0.0376 70	0.36125 0.0021 70	-0.36906 0.0018 69	-0.31887 0.0071 70	-0.31333 0.0176 57	0.06533 0.5911 70	-0.15643 0.1959 70	0.13485 0.2657 70	-0.05019 0.6821 69	0.00074 0.9952 68	-0.37141 0.0030 62	-0.10267 0.6852 18	-0.04817 0.7020 64	-0.00416 0.9728 70	0.12959 0.3599 52	-0.14123 0.2580 66	-0.30457 0.0799 34	-0.39899 0.0006 70	-0.04526 0.8025 33	-0.10749 0.3758 70	-0.10578 0.3835 70	-0.02148 0.8470 70	-0.23821 0.0471 70	MNO
MGO					1.00000 0.0000 70	0.29161 0.0143 70	0.56156 0.0001 69	0.34734 0.0032 70	0.49347 0.0001 57	0.13473 0.2661 70	0.16669 0.1678 70	-0.27035 0.0236 70	-0.08496 0.4108 69	-0.00508 0.9672 68	-0.17951 0.1627 62	-0.44952 0.0613 18	-0.31770 0.0105 64	0.08570 0.4806 70	0.00954 0.9465 52	0.06381 0.6107 66	0.82152 0.0001 34	0.07650 0.5290 70	-0.28773 0.1044 33	0.01198 0.9216 70	0.37882 0.0012 70	0.16030 0.1850 70	-0.19946 0.0978 70	MGO
CAO						1.00000 0.0000 70	0.10045 0.4115 69	0.00278 0.9818 70	0.03604 0.7901 57	0.02115 0.8621 70	-0.07755 0.5234 70	0.08493 0.4845 70	-0.22103 0.0680 69	-0.19492 0.2184 68	-0.24858 0.0554 62	-0.15407 0.5416 18	-0.27122 0.0302 64	-0.07495 0.5402 70	0.05398 0.7039 52	0.02056 0.8699 66	-0.25378 0.1475 34	-0.09972 0.4115 70	-0.32833 0.0621 33	-0.17183 0.1549 70	0.01827 0.8807 70	-0.19898 0.0987 70	-0.19840 0.0995 70	CAO
NA20							1.00000 0.0000 69	0.58708 0.0001 69	0.43163 0.0009 56	0.00266 0.9827 69	0.61723 0.0001 69	-0.06315 0.6062 69	-0.04108 0.7394 68	0.10357 0.4043 67	0.03220 0.8038 62	-0.39910 0.1125 17	-0.33448 0.0074 63	0.01522 0.9012 69	0.14891 0.2921 52	0.48102 0.0001 66	0.08529 0.6315 34	0.53047 0.0001 69	-0.31151 0.0826 32	-0.01445 0.9062 69	0.08002 0.5133 69	-0.08824 0.4709 69	0.05786 0.6368 69	NA20
K20								1.00000 0.0000 70	0.27644 0.0374 57	0.02992 0.8058 70	0.50889 0.0001 70	-0.03959 0.7449 70	0.05811 0.6352 69	0.13874 0.2592 68	0.02702 0.8349 62	-0.41265 0.0888 18	-0.17526 0.1660 64	0.08178 0.5010 70	0.20877 0.1375 52	0.63084 0.0001 66	-0.38882 0.0230 34	0.38414 0.0010 70	-0.09812 0.5870 33	0.03387 0.7808 70	0.08849 0.4661 70	-0.14624 0.2270 70	0.32574 0.0059 70	K20
P205									1.00000 0.0000 57	-0.14843 0.2705 57	0.17860 0.1838 57	-0.11101 0.4110 57	-0.09945 0.4617 57	0.12304 0.3708 55	0.10505 0.4632 51	-0.45553 0.0762 16	-0.07701 0.5874 52	0.07658 0.5712 57	0.12153 0.4433 42	-0.[illegible]710 0.7647 53	0.29569 0.1194 29	0.22566 0.0915 57	-0.00909 0.9627 29	0.03779 0.7802 57	0.14962 0.2666 57	0.05869 0.6645 57	-0.21715 0.1047 57	P205
AU										1.00000 0.0000 70	0.02845 0.8151 70	0.35878 0.0023 70	-0.07617 0.5139 69	0.07656 0.5549 68	0.08454 0.5136 62	-0.27997 0.2605 18	-0.08460 0.5063 64	-0.10554 0.3846 70	-0.06937 0.6251 52	0.11941 0.3396 66	0.10652 0.5488 34	-0.05715 0.6384 70	0.02768 0.8785 33	0.01665 0.8912 70	-0.06518 0.5919 70	0.06144 0.6021 70	-0.00612 0.9599 70	AU
BA											1.00000 0.0000 70	0.28072 0.0186 70	0.02427 0.8434 69	0.17166 0.1616 68	-0.06813 0.5988 62	-0.43658 0.0701 18	-0.22230 0.0775 64	-0.25100 0.0361 70	0.17447 0.2161 52	0.60244 0.0001 66	-0.41174 0.0155 34	0.57787 0.0001 70	-0.06400 0.7235 33	-0.06780 0.5771 70	-0.19558 0.1047 70	-0.01782 0.9161 70	0.21514 0.0717 70	BA
CO												1.00000 0.0000 70	-0.01951 0.7472 69	0.14539 0.2368 68	-0.07996 0.5367 62	-0.50665 0.0319 18	-0.09784 0.4418 64	-0.29582 0.0129 70	0.05759 0.6851 52	0.28067 0.0224 66	-0.48876 0.0034 34	0.15351 0.2085 70	0.09456 0.6007 33	-0.23948 0.0459 70	-0.56537 0.0001 70	0.03891 0.7491 70	0.19594 0.1060 70	CO
CR													1.00000 0.0000 69	0.26799 0.0283 67	0.21406 0.0976 61	0.39670 0.1031 18	0.18809 0.1366 64	0.47409 0.0001 69	0.11164 0.4307 52	0.28443 0.0217 65	-0.11242 0.5267 34	-0.09789 0.4236 69	0.25602 0.1573 32	0.34906 0.0033 69	-0.00839 0.9455 69	-0.33739 0.0053 69	0.05665 0.6438 69	CR
CU														1.00000 0.0000 68	-0.06770 0.6081 61	-0.04122 0.8710 18	0.13163 0.3078 62	0.36433 0.0023 68	0.10406 0.4721 50	0.18713 0.1387 64	-0.23009 0.1977 33	-0.03743 0.7619 68	0.19873 0.2756 32	0.03770 0.7602 68	0.04848 0.6946 68	-0.19329 0.1143 68	-0.03669 0.7667 68	CU
GA															1.00000 0.0000 62	-0.35954 0.2276 13	0.03519 0.7968 56	0.35247 0.0050 62	-0.10272 0.4825 49	-0.12804 0.3254 61	0.26629 0.1407 32	0.05075 0.6953 62	0.16319 0.3889 30	0.14393 0.2644 62	-0.06322 0.6254 62	0.19986 0.1194 62	0.03195 0.8053 62	GA
MO																1.00000 0.0000 18	0.71547 0.0008 18	0.06157 0.8182 18	-0.71250 0.0139 11	-0.33265 0.2452 14	-0.10541 0.8946 4	-0.38484 0.1148 18	0.84067 0.0178 7	0.26856 0.2812 18	0.60924 0.0073 18	-0.36928 0.1116 18	-0.17908 0.4772 18	MO
NB																	1.00000 0.0000 64	0.02692 0.8328 64	-0.21312 0.1332 51	-0.36769 0.0039 60	-0.25123 0.1654 32	-0.23699 0.0594 64	0.29900 0.1085 30	0.16089 0.2041 64	0.10235 0.4210 64	0.05622 0.6590 64	-0.10869 0.3918 64	NB
NI																		1.00000 0.0000 70	0.01090 0.9389 52	0.02007 0.8729 66	0.06856 0.7001 34	-0.28374 0.0173 70	-0.01237 0.9455 33	0.48525 0.0001 70	0.20686 0.0858 70	-0.27452 0.0215 70	-0.11222 0.1540 70	NI
PB																			1.00000 0.0000 52	0.17096 0.2256 52	-0.01677 0.9325 28	-0.05365 0.7056 52	-0.27368 0.1672 27	-0.06589 0.6426 52	0.01513 0.9152 52	-0.07941 0.5751 52	0.24328 0.0822 52	PB
RB																				1.00000 0.0000 66	-0.44417 0.0109 32	0.47877 0.0001 66	0.01016 0.9567 31	0.00711 0.9548 66	-0.17572 0.1581 66	-0.23933 0.0529 66	0.33338 0.0062 66	RB
SC																					1.00000 0.0000 34	-0.30132 0.0833 34	0.04927 0.8321 21	0.24878 0.1560 34	0.52731 0.0014 34	0.38173 0.0251 34	-0.39901 0.0194 34	SC
SR																						1.00000 0.0000 70	-0.28100 0.1132 33	-0.09005 0.4585 70	-0.27429 0.0216 70	0.16168 0.1812 70	0.39873 0.0006 70	SR
U																							1.00000 0.0000 33	-0.09072 0.6156 33	-0.20782 0.2458 33	0.00454 0.9800 33	-0.12725 0.4804 33	U
V																								1.00000 0.0000 70	0.33768 0.0043 70	0.00900 0.9411 70	0.07312 0.5475 70	V
Y																									1.00000 0.0000 70	0.02468 0.8393 70	-0.10738 0.3763 70	Y
ZN																										1.00000 0.0000 70	0.28443 0.0170 70	ZN
ZR																											1.00000 0.0000 70	ZR

APPENDIX 4

Spearman correlation matrix for major- and trace element content of Waaikraal pyroxenite (a) and magnetite-rich rock (b). The computed level of significance (given underneath the correlation coefficient) is based on the respective number of observations above the lower limit of detection (given below the level of significance).

b: Magnetite-Rich Rock

	TIO2	AL2O3	FE2O3	MNO	MGO	CAO	NA2O	K2O	P2O5	AU	BA	CO	CR	CU	GA	MO	NB	NI	RB	SR	U	V	Y	ZN	ZR	
SIO2	0.35981 0.0075 54	0.81047 0.0001 54	-0.97565 0.0001 24	0.22227 0.1062 54	0.64729 0.0001 54	0.86583 0.0001 54	0.31227 0.0930 30	0.65085 0.0001 53	0.37813 0.0685 24	-0.29852 0.0306 54	0.44317 0.0008 54	0.17862 0.2408 47	0.25088 0.0673 54	0.22039 0.1093 54	-0.16465 0.2688 47	-0.24526 0.0797 52	0.23943 0.0812 54	-0.12546 0.4171 44	0.15619 0.5635 16	0.46960 0.0008 48	-0.03251 0.8887 21	0.21302 0.1417 49	0.71761 0.0001 54	-0.63337 0.0001 54	0.57780 0.0001 52	SIO2
TIO2	1.00000 0.0000 54	0.23885 0.0820 54	-0.66797 0.0004 24	-0.08874 0.5234 54	0.55829 0.0001 54	0.28202 0.0388 54	0.37496 0.0412 30	0.32578 0.0173 53	0.22293 0.2951 24	-0.17145 0.2151 54	0.32114 0.0179 54	0.70240 0.0001 47	0.33017 0.0198 54	0.24173 0.0782 54	-0.21484 0.1470 47	0.03147 0.8248 52	0.02706 0.8460 54	0.39817 0.0074 44	0.20455 0.4473 16	0.15062 0.3068 48	0.08683 0.7082 21	0.31692 0.0265 49	0.19151 0.1654 54	-0.11190 0.4205 54	0.05557 0.6956 52	TIO2
AL2O3		1.00000 0.0000 54	-0.83565 0.0001 24	0.08842 0.5249 54	0.48196 0.0008 54	0.80243 0.0001 54	-0.18901 0.3172 30	0.50213 0.0001 53	0.33047 0.1187 24	-0.28173 0.0390 54	0.44276 0.0008 54	-0.09029 0.5461 47	0.19263 0.1629 54	-0.03366 0.8091 54	-0.07696 0.6072 47	-0.18206 0.1964 52	0.57173 0.0001 54	-0.13554 0.3803 44	0.07509 0.7822 16	0.36957 0.0097 48	0.06762 0.7709 21	0.27840 0.0527 49	0.88315 0.0001 54	-0.75708 0.0001 54	0.59595 0.0001 52	AL2O3
FE2O3			1.00000 0.0000 24	0.10845 0.6140 24	-0.71469 0.0001 24	-0.90609 0.0001 24	-0.37325 0.2321 12	-0.54177 0.0076 23	-0.15936 0.6821 9	0.21308 0.3175 24	-0.51217 0.0105 24	-0.32942 0.1448 21	-0.21270 0.3183 24	-0.30897 0.1413 24	-0.07138 0.7585 21	0.26445 0.2227 23	-0.30398 0.1487 24	-0.13113 0.6040 18	-0.28694 0.4541 9	-0.41766 0.0531 16	-0.36820 0.3296 9	-0.18550 0.3855 24	-0.63446 0.0009 24	0.48114 0.0173 24	-0.69068 0.0004 22	FE2O3
MNO				1.00000 0.0000 54	0.02449 0.8605 54	-0.05364 0.7001 54	0.01485 0.9379 30	0.01189 0.9327 53	0.09413 0.6618 24	-0.32039 0.0182 54	-0.13510 0.3300 54	0.16333 0.2726 47	-0.08814 0.5262 54	0.09951 0.4740 54	-0.04287 0.7748 47	0.06185 0.6631 52	-0.07485 0.5906 54	-0.35066 0.0196 44	-0.01654 0.9515 16	0.09920 0.5423 48	-0.26891 0.2385 21	-0.08588 0.5574 49	-0.00527 0.9698 54	-0.17335 0.2100 54	-0.01671 0.9176 52	MNO
MGO					1.00000 0.0000 54	0.96418 0.0001 54	0.69116 0.0001 30	0.37231 0.0060 53	0.05587 0.7954 24	0.00409 0.9766 54	0.26724 0.0508 54	0.44885 0.0016 47	0.35101 0.0088 54	0.33805 0.0124 54	-0.13052 0.3819 47	-0.20876 0.1375 52	-0.07564 0.5867 54	0.21953 0.1522 44	0.31273 0.1551 16	0.31781 0.0277 48	-0.04556 0.8445 21	0.28455 0.0475 49	0.31683 0.0050 54	-0.30000 0.0275 54	0.35685 0.0094 52	MGO
CAO						1.00000 0.0000 54	0.21353 0.2572 30	0.52495 0.0001 53	0.28235 0.1811 24	-0.23886 0.0820 54	0.42597 0.0013 54	0.06678 0.6556 47	0.26384 0.0539 54	0.07879 0.5741 54	-0.02852 0.8700 47	-0.17642 0.2109 52	0.45992 0.0005 54	-0.14583 0.3449 44	0.31238 0.2388 16	0.42795 0.0024 48	0.02796 0.9082 21	0.15697 0.2814 49	0.77865 0.0001 54	-0.59321 0.0001 54	0.68795 0.0001 52	CAO
NA2O							1.00000 0.0000 30	0.38513 0.0356 30	0.04030 0.8866 15	0.02203 0.9080 30	0.04814 0.8005 30	0.29248 0.1236 29	0.25968 0.1661 30	0.40335 0.0271 30	-0.07237 0.7253 26	-0.45818 0.0133 29	-0.54930 0.0017 30	0.28131 0.1470 28	-0.41476 0.3169 8	0.29916 0.1149 29	0.04951 0.8052 13	-0.09359 0.6357 28	-0.20544 0.2761 30	0.07036 0.7118 30	-0.01286 0.9462 30	NA2O
K2O								1.00000 0.0000 53	0.52047 0.0109 23	-0.31717 0.0207 53	0.67896 0.0001 53	0.03764 0.8039 46	0.19418 0.1635 51	0.18013 0.4747 51	-0.15117 0.3095 46	-0.12765 0.3720 51	0.09201 0.5123 53	-0.13008 0.4057 43	-0.16883 0.5319 16	0.72357 0.0001 47	-0.32930 0.1563 20	0.19096 0.1916 48	0.45515 0.0006 53	-0.30840 0.0247 53	0.39386 0.0039 52	K2O
P2O5									1.00000 0.0000 24	-0.08260 0.7012 24	0.45721 0.0247 24	0.26460 0.2464 21	-0.00204 0.9924 24	-0.10930 0.6112 24	-0.52912 0.0113 22	-0.15130 0.4804 24	0.05447 0.8018 24	-0.35961 0.1093 21	-0.19528 0.5101 5	0.46856 0.0278 22	-0.29254 0.3321 13	0.32150 0.1669 20	0.35801 0.0858 24	-0.27614 0.1915 24	0.07823 0.7364 23	P2O5
AU										1.00000 0.0000 54	-0.37057 0.0058 54	-0.06580 0.6603 47	0.01416 0.9190 54	-0.06951 0.6174 54	0.19946 0.1789 47	-0.23306 0.0964 52	-0.16121 0.2482 54	0.36656 0.0144 44	-0.17848 0.5184 16	-0.08713 0.5560 48	0.01106 0.9621 21	-0.01095 0.9405 49	-0.22398 0.1035 54	0.35584 0.0083 54	-0.22346 0.1113 52	AU
BA											1.00000 0.0000 54	0.09326 0.5329 47	0.19200 0.1643 54	-0.00380 0.9782 54	-0.33711 0.0205 47	-0.09327 0.5108 52	0.26274 0.0549 54	-0.21307 0.1649 44	-0.20725 0.4412 16	0.46854 0.0008 48	-0.01756 0.9398 21	0.29537 0.0394 49	0.49325 0.0002 54	-0.29178 0.0323 54	0.34108 0.0133 52	BA
CO												1.00000 0.0000 47	0.19511 0.1888 47	0.26734 0.0693 47	-0.11240 0.4881 47	0.12103 0.4284 45	-0.19088 0.1987 47	0.26023 0.1049 40	0.46640 0.0927 14	-0.02393 0.8789 43	0.16816 0.5048 18	0.20202 0.1995 42	-0.14616 0.3269 47	0.14365 0.3394 47	-0.11345 0.4581 45	CO
CR													1.00000 0.0000 54	-0.11202 0.4200 54	-0.15745 0.2905 47	-0.19884 0.1505 52	0.09778 0.4818 54	0.34851 0.0204 44	0.10521 0.6982 16	-0.01577 0.9153 48	-0.15317 0.5074 21	0.13999 0.3374 49	0.17304 0.2108 54	-0.24395 0.0755 54	0.09793 0.4897 52	CR
CU														1.00000 0.0000 54	-0.28698 0.0505 47	-0.07721 0.5864 52	-0.22581 0.1006 54	0.22331 0.1451 44	-0.07850 0.7126 16	0.06303 0.6704 48	0.22135 0.3349 21	0.02299 0.8754 49	-0.00053 0.9969 54	-0.00547 0.9687 54	0.02836 0.8418 52	CU
GA															1.00000 0.0000 47	0.24139 0.1102 45	0.06442 0.6671 47	-0.07629 0.6489 38	0.53989 0.0568 13	0.09828 0.7643 41	0.15561 0.5247 19	-0.33609 0.0257 44	-0.14438 0.3329 47	0.16396 0.2708 47	-0.00790 0.9589 45	GA
MO																1.00000 0.0000 52	0.07234 0.6103 52	-0.19448 0.2171 42	0.38383 0.1578 15	0.04701 0.7537 47	0.28352 0.2130 21	0.02205 0.8831 47	-0.12938 0.3606 52	0.14611 0.3013 52	-0.10521 0.4671 50	MO
NB																	1.00000 0.0000 54	-0.30623 0.0432 44	0.00751 0.9780 16	0.13715 0.3526 48	0.03902 0.8666 21	-0.01044 0.9432 49	0.66948 0.0001 54	-0.48476 0.0002 54	0.35229 0.0106 52	NB
NI																		1.00000 0.0000 44	-0.02658 0.9313 13	-0.18101 0.2574 41	0.29432 0.2078 20	0.02075 0.8989 40	-0.22719 0.1181 44	0.22568 0.1408 44	-0.33187 0.0318 42	NI
RB																			1.00000 0.0000 16	0.05175 0.8605 14	0.61721 0.1917 6	-0.21250 0.4470 15	-0.02703 0.9208 16	0.16832 0.5332 16	0.14432 0.6078 15	RB
SR																				1.00000 0.0000 48	0.09278 0.6912 20	0.06263 0.6899 43	0.39098 0.0060 48	-0.14315 0.3317 48	0.35830 0.0145 46	SR
U																					1.00000 0.0000 21	-0.27509 0.2544 19	0.10923 0.6374 21	0.12406 0.5921 21	-0.27369 0.2569 19	U
V																						1.00000 0.0000 49	0.09731 0.5059 49	-0.07351 0.6157 49	0.29579 0.0435 47	V
Y																							1.00000 0.0000 54	-0.73875 0.0001 54	0.53588 0.0001 52	Y
ZN																								1.00000 0.0000 54	-0.35545 0.0097 52	ZN

APPENDIX 5

5.1 Results of microprobe analyses of clinopyroxenes together with the number of ions on the basis of 6 oxygen atoms (all iron as FeO, <lld = less than the lower limit of detection).

a: Pyroxenite

SAMPLE	SiO_2 Si	TiO_2 Ti	Al_2O_3 Al	Cr_2O_3 Cr	FeO Fe	MnO Mn	MgO Mg	CaO Ca	Na_2O Na	K_2O K	TOTAL
WK3.2	48.10	0.14	0.96	<lld	27.37	0.73	1.93	20.52	0.17	<lld	99.77
	1.971	-	0.046	-	0.938	0.025	0.118	0.901	0.014	-	
WK3.2	47.69	0.11	1.09	<lld	27.94	0.78	1.93	20.06	0.20	<lld	99.68
	1.961	-	0.053	-	0.961	0.027	0.118	0.884	0.016	-	
WK3.2	47.66	0.10	0.60	<lld	27.13	0.72	2.06	20.25	0.11	<lld	98.54
	1.978	-	0.030	-	0.941	0.025	0.128	0.900	0.009	-	
WK3.2	47.48	0.09	0.53	<lld	27.40	0.76	2.12	20.53	0.12	<lld	98.95
	1.968	-	0.026	-	0.950	0.027	0.131	0.912	0.010	-	
WK3.2	47.76	0.16	0.98	<lld	27.97	0.75	2.18	20.16	0.17	<lld	99.97
	1.959	-	0.047	-	0.959	0.026	0.133	0.886	0.014	-	
WK3.2	47.81	0.13	0.97	<lld	27.75	0.77	2.16	19.96	0.18	<lld	99.60
	1.965	-	0.047	-	0.954	0.027	0.132	0.879	0.014	-	
WK3.2	48.60	<lld	0.09	<lld	27.08	0.79	2.24	21.30	0.09	<lld	100.18
	1.985	-	0.004	-	0.925	0.027	0.136	0.932	0.007	-	
WK3.2	48.46	0.02	0.08	<lld	26.91	0.78	2.25	20.84	0.09	<lld	99.40
	1.992	-	0.004	-	0.925	0.027	0.138	0.918	0.007	-	
WK5.2	48.30	0.17	1.13	<lld	27.82	0.70	2.22	20.71	0.16	<lld	101.04
	1.957	-	0.054	-	0.942	0.024	0.134	0.899	0.012	-	
WK5.2	47.77	0.19	1.21	<lld	28.13	0.61	2.21	20.65	0.18	<lld	100.77
	1.945	-	0.058	-	0.958	0.021	0.134	0.901	0.014	-	
WK5.2	46.97	0.07	0.60	<lld	27.79	0.67	2.19	20.59	0.15	<lld	98.97
	1.953	-	0.029	-	0.966	0.024	0.136	0.917	0.012	-	
WK5.2	46.94	0.09	0.58	0.02	28.17	0.70	2.18	20.51	0.16	<lld	99.24
	1.950	-	0.028	-	0.979	0.025	0.135	0.913	0.013	-	
WK5.2	46.56	0.24	1.57	0.03	28.35	0.80	2.12	19.20	0.20	<lld	98.79
	1.937	-	0.077	-	0.987	0.028	0.131	0.856	0.016	-	
WK5.2	46.68	0.25	1.61	0.03	28.45	0.73	2.14	19.30	0.20	<lld	99.12
	1.936	-	0.079	-	0.987	0.026	0.132	0.857	0.016	-	
WK5.2	46.19	0.37	1.24	<lld	30.04	0.63	2.16	18.57	0.17	<lld	99.01
	1.931	-	0.061	-	1.050	0.022	0.135	0.832	0.014	-	
WK5.2	46.19	0.39	1.25	<lld	30.08	0.69	2.20	18.74	0.20	<lld	99.35
	1.926	-	0.062	-	1.049	0.024	0.137	0.837	0.016	-	
WK5.2	47.19	0.26	1.43	0.02	28.18	0.65	2.07	19.75	0.20	<lld	99.47
	1.947	-	0.069	-	0.972	0.023	0.127	0.873	0.016	-	
WK6.3	47.62	0.08	1.38	0.02	29.14	0.76	1.69	19.50	0.11	0.10	100.30
	1.953	-	0.067	-	0.999	0.027	0.103	0.857	0.009	0.005	
WK6.3	46.93	0.34	1.92	<lld	28.09	0.67	2.14	19.70	0.25	<lld	99.70
	1.931	-	0.093	-	0.966	0.023	0.131	0.868	0.020	-	
WK6.3	48.10	0.10	0.75	<lld	28.31	0.76	2.22	20.30	0.18	<lld	100.61
	1.962	-	0.036	-	0.966	0.026	0.135	0.887	0.014	-	
WK6.3	48.14	0.09	0.77	<lld	27.98	0.71	2.25	20.35	0.20	<lld	100.41
	1.965	-	0.037	-	0.955	0.025	0.137	0.890	0.016	-	
WK6.3	47.73	0.24	1.45	0.01	28.40	0.63	2.13	19.26	0.24	<lld	99.85
	1.957	-	0.070	-	0.973	0.022	0.130	0.846	0.019	-	
WK6.3	47.73	0.28	1.54	<lld	28.42	0.68	2.17	19.94	0.24	<lld	100.72
	1.944	-	0.074	-	0.968	0.024	0.131	0.870	0.019	-	
WK6.3	48.55	0.06	0.40	0.02	28.58	0.79	2.26	19.15	0.10	<lld	99.83
	1.990	-	0.019	-	0.980	0.027	0.138	0.841	0.008	-	
WK6.3	48.46	0.07	0.35	<lld	28.55	0.78	2.28	20.09	0.13	<lld	100.64
	1.976	-	0.017	-	0.974	0.027	0.139	0.878	0.010	-	
WK6.3	48.59	0.08	0.55	0.01	28.22	0.74	2.36	19.37	0.16	<lld	100.00
	1.986	-	0.026	-	0.965	0.026	0.144	0.848	0.013	-	
WK6.3	48.46	0.08	0.62	0.03	28.48	0.78	2.34	19.31	0.33	<lld	100.32
	1.978	-	0.030	-	0.972	0.027	0.143	0.845	0.026	-	

SAMPLE	SiO_2 Si	TiO_2 Ti	Al_2O_3 Al	Cr_2O_3 Cr	FeO Fe	MnO Mn	MgO Mg	CaO Ca	Na_2O Na	K_2O K	TOTAL
WK11.2	48.17	0.11	1.02	0.03	28.76	0.82	1.30	20.99	0.17	<11d	101.24
	1.960	-	0.049	-	0.978	0.028	0.079	0.915	0.014	-	
WK11.2	47.56	0.09	1.04	0.02	28.82	0.83	1.21	20.77	0.16	<11d	100.39
	1.955	-	0.051	-	0.991	0.029	0.074	0.914	0.013	-	
WK11.2	47.57	0.06	0.81	0.03	29.63	0.78	1.46	19.78	0.13	<11d	100.17
	1.962	-	0.039	-	1.022	0.027	0.090	0.874	0.010	-	
WK11.2	47.76	0.10	0.99	0.04	29.70	0.82	1.19	20.13	0.18	<11d	100.77
	1.959	-	0.048	-	1.018	0.029	0.073	0.884	0.014	-	
WK11.2	47.90	0.13	1.07	0.04	29.67	0.83	1.24	19.96	0.18	<11d	100.85
	1.960	-	0.051	-	1.015	0.029	0.076	0.875	0.014	-	
WK11.2	47.85	0.06	0.97	0.01	30.17	0.85	1.24	19.95	0.16	<11d	101.20
	1.956	-	0.047	-	1.032	0.030	0.076	0.874	0.013	-	
WK11.2	47.69	0.05	0.95	0.04	29.71	0.83	1.18	19.82	0.17	<11d	100.35
	1.963	-	0.046	-	1.023	0.029	0.073	0.874	0.014	-	
WK11.2	47.52	0.07	1.15	0.02	30.16	0.82	1.32	19.62	0.21	<11d	100.80
	1.950	-	0.056	-	1.035	0.028	0.081	0.863	0.016	-	
WK11.2	47.26	0.07	1.14	0.04	29.59	0.73	1.26	19.43	0.16	<11d	99.56
	1.959	-	0.056	-	1.026	0.025	0.078	0.863	0.013	-	
WK12.2	46.86	0.07	1.22	<11d	28.99	0.73	2.06	19.83	0.17	<11d	99.87
	1.936	-	0.059	-	1.002	0.026	0.127	0.878	0.014	-	
WK12.2	45.23	0.08	2.22	0.01	29.31	0.67	1.63	19.92	0.19	<11d	99.18
	1.892	-	0.109	-	1.025	0.024	0.102	0.893	0.016	-	
WK12.2	45.72	0.09	2.16	0.01	29.29	0.67	1.69	20.11	0.25	<11d	99.88
	1.897	-	0.106	-	1.016	0.024	0.104	0.894	0.020	-	
WK12.2	45.70	0.04	2.16	<11d	30.23	0.73	1.49	19.83	0.19	<11d	100.34
	1.894	-	0.106	-	1.048	0.026	0.092	0.881	0.015	-	
WK12.2	45.10	0.05	2.19	<11d	29.66	0.72	1.44	19.53	0.21	<11d	98.86
	1.895	-	0.108	-	1.042	0.026	0.090	0.879	0.018	-	
WK12.2	45.75	0.02	1.59	<11d	29.59	0.77	1.55	20.07	0.18	<11d	99.52
	1.910	-	0.078	-	1.033	0.027	0.097	0.898	0.015	-	
WK12.2	45.72	0.03	1.59	<11d	30.13	0.73	1.63	19.95	0.18	<11d	99.93
	1.905	-	0.078	-	1.049	0.026	0.101	0.890	0.014	-	
WK12.2	45.16	0.04	2.72	<11d	29.55	0.72	1.36	19.51	0.21	<11d	99.24
	1.887	-	0.134	-	1.032	0.025	0.085	0.873	0.017	-	
WK12.2	45.52	0.01	2.61	<11d	29.23	0.64	1.40	20.17	0.22	<11d	99.80
	1.889	-	0.128	-	1.015	0.023	0.086	0.897	0.018	-	
WK12.3	48.85	<11d	0.06	<11d	26.41	0.92	2.57	21.77	0.10	<11d	100.69
	1.981	-	0.003	-	0.896	0.032	0.155	0.946	0.008	-	
WK12.3	48.16	<11d	0.06	<11d	27.05	0.91	2.49	22.00	0.11	<11d	100.78
	1.963	-	0.003	-	0.922	0.032	0.151	0.961	0.009	-	
WK12.3	47.95	0.02	0.35	<11d	27.60	0.95	2.63	20.73	0.16	<11d	100.38
	1.961	-	0.017	-	0.944	0.033	0.161	0.908	0.013	-	
WK12.3	47.33	0.03	0.34	<11d	27.33	0.84	2.60	20.84	0.17	<11d	99.45
	1.956	-	0.016	-	0.945	0.029	0.160	0.923	0.014	-	
WK12.3	47.36	0.06	0.71	<11d	28.13	0.89	2.47	20.44	0.17	<11d	100.17
	1.946	-	0.035	-	0.967	0.031	0.151	0.900	0.014	-	
WK12.3	47.58	0.06	0.72	<11d	28.34	0.82	2.41	20.57	0.15	<11d	100.60
	1.947	-	0.035	-	0.970	0.029	0.147	0.902	0.012	-	
WK12.3	48.17	0.02	0.27	<11d	28.42	0.94	2.41	19.88	0.14	<11d	100.24
	1.974	-	0.013	-	0.974	0.033	0.147	0.873	0.011	-	
WK12.3	47.81	0.01	0.32	<11d	28.08	0.93	2.40	20.56	0.13	<11d	100.24
	1.962	-	0.016	-	0.964	0.032	0.147	0.904	0.011	-	
WK12.3	47.75	0.04	0.62	<11d	28.48	1.04	2.32	19.49	0.16	<11d	99.85
	1.965	-	0.030	-	0.980	0.036	0.142	0.859	0.013	-	
WK12.3	47.95	0.06	0.57	<11d	28.28	0.93	2.39	19.49	0.15	<11d	99.76
	1.971	-	0.028	-	0.972	0.032	0.147	0.859	0.012	-	

SAMPLE	SiO_2	TiO_2	Al_2O_3	Cr_2O_3	FeO	MnO	MgO	CaO	Na_2O	K_2O	TOTAL
	Si	Ti	Al	Cr	Fe	Mn	Mg	Ca	Na	K	
WK12.4	47.45	0.24	1.25	<11d	28.78	0.81	2.43	18.83	0.24	<11d	99.78
	1.952	-	0.061	-	0.990	0.028	0.149	0.830	0.019	-	
WK12.4	47.07	0.21	1.30	0.01	29.31	0.84	2.42	19.56	0.22	<11d	100.73
	1.929	-	0.063	-	1.004	0.029	0.148	0.859	0.017	-	
WK12.4	48.35	0.08	0.54	<11d	28.93	0.88	2.39	18.58	0.12	<11d	99.78
	1.985	-	0.026	-	0.993	0.030	0.146	0.817	0.010	-	
WK12.4	48.14	0.09	0.60	0.01	28.67	0.90	2.38	19.93	0.13	<11d	100.74
	1.964	-	0.029	-	0.978	0.031	0.145	0.871	0.010	-	
WK12.4	47.56	0.14	1.35	0.01	26.93	0.77	2.08	21.20	0.26	<11d	100.16
	1.945	-	0.065	-	0.921	0.027	0.127	0.929	0.021	-	
WK12.4	47.42	0.17	1.22	0.01	26.95	0.79	2.07	20.73	0.24	<11d	99.43
	1.952	-	0.059	-	0.928	0.028	0.127	0.914	0.019	-	
WK12.4	47.10	0.16	1.27	0.06	30.11	0.94	2.33	18.70	0.21	<11d	100.67
	1.934	-	0.061	-	1.034	0.033	0.143	0.823	0.017	-	
WK12.4	47.35	0.19	1.27	<11d	30.09	0.87	2.21	18.79	0.21	<11d	100.80
	1.940	-	0.061	-	1.031	0.030	0.135	0.825	0.017	-	
WK12.4	47.63	0.17	0.82	0.03	28.79	0.79	2.13	18.47	0.13	<11d	98.76
	1.977	-	0.040	-	0.999	0.028	0.131	0.821	0.011	-	
WK12.4	47.87	0.21	0.84	0.04	27.95	0.74	2.17	20.42	0.11	<11d	100.11
	1.961	-	0.041	-	0.957	0.026	0.132	0.896	0.009	-	
WK13.2	47.86	0.11	0.58	0.02	29.78	0.92	2.39	19.24	0.16	<11d	100.94
	1.957	-	0.028	-	1.018	0.032	0.146	0.843	0.013	-	
WK13.2	47.23	0.08	0.59	0.04	29.55	0.99	2.32	19.46	0.15	<11d	100.30
	1.948	-	0.029	-	1.019	0.035	0.143	0.860	0.012	-	
WK13.2	47.68	0.08	0.75	<11d	27.67	0.88	2.58	19.94	0.16	<11d	99.68
	1.960	-	0.037	-	0.951	0.031	0.158	0.878	0.013	-	
WK13.2	48.10	0.08	0.74	0.02	28.02	0.84	2.64	20.10	0.18	<11d	100.63
	1.959	-	0.036	-	0.954	0.029	0.160	0.877	0.014	-	
WK13.2	46.82	0.15	1.12	0.01	27.04	0.71	2.46	21.07	0.21	<11d	99.43
	1.934	-	0.055	-	0.934	0.025	0.151	0.932	0.017	-	
WK13.2	46.72	0.15	1.11	0.02	26.42	0.71	2.48	21.03	0.21	<11d	98.69
	1.939	-	0.054	-	0.917	0.025	0.153	0.935	0.017	-	
WK13.2	47.26	0.12	1.04	<11d	27.18	0.75	2.53	21.17	0.24	<11d	100.17
	1.937	-	0.050	-	0.931	0.026	0.154	0.930	0.019	-	
WK13.2	47.38	0.12	1.03	0.01	26.93	0.76	2.49	21.14	0.21	<11d	99.93
	1.943	-	0.050	-	0.924	0.026	0.152	0.929	0.017	-	
WK13.2	47.92	0.10	0.66	0.03	27.89	0.79	2.55	20.68	0.15	<11d	100.64
	1.955	-	0.032	-	0.951	0.027	0.155	0.904	0.012	-	
WK13.2	47.88	0.13	0.71	0.01	28.07	0.91	2.61	20.67	0.15	<11d	101.00
	1.948	-	0.034	-	0.955	0.031	0.158	0.901	0.012	-	
WK13.2	48.81	0.07	0.39	<11d	27.26	0.94	2.55	20.38	0.13	<11d	100.46
	1.983	-	0.019	-	0.926	0.032	0.155	0.887	0.010	-	
WK13.2	47.94	0.08	0.35	<11d	29.16	0.89	2.41	18.78	0.15	<11d	99.68
	1.977	-	0.017	-	1.006	0.031	0.148	0.830	0.012	-	
WK14.4	47.78	0.08	0.50	<11d	28.85	0.90	2.25	19.81	0.13	<11d	100.23
	1.963	-	0.024	-	0.991	0.031	0.138	0.872	0.011	-	
WK14.4	47.15	0.04	0.49	<11d	28.69	0.84	2.10	19.40	0.15	<11d	98.82
	1.966	-	0.024	-	1.000	0.030	0.130	0.866	0.012	-	
WK14.4	47.45	0.03	0.78	<11d	28.61	0.79	2.13	20.10	0.20	<11d	100.07
	1.953	-	0.038	-	0.985	0.028	0.131	0.886	0.016	-	
WK14.4	47.44	0.02	0.79	<11d	28.66	0.83	2.13	20.13	0.17	<11d	100.15
	1.951	-	0.038	-	0.986	0.029	0.131	0.887	0.013	-	
WK14.4	47.74	0.07	0.75	<11d	28.00	0.85	2.19	20.77	0.21	<11d	100.51
	1.953	-	0.036	-	0.958	0.029	0.134	0.910	0.016	-	
WK14.4	47.65	0.05	0.71	<11d	28.22	0.79	2.24	20.61	0.20	<11d	100.42
	1.953	-	0.034	-	0.967	0.028	0.137	0.905	0.016	-	
WK14.4	47.03	0.05	0.71	<11d	30.54	1.56	2.48	18.28	0.16	<11d	100.76
	1.938	-	0.035	-	1.052	0.054	0.152	0.807	0.013	-	
WK14.4	47.26	0.04	0.75	0.01	30.73	0.83	2.15	18.14	0.18	<11d	100.04
	1.955	-	0.037	-	1.063	0.029	0.132	0.804	0.015	-	
WK14.4	46.84	0.19	1.32	<11d	27.66	0.72	1.99	20.77	0.24	<11d	99.55
	1.935	-	0.064	-	0.955	0.025	0.123	0.920	0.019	-	
WK14.4	46.46	0.20	1.23	<11d	27.62	0.71	2.09	20.50	0.23	<11d	98.85
	1.935	-	0.060	-	0.962	0.025	0.130	0.915	0.019	-	

SAMPLE	SiO_2	TiO_2	Al_2O_3	Cr_2O_3	FeO	MnO	MgO	CaO	Na_2O	K_2O	TOTAL
	Si	Ti	Al	Cr	Fe	Mn	Mg	Ca	Na	K	
WK16.2	46.53	0.09	1.44	<11d	30.65	0.75	1.00	20.54	0.25	<11d	101.16
	1.917	-	0.070	-	1.056	0.026	0.062	0.907	0.020	-	
WK16.2	46.63	0.09	1.51	<11d	30.14	0.70	1.04	20.47	0.26	<11d	100.76
	1.923	-	0.073	-	1.039	0.024	0.064	0.904	0.021	-	
WK16.2	46.92	0.11	1.24	<11d	29.38	0.82	0.97	19.98	0.21	<11d	99.51
	1.950	-	0.061	-	1.021	0.029	0.060	0.890	0.017	-	
WK16.2	46.72	0.11	1.22	<11d	29.38	0.74	0.91	20.89	0.24	<11d	100.10
	1.936	-	0.060	-	1.018	0.026	0.056	0.928	0.019	-	
WK16.2	47.09	0.01	0.80	<11d	28.57	0.83	0.96	21.25	0.16	<11d	99.68
	1.955	-	0.039	-	0.992	0.029	0.060	0.945	0.013	-	
WK16.2	46.59	<11d	0.80	<11d	28.61	0.72	0.93	20.98	0.13	<11d	98.76
	1.953	-	0.040	-	1.003	0.025	0.058	0.942	0.010	-	
WK16.2	47.10	0.02	0.86	0.02	29.47	0.87	1.03	19.53	0.21	<11d	99.06
	1.966	-	0.042	-	1.028	0.031	0.064	0.873	0.017	-	
WK20.5	49.22	<11d	0.19	<11d	26.21	0.80	3.38	21.30	0.10	<11d	101.21
	1.978	-	0.009	-	0.881	0.027	0.202	0.917	0.008	-	
WK20.5	48.70	0.03	0.19	<11d	26.59	0.88	3.21	21.01	0.15	<11d	100.74
	1.972	-	0.009	-	0.901	0.030	0.194	0.912	0.012	-	
WK20.5	48.50	0.07	0.42	<11d	26.21	0.77	3.63	20.79	0.16	<11d	100.48
	1.964	-	0.020	-	0.888	0.026	0.219	0.902	0.012	-	
WK20.5	48.37	0.04	0.49	<11d	26.34	0.79	3.43	19.20	0.19	<11d	98.81
	1.985	-	0.024	-	0.904	0.028	0.210	0.845	0.015	-	
WK20.5	48.51	0.04	0.50	<11d	26.52	0.86	3.39	19.98	0.17	<11d	99.93
	1.974	-	0.024	-	0.903	0.030	0.206	0.871	0.014	-	
WK20.5	49.01	0.02	0.11	<11d	25.35	0.84	3.58	20.58	0.12	<11d	99.58
	1.992	-	0.005	-	0.861	0.029	0.217	0.896	0.009	-	
WK20.5	48.87	0.03	0.10	<11d	25.43	0.83	3.52	21.10	0.12	<11d	99.97
	1.983	-	0.005	-	0.863	0.029	0.213	0.917	0.009	-	
WK20.5	49.14	0.04	0.29	0.05	24.50	0.92	3.57	22.18	0.11	<11d	100.71
	1.975	-	0.014	-	0.823	0.031	0.214	0.955	0.009	-	
WK21.5	49.15	0.03	0.08	0.02	24.65	1.01	2.93	23.47	0.07	<11d	101.36
	1.973	-	0.004	-	0.827	0.034	0.176	1.009	0.006	-	
WK21.5	48.67	0.03	0.17	0.01	25.67	0.84	3.42	21.08	0.16	<11d	100.02
	1.978	-	0.008	-	0.872	0.029	0.207	0.918	0.013	-	
WK21.5	48.73	0.05	0.14	<11d	26.19	0.86	3.58	19.56	0.14	<11d	99.20
	1.992	-	0.007	-	0.895	0.030	0.218	0.857	0.011	-	
WK21.5	49.13	0.01	0.21	<11d	25.42	0.81	3.49	21.69	0.15	<11d	100.90
	1.976	-	0.010	-	0.855	0.028	0.209	0.935	0.012	-	
WK21.5	48.68	<11d	0.07	<11d	25.36	0.78	3.46	21.04	0.14	<11d	99.53
	1.984	-	0.004	-	0.864	0.027	0.210	0.919	0.011	-	
WK21.5	48.74	0.01	0.08	<11d	25.35	0.81	3.42	22.36	0.13	<11d	100.89
	1.967	-	0.004	-	0.855	0.028	0.206	0.967	0.010	-	
WK21.5	48.64	0.03	0.10	<11d	25.34	0.77	3.54	22.15	0.09	<11d	100.63
	1.967	-	0.005	-	0.857	0.026	0.214	0.959	0.007	-	
WK21.5	48.69	0.03	0.10	<11d	25.22	0.84	3.53	20.62	0.11	<11d	99.11
	1.990	-	0.005	-	0.862	0.029	0.215	0.903	0.009	-	
WK26.2	48.81	0.13	0.90	0.03	25.29	0.55	4.21	21.12	0.13	<11d	101.01
	1.954	-	0.042	-	0.847	0.019	0.252	0.906	0.010	-	
WK26.2	48.18	0.08	0.82	<11d	24.55	0.51	4.17	20.98	0.13	<11d	99.34
	1.959	-	0.039	-	0.835	0.017	0.253	0.914	0.010	-	
WK26.2	48.69	0.11	0.59	0.04	24.60	0.50	4.31	21.42	0.06	<11d	100.17
	1.963	-	0.028	-	0.829	0.017	0.259	0.925	0.004	-	
WK26.2	48.60	0.10	0.60	0.04	24.38	0.55	4.40	20.73	0.07	<11d	99.34
	1.971	-	0.029	-	0.827	0.019	0.266	0.901	0.006	-	
WK26.2	47.76	0.24	0.79	0.01	27.14	0.71	2.63	20.74	0.21	<11d	99.97
	1.956	-	0.038	-	0.929	0.025	0.160	0.910	0.016	-	
WK26.2	47.83	0.24	0.74	0.04	26.69	0.68	2.53	20.08	0.21	<11d	98.76
	1.975	-	0.036	-	0.921	0.024	0.156	0.888	0.017	-	
WK26.2	48.22	0.14	0.66	0.06	26.84	0.69	3.21	19.81	0.18	<11d	99.61
	1.971	-	0.032	-	0.917	0.024	0.195	0.867	0.014	-	
WK26.2	47.87	0.11	0.64	0.03	26.13	0.65	3.17	20.54	0.19	<11d	99.19
	1.965	-	0.031	-	0.897	0.023	0.194	0.903	0.015	-	

SAMPLE	SiO_2	TiO_2	Al_2O_3	Cr_2O_3	FeO	MnO	MgO	CaO	Na_2O	K_2O	TOTAL
	Si	Ti	Al	Cr	Fe	Mn	Mg	Ca	Na	K	
WK26.2	48.60	0.06	0.23	0.03	25.70	0.77	3.42	21.52	0.15	<11d	100.39
	1.970	-	0.011	-	0.871	0.026	0.207	0.934	0.012	-	
WK26.2	48.90	0.02	0.17	0.03	25.55	0.73	3.46	21.38	0.15	<11d	100.34
	1.979	-	0.008	-	0.864	0.025	0.209	0.927	0.012	-	
WK28.4	49.70	0.03	0.22	<11d	23.66	0.70	5.39	20.85	0.17	<11d	100.69
	1.979	-	0.010	-	0.788	0.024	0.320	0.889	0.013	-	
WK28.4	49.52	0.03	0.22	<11d	23.53	0.73	5.40	20.07	0.16	<11d	99.63
	1.988	-	0.011	-	0.790	0.025	0.323	0.863	0.012	-	
WK28.4	49.49	0.03	0.22	<11d	23.58	0.74	5.53	20.72	0.16	<11d	100.44
	1.976	-	0.010	-	0.787	0.025	0.329	0.886	0.013	-	
WK28.4	47.87	0.27	1.54	<11d	24.86	0.58	3.85	21.13	0.23	<11d	100.07
	1.936	-	0.073	-	0.841	0.020	0.232	0.916	0.018	-	
WK28.4	48.04	0.26	1.48	<11d	24.35	0.61	3.90	21.21	0.24	<11d	99.84
	1.943	-	0.070	-	0.824	0.021	0.235	0.919	0.019	-	
WK28.4	48.38	0.25	1.44	<11d	24.51	0.62	4.75	19.44	0.24	<11d	99.38
	1.955	-	0.068	-	0.828	0.021	0.286	0.841	0.019	-	
WK28.4	48.45	0.24	1.47	<11d	24.94	0.65	4.76	20.16	0.23	<11d	100.67
	1.940	-	0.069	-	0.835	0.022	0.284	0.865	0.018	-	
WK28.4	47.91	0.19	1.50	<11d	25.25	0.58	4.53	18.90	0.21	0.06	98.95
	1.951	-	0.072	-	0.860	0.020	0.275	0.825	0.017	0.003	

b: Magnetite-Rich Rock

SAMPLE	SiO_2	TiO_2	Al_2O_3	Cr_2O_3	FeO	MnO	MgO	CaO	Na_2O	K_2O	TOTAL
	Si	Ti	Al	Cr	Fe	Mn	Mg	Ca	Na	K	
WK4.1	47.22	0.11	1.72	<11d	29.17	0.75	1.53	20.24	0.18	<11d	100.81
	1.932	-	0.083	-	0.998	0.026	0.093	0.887	0.014	-	
WK4.1	47.02	0.12	1.80	0.01	29.67	0.72	1.61	20.28	0.19	<11d	101.30
	1.920	-	0.087	-	1.013	0.025	0.098	0.887	0.015	-	
WK4.1	46.94	0.11	2.11	0.02	29.34	0.64	1.53	19.26	0.18	<11d	100.00
	1.932	-	0.103	-	1.010	0.022	0.094	0.849	0.014	-	
WK4.1	46.94	0.10	2.04	0.02	29.33	0.76	1.55	20.15	0.17	<11d	100.94
	1.920	-	0.098	-	1.003	0.026	0.094	0.883	0.013	-	
WK4.1	46.85	0.08	1.90	<11d	29.09	0.63	1.50	20.15	0.21	<11d	100.33
	1.926	-	0.092	-	1.000	0.022	0.092	0.887	0.017	-	
WK4.1	46.84	0.12	1.98	0.02	29.05	0.72	1.52	19.48	0.20	<11d	99.79
	1.933	-	0.097	-	1.002	0.025	0.093	0.861	0.016	-	
WK4.1	46.86	0.13	1.89	0.03	30.14	0.74	1.24	19.36	0.19	<11d	100.43
	1.930	-	0.092	-	1.038	0.026	0.076	0.854	0.015	-	
WK4.1	46.64	0.09	1.93	0.02	29.90	0.74	1.29	18.19	0.20	<11d	98.89
	1.944	-	0.095	-	1.042	0.026	0.080	0.813	0.016	-	
WK4.1	46.61	0.11	2.10	<11d	29.75	0.66	1.40	20.11	0.22	<11d	100.85
	1.913	-	0.102	-	1.021	0.023	0.086	0.884	0.018	-	
WK4.1	46.45	0.08	2.16	<11d	29.33	0.66	1.40	20.22	0.22	<11d	100.44
	1.912	-	0.105	-	1.010	0.023	0.086	0.892	0.018	-	
WK4.1	46.56	0.15	1.49	0.02	29.98	0.79	1.63	20.02	0.19	<11d	100.65
	1.919	-	0.072	-	1.034	0.027	0.100	0.884	0.015	-	
WK4.1	46.67	0.12	1.52	0.01	29.74	0.66	1.56	19.24	0.16	<11d	99.56
	1.937	-	0.074	-	1.032	0.023	0.097	0.856	0.013	-	
WK4.1	46.33	0.14	1.78	<11d	29.20	0.71	1.57	20.14	0.17	<11d	99.90
	1.918	-	0.087	-	1.011	0.025	0.097	0.893	0.014	-	
WK4.1	46.36	0.13	1.73	0.01	29.37	0.70	1.59	20.18	0.20	<11d	100.13
	1.917	-	0.084	-	1.015	0.024	0.098	0.894	0.016	-	
WK4.1	47.05	0.17	1.90	<11d	29.49	0.75	1.52	18.79	0.16	<11d	99.67
	1.943	-	0.093	-	1.018	0.026	0.094	0.831	0.013	-	
WK4.1	47.17	0.12	1.49	<11d	29.82	0.78	1.58	19.52	0.17	<11d	100.54
	1.938	-	0.072	-	1.025	0.027	0.097	0.859	0.014	-	
WK4.1	47.17	0.12	1.55	<11d	29.85	0.76	1.55	20.26	0.21	<11d	101.35
	1.927	-	0.074	-	1.019	0.026	0.095	0.887	0.017	-	
WK4.1	47.50	0.06	1.29	0.01	29.92	0.79	1.66	19.58	0.16	<11d	100.91
	1.944	-	0.062	-	1.024	0.028	0.101	0.859	0.013	-	

SAMPLE	SiO_2	TiO_2	Al_2O_3	Cr_2O_3	FeO	MnO	MgO	CaO	Na_2O	K_2O	TOTAL
	Si	Ti	Al	Cr	Fe	Mn	Mg	Ca	Na	K	
WK4.1	47.59	0.07	1.32	0.01	29.59	0.70	1.72	19.95	0.15	<lld	101.02
	1.943	-	0.063	-	1.011	0.024	0.105	0.873	0.012	-	
WK8.3	46.65	0.04	2.40	<lld	29.49	0.65	1.45	19.98	0.19	<lld	100.81
	1.911	-	0.116	-	1.010	0.023	0.089	0.877	0.015	-	
WK8.3	46.46	0.03	2.15	0.03	29.41	0.73	1.49	18.67	0.21	<lld	99.12
	1.931	-	0.105	-	1.022	0.026	0.092	0.831	0.017	-	
WK8.3	46.53	0.01	2.20	0.03	29.22	0.69	1.50	18.83	0.21	<lld	99.18
	1.931	-	0.108	-	1.014	0.024	0.093	0.837	0.017	-	
WK8.3	46.30	0.02	2.55	<lld	29.07	0.68	1.38	20.03	0.21	<lld	100.21
	1.907	-	0.124	-	1.001	0.024	0.084	0.884	0.017	-	
WK8.3	46.56	<lld	2.54	<lld	28.95	0.62	1.36	19.94	0.16	<lld	100.13
	1.915	-	0.123	-	0.996	0.022	0.084	0.879	0.013	-	
WK8.3	46.63	0.01	1.93	<lld	29.13	0.74	1.53	19.80	0.21	<lld	99.97
	1.925	-	0.094	-	1.005	0.026	0.094	0.876	0.016	-	
WK8.3	46.99	0.02	1.88	<lld	29.11	0.73	1.61	19.67	0.17	<lld	100.17
	1.932	-	0.091	-	1.001	0.025	0.099	0.867	0.014	-	
WK8.3	47.12	<lld	1.62	0.02	29.38	0.75	1.61	19.80	0.14	<lld	100.41
	1.936	-	0.078	-	1.009	0.026	0.098	0.871	0.011	-	
WK8.3	47.13	0.03	1.59	0.02	29.69	0.83	1.62	19.34	0.20	<lld	100.41
	1.938	-	0.077	-	1.021	0.029	0.099	0.852	0.016	-	
WK8.3	47.32	0.01	1.50	<lld	29.41	0.74	1.66	18.62	0.16	<lld	99.40
	1.957	-	0.073	-	1.017	0.026	0.102	0.825	0.013	-	
WK8.3	47.41	<lld	1.49	0.04	29.45	0.77	1.58	19.77	0.16	<lld	100.65
	1.943	-	0.072	-	1.009	0.027	0.096	0.868	0.013	-	
WK12.1	45.77	0.04	2.11	<lld	28.23	0.86	1.89	19.70	0.16	<lld	98.73
	1.911	-	0.104	-	0.986	0.030	0.118	0.881	0.013	-	
WK12.1	45.78	0.01	2.45	0.01	27.88	0.89	1.72	20.00	0.19	<lld	98.91
	1.906	-	0.120	-	0.971	0.031	0.107	0.892	0.016	-	
WK12.1	45.81	0.04	2.54	0.02	28.45	0.77	1.60	19.99	0.18	<lld	99.35
	1.902	-	0.124	-	0.988	0.027	0.099	0.889	0.014	-	
WK12.1	46.28	0.01	2.17	<lld	27.98	0.80	1.85	20.06	0.15	<lld	99.28
	1.917	-	0.106	-	0.969	0.028	0.114	0.890	0.012	-	
WK12.1	46.12	0.04	2.22	0.34	28.10	0.76	1.74	19.94	0.15	<lld	99.04
	1.916	-	0.109	-	0.976	0.027	0.108	0.888	0.012	-	
WK14.1	47.16	<lld	1.34	<lld	27.96	0.95	2.04	20.19	0.19	<lld	99.84
	1.942	-	0.065	-	0.962	0.033	0.125	0.891	0.015	-	
WK14.1	46.85	<lld	1.43	<lld	27.61	0.98	2.06	19.79	0.18	<lld	98.90
	1.944	-	0.070	-	0.958	0.034	0.127	0.880	0.014	-	
WK14.1	47.21	<lld	1.13	<lld	28.33	1.00	2.19	19.05	0.12	<lld	99.05
	1.957	-	0.055	-	0.982	0.035	0.136	0.846	0.010	-	
WK14.1	47.01	<lld	1.23	<lld	27.98	0.91	2.33	19.29	0.16	<lld	98.93
	1.950	-	0.060	-	0.970	0.032	0.144	0.857	0.013	-	
WK14.1	46.57	<lld	1.24	<lld	27.39	0.95	2.30	20.47	0.15	<lld	99.08
	1.933	-	0.061	-	0.950	0.033	0.142	0.910	0.012	-	
WK14.1	46.72	<lld	1.34	<lld	27.59	0.94	2.20	20.24	0.16	<lld	99.20
	1.936	-	0.065	-	0.956	0.033	0.136	0.898	0.013	-	
WK14.1	46.87	<lld	1.35	<lld	27.50	0.87	2.25	20.12	0.16	<lld	99.12
	1.941	-	0.066	-	0.952	0.031	0.139	0.892	0.013	-	
WK14.1	47.32	<lld	1.08	<lld	27.74	0.96	2.48	19.97	0.14	<lld	99.69
	1.948	-	0.052	-	0.955	0.033	0.152	0.881	0.011	-	
WK14.1	47.30	<lld	1.04	<lld	27.81	0.99	2.40	20.12	0.15	<lld	99.82
	1.946	-	0.050	-	0.957	0.034	0.147	0.887	0.012	-	
WK14.1	47.30	<lld	1.07	<lld	27.34	0.90	2.33	20.47	0.15	<lld	99.56
	1.948	-	0.052	-	0.942	0.031	0.143	0.903	0.012	-	
WK14.1	47.19	<lld	1.03	<lld	27.18	0.92	2.32	20.38	0.16	<lld	99.17
	1.951	-	0.050	-	0.940	0.032	0.143	0.903	0.013	-	
WK15.3	47.14	<lld	2.10	<lld	29.36	0.97	1.53	19.98	0.13	<lld	101.20
	1.922	-	0.101	-	1.001	0.033	0.093	0.873	0.010	-	
WK15.3	46.22	0.02	2.11	<lld	29.04	0.98	1.47	20.64	0.14	<lld	100.59
	1.903	-	0.102	-	1.000	0.034	0.090	0.911	0.011	-	
WK15.3	45.91	0.05	2.55	<lld	29.25	0.93	1.41	20.19	0.17	<lld	100.42
	1.894	-	0.124	-	1.009	0.033	0.087	0.892	0.014	-	

SAMPLE	SiO_2 Si	TiO_2 Ti	Al_2O_3 Al	Cr_2O_3 Cr	FeO Fe	MnO Mn	MgO Mg	CaO Ca	Na_2O Na	K_2O K	TOTAL
WK15.3	45.88	0.03	2.56	<11d	28.94	0.98	1.41	20.24	0.17	<11d	100.18
	1.895	-	0.125	-	1.000	0.034	0.087	0.896	0.014	-	
WK15.3	46.30	<11d	2.49	<11d	28.67	0.97	1.44	20.87	0.16	<11d	100.91
	1.897	-	0.120	-	0.982	0.034	0.088	0.916	0.013	-	
WK15.3	46.35	0.04	2.47	<11d	29.23	0.98	1.51	20.59	0.19	<11d	101.32
	1.894	-	0.119	-	0.999	0.034	0.092	0.901	0.015	-	
WK15.3	46.94	0.02	1.81	<11d	28.34	0.95	1.58	20.83	0.12	<11d	100.56
	1.924	-	0.087	-	0.972	0.033	0.096	0.915	0.010	-	
WK15.3	46.98	<11d	1.79	<11d	28.43	1.01	1.64	20.63	0.14	<11d	100.63
	1.925	-	0.086	-	0.974	0.035	0.100	0.906	0.011	-	
WK15.3	46.10	0.01	2.53	<11d	29.24	0.79	1.47	20.54	0.17	<11d	100.83
	1.893	-	0.122	-	1.004	0.027	0.090	0.903	0.013	-	
WK15.3	46.08	0.01	2.53	<11d	28.50	0.81	1.41	20.55	0.16	<11d	100.05
	1.901	-	0.123	-	0.983	0.028	0.087	0.909	0.013	-	
WK15.3	47.04	0.02	1.80	<11d	28.87	0.93	1.63	20.70	0.17	<11d	101.15
	1.920	-	0.087	-	0.986	0.032	0.099	0.905	0.014	-	
WK15.3	45.81	<11d	2.05	<11d	28.72	0.96	1.47	20.56	0.20	<11d	99.76
	1.902	-	0.100	-	0.997	0.034	0.091	0.915	0.016	-	
WK15.3	45.41	<11d	2.00	<11d	28.78	0.81	1.52	20.19	0.19	<11d	98.91
	1.903	-	0.099	-	1.008	0.029	0.095	0.906	0.015	-	
WK15.3	47.26	<11d	1.22	<11d	29.40	1.13	1.72	20.21	0.11	<11d	101.05
	1.935	-	0.059	-	1.007	0.039	0.105	0.886	0.009	-	
WK15.3	47.54	0.02	1.17	<11d	29.21	1.15	1.65	20.16	0.13	<11d	101.01
	1.944	-	0.056	-	0.999	0.040	0.101	0.883	0.010	-	
WK28.3	46.85	0.03	2.62	0.01	28.77	0.89	1.96	18.42	0.18	<11d	99.70
	1.926	-	0.127	-	0.989	0.031	0.120	0.811	0.015	-	
WK28.3	46.09	0.01	2.68	<11d	28.49	0.93	1.95	18.47	0.18	<11d	98.78
	1.915	-	0.131	-	0.990	0.033	0.121	0.822	0.014	-	
WK28.3	45.56	0.02	2.86	0.01	28.42	0.78	1.73	19.24	0.16	<11d	98.75
	1.899	-	0.141	-	0.991	0.028	0.107	0.859	0.013	-	
WK28.3	46.60	0.02	2.20	<11d	28.41	0.96	2.16	19.02	0.19	<11d	99.53
	1.922	-	0.107	-	0.980	0.033	0.133	0.841	0.015	-	
WK28.3	47.32	<11d	0.98	<11d	28.44	1.11	2.41	18.19	0.09	<11d	98.55
	1.968	-	0.048	-	0.989	0.039	0.150	0.810	0.007	-	
WK28.3	47.42	0.03	1.00	0.01	28.40	1.17	2.41	18.57	0.09	<11d	99.06
	1.963	-	0.049	-	0.983	0.041	0.148	0.824	0.007	-	
WK28.3	46.96	0.02	1.34	<11d	28.77	0.96	2.52	18.16	0.17	<11d	98.88
	1.949	-	0.065	-	0.999	0.034	0.156	0.808	0.014	-	
WK28.3	46.91	0.03	1.37	<11d	28.92	0.92	2.42	18.39	0.16	<11d	99.08
	1.946	-	0.067	-	1.003	0.032	0.149	0.817	0.013	-	
WK28.3	47.19	0.01	1.58	<11d	28.66	1.00	2.41	19.61	0.13	<11d	100.58
	1.930	-	0.076	-	0.980	0.035	0.147	0.859	0.010	-	
WK28.3	47.61	0.02	1.28	0.01	28.24	1.05	2.51	18.45	0.16	<11d	99.31
	1.961	-	0.062	-	0.973	0.037	0.154	0.814	0.013	-	
WK28.3	47.42	0.02	1.32	<11d	28.51	1.05	2.58	17.95	0.15	<11d	98.99
	1.960	-	0.064	-	0.986	0.037	0.159	0.795	0.012	-	

c: Pyroxene Hornfels

SAMPLE	SiO_2 Si	TiO_2 Ti	Al_2O_3 Al	Cr_2O_3 Cr	FeO Fe	MnO Mn	MgO Mg	CaO Ca	Na_2O Na	K_2O K	TOTAL
HF2	46.24	0.41	1.62	0.02	25.37	0.97	1.95	22.59	0.10	<11d	98.83
	1.919	-	0.079	-	0.881	0.034	0.120	1.004	0.008	-	
HF2	46.23	0.49	1.69	0.04	24.92	0.93	1.97	22.73	0.07	<11d	98.55
	1.920	-	0.083	-	0.866	0.033	0.122	1.012	0.005	-	
HF2	46.26	0.48	1.66	<11d	25.37	0.98	1.86	22.85	0.09	<11d	99.08
	1.916	-	0.081	-	0.879	0.034	0.115	1.014	0.007	-	
HF2	46.64	0.41	1.62	<11d	25.29	0.94	1.93	22.54	0.07	<11d	99.04
	1.927	-	0.079	-	0.874	0.033	0.119	0.998	0.006	-	
HF2	46.27	0.47	1.59	<11d	25.18	0.96	1.90	22.92	0.08	<11d	98.90
	1.919	-	0.078	-	0.873	0.034	0.117	1.018	0.007	-	
HF2	46.85	0.38	1.58	<11d	25.23	1.00	1.95	22.99	0.11	<11d	99.71
	1.924	-	0.076	-	0.866	0.035	0.120	1.012	0.009	-	
HF2	46.76	0.42	1.55	<11d	25.21	0.96	1.84	22.75	0.07	<11d	99.14
	1.930	-	0.075	-	0.870	0.033	0.113	1.006	0.006	-	
HF2	46.53	0.46	1.69	<11d	25.53	0.97	1.96	22.71	0.10	<11d	99.51
	1.918	-	0.082	-	0.880	0.034	0.121	1.003	0.008	-	
HF2	46.47	0.45	1.73	0.01	25.98	0.95	1.83	22.76	0.10	<11d	99.82
	1.913	-	0.084	-	0.894	0.033	0.112	1.004	0.008	-	
HF2	46.05	0.47	1.79	<11d	25.40	0.93	1.84	22.86	0.07	<11d	98.94
	1.911	-	0.088	-	0.881	0.033	0.114	1.016	0.006	-	
HF2	46.20	0.51	1.74	0.01	25.19	1.06	1.89	23.08	0.09	<11d	99.25
	1.911	-	0.085	-	0.871	0.037	0.117	1.023	0.007	-	
HF2	46.59	0.45	1.56	<11d	25.44	0.93	1.86	23.01	0.09	<11d	99.48
	1.921	-	0.076	-	0.877	0.032	0.114	1.016	0.007	-	
HF2	46.63	0.44	1.60	<11d	25.60	0.94	1.90	22.68	0.08	<11d	99.42
	1.923	-	0.078	-	0.883	0.033	0.117	1.002	0.006	-	
HF2	46.97	0.41	1.64	<11d	25.17	0.95	1.85	23.01	0.09	<11d	99.69
	1.928	-	0.079	-	0.864	0.033	0.113	1.012	0.008	-	
HF2	46.59	0.41	1.55	<11d	25.09	0.94	1.87	22.84	0.09	<11d	98.97
	1.927	-	0.076	-	0.868	0.033	0.115	1.012	0.007	-	

d: Magnetite Gabbro

SAMPLE	SiO_2 Si	TiO_2 Ti	Al_2O_3 Al	Cr_2O_3 Cr	FeO Fe	MnO Mn	MgO Mg	CaO Ca	Na_2O Na	K_2O K	TOTAL
MG1	50.60	0.43	1.48	<11d	15.60	0.33	10.53	20.94	0.22	<11d	99.70
	1.953	-	0.067	-	0.503	0.011	0.606	0.866	0.017	-	
MG1	50.50	0.52	1.54	0.02	15.35	0.32	10.53	21.07	0.22	<11d	99.53
	1.951	-	0.070	-	0.496	0.010	0.606	0.872	0.017	-	
MG1	49.84	0.58	1.62	0.04	14.91	0.42	10.80	21.47	0.22	<11d	99.29
	1.933	-	0.074	-	0.484	0.014	0.624	0.892	0.017	-	
MG1	49.77	0.37	1.15	<11d	15.22	0.37	10.74	21.06	0.20	<11d	98.52
	1.947	-	0.053	-	0.498	0.012	0.626	0.883	0.015	-	
MG1	50.77	0.35	1.17	0.02	14.91	0.37	10.85	21.44	0.17	<11d	99.68
	1.956	-	0.053	-	0.480	0.012	0.623	0.885	0.012	-	
MG1	50.15	0.35	1.30	0.44	14.87	0.38	10.45	21.74	0.24	<11d	99.14
	1.948	-	0.059	-	0.483	0.013	0.605	0.905	0.018	-	
MG1	50.13	0.36	1.30	<11d	14.92	0.30	10.30	21.35	0.23	<11d	98.53
	1.956	-	0.060	-	0.487	0.010	0.599	0.893	0.017	-	
MG1	50.04	0.47	1.44	<11d	14.54	0.38	10.70	21.38	0.21	<11d	98.69
	1.948	-	0.066	-	0.473	0.012	0.621	0.891	0.016	-	
MG1	50.04	0.39	1.38	<11d	14.63	0.32	10.78	21.25	0.20	<11d	98.61
	1.949	-	0.064	-	0.477	0.011	0.626	0.887	0.015	-	
MG1	49.70	0.50	1.30	0.03	15.55	0.38	10.73	20.67	0.20	<11d	98.54
	1.944	-	0.060	-	0.509	0.013	0.626	0.866	0.015	-	

SAMPLE	SiO_2	TiO_2	Al_2O_3	Cr_2O_3	FeO	MnO	MgO	CaO	Na_2O	K_2O	TOTAL
	Si	Ti	Al	Cr	Fe	Mn	Mg	Ca	Na	K	
MG2	50.09	0.57	1.57	<11d	15.17	0.36	10.55	20.60	0.23	<11d	98.57
	1.952	-	0.072	-	0.494	0.012	0.613	0.860	0.017	-	
MG2	50.15	0.56	1.53	0.02	15.21	0.38	10.49	20.83	0.22	<11d	98.80
	1.951	-	0.070	-	0.495	0.012	0.609	0.868	0.017	-	
MG2	50.53	0.51	1.54	<11d	15.54	0.33	10.79	20.52	0.20	<11d	99.46
	1.952	-	0.070	-	0.502	0.011	0.621	0.849	0.015	-	
MG2	50.16	0.59	1.42	<11d	15.26	0.35	10.73	20.74	0.23	0.04	98.95
	1.950	-	0.065	-	0.496	0.012	0.622	0.864	0.017	0.002	
MG3	51.08	0.29	1.10	<11d	15.41	0.38	11.12	19.98	0.18	<11d	99.25
	1.971	-	0.050	-	0.497	0.012	0.640	0.826	0.014	-	
MG3	50.48	0.28	1.14	<11d	15.79	0.35	10.79	20.01	0.19	<11d	98.76
	1.964	-	0.052	-	0.514	0.012	0.626	0.834	0.014	-	
MG3	49.36	0.45	1.43	<11d	16.32	0.44	10.83	20.94	0.21	<11d	99.52
	1.923	-	0.065	-	0.531	0.014	0.629	0.874	0.016	-	
MG3	50.91	0.42	1.23	<11d	15.79	0.38	10.99	20.59	0.18	<11d	100.07
	1.956	-	0.056	-	0.507	0.012	0.629	0.848	0.014	-	
MG3	50.51	0.45	1.20	<11d	16.23	0.36	10.91	20.43	0.21	<11d	99.85
	1.950	-	0.055	-	0.524	0.012	0.628	0.845	0.015	-	
MG3	50.52	0.47	1.44	<11d	17.67	0.41	10.83	18.43	0.22	<11d	99.52
	1.958	-	0.066	-	0.573	0.013	0.625	0.765	0.016	-	
MG3	50.01	0.44	1.43	0.02	17.56	0.39	10.88	19.05	0.17	<11d	99.49
	1.944	-	0.065	-	0.571	0.013	0.630	0.793	0.013	-	

5.2 Results of microprobe analyses of plagioclase together with the number of ions on the basis of 32 oxygen atoms and mol per cent albite, anorthite and orthoclase (all iron as FeO, <lld = less than the lower limit of detection).

a: Pyroxenite

SAMPLE	SiO_2	TiO_2	Al_2O_3	FeO	MgO	CaO	Na_2O	K_2O	TOTAL		
	Si	Ti	Al	Fe	Mg	Ca	Na	K	Ab	An	Or
WK3.2	59.81	<lld	25.39	0.59	<lld	9.05	5.68	0.55	101.07		
	10.601	-	5.303	0.087	-	1.718	1.952	0.124	51	45	4
WK3.2	58.01	<lld	26.25	0.54	<lld	8.41	6.62	0.51	100.34		
	10.392	-	5.542	0.081	-	1.614	2.299	0.117	57	40	3
WK3.2	57.77	<lld	26.34	0.55	<lld	8.21	6.55	0.51	99.93		
	10.384	-	5.580	0.083	-	1.581	2.282	0.117	57	40	3
WK3.2	57.26	<lld	26.59	0.60	<lld	9.40	6.47	0.34	100.66		
	10.260	-	5.615	0.090	-	1.804	2.248	0.078	54	44	2
WK3.2	57.60	<lld	27.10	0.66	<lld	9.31	6.48	0.22	101.37		
	10.237	-	5.676	0.098	-	1.773	2.233	0.050	55	44	1
WK3.2	57.65	<lld	26.46	0.41	<lld	9.08	6.58	0.31	100.49		
	10.322	-	5.583	0.061	-	1.742	2.284	0.071	56	43	1
WK3.2	57.40	<lld	26.65	0.48	<lld	9.28	6.53	0.24	100.58		
	10.277	-	5.623	0.072	-	1.780	2.267	0.055	55	43	2
WK3.2	56.69	<lld	26.71	0.46	<lld	9.10	6.53	0.31	99.80		
	10.234	-	5.683	0.069	-	1.760	2.285	0.071	56	43	1
WK3.2	57.77	<lld	26.53	0.51	<lld	9.14	6.51	0.22	100.68		
	10.321	-	5.586	0.076	-	1.749	2.255	0.050	56	43	1
WK5.2	57.08	<lld	27.20	0.46	<lld	9.62	6.24	0.31	100.91		
	10.194	-	5.725	0.069	-	1.841	2.160	0.071	53	45	2
WK5.2	56.56	<lld	27.42	0.38	<lld	9.34	6.01	0.22	99.93		
	10.175	-	5.813	0.057	-	1.800	2.096	0.050	53	46	1
WK5.2	56.82	<lld	27.24	0.35	<lld	9.89	6.10	0.29	100.69		
	10.170	-	5.746	0.052	-	1.896	2.117	0.066	52	46	2
WK5.2	57.76	<lld	26.75	0.35	<lld	8.79	6.77	0.40	100.82		
	10.307	-	5.625	0.052	-	1.680	2.342	0.091	57	41	2
WK5.2	57.62	<lld	25.98	0.61	<lld	8.50	6.63	0.32	99.66		
	10.393	-	5.522	0.092	-	1.642	2.318	0.074	57	41	2
WK5.2	57.50	<lld	26.44	0.53	<lld	8.62	6.71	0.24	100.04		
	10.333	-	5.599	0.080	-	1.659	2.338	0.055	58	41	1
WK5.2	64.77	<lld	22.67	0.30	<lld	1.60	9.03	1.47	99.84		
	11.434	-	4.716	0.044	-	0.303	3.090	0.331	83	8	9
WK6.3	58.01	<lld	26.49	0.46	<lld	8.65	7.00	0.28	100.89		
	10.344	-	5.567	0.069	-	1.652	2.420	0.064	59	40	1
WK6.3	56.27	<lld	27.47	0.53	<lld	9.80	5.99	0.44	100.50		
	10.109	-	5.816	0.080	-	1.886	2.086	0.101	51	46	3
WK6.3	56.83	<lld	27.52	0.40	<lld	9.19	6.12	0.35	100.41		
	10.180	-	5.810	0.060	-	1.764	2.125	0.080	54	44	2
WK6.3	57.78	<lld	26.29	0.47	<lld	7.88	6.97	0.27	99.66		
	10.399	-	5.576	0.071	-	1.519	2.432	0.062	61	38	1
WK6.3	58.17	<lld	26.69	0.46	<lld	8.57	7.00	0.24	101.13		
	10.340	-	5.591	0.068	-	1.632	2.412	0.054	59	40	1
WK12.2	49.10	<lld	32.59	0.92	<lld	16.06	2.64	0.09	101.40		
	8.907	-	6.967	0.140	-	3.121	0.928	0.021	23	77	0
WK12.2	46.52	<lld	34.50	1.06	<lld	16.60	1.72	0.05	100.45		
	8.536	-	7.460	0.163	-	3.263	0.612	0.012	16	84	0
WK12.2	50.35	<lld	31.32	0.43	<lld	13.79	3.73	0.19	99.81		
	9.210	-	6.752	0.066	-	2.702	1.323	0.044	33	66	1
WK12.2	51.21	<lld	31.00	0.72	<lld	13.91	3.81	0.21	100.86		
	9.282	-	6.622	0.109	-	2.701	1.339	0.049	33	66	1
WK12.2	46.68	<lld	34.33	0.78	<lld	17.36	1.93	0.07	101.15		
	8.525	-	7.389	0.119	-	3.397	0.683	0.016	17	83	0
WK12.2	46.62	<lld	34.52	0.66	<lld	17.23	1.82	0.08	100.93		
	8.520	-	7.435	0.101	-	3.374	0.645	0.019	16	84	0
WK12.2	46.72	<lld	34.20	0.99	<lld	17.39	1.89	0.08	101.27		
	8.531	-	7.360	0.151	-	3.402	0.669	0.019	16	83	1

SAMPLE	SiO_2 Si	TiO_2 Ti	Al_2O_3 Al	FeO Fe	MgO Mg	CaO Ca	Na_2O Na	K_2O K	TOTAL Ab	An	Or
WK12.2	50.69	<11d	31.44	0.65	<11d	14.38	3.59	0.26	101.01		
	9.187	-	6.716	0.099	-	2.792	1.261	0.060	31	68	1
WK12.4	56.32	<11d	28.28	0.50	<11d	8.78	5.45	1.08	100.41		
	10.101	-	5.977	0.075	-	1.687	1.895	0.247	49	44	7
WK12.4	55.26	<11d	28.72	0.30	<11d	10.52	5.97	0.19	100.96		
	9.894	-	6.060	0.045	-	2.018	2.072	0.043	50	49	1
WK13.2	57.12	<11d	27.20	0.64	<11d	8.36	6.55	0.44	100.31		
	10.243	-	5.748	0.096	-	1.606	2.277	0.101	57	40	3
WK14.4	74.41	<11d	20.08	0.11	<11d	0.13	5.27	0.07	100.07		
	12.552	-	3.992	0.016	-	0.023	1.723	0.015	98	1	1
WK14.4	55.54	<11d	28.05	0.52	<11d	10.67	5.52	0.45	100.75		
	9.975	-	5.937	0.078	-	2.053	1.922	0.103	47	50	3
WK14.4	55.33	<11d	27.74	0.45	<11d	10.65	5.55	0.38	100.10		
	9.997	-	5.907	0.068	-	2.062	1.944	0.088	47	50	3
WK14.4	55.11	<11d	27.57	0.30	<11d	10.52	5.78	0.25	99.53		
	10.006	-	5.899	0.046	-	2.046	2.035	0.058	49	49	2
WK14.4	57.05	<11d	26.29	0.47	<11d	9.05	6.73	0.22	99.81		
	10.295	-	5.591	0.071	-	1.750	2.355	0.051	57	42	1
WK16.2	68.56	<11d	18.96	1.04	<11d	<11d	10.41	0.07	99.04		
	12.078	-	3.936	0.153	-	-	3.555	0.016	100	0	0
WK16.2	68.88	<11d	19.46	<11d	<11d	<11d	11.55	<11d	99.89		
	12.021	-	4.002	-	-	-	3.908	-	100	0	0
WK16.2	69.42	<11d	19.82	<11d	<11d	<11d	11.72	0.04	101.00		
	11.991	-	4.035	-	-	-	3.925	0.009	100	0	0
WK28.4	57.48	<11d	27.48	0.17	<11d	9.49	5.75	0.27	100.64		
	10.242	-	5.770	0.025	-	1.812	1.986	0.061	51	47	2
WK28.4	57.52	<11d	27.37	0.25	<11d	8.56	6.61	0.25	100.56		
	10.262	-	5.754	0.037	-	1.636	2.286	0.057	57	41	2
WK28.4	56.07	<11d	28.22	0.29	<11d	9.50	6.16	0.25	100.56		
	10.043	-	5.957	0.043	-	1.823	2.139	0.057	53	45	2
WK28.4	59.20	<11d	26.24	0.38	<11d	7.07	7.41	0.26	100.62		
	10.519	-	5.495	0.056	-	1.346	2.553	0.059	65	34	1
WK28.4	55.41	<11d	28.45	0.56	<11d	9.27	6.18	0.23	100.17		
	9.976	-	6.037	0.084	-	1.788	2.157	0.053	54	45	1
WK28.4	54.84	<11d	29.20	0.31	<11d	10.01	5.49	0.26	100.11		
	9.872	-	6.195	0.047	-	1.930	1.916	0.060	49	49	2
WK28.4	56.17	<11d	27.95	0.29	<11d	9.23	6.00	0.20	99.84		
	10.108	-	5.928	0.044	-	1.779	2.093	0.046	53	45	2
WK28.4	55.61	<11d	28.17	0.34	<11d	9.72	6.10	0.25	100.19		
	10.009	-	5.975	0.051	-	1.874	2.129	0.057	52	46	2
WK28.4	55.31	<11d	28.23	0.65	<11d	9.16	6.01	0.30	99.72		
	10.001	-	6.016	0.098	-	1.774	2.107	0.069	53	45	2
WK28.4	56.15	<11d	28.49	0.34	<11d	9.83	6.02	0.29	101.18		
	10.006	-	5.983	0.051	-	1.877	2.080	0.066	52	47	1

b: Magnetite-Rich Rock

SAMPLE	SiO_2 Si	TiO_2 Ti	Al_2O_3 Al	FeO Fe	MgO Mg	CaO Ca	Na_2O Na	K_2O K	TOTAL Ab	An	Or
WK4.1	53.37	<11d	29.43	0.74	<11d	12.74	4.49	0.32	101.09		
	9.617	-	6.250	0.111	-	2.459	1.569	0.074	38	60	2
WK4.1	49.24	<11d	32.19	0.87	<11d	15.88	2.61	0.18	100.97		
	8.964	-	6.907	0.132	-	3.097	0.921	0.042	23	76	1
WK4.1	51.14	<11d	30.78	0.68	<11d	14.39	3.47	0.27	100.73		
	9.287	-	6.587	0.103	-	2.800	1.222	0.063	30	69	1
WK4.1	54.94	<11d	28.20	0.49	<11d	10.92	5.06	0.46	100.07		
	9.931	-	6.007	0.074	-	2.115	1.773	0.106	44	53	3
WK4.1	55.37	<11d	28.29	0.51	<11d	11.12	5.24	0.45	100.98		
	9.929	-	5.978	0.076	-	2.136	1.822	0.103	45	53	2
WK4.1	55.72	<11d	27.90	0.47	<11d	10.96	5.46	0.46	100.97		
	9.990	-	5.895	0.070	-	2.105	1.898	0.105	46	51	3
WK4.1	56.47	<11d	27.19	0.49	<11d	9.75	6.09	0.39	100.38		
	10.151	-	5.760	0.074	-	1.878	2.122	0.089	52	46	2
WK12.1	59.72	<11d	25.81	0.41	<11d	9.32	5.80	0.21	101.27		
	10.550	-	5.373	0.061	-	1.764	1.986	0.047	52	46	2
WK12.1	57.31	<11d	25.81	0.40	<11d	8.77	6.81	0.28	99.38		
	10.375	-	5.507	0.061	-	1.701	2.390	0.065	58	41	1
WK12.1	54.07	<11d	27.65	0.36	<11d	10.90	5.57	0.11	98.75		
	9.911	-	5.973	0.055	-	2.141	1.979	0.026	48	52	0
WK12.1	54.22	<11d	27.26	0.45	<11d	10.77	5.79	0.10	98.59		
	9.959	-	5.901	0.069	-	2.119	2.062	0.023	49	50	1
WK12.1	56.52	<11d	26.59	0.37	<11d	9.50	6.63	0.25	99.86		
	10.212	-	5.662	0.056	-	1.839	2.322	0.058	55	44	1
WK12.1	55.86	<11d	26.50	0.47	<11d	9.42	6.47	0.21	98.93		
	10.188	-	5.696	0.072	-	1.841	2.288	0.049	55	44	1
WK12.1	55.64	<11d	26.53	1.30	<11d	9.19	6.17	0.36	99.19		
	10.156	-	5.707	0.198	-	1.797	2.183	0.084	54	44	2
WK14.1	47.98	<11d	32.87	1.02	<11d	17.14	2.04	0.13	101.18		
	8.756	-	7.070	0.156	-	3.351	0.722	0.030	18	82	0
WK14.1	47.44	<11d	33.56	1.20	<11d	16.91	2.05	0.11	101.27		
	8.656	-	7.216	0.183	-	3.305	0.725	0.026	18	81	1
WK28.3	47.32	<11d	32.98	0.79	<11d	17.19	1.98	0.10	100.36		
	8.703	-	7.148	0.121	-	3.387	0.706	0.023	17	82	1

c: Magnetite-Gabbro

SAMPLE	SiO_2 Si	TiO_2 Ti	Al_2O_3 Al	FeO Fe	MgO Mg	CaO Ca	Na_2O Na	K_2O K	TOTAL Ab	An	Or
MG1	57.63	<11d	27.27	0.29	<11d	10.22	5.24	0.42	101.13		
	10.241	-	5.711	0.043	-	1.946	1.805	0.095	47	51	2
MG1	55.46	<11d	28.21	0.24	<11d	9.90	5.86	0.40	100.07		
	9.997	-	5.993	0.036	-	1.912	2.048	0.092	51	47	2
MG1	55.72	<11d	28.11	0.24	<11d	10.10	5.78	0.34	100.29		
	10.019	-	5.956	0.036	-	1.946	2.015	0.078	50	48	2
MG1	56.84	<11d	27.17	0.26	<11d	8.69	6.38	0.39	99.73		
	10.237	-	5.767	0.039	-	1.677	2.228	0.090	56	42	2
MG1	55.85	<11d	27.59	0.29	<11d	9.88	5.86	0.43	99.96		
	10.079	-	5.868	0.044	-	1.910	2.050	0.099	51	47	2
MG1	56.27	<11d	28.42	0.27	<11d	10.10	5.89	0.36	101.31		
	10.017	-	5.962	0.040	-	1.926	2.033	0.082	50	48	2
MG1	55.66	<11d	28.13	0.22	<11d	9.72	5.79	0.43	99.95		
	10.033	-	5.976	0.033	-	1.877	2.023	0.099	51	47	2
MG1	56.51	<11d	27.72	0.29	<11d	9.19	5.99	0.45	100.15		
	10.148	-	5.866	0.044	-	1.768	2.085	0.103	53	45	2
MG1	55.58	<11d	27.65	0.22	<11d	10.16	5.83	0.41	99.85		
	10.047	-	5.891	0.033	-	1.968	2.043	0.095	50	48	2
MG1	55.58	<11d	27.62	0.42	0.05	9.65	5.85	0.46	99.69		
	10.061	-	5.892	0.064	0.013	1.871	2.053	0.106	51	46	3
MG1	56.13	<11d	27.88	0.29	<11d	9.72	5.97	0.42	100.41		
	10.076	-	5.898	0.044	-	1.869	2.078	0.096	51	46	3
MG2	56.34	<11d	27.16	0.18	<11d	10.27	5.15	0.44	99.54		
	10.179	-	5.783	0.027	-	1.988	1.804	0.101	46	51	3
MG2	55.90	<11d	27.03	0.25	<11d	9.09	6.03	0.44	98.74		
	10.184	-	5.803	0.038	-	1.774	2.130	0.102	53	44	3
MG2	57.67	<11d	27.19	0.18	<11d	9.84	5.36	0.38	100.62		
	10.279	-	5.711	0.027	-	1.879	1.852	0.086	49	49	2
MG2	56.16	<11d	27.58	0.14	<11d	9.63	6.07	0.36	99.94		
	10.118	-	5.856	0.021	-	1.859	2.120	0.083	52	46	2
MG2	56.06	<11d	28.02	0.22	<11d	9.97	5.85	0.47	100.59		
	10.051	-	5.920	0.033	-	1.915	2.033	0.107	50	47	3
MG2	55.80	<11d	27.84	0.20	<11d	10.04	5.75	0.47	100.10		
	10.053	-	5.911	0.030	-	1.938	2.008	0.108	50	48	2
MG2	55.87	<11d	28.14	0.28	<11d	10.24	5.76	0.41	100.70		
	10.014	-	5.944	0.042	-	1.966	2.002	0.094	49	48	3
MG2	55.78	<11d	28.06	0.30	<11d	10.14	5.90	0.44	100.62		
	10.012	-	5.936	0.045	-	1.950	2.053	0.101	50	48	2
MG2	55.92	<11d	28.26	0.32	<11d	10.06	5.82	0.44	100.82		
	10.010	-	5.962	0.048	-	1.929	2.020	0.100	50	48	2
MG2	55.24	<11d	27.93	0.35	<11d	9.85	5.89	0.25	99.51		
	10.011	-	5.965	0.053	-	1.912	2.069	0.058	51	47	2
MG2	55.54	<11d	27.49	0.22	<11d	9.96	5.89	0.38	99.48		
	10.071	-	5.874	0.033	-	1.935	2.070	0.088	51	47	2
MG3	56.02	<11d	28.23	0.37	<11d	10.03	5.76	0.47	100.88		
	10.021	-	5.951	0.055	-	1.922	1.998	0.107	50	48	2
MG3	56.25	<11d	28.32	0.24	<11d	9.76	5.86	0.42	100.85		
	10.046	-	5.961	0.036	-	1.868	2.029	0.096	51	47	2

5.3 Results of microprobe analyses of amphibole in pyroxenite (all iron as FeO) together with the number of ions calculated according to Spear and Kimball (1984) (average Fe^{3+} content).

SAMPLE	SiO_2	Al_2O_3	TiO_2	MgO	FeO		MnO	CaO	Na_2O	K_2O	TOTAL
	Si	Al	Ti	Mg	Fe^{3+}	Fe^{2+}	Mn	Ca	Na	K	
WK3.2	38.05	10.12	0.88	0.83	32.91		0.32	11.08	1.34	2.35	97.89
	6.221	1.951	0.108	0.203	0.537	3.962	0.045	1.941	0.426	0.491	
WK3.2	37.09	9.93	0.93	0.74	33.52		0.35	10.54	1.41	2.19	96.70
	6.138	1.938	0.116	0.182	0.780	3.858	0.049	1.869	0.452	0.463	
WK3.2	37.15	10.16	0.75	0.90	33.70		0.35	10.76	1.58	1.90	97.25
	6.098	1.966	0.092	0.220	0.869	3.758	0.049	1.892	0.504	0.398	
WK3.2	37.44	9.87	0.83	0.92	33.68		0.44	10.90	1.25	2.41	97.75
	6.131	1.905	0.102	0.224	0.819	3.794	0.062	1.913	0.396	0.504	
WK3.2	36.82	10.46	1.17	0.90	32.84		0.38	11.08	1.23	2.44	97.33
	6.057	2.029	0.145	0.220	0.710	3.807	0.053	1.953	0.393	0.513	
WK3.2	36.95	9.63	0.84	0.96	32.53		0.38	10.16	1.37	2.23	95.06
	6.202	1.906	0.107	0.241	0.735	3.832	0.054	1.828	0.446	0.477	
WK3.2	37.41	9.72	1.16	1.00	33.10		0.38	10.54	1.36	2.18	96.85
	6.166	1.889	0.144	0.245	0.743	3.819	0.054	1.861	0.434	0.458	
WK3.2	37.96	10.27	0.95	0.93	33.13		0.35	10.92	1.36	2.18	98.06
	6.175	1.970	0.117	0.226	0.670	3.838	0.049	1.904	0.428	0.453	
WK5.2	38.32	9.45	0.75	0.89	33.91		0.34	10.49	1.46	2.18	97.78
	6.261	1.820	0.092	0.216	0.726	3.908	0.048	1.836	0.464	0.454	
WK5.2	38.01	9.73	1.07	0.96	33.21		0.32	10.35	1.44	2.22	97.33
	6.234	1.881	0.132	0.236	0.655	3.900	0.045	1.819	0.459	0.465	
WK5.2	37.93	10.17	0.95	1.01	33.14		0.39	10.20	1.50	2.25	97.55
	6.195	1.959	0.117	0.245	0.700	3.826	0.054	1.784	0.477	0.468	
WK5.5	37.89	10.42	0.92	0.88	32.66		0.39	10.96	1.60	2.16	97.88
	6.188	2.006	0.113	0.245	0.524	3.937	0.054	1.918	0.505	0.450	
WK5.2	37.25	10.92	0.47	0.74	33.40		0.33	10.51	1.31	2.61	97.53
	6.102	2.108	0.058	0.181	0.776	3.800	0.045	1.844	0.417	0.545	
WK5.2	37.65	10.20	0.93	0.91	32.93		0.31	10.92	1.48	2.17	97.51
	6.169	1.970	0.115	0.222	0.621	3.893	0.044	1.918	0.472	0.453	
WK5.2	37.71	10.42	0.90	0.94	33.13		0.40	9.63	1.43	2.25	96.82
	6.184	2.014	0.111	0.230	0.796	3.747	0.056	1.692	0.454	0.471	
WK5.2	38.32	10.47	0.25	1.11	32.52		0.42	9.93	1.41	2.19	96.63
	6.279	2.024	0.031	0.270	0.724	3.732	0.058	1.744	0.447	0.459	
WK5.2	36.30	11.30	0.14	0.93	32.83		0.45	9.64	1.57	2.38	95.54
	6.034	2.214	0.017	0.231	0.997	3.566	0.064	1.716	0.505	0.505	
WK5.2	37.08	9.82	1.29	0.81	32.71		0.32	10.38	1.37	2.37	96.15
	6.176	1.928	0.161	0.202	0.611	3.945	0.046	1.852	0.441	0.504	
WK6.3	37.77	9.26	0.82	1.03	33.00		0.45	10.91	1.48	2.14	96.85
	6.246	1.804	0.101	0.254	0.648	3.915	0.063	1.933	0.474	0.451	
WK6.3	37.75	9.09	1.08	1.14	32.59		0.39	10.70	1.49	1.80	96.02
	6.268	1.779	0.135	0.281	0.655	3.870	0.054	1.904	0.479	0.382	
WK6.3	37.60	9.53	1.14	0.70	32.96		0.45	11.02	1.46	2.00	96.85
	6.222	1.859	0.142	0.173	0.572	3.990	0.063	1.954	0.468	0.421	
WK6.3	38.50	10.00	0.52	0.99	32.47		0.42	11.03	1.42	2.12	97.48
	6.297	1.928	0.065	0.242	0.527	3.914	0.058	1.932	0.451	0.443	
WK6.3	37.30	10.76	0.15	1.10	32.45		0.42	10.73	1.41	2.42	96.76
	6.124	2.090	0.019	0.271	0.743	3.726	0.059	1.893	0.451	0.509	
WK6.3	37.84	9.84	1.33	0.98	32.13		0.31	11.18	1.36	2.14	97.11
	6.228	1.910	0.164	0.240	0.449	3.972	0.044	1.972	0.433	0.449	
WK6.3	38.64	9.28	1.06	1.01	33.29		0.40	11.15	1.43	1.90	98.18
	6.285	1.780	0.130	0.245	0.602	3.927	0.055	1.943	0.451	0.395	
WK6.3	38.63	9.37	1.55	1.07	32.46		0.40	10.84	1.50	1.99	97.82
	6.301	1.802	0.190	0.261	0.429	3.999	0.056	1.895	0.475	0.414	
WK6.3	37.02	10.99	0.11	1.03	32.27		0.44	10.97	1.35	2.60	96.78
	6.109	2.137	0.014	0.254	0.703	3.750	0.061	1.940	0.431	0.584	

SAMPLE	SiO_2	Al_2O_3	TiO_2	MgO	FeO		MnO	CaO	Na_2O	K_2O	TOTAL
	Si	Al	Ti	Mg	Fe^{3+}	Fe^{2+}	Mn	Ca	Na	K	
WK11.2	37.46	9.96	0.45	0.73	34.11		0.34	11.09	1.29	2.41	97.84
	6.138	1.924	0.056	0.178	0.824	3.849	0.048	1.946	0.410	0.503	
WK11.2	36.71	10.58	0.85	0.52	34.36		0.30	9.96	1.04	3.10	97.43
	6.045	2.054	0.105	0.128	0.914	3.819	0.042	1.757	0.334	0.652	
WK11.2	41.51	6.48	0.75	0.96	35.10		0.52	10.11	1.01	1.32	97.78
	6.768	1.246	0.092	0.234	0.482	4.304	0.072	1.767	0.319	0.274	
WK11.2	38.09	10.38	0.75	0.67	33.78		0.41	10.18	1.72	1.13	97.12
	6.200	1.991	0.092	0.162	0.882	3.716	0.057	1.775	0.544	0.235	
WK11.2	36.58	11.14	0.51	0.47	33.86		0.37	10.71	1.74	1.60	96.98
	6.010	2.157	0.063	0.115	0.925	3.728	0.051	1.885	0.554	0.336	
WK11.2	39.89	9.82	0.19	0.64	34.00		0.38	10.69	1.05	2.56	99.23
	6.410	1.860	0.023	0.153	0.584	3.985	0.052	1.841	0.329	0.526	
WK11.2	37.58	10.19	0.59	0.74	33.11		0.35	10.83	1.29	2.52	97.21
	6.192	1.980	0.074	0.181	0.637	3.925	0.048	1.912	0.413	0.529	
WK11.2	37.20	10.36	0.52	0.55	33.74		0.34	10.48	1.28	2.25	96.73
	6.141	2.016	0.065	0.136	0.842	3.817	0.048	1.854	0.410	0.474	
WK11.2	35.86	11.49	0.11	0.58	33.92		0.30	11.23	1.16	2.59	97.24
	5.906	2.231	0.014	0.142	1.035	3.638	0.042	1.982	0.369	0.544	
WK11.2	36.76	10.94	0.05	0.55	33.71		0.27	10.57	1.11	2.73	96.70
	6.081	2.133	0.007	0.136	0.894	3.770	0.038	1.874	0.355	0.576	
WK11.2	36.29	10.15	0.91	0.59	33.58		0.37	10.93	1.28	2.38	96.47
	6.041	1.993	0.114	0.147	0.832	3.843	0.052	1.950	0.412	0.505	
WK12.3	38.65	9.17	1.24	1.14	34.12		0.38	10.81	1.48	1.91	98.91
	6.258	1.751	0.151	0.276	0.606	4.014	0.052	1.875	0.464	0.394	
WK12.3	37.59	9.91	0.74	1.04	32.91		0.41	10.49	1.67	1.97	96.73
	6.198	1.926	0.091	0.257	0.703	3.836	0.057	1.853	0.534	0.415	
WK12.3	37.17	10.57	1.48	0.93	33.00		0.38	11.04	1.51	1.97	98.06
	6.052	2.029	0.181	0.226	0.697	3.795	0.053	1.927	0.467	0.409	
WK12.3	37.17	10.12	1.27	0.81	33.61		0.37	11.04	1.67	2.07	98.14
	6.078	1.951	0.156	0.198	0.690	3.906	0.051	1.933	0.530	0.432	
WK12.3	37.09	10.52	1.32	1.07	32.58		0.40	11.00	1.51	2.30	97.79
	6.067	2.030	0.162	0.261	0.632	3.826	0.056	1.928	0.479	0.479	
WK12.3	36.73	11.00	0.12	0.88	34.07		0.43	11.29	1.44	2.69	98.65
	5.976	2.109	0.014	0.212	0.945	3.692	0.060	1.967	0.456	0.559	
WK12.3	36.98	10.67	1.10	0.98	33.35		0.44	11.02	1.73	1.93	98.20
	6.019	2.047	0.134	0.237	0.782	3.757	0.060	1.921	0.547	0.401	
WK12.3	36.62	10.06	0.88	0.87	33.47		0.41	10.84	1.39	2.50	97.03
	6.060	1.962	0.109	0.214	0.808	3.825	0.058	1.923	0.447	0.527	
WK12.4	37.32	10.33	0.17	1.12	33.11		0.36	11.19	1.39	2.57	97.58
	6.125	2.000	0.021	0.274	0.761	3.784	0.050	1.968	0.444	0.537	
WK12.4	36.30	11.69	0.33	0.92	33.28		0.44	11.04	1.31	2.67	97.98
	5.920	2.248	0.041	0.223	0.933	3.606	0.061	1.930	0.416	0.555	
WK12.4	38.17	9.63	0.38	1.12	33.80		0.40	10.68	1.33	2.15	97.67
	6.226	1.851	0.046	0.273	0.879	3.732	0.055	1.866	0.422	0.447	
WK12.4	36.62	10.53	1.09	0.89	32.65		0.31	10.86	1.28	2.41	96.65
	6.061	2.055	0.136	0.220	0.711	3.809	0.043	1.926	0.410	0.510	
WK12.4	36.63	10.43	0.80	0.77	34.34		0.33	10.86	1.43	1.97	97.56
	6.003	2.015	0.099	0.187	0.980	3.727	0.046	1.908	0.456	0.413	
WK12.4	37.96	10.04	0.13	1.37	33.51		0.47	10.28	1.74	2.31	97.80
	6.179	1.927	0.015	0.331	0.910	3.652	0.065	1.792	0.549	0.481	
WK12.4	37.40	10.66	0.94	1.10	33.19		0.35	11.02	1.55	2.26	98.46
	6.068	2.039	0.114	0.266	0.734	3.769	0.048	1.916	0.487	0.467	
WK12.4	37.46	9.64	1.07	0.95	32.57		0.32	11.09	1.41	2.17	96.70
	6.205	1.883	0.134	0.235	0.559	3.952	0.045	1.968	0.454	0.459	
WK13.2	37.00	10.29	1.27	1.12	33.04		0.41	9.70	1.41	2.13	96.38
	6.092	1.997	0.158	0.275	0.911	3.639	0.058	1.712	0.451	0.446	
WK13.2	36.69	9.96	1.30	1.10	33.18		0.47	10.30	1.52	1.79	96.31
	6.078	1.946	0.162	0.273	0.796	3.801	0.066	1.828	0.487	0.378	
WK13.2	36.69	10.19	1.13	1.05	33.67		0.36	9.50	1.66	1.79	96.05
	6.077	1.991	0.141	0.260	0.911	3.753	0.051	1.686	0.532	0.378	
WK13.2	36.95	9.94	1.63	1.16	33.12		0.43	10.05	1.51	1.79	96.59
	6.100	1.935	0.202	0.287	0.730	3.842	0.061	1.777	0.483	0.377	

SAMPLE	SiO_2 / Si	Al_2O_3 / Al	TiO_2 / Ti	MgO / Mg	FeO / Fe^{3+}	Fe^{2+}	MnO / Mn	CaO / Ca	Na_2O / Na	K_2O / K	TOTAL
WK13.2	37.07	9.96	1.29	0.99	32.46		0.49	10.22	1.42	2.24	96.15
	6.151	1.948	0.161	0.246	0.688	3.817	0.069	1.818	0.456	0.475	
WK13.2	36.56	10.60	1.12	1.19	32.90		0.46	10.86	1.15	2.51	97.34
	5.994	2.048	0.138	0.290	0.900	3.610	0.064	1.907	0.364	0.525	
WK13.2	37.16	9.99	1.29	1.16	33.58		0.41	10.85	1.34	2.21	98.01
	6.075	1.926	0.159	0.283	0.723	3.869	0.057	1.901	0.423	0.461	
WK14.4	36.62	10.15	1.28	0.82	32.91		0.35	10.38	1.48	2.21	96.20
	6.088	1.990	0.160	0.203	0.728	3.848	0.050	1.849	0.476	0.469	
WK14.4	37.37	9.85	0.94	0.88	33.39		0.41	10.14	1.46	2.03	96.48
	6.172	1.918	0.117	0.218	0.826	3.785	0.057	1.794	0.468	0.428	
WK14.4	36.75	10.80	0.16	0.92	33.38		0.37	10.92	1.37	2.43	97.11
	6.047	2.095	0.020	0.226	0.901	3.693	0.052	1.925	0.438	0.511	
WK14.4	36.63	10.62	0.74	0.83	33.09		0.34	10.35	1.51	2.18	96.30
	6.067	2.074	0.092	0.205	0.830	3.754	0.048	1.837	0.485	0.461	
WK14.4	36.09	10.61	0.70	0.74	33.56		0.39	10.52	1.37	2.56	96.55
	5.994	2.077	0.087	0.184	0.915	3.747	0.055	1.873	0.441	0.542	
WK14.4	36.38	9.95	0.66	0.77	33.87		0.35	10.82	1.38	2.48	96.65
	6.056	1.954	0.082	0.191	0.832	3.884	1.931	1.931	0.444	0.526	
WK14.4	36.82	10.23	0.62	0.89	32.57		0.46	10.46	1.36	2.34	95.76
	6.142	2.011	0.078	0.221	0.750	3.793	0.065	1.870	0.441	0.497	
WK14.4	36.86	10.29	1.02	0.93	33.08		0.33	10.04	1.69	1.71	95.94
	6.107	2.009	0.128	0.229	0.851	3.732	0.046	1.782	0.544	0.362	
WK14.4	37.09	10.19	0.48	0.91	32.48		0.48	10.42	1.34	2.41	95.80
	6.181	2.003	0.060	0.226	0.717	3.810	0.068	1.862	0.435	0.513	
WK14.4	37.49	9.85	0.93	0.99	32.98		0.39	10.45	1.40	2.11	96.59
	6.187	1.917	0.115	0.244	0.748	3.804	0.054	1.848	0.449	0.444	
WK16.2	39.78	11.70	0.39	0.70	32.93		0.48	11.18	1.71	0.01	98.87
	6.265	2.173	0.046	0.165	0.801	3.536	0.063	1.886	0.521	0.001	
WK16.2	36.94	11.06	0.47	0.52	33.80		0.34	10.82	1.16	2.05	97.19
	6.048	2.135	0.058	0.128	0.961	3.668	0.048	1.899	0.369	0.429	
WK16.2	38.14	10.77	0.56	0.68	33.94		0.41	10.98	1.02	1.89	98.40
	6.142	2.044	0.068	0.164	0.940	3.632	0.057	1.895	0.319	0.388	
WK16.2	36.52	9.47	0.17	0.20	34.87		0.35	10.72	1.63	1.61	95.56
	6.138	1.876	0.022	0.051	0.975	3.927	0.050	1.931	0.530	0.346	
WK20.5	38.27	9.81	1.01	1.71	32.92		0.39	10.65	1.51	2.27	98.54
	6.177	1.867	0.123	0.412	0.757	3.688	0.054	1.842	0.473	0.468	
WK20.5	39.94	8.70	0.76	2.17	32.06		0.49	11.12	1.42	1.86	98.52
	6.411	1.646	0.092	0.520	0.619	3.686	0.067	1.913	0.442	0.381	
WK20.5	36.90	10.28	1.05	1.47	32.72		0.47	10.19	1.46	2.17	96.72
	6.062	1.992	0.130	0.361	0.908	3.587	0.066	1.793	0.464	0.454	
WK20.5	37.53	9.66	1.47	1.67	32.32		0.36	10.15	1.55	1.89	96.62
	6.170	1.873	0.182	0.410	0.694	3.751	0.051	1.789	0.494	0.396	
WK20.5	37.07	10.61	0.83	1.41	32.43		0.42	11.07	1.51	2.26	97.62
	6.054	2.043	0.102	0.343	0.764	3.665	0.059	1.936	0.477	0.472	
WK20.5	37.21	10.19	0.55	1.32	32.98		0.39	10.26	1.47	2.22	96.60
	6.124	1.977	0.069	0.324	0.905	3.633	0.054	1.809	0.470	0.465	
WK20.5	37.56	9.89	0.81	1.39	33.09		0.41	10.04	1.57	2.09	96.85
	6.160	1.913	0.100	0.340	0.881	3.657	0.057	1.764	0.500	0.437	
WK20.5	36.58	10.53	0.92	1.39	32.72		0.39	9.93	1.55	2.02	96.03
	6.035	2.049	0.114	0.343	0.990	3.525	0.055	1.756	0.496	0.426	
WK20.5	37.17	9.79	1.09	1.65	32.25		0.42	10.21	1.52	2.27	96.37
	6.140	1.906	0.135	0.407	0.747	3.709	0.058	1.808	0.487	0.478	
WK20.5	36.62	10.50	1.52	1.41	31.98		0.42	10.27	1.46	1.96	96.13
	6.039	2.041	0.188	0.347	0.821	3.589	0.058	1.816	0.466	0.413	
WK21.5	37.64	10.06	0.96	1.44	32.67		0.45	11.04	1.42	2.40	98.08
	6.127	1.931	0.118	0.349	0.712	3.736	0.062	1.925	0.449	0.499	
WK21.5	37.44	10.31	0.73	1.45	32.49		0.44	11.09	1.38	2.48	97.81
	6.106	1.983	0.090	0.353	0.737	3.694	0.061	1.938	0.435	0.515	
WK21.5	36.60	9.97	1.29	1.35	31.80		0.42	10.99	1.49	2.25	96.16
	6.083	1.953	0.162	0.333	0.635	3.786	0.059	1.958	0.481	0.478	
WK21.5	37.07	10.64	1.02	1.47	32.20		0.45	10.61	1.37	2.64	97.48
	6.060	2.051	0.125	0.359	0.739	3.664	0.062	1.858	0.436	0.551	

SAMPLE	SiO_2	Al_2O_3	TiO_2	MgO	FeO		MnO	CaO	Na_2O	K_2O	TOTAL
	Si	Al	Ti	Mg	Fe^{3+}	Fe^{2+}	Mn	Ca	Na	K	
WK21.5	36.84	10.24	0.94	1.40	32.10		0.38	10.92	1.54	2.27	96.64
	6.082	1.994	0.117	0.345	0.702	3.731	0.054	1.932	0.492	0.479	
WK21.5	37.01	10.71	1.28	1.49	32.62		0.40	10.66	1.36	2.53	98.06
	6.012	2.050	0.156	0.362	0.814	3.618	0.054	1.856	0.428	0.525	
WK21.5	38.72	9.50	0.17	1.88	32.19		0.46	9.97	1.48	1.91	96.28
	6.336	1.833	0.021	0.458	0.855	3.550	0.064	1.747	0.470	0.398	
WK21.5	37.08	10.63	1.29	1.40	31.79		0.43	11.35	1.48	2.27	97.72
	6.055	2.047	0.159	0.340	0.594	3.748	0.059	1.986	0.468	0.474	
WK21.5	44.98	4.41	0.18	3.12	31.48		0.56	11.25	0.84	0.51	97.33
	7.181	0.829	0.021	0.743	0.439	3.765	0.075	1.925	0.259	0.105	
WK26.2	38.32	9.59	1.04	1.62	31.58		0.34	10.55	1.88	1.52	96.45
	6.296	1.857	0.129	0.397	0.530	3.810	0.048	1.857	0.598	0.320	
WK26.2	37.61	10.05	1.31	1.65	32.03		0.36	10.70	1.85	1.58	97.14
	6.139	1.935	0.161	0.401	0.687	3.686	0.049	1.872	0.584	0.329	
WK26.2	37.44	10.26	1.46	2.16	31.14		0.33	10.82	1.85	0.97	96.43
	6.096	1.969	0.179	0.523	0.818	3.422	0.046	1.888	0.584	0.201	
WK26.2	37.57	9.45	1.46	1.70	32.54		0.25	10.77	1.62	1.82	97.19
	6.170	1.830	0.180	0.416	0.573	3.896	0.035	1.896	0.517	0.381	
WK26.2	37.70	10.38	1.24	1.63	31.75		0.34	10.19	1.66	1.91	96.80
	6.162	2.000	0.152	0.398	0.679	3.660	0.047	1.785	0.525	0.397	
WK26.2	40.55	8.85	1.44	2.42	30.94		0.33	10.56	1.61	1.15	97.86
	6.485	1.669	0.173	0.578	0.485	3.654	0.045	1.809	0.500	0.234	
WK26.2	38.72	8.78	1.21	1.95	31.88		0.31	10.99	1.46	1.48	96.81
	6.327	1.691	0.149	0.476	0.651	3.705	0.043	1.925	0.464	0.310	
WK28.4	41.29	7.92	1.31	3.50	30.77		0.44	10.79	1.83	0.94	98.81
	6.538	1.479	0.157	0.827	0.447	3.629	0.060	1.830	0.561	0.190	
WK28.4	40.24	8.82	1.67	3.56	30.44		0.41	10.55	1.69	1.43	98.82
	6.378	1.649	0.199	0.841	0.485	3.549	0.055	1.791	0.520	0.289	
WK28.4	39.24	9.39	1.54	3.21	30.39		0.32	10.77	1.70	1.75	98.32
	6.267	1.768	0.185	0.763	0.570	0.490	0.043	1.842	0.527	0.356	
WK28.4	39.50	9.66	1.77	3.24	29.95		0.35	11.11	1.74	1.57	98.90
	6.256	1.804	0.211	0.765	0.530	3.437	0.047	1.886	0.534	0.318	
WK28.4	39.80	9.58	1.66	3.35	30.08		0.39	10.67	1.71	1.55	98.80
	6.290	1.784	0.197	0.790	0.611	3.365	0.053	1.807	0.525	0.314	
WK28.4	39.13	9.78	1.64	3.05	30.45		0.40	9.94	1.70	1.70	97.78
	6.248	1.841	0.197	0.726	0.711	3.356	0.054	1.702	0.526	0.346	
WK28.4	39.93	9.59	1.67	3.31	30.30		0.41	10.26	1.66	1.74	98.87
	6.305	1.785	0.198	0.778	0.632	3.369	0.055	1.736	0.509	0.350	
WK28.4	39.79	9.02	1.52	3.43	30.43		0.38	10.89	1.63	1.48	98.57
	6.326	1.690	0.182	0.812	0.544	3.502	0.051	1.855	0.503	0.301	
WK28.4	38.82	10.12	1.75	3.43	30.28		0.33	10.90	1.75	1.92	99.31
	6.142	1.888	0.209	0.808	0.597	3.409	0.044	1.848	0.538	0.387	
WK36.8	39.77	9.42	0.58	1.65	31.45		0.45	11.50	1.34	1.51	97.66
	6.425	1.794	0.070	0.398	0.488	3.761	0.061	1.990	0.420	0.311	
WK36.8	39.40	9.65	0.66	1.77	30.48		0.41	10.47	1.44	1.38	95.65
	6.458	1.864	0.081	0.432	0.481	3.697	0.057	1.838	0.457	0.288	
WK36.8	39.58	9.73	0.42	1.76	30.72		0.42	11.20	1.40	1.34	96.57
	6.436	1.865	0.051	0.426	0.484	3.694	0.058	1.952	0.441	0.279	
WK36.8	48.98	1.16	0.17	4.20	30.14		0.56	10.92	0.32	0.22	96.68
	7.792	0.217	0.020	0.008	0.049	3.961	0.075	1.862	0.098	0.045	
WK36.8	48.95	1.25	0.18	4.16	30.00		0.67	11.26	0.34	0.24	97.06
	7.766	0.234	0.021	0.985	0.030	3.950	0.090	1.915	0.104	0.048	

5.4 Results of microprobe analyses of olivine in magnetite-rich rocks together with the number of ions on the basis of 4 oxygen atoms (<11d = less than the lower limit of detection).

SAMPLE	SiO_2 Si	TiO_2 Ti	Al_2O_3 Al	FeO Fe	MnO Mn	MgO Mg	CaO Ca	Na_2O Na	K_2O K	TOTAL
WK14.1	29.79	<11d	<11d	66.52	2.79	1.67	0.07	<11d	<11d	100.8
	0.990	-	-	1.850	0.080	0.080	-	-	-	
WK14.1	29.80	<11d	0.05	66.34	2.74	1.67	0.08	<11d	<11d	100.6
	0.990	-	-	1.850	0.080	0.080	-	-	-	
WK14.1	29.66	<11d	<11d	66.74	2.82	1.70	0.11	<11d	<11d	101.0
	0.990	-	-	1.860	0.080	0.080	-	-	-	
WK14.1	29.52	<11d	<11d	66.08	2.74	1.66	0.13	<11d	<11d	100.1
	0.990	-	-	1.850	0.080	0.080	-	-	-	
WK14.1	29.58	<11d	<11d	66.29	2.79	1.64	0.11	<11d	<11d	100.4
	0.990	-	-	1.860	0.080	0.080	-	-	-	

5.5 Results of microprobe analyses of magnetite (mt) and ilmenite (il) in pyroxenite, magnetite-rich rock and magnetite gabbro; recalculated to determine the Fe^{3+} content assuming stoichiometry (<11d = less than lower limit of detection).

a: Pyroxenite

SAMPLE	OXIDE	SiO_2	TiO_2	Al_2O_3	Cr_2O_3	Fe_2O_3	FeO	MnO	MgO	CaO	V_2O_3	TOTAL
WK5.2	mt	<11d	3.07	0.24	0.12	62.10	33.40	0.22	0.03	<11d	<11d	99.18
WK5.2	mt	<11d	1.11	0.26	0.11	66.70	32.07	0.11	0.04	<11d	<11d	100.40
WK5.2	mt	<11d	0.63	0.20	0.10	67.42	31.49	0.05	0.07	<11d	<11d	99.96
WK5.2	mt	<11d	2.57	0.22	0.17	63.96	33.49	0.16	<11d	<11d	0.06	100.63
WK5.2	mt	<11d	2.76	0.11	0.19	63.73	33.67	0.18	<11d	<11d	0.06	100.70
WK5.2	mt	<11d	4.57	0.16	0.20	59.91	35.09	0.29	<11d	<11d	0.06	100.28
WK6.3	mt	0.09	4.75	0.47	0.08	59.22	35.44	0.33	<11d	<11d	0.04	100.42
WK6.3	mt	0.09	4.42	0.52	0.04	59.90	35.16	0.31	0.03	<11d	0.05	100.52
WK6.3	mt	<11d	2.21	0.75	0.06	64.15	33.32	0.10	<11d	<11d	0.06	100.65
WK6.3	il	<11d	51.42	<11d	<11d	3.77	44.20	2.01	<11d	<11d	<11d	101.40
WK6.3	il	<11d	51.36	<11d	<11d	3.89	44.16	2.00	<11d	<11d	0.04	101.45
WK6.3	il	<11d	51.02	<11d	<11d	4.22	43.84	2.01	<11d	<11d	<11d	101.09
WK12.4	mt	<11d	1.65	0.13	0.20	66.15	32.81	0.13	<11d	<11d	0.06	101.13
WK12.4	mt	0.10	2.37	0.23	0.24	64.35	33.53	0.20	<11d	<11d	0.06	101.08
WK12.4	mt	<11d	1.74	0.18	0.18	65.75	32.80	0.16	<11d	<11d	0.08	100.89
WK12.4	mt	<11d	1.76	0.20	0.23	65.92	32.92	0.17	<11d	<11d	0.04	101.24
WK12.4	mt	<11d	2.42	0.21	0.21	64.21	33.36	0.17	<11d	<11d	0.09	100.67
WK12.4	mt	<11d	1.29	0.19	0.22	66.94	32.44	0.09	0.03	<11d	0.06	101.26
WK12.4	mt	<11d	1.57	0.15	0.19	65.83	32.50	0.14	<11d	<11d	0.05	100.43
WK12.4	mt	<11d	1.34	0.11	0.21	66.66	32.50	0.10	<11d	<11d	0.05	100.97
WK12.4	mt	<11d	1.37	0.16	<11d	66.34	32.43	0.12	<11d	<11d	0.05	100.47
WK12.4	mt	<11d	1.49	0.34	0.21	66.37	32.80	0.09	<11d	<11d	0.06	101.36
WK12.4	mt	<11d	0.74	0.22	0.18	67.95	32.14	<11d	<11d	<11d	0.05	101.28
WK12.4	mt	0.17	9.38	0.41	0.29	49.84	39.44	0.46	0.11	<11d	0.06	100.16
WK12.4	mt	<11d	20.30	0.13	0.13	28.76	48.63	0.97	<11d	<11d	0.03	98.95
WK12.4	mt	0.17	2.01	0.83	0.40	63.76	33.10	0.15	0.13	<11d	0.03	100.58
WK12.4	mt	0.18	1.73	0.71	0.39	64.03	32.58	0.11	0.19	<11d	0.04	99.96
WK12.4	mt	0.19	4.34	0.78	0.39	58.68	34.90	0.24	0.14	<11d	0.03	99.69
WK12.4	mt	0.22	4.39	0.75	0.38	58.04	34.71	0.21	0.18	<11d	0.04	98.92
WK12.4	mt	0.18	1.98	0.92	0.39	63.53	32.84	0.24	0.19	<11d	0.04	100.31
WK12.4	mt	0.18	1.98	0.88	0.40	63.64	33.08	0.20	0.10	<11d	0.03	100.49
WK12.4	il	<11d	51.20	<11d	<11d	4.03	43.69	2.32	<11d	<11d	<11d	101.24
WK12.4	il	<11d	51.09	<11d	<11d	3.74	43.60	2.32	<11d	<11d	<11d	100.75
WK12.4	il	<11d	51.29	<11d	0.14	2.95	43.89	2.18	0.02	<11d	<11d	100.47
WK12.4	il	<11d	51.19	<11d	<11d	3.80	43.75	2.25	<11d	<11d	<11d	100.99
WK12.4	il	<11d	51.99	<11d	<11d	2.01	44.67	2.06	<11d	<11d	<11d	100.73
WK12.4	il	<11d	52.06	<11d	<11d	2.21	44.71	2.08	<11d	<11d	0.04	101.10
WK12.4	il	<11d	51.66	<11d	0.11	2.11	44.21	2.13	0.04	<11d	<11d	100.26
WK12.4	il	<11d	51.62	<11d	0.11	2.48	44.27	2.10	<11d	<11d	<11d	100.58
WK12.4	il	<11d	51.30	<11d	0.13	2.89	43.85	2.21	0.02	<11d	<11d	100.40
WK12.4	il	<11d	51.68	<11d	<11d	3.31	44.41	2.02	<11d	<11d	<11d	101.42

b: Magnetite-Rich Rock

SAMPLE	OXIDE	SiO_2	TiO_2	Al_2O_3	Cr_2O_3	Fe_2O_3	FeO	MnO	MgO	CaO	V_2O_3	TOTAL
WK8.3	mt	0.06	1.02	0.79	0.05	65.91	32.00	0.19	<11d	<11d	<11d	100.02
WK8.3	mt	<11d	0.92	1.11	0.06	66.32	31.92	0.22	0.09	<11d	<11d	100.64
WK8.3	mt	<11d	0.93	1.42	0.06	66.03	31.98	0.22	0.10	<11d	<11d	100.74
WK8.3	mt	<11d	0.96	1.40	0.06	66.11	32.28	0.17	0.02	<11d	<11d	101.00
WK8.3	mt	<11d	1.46	1.97	0.04	64.57	32.75	0.30	0.02	<11d	<11d	101.11
WK8.3	mt	<11d	0.95	1.60	0.34	65.72	32.21	0.20	<11d	<11d	<11d	101.02
WK8.3	mt	<11d	0.94	0.63	<11d	66.14	31.76	0.13	<11d	<11d	<11d	99.60
WK8.3	mt	<11d	0.93	0.98	<11d	65.94	31.85	0.19	<11d	<11d	<11d	99.89
WK8.3	mt	<11d	1.03	1.21	0.02	66.00	32.21	0.20	<11d	<11d	<11d	100.67
WK8.3	mt	0.15	0.94	0.95	<11d	66.34	32.36	0.17	0.02	<11d	<11d	100.93
WK8.3	mt	<11d	0.99	2.21	0.13	65.25	32.48	0.23	<11d	<11d	<11d	101.29
WK8.3	mt	<11d	0.94	0.97	0.02	66.71	32.20	0.18	<11d	<11d	<11d	101.02
WK8.3	mt	<11d	0.99	1.34	0.04	65.96	32.20	0.22	<11d	<11d	<11d	100.75
WK12.1	mt	<11d	0.69	0.82	0.04	67.05	31.79	0.15	0.06	<11d	<11d	100.60
WK12.1	mt	<11d	0.62	1.73	0.04	66.33	31.96	0.20	0.06	<11d	<11d	100.94
WK12.1	mt	<11d	0.62	1.26	0.04	65.97	31.51	0.20	<11d	<11d	<11d	99.60
WK12.1	mt	0.26	0.55	0.54	0.03	66.64	31.82	0.10	<11d	<11d	<11d	99.94
WK12.1	mt	<11d	2.34	1.74	0.05	62.31	33.22	0.29	<11d	<11d	0.03	99.98
WK12.1	mt	<11d	2.45	1.94	0.05	62.41	33.57	0.30	<11d	<11d	0.04	100.76
WK12.1	mt	<11d	2.28	1.81	0.06	61.65	32.93	0.28	<11d	<11d	0.03	99.04
WK12.1	mt	<11d	1.88	1.33	0.02	63.12	32.49	0.23	<11d	<11d	<11d	99.07
WK12.1	mt	<11d	2.11	1.14	0.03	62.82	32.99	0.32	0.02	<11d	0.03	99.46
WK12.1	mt	<11d	1.92	1.73	0.03	63.32	32.90	0.24	0.02	<11d	<11d	100.16

c: Magnetite-Gabbro

SAMPLE	OXIDE	SiO_2	TiO_2	Al_2O_3	Cr_2O_3	Fe_2O_3	FeO	MnO	MgO	CaO	V_2O_3	TOTAL
MG1	mt	0.20	15.89	0.80	0.04	36.55	45.78	0.29	0.02	<11d	0.04	99.61
MG1	mt	0.20	13.80	0.83	0.04	40.86	44.00	0.26	0.03	<11d	0.06	100.08
MG1	mt	0.13	11.58	1.16	0.04	44.80	41.95	0.20	<11d	<11d	0.09	99.95
MG1	mt	0.17	11.40	1.16	0.06	45.79	42.13	0.19	0.03	<11d	0.04	100.97
MG1	il	<11d	51.91	<11d	<11d	1.81	45.73	0.97	<11d	<11d	<11d	100.42
MG1	il	<11d	51.80	<11d	<11d	2.51	45.49	0.98	<11d	<11d	<11d	100.78
MG1	il	<11d	52.00	<11d	<11d	2.56	45.79	0.65	0.18	<11d	<11d	101.18
MG1	il	<11d	51.80	<11d	<11d	2.49	45.56	0.72	0.16	<11d	<11d	100.73
MG2	mt	0.13	12.03	0.97	0.04	43.94	42.11	0.29	0.02	<11d	0.05	99.58
MG2	mt	0.12	12.22	0.97	0.04	44.19	42.53	0.29	0.02	<11d	0.06	100.44
MG2	mt	0.27	10.33	0.66	0.04	48.08	41.04	0.24	0.03	<11d	0.04	100.73
MG2	mt	0.28	9.88	0.65	0.03	48.26	40.27	0.24	0.04	<11d	0.05	99.70
MG2	mt	0.14	14.03	0.68	0.04	39.93	43.66	0.36	0.03	<11d	0.07	98.94
MG2	mt	0.11	14.61	0.70	0.03	39.12	44.24	0.39	0.02	<11d	0.06	99.28
MG2	il	<11d	51.63	0.04	<11d	3.64	44.86	0.52	0.61	<11d	<11d	101.30
MG2	il	<11d	51.65	0.04	<11d	3.80	44.60	0.59	0.72	<11d	<11d	101.40
MG2	il	<11d	51.02	0.04	<11d	4.02	44.05	0.58	0.72	<11d	<11d	100.43
MG3	il	<11d	51.86	<11d	<11d	2.16	44.90	0.57	0.65	<11d	<11d	100.14

5.6 Results of microprobe analyses of clinozoisite in magnetite-rich rock (<11d = less than lower limit of detection , all iron as FeO).

SAMPLE	SiO_2	Al_2O_3	TiO_2	MgO	FeO	MnO	CaO	Na_2O	K_2O	TOTAL
WK8.3	39.19	29.35	<11d	<11d	4.75	0.15	23.65	0.05	<11d	97.15
WK8.3	38.81	28.04	<11d	<11d	6.19	0.07	23.60	0.10	<11d	96.80
WK8.3	41.44	29.10	<11d	<11d	3.39	0.06	22.51	0.61	0.60	97.71

APPENDIX 6

Results of microprobe analyses of Waaikraal ore minerals (rock type: px = pyroxenite, mt = magnetite-rich rock).

6.1 Gold and Gold Compounds (Pd, Rh and Hg below the lower limit of detection)

Sample	Rock Type	Au	Ag	Bi	Cu	Fe	Total	Mineral
WK 5.2	px	99.87	0.50	<11d	0.11	0.02	100.50	gold
WK 5.2	px	100.24	0.30	<11d	0.10	<11d	100.64	gold
WK 5.2	px	100.75	0.40	<11d	0.07	<11d	101.22	gold
WK 5.2	px	100.50	0.34	<11d	0.05	0.04	100.93	gold
WK 5.2	px	99.86	0.72	<11d	0.09	0.06	100.73	gold
WK 5.2	px	100.42	0.50	<11d	0.04	0.03	100.99	gold
WK 5.2	px	99.51	0.29	<11d	0.07	<11d	99.89	gold
WK 6.3	px	99.89	1.26	<11d	0.06	0.03	101.24	gold
WK 6.3	px	97.99	1.07	<11d	0.24	0.12	99.42	gold
WK 6.3	px	99.36	1.03	<11d	0.05	0.04	100.48	gold
WK 28.4	px	100.58	0.18	<11d	0.18	0.03	100.97	gold
WK 28.4	px	99.55	<11d	<11d	0.20	0.04	99.79	gold
WK 28.4	px	101.14	<11d	<11d	0.09	0.15	101.38	gold
WK 52.3	mt	90.37	0.17	<11d	9.66	0.33	100.53	$CuAu_3$
WK 52.3	mt	66.77	<11d	34.44	<11d	0.05	101.26	maldonite
WK 52.3	mt	66.22	<11d	34.42	<11d	0.16	100.80	maldonite
WK 52.3	mt	65.83	0.13	33.86	<11d	0.18	100.00	maldonite
WK 52.3	mt	65.87	<11d	33.78	<11d	0.12	99.77	maldonite
WK 52.3	mt	65.60	0.10	33.46	<11d	0.13	99.29	maldonite

6.2 Bismuth Minerals

Sample	Rock Type	S	Bi	Te	Co	Ni	Sb	As	Total	Mineral
WK 5.2	px	18.95	80.51	<11d	<11d	<11d	0.02	<11d	99.46	bismuthinite
WK 5.2	px	18.80	80.32	<11d	<11d	<11d	0.03	<11d	99.15	bismuthinite
WK 5.2	px	2.85	75.74	21.80	0.04	0.07	0.20	0.78	101.48	joseite-B
WK 5.2	px	2.69	75.55	21.43	<11d	<11d	0.10	<11d	99.77	joseite-B
WK 5.2	px	2.69	75.56	21.51	<11d	<11d	0.10	<11d	99.86	joseite-B
WK 5.2	px	2.93	73.74	21.83	<11d	<11d	0.04	0.30	98.84	joseite-B
WK 5.2	px	2.93	73.85	21.76	<11d	<11d	0.05	<11d	98.59	joseite-B
WK 5.2	px	2.94	74.31	22.05	<11d	<11d	0.05	0.27	99.62	joseite-B
WK 5.2	px	2.97	74.11	21.78	<11d	<11d	0.04	<11d	98.90	joseite-B
WK 5.2	px	2.92	75.80	21.70	<11d	<11d	0.05	<11d	100.47	joseite-B
WK 5.2	px	2.93	75.38	21.79	<11d	<11d	0.03	0.26	100.39	joseite-B
WK 6.3	px	18.65	80.51	<11d	<11d	<11d	0.01	<11d	99.17	bismuthinite
WK 6.3	px	18.92	80.61	<11d	<11d	<11d	0.02	<11d	99.55	bismuthinite
WK 6.3	px	6.49	74.74	5 17.8	<11d	0.04	0.13	0.60	99.85	joseite-B
WK 6.3	px	2.90	75.61	7 21.8	0.05	0.07	0.16	0.83	101.49	joseite-B
WK 6.3	px	2.68	75.32	5 21.3	<11d	<11d	0.08	<11d	99.43	joseite-B
WK 6.3	px	2.67	76.18	8 21.2	<11d	<11d	0.08	<11d	100.21	joseite-B
WK 12.4	px	<11d	99.03	<11d	0.11	0.15	0.11	1.55	100.96	nat. bismuth
WK 12.4	px	<11d	99.04	<11d	0.08	0.06	<11d	0.79	99.97	nat. bismuth
WK 12.4	px	<11d	99.67	<11d	0.07	0.07	<11d	0.84	100.65	nat. bismuth
WK 12.4	px	<11d	99.14	<11d	0.07	0.08	<11d	0.73	100.03	nat. bismuth
WK 12.4	px	<11d	99.38	<11d	0.07	0.06	<11d	0.76	100.27	nat. bismuth
WK 12.4	px	18.29	81.67	<11d	<11d	<11d	<11d	<11d	99.96	bismuthinite
WK 12.4	px	18.15	81.50	<11d	0.04	<11d	<11d	<11d	99.69	bismuthinite
WK 12.4	px	6.66	74.85	17.51	<11d	0.05	0.12	0.64	99.83	joseite-B

Sample	Rock Type	S	Bi	Te	Co	Ni	Sb	As	Total	Mineral
WK 12.4	px	2.66	76.03	21.47	<11d	<11d	0.09	<11d	100.25	joseite-B
WK 12.4	px	2.66	75.18	21.43	<11d	<11d	0.08	<11d	99.35	joseite-B
WK 12.4	px	6.14	79.59	12.39	<11d	<11d	0.15	0.53	98.80	joseite-A
WK 12.4	px	3.18	77.03	18.58	<11d	<11d	0.09	<11d	98.88	joseite-B
WK 12.4	px	2.79	75.30	20.83	<11d	<11d	0.03	<11d	98.95	joseite-B
WK 12.4	px	2.94	75.44	21.38	<11d	<11d	0.06	<11d	99.82	joseite-B
WK 12.4	px	2.92	75.59	21.37	<11d	<11d	0.06	<11d	99.94	joseite-B
WK 12.4	px	2.89	74.72	21.59	<11d	<11d	0.06	<11d	99.26	joseite-B
WK 12.4	px	2.99	75.20	21.70	<11d	<11d	0.05	<11d	99.94	joseite-B
WK 12.4	px	2.98	75.54	21.54	<11d	<11d	0.05	<11d	100.11	joseite-B
WK 12.4	px	2.93	75.51	21.70	<11d	<11d	0.04	<11d	100.18	joseite-B
WK 12.4	px	2.89	75.23	21.72	<11d	<11d	0.05	<11d	99.89	joseite-B
WK 12.4	px	2.91	75.26	21.74	<11d	<11d	0.06	<11d	99.97	joseite-B
WK 12.4	px	2.89	75.43	21.62	<11d	<11d	0.07	<11d	100.01	joseite-B
WK 12.4	px	2.92	75.78	21.73	<11d	<11d	0.04	<11d	100.47	joseite-B
WK 12.4	px	2.97	75.31	21.59	<11d	<11d	0.05	<11d	99.92	joseite-B
WK 12.4	px	2.88	73.19	22.52	<11d	<11d	0.07	<11d	98.66	joseite-B
WK 12.4	px	2.91	73.44	22.52	<11d	<11d	0.09	<11d	98.90	joseite-B
WK 12.4	px	2.97	75.77	21.78	<11d	<11d	0.07	<11d	100.59	joseite-B
WK 12.4	px	2.97	75.47	21.76	<11d	<11d	0.07	<11d	100.27	joseite-B
WK 12.4	px	2.81	75.11	21.23	<11d	<11d	0.04	<11d	99.20	joseite-B
WK 12.4	px	2.90	74.53	21.36	<11d	<11d	0.05	<11d	98.84	joseite-B

6.3 Diarsenides (Sb below the lower limit of detection)

Sample	Rock Type	No.	S	Co	Ni	Fe	As	Bi	Total	Mineral
WK 3.2	px	7	0.75	9.86	0.61	17.23	72.65	<11d	101.10	safflorite
WK 3.2	px	8	0.98	7.93	0.43	19.67	69.78	<11d	98.79	safflorite
WK 3.2	px	9	0.61	17.03	1.16	10.22	71.36	<11d	100.38	safflorite
WK 5.2	px	13	0.89	2.96	2.41	22.11	72.47	<11d	100.84	safflorite
WK 5.2	px	14	0.65	3.70	2.53	20.38	72.42	<11d	99.68	safflorite
WK 5.2	px	16	0.64	17.79	1.24	9.02	70.25	0.92	99.86	safflorite
WK 12.3	px	3	0.35	21.28	1.23	5.40	71.18	1.72	101.16	safflorite
WK 12.3	px	4	0.34	21.34	1.32	5.39	70.84	1.38	100.61	safflorite
WK 12.3	px	5	0.70	15.82	1.04	11.16	70.89	1.05	100.66	safflorite
WK 14.4	px	1	0.60	12.49	0.72	14.31	71.39	0.82	100.33	safflorite
WK 14.4	px	2	0.60	12.56	0.73	14.44	71.50	<11d	99.83	safflorite
WK 28.4	px	6	0.72	0.89	0.17	26.09	73.54	<11d	101.43	safflorite
WK 52.3	mt	10	0.21	11.07	0.57	15.84	71.88	<11d	99.57	safflorite
WK 52.3	mt	11	0.22	10.85	0.57	16.00	72.67	<11d	100.31	safflorite
WK 52.3	mt	12	0.19	10.92	0.57	15.83	73.22	<11d	100.73	safflorite

6.4 Sulpharsenides (as-py= arsenopyrite)

Sample	Rock Type	No.	S	Co	Ni	Fe	As	Sb	Bi	Total	Mineral
WK 5.2	px	13	17.96	0.17	1.84	31.82	46.96	<lld	0.87	99.62	as-py
WK 5.2	px	14	18.47	0.13	4.73	29.01	46.83	<lld	<lld	99.16	as-py
WK 6.3	px	1	19.40	0.06	<lld	34.64	44.59	<lld	<lld	98.69	as-py
WK 6.3	px	2	19.72	0.05	<lld	34.67	44.45	<lld	<lld	98.89	as-py
WK 6.3	px	3	19.83	0.04	<lld	34.87	43.76	<lld	<lld	98.50	as-py
WK 6.3	px	4	21.42	0.05	<lld	35.44	42.82	<lld	<lld	99.73	as-py
WK 6.3	px	5	21.28	0.05	<lld	35.35	42.24	<lld	<lld	98.92	as-py
WK 6.3	px	6	19.51	0.03	<lld	34.32	44.21	<lld	1.19	99.26	as-py
WK 6.3	px	7	19.44	0.04	<lld	34.35	44.47	<lld	0.93	99.23	as-py
WK 6.3	px	11	17.55	3.60	3.38	25.44	44.00	<lld	4.73	98.70	as-py
WK 6.3	px	12	17.72	7.09	3.56	22.15	43.78	<lld	4.28	98.58	as-py
WK 12.3	px	16	20.27	28.11	1.54	5.78	42.70	0.10	<lld	98.50	cobaltite
WK 12.3	px	17	17.74	29.90	2.71	2.42	46.69	<lld	<lld	99.46	cobaltite
WK 12.3	px	18	17.84	30.16	2.60	2.42	47.40	<lld	<lld	100.42	cobaltite
WK 12.4	px	15	18.47	2.15	2.22	29.77	47.35	<lld	1.30	101.26	as-py
WK 14.4	px	8	20.36	0.07	<lld	34.09	44.05	0.04	1.03	99.64	as-py
WK 14.4	px	9	21.58	0.02	<lld	34.71	42.65	<lld	<lld	98.96	as-py
WK 14.4	px	10	21.55	0.04	<lld	34.48	41.85	<lld	0.81	98.73	as-py
WK 21.5	px	19	18.46	31.84	1.54	1.64	46.78	<lld	<lld	100.26	cobaltite
WK 28.4	px	12	20.58	34.34	<lld	2.10	42.14	<lld	<lld	99.16	cobaltite

6.5 Pyrrhotite (selected analyses, ipo = intermediate pyrrhotite, mpo = monoclinic pyrrhotite, As below the lower limit of detection)

Sample	Rock Type	S	Fe	Cu	Ni	Co	Total	atomic % S	atomic % Fe	Mineral
WK 1	mt	39.14	60.06	<lld	<lld	0.21	99.41	53.08	46.76	mpo
WK 1	mt	39.51	59.51	<lld	0.03	0.28	99.33	53.50	46.27	mpo
WK 1	mt	39.73	59.62	<lld	0.03	0.14	99.52	53.66	46.23	mpo
WK 1	mt	39.25	60.94	0.08	0.06	0.23	100.56	52.74	47.51	ipo
WK 1	mt	38.50	61.50	<lld	0.05	0.20	100.25	52.07	47.75	ipo
WK 1	mt	39.01	61.28	<lld	<lld	0.14	100.43	52.52	47.38	ipo
WK 1	mt	38.46	61.10	<lld	0.03	0.14	99.73	52.23	47.64	ipo
WK 1	mt	38.93	60.88	<lld	<lld	0.23	100.04	52.60	47.23	ipo
WK 1	mt	38.81	60.99	<lld	0.04	0.21	100.05	52.48	47.34	ipo
WK 1	mt	37.59	61.73	<lld	0.04	0.08	99.41	51.44	48.49	ipo
WK 1	mt	38.80	61.66	<lld	0.05	0.06	100.57	52.25	47.67	ipo
WK 1	mt	38.80	61.84	<lld	0.06	0.06	100.76	52.17	47.74	ipo
WK 1	mt	38.54	61.59	<lld	0.06	0.06	100.25	52.10	47.81	ipo
WK 1	mt	38.37	60.89	<lld	0.04	0.27	99.57	52.20	47.57	ipo
WK 1	mt	38.25	60.48	<lld	0.03	0.25	99.01	52.31	47.48	ipo

6.6 Chalcopyrite

Sample	Rock Type	S	Fe	Cu	Ni	Co	Total
WK 1	mt	34.91	30.77	35.21	<11d	0.03	100.92
WK 1	mt	34.56	31.37	34.93	<11d	0.03	100.89
WK 1	mt	34.75	31.43	34.77	<11d	0.03	100.97
WK 1	mt	35.21	28.98	35.23	<11d	0.04	99.46
WK 1	mt	35.22	30.20	34.89	<11d	0.03	100.34
WK 1	mt	35.27	30.25	34.76	<11d	0.05	100.33
WK 5.2	px	34.39	30.48	34.42	<11d	0.02	99.31
WK 5.2	px	33.39	30.58	34.82	<11d	0.03	98.82
WK 6.3	px	34.52	30.75	35.21	<11d	<11d	100.48
WK 6.3	px	34.11	30.96	34.99	<11d	0.03	100.09
WK 6.3	px	34.22	30.75	35.15	<11d	0.04	100.16
WK 6.3	px	34.47	30.22	34.36	<11d	<11d	99.05
WK 6.3	px	34.72	30.27	34.98	<11d	0.03	100.00
WK 6.3	px	34.38	30.29	34.83	<11d	<11d	99.50
WK 6.3	px	34.19	30.10	34.53	<11d	0.03	98.85